THE UNIVERSITY
of EDINBURGH

Susceptibility to hypertensive renal injury mediated by P2X receptors

Robert Ian Menzies

A thesis submitted for the degree of

PhilosophiæDoctor (Ph.D)

University of Edinburgh

February 2014

Declaration

I declare that this thesis was compiled by myself and that all the work presented is my own, except where otherwise stated.

Robert Ian Menzies

Acknowledgements

I would like to acknowledge my supervisors Dr Matthew Bailey and Professor John Mullins for their support and direction throughout my PhD. Also the British Heart Foundation for funding my studentship. It's been a rewarding and steep learning curve following a physics MPhys: I hope I have honoured the ambitions of the Centre of Research Excellence in my studies.

Drs. Guido Sanguinetti and Andrew Zammit-Mangion (School of Informatics, Edinburgh) were fantastic to work with. Their knowledge of signal analysis methodologies advanced the BOLD MRI studies towards robust and reasoned image analysis. I would like to thank Dr Maurits Jansen and Ross Lennon without whom the MRI scanner would not have run. Dr Chris Kenyon who's experience and perspective has helped me cut to the chase on several occasions. The BRF staff provided excellent technical assistance throughout my PhD, particularly super tech' Will who made light work of tail vein catheterisation and everyone in the Molecular Physiology lab who has assisted me over the years, especially Jessica Ivy for teaching me Western blotting and Charlotte Buckley for upholding the time honoured tradition of tea time in our office.

I would like to thank Dr Allen W. Cowley Jr. for supporting my visit as a short-term scholar to Wisconsin as well as Drs. Daniel A. Beard and Brain E. Carlson all of whom supervised my work under the NIH Centre for Systems Biology. I enjoyed many discussions with Dr Cowley on the nature of the pressure-natriuresis mechanism and the studies of Arthur C. Guyton which influenced to the surgical pressure ramping protocol I developed in Edinburgh. I would also like to thank the University of Edinburgh's Innovation Initiative Grant scheme for awarding me the funds to purchase the Doppler flow-probe used in the surgical studies presented in this thesis. I would also like to thank Dr Ranjan K. Dash whose suggestions regarding modelling ligand gated ion channels facilitated the biophysically considerate models of P2X receptor voltage-current relationships.

Abstract

The renin angiotensin aldosterone system is the dominant hormonal regulatory system controlling sodium balance and therefore blood pressure homeostasis. Abnormal modulation of this system is implicated in the pathogenesis of hypertension and end organ injury. We have previously developed the *Cyp1a1-Ren2* transgenic rat to model angiotensin II (ANG II) dependent hypertension. In this model hypertension causes renal injury, predominantly in the preglomerular vasculature. The susceptibility to renal injury has a genetic component. A consomic/congenic study identified angiotensin converting enzyme (*Ace*) as an important modifier.

However, renal injury is unlikely to be influenced by a single gene. In this thesis it was hypothesised that examination of a renal microarray to compare the relative expression in F344 (susceptible) and Lewis (relatively protected) strains would reveal further genetic factors mediating renal injury susceptibility. Genome wide expression analysis confirmed that *Ace* was a key modifier gene. Furthermore, the purinergic receptors *P2x7* and *P2x4* were identified as additional candidates. Gene and protein expression of these P2X receptors were both higher in F344 compared with Lewis. Immunohistochemistry localised P2X7 and P2X4 to the renal vasculature and tubules: the expression pattern was similar in both strains but became distinct in the renal medulla.

F344, but not Lewis, responded to acute antagonism of P2X7 and P2X4. F344 showed a significant drop in blood pressure but maintained renal blood flow, indicative of tonic renal vasoconstriction. When ANG II was infused into F344 rats, there was a modest increase in blood pressure and an impairment of the pressure-natriuresis mechanism but no overt injury. Blood oxygenation-level dependent magnetic resonance imaging of the kidney identified a decrease in renal R2* signal following P2X7 and P2X4 antagonism in ANG II infused F344 rats. P2X7/4 receptor activation reduces oxygenation and suppresses pressure-natriuresis. These effects are pro-fibrotic and may underpin susceptibility to renal injury.

Contents

Glossary

Ac-SDKP N-acetyl-Ser-Asp-Lys-Pro

ACE2 Angiotensin converting enzyme 2

AGT Angiotensinogen

ANG 1-7 Angiotensin 1-7

ANG 1-9 Angiotensin 1-9

ANG I Angiotensin I

ANG II Angiotensin II

ANG III (2-8) Angiotensin III (a.k.a. 2-8)

ANG IV Angiotensin IV (a.k.a. 3-7)

ANOVA Analysis of variance

AQP1-4 Aquaporins 1-4

ASDN Aldosterone sensitive distal nephron

AT1 Angiotensin Type I Receptor

AT1a angiotensin receptor type 1a

AT1b angiotensin receptor type 1b

AT2 Angiotensin Type II Receptor

ATP Adenosine-5'-triphosphate

BBG Brilliant Blue G

BOLD Blood oxygenation level-dependent

bp base pair

CCD Cortical collecting duct

CD68 Cluster of differentiation 68 a.k.a ED-1

cGP Causally cohesive genotype phenotype mapping

CHARGE Cohorts for heart and ageing research in genomic epidemiology

CKD Chronic Kidney Disease

CRP C-reactive proteins

CTGF Connecting tubule glomerular feedback

DAB 3,3′-Diaminobenzidine

DBP Diastolic blood pressure

DCT Distal convoluted tubule

DL Descending limb

DNA Deoxyribonucleic acid

DOCA deoxycorticosterone acetate

ECL enhanced chemiluminescence

EDTA Ethylenediaminetetraacetic acid

ENaC Epithelial sodium channel

GFR Glomerular filtration rate

GWAS Genome wide association studies

H&E Hematoxylin and eosin

HIER Heat-induced epitope recovery

HRP Horseradish Peroxidase

I3C Indole-3-carbinol

IL-6 Interleukin 6

JGA Juxtaglomerular apparatus

L-NAME N-Nitro-L-arginine methyl ester hydrochloride

LIMMA Linear models for microarray data

LOD Logarithm (base 10) of odds

mmHg Millimetres of mercury

MRI Magnetic resonance imaging

NaCl Sodium chloride

NaF Sodium fluoride

NCC Thiazide-sensitive NaCl cotransporter

NHE3 Sodiumhydrogen antiporter 3

NKCC2 $Na^+ - K^+ - 2Cl^-$ cotransporter

NO Nitric oxide

NOS Nitric oxide synthase

PAS periodic acid-Schiff

PBS Phosphate buffered saline

PCT Proximal convoluted tubule

PKD Polycystic kidney disease

pO_2 Partial pressure of oxygen

qRT-PCR Quantitative real time polymerase chain reaction

QTL Quantitative trait loci

RAS Renin Angiotensin System

RBF Renal blood flow

RIHP Renal interstitial hydrostatic pressure

RMA Robust multi-array average

RNA Ribonucleic acid

ROI Region(s) of interest

ROMK Renal outer medulla potassium channel

RVR renal vascular resistance ($mmHg/ml.min^{-1}$)

SBP Systolic blood pressure

SEM Standard error of the mean

SNP(s) Single nucleotide polymorphism(s)

TAL Thick ascending limb

TGF Tubuloglomerular feedback

Tris tris(hydroxymethyl)aminomethane

TRP Transient receptor potential

WNK lysine deficient protein kinases

WTCC Wellcome Trust case control consortium

List of Figures

For my parents James and Christine.

1
INTRODUCTION

1.1 The Genetics of Hypertension

Hypertension is defined as systolic blood pressure (SBP) $\geq$140 mmHg or diastolic blood pressure (DBP) $\geq$90 mmHg and affects around one third of the Earth's population (250). Hypertension is a major risk factor for future cardiovascular and kidney diseases (290, 345, 436) and therefore exerts a profound socioeconomic burden on most societies.

Hypertension has a heritable component. On average, half of blood pressure variability has been ascribed to inherited genetics (187, 297, 327). Genetic variability within families is also important as evidenced by the greater similarity of blood pressure between monozygotic, compared to dizygotic, twins (124). Furthermore cardiovascular morbidity confers greater risk for a surviving monozygotic, compared with dizygotic, twin (124, 203).

Hypertension is either essential (primary), whereby the origin of the blood pressure rise is unknown, or secondary, in cases where a causal mechanism can be defined. Essential hypertension is almost certainly polygenic and by far the most prevalent form of hypertension, affecting 90-95% of hypertensive patients (59) who are typically treated with a drug, or drugs, targeting the renin angiotensin system (see section 1.3), calcium channel blockers or diuretics (111, 307). Common secondary forms hypertension are predominantly caused by sleep apnoea or renal parenchymal disease (also see Table 1 of (426)). The rarest forms of secondary hypertension have a strong genetic component (511) and might present an opportunity for high specificity pharmacotherapy (111). This is consistent with the observation that single gene variants with large effects on blood pressure are rare (see sections 1.1.1 & 1.2.4) whilst multiple genes each with small effects are more common (see section 1.1.2).

Long term population-wide studies (particularly the Framingham studies (134)) have identified hypertension as a major, modifiable, risk factor for cardiovascular disease and morbidity. Environmental factors also play a causative role in cardiovascular disease (82). Low birth weight confers cardiovascular disease susceptibility (23) and a number of contributing factors are implicated (8), for example glucocorticoid overexposure (30). Together these studies support the present understand-

ing that the molecular aetiology of hypertension is complex and key mechanisms remain elusive.

1.1.1 Monogenic hypertension

Monogenic forms of hypertension are rare, accounting for only a small proportion of secondary forms of hypertension. These can be described by three convergent mechanisms (463). First, Liddle's syndrome (457) and Gordon's syndrome (68) are caused by deleterious mutations in salt transporters causing increased renal sodium reabsorption. Secondly, deficiencies in adrenal steroid synthesis lead to increased plasma volume, examples of this are congenital adrenal hyperplasia (472), or the syndrome of apparent mineralocorticoid excess (534). The third major monogenic mechanism is caused by abhorrently high aldosterone synthesis which perpetuates volume dependence and decreased renin release as seen in glucocorticoid remedial aldosteronism (288, 289). For example, somatic mutations in ion channels of the adrenal gland are associated with aldosterone producing adenomas (14, 32).

Monogenic human hypertension has been recapitulated in animal models (485). Specifically, gene targeting in rats and mice (148, 220, 489) including cell specific (382) and inducible (276) mutagenesis techniques have provided deeper mechanistic insights into the renal physiology than would be ethically viable in human studies (see section 1.2.4). These approaches have validated the concept that impaired renal salt homeostasis is found in all monogenic forms of hypertension (181). Importantly however this does not necessarily equate to causality since causative genes are often expressed in multiple tissues and major endocrine systems affect multiple organs.

1.1.2 Polygenic hypertension

Essential hypertension is likely polygenic but genetic mechanisms are not clear-cut. Broadly speaking, attempts to define critical genetic factors fall into two categories. Firstly, familial based genetic linkage studies, such as (376), assert that heritable traits are tractable within related subjects with comparable phenotype. Secondly, genome wide association studies (GWAS), such as the Wellcome Trust case control consortium (WTCCC) (532), are designed on the assertion that common genetic variants cause common complex disease at the population scale. Both approaches have made important contributions to the study of essential hypertension, and both have their respective caveats. Linkage analysis identifies rare variants with large effects on phenotype: GWAS identify multiple variants each with small additive effects on phenotype (308).

Blood pressure quantitative trait loci (QTL) have been established in animal models through microsatellite guided selective breeding to produce ever refined

congenic strains (144, 316, 415). Enrichment of these refined QTLs by methods such as gene network analysis (reviewed (242)) provide a holistic strategy for the identification of causation (provided all/most causative genes are captured by the congenic region) in these complex polygenic phenotypes (81, 100).

1.1.2.1 Genetic linkage analysis

Genes located in close proximity to each other on the chromosome are said to be genetically linked as they tend to segregate into the same chromatid during meiosis (25, 321, 338). Genetic linkage analysis utilises this property to study inherited diseases (for examples see section 1.2.4).

Pedigree studies are, however, limited in their applicability to populations. One of the earliest major studies which tried to address this was the Framingham cohort which began in 1948 with the aim of identifying population wide cardiovascular risk factors (93, 94, 238). Framingham cohort studies have produced far-reaching, even policy forming, insights: cigarette smoking (93), lipoprotein profile in men (239), obesity (204) and arterial fibrillation (539) were all identified by Framingham studies as risk factors for cardiovascular disease.

1.1.2.2 Genome wide association studies

The most common genetic variations are single point variants or single nucleotide polymorphisms (SNPs) occurring approximately every 1,000 bp (482). SNPs have the potential to alter protein function and associations between multiple SNPs and physiological measures such as blood pressure provide an opportunity to unlock polygenic mechanisms. There is thus an assertion that multiple SNPs found frequently in hypertensive individuals are informative in identifying mechanisms of polygenic hypertension.

GWAS requires *a priori* that common complex disease is caused by common genetic variants (427). This assertion has provided limited functional insights since SNPs frequently occur in non-coding regions and such variation cannot be clearly tied to function (482) and is not absolute: phenotypic consequences of both common and rare gene variants might be important (149). This presents a challenge in tying SNPs from genotype to phenotype. Mechanistically, small variants in renal transporters appear important (224) but many other small effect variants have also been identified (389). Most of the SNPs identified by GWAS to date cannot be reconciled mechanistically with known physiological mechanisms of blood pressure rise (24).

Statistical methods can provide association of genes and their phenotypes. This lacks causation, and therefore the prediction of acquired phenotypes. Causally cohesive genotype phenotype mapping (cGP) has been proposed as one method to

bridge this conceptual gap (381, 412). This method argues that the unexplained variance, also known as the problem of missing heritability (308), found in genetic association studies might map to the variance found in physiologically measurable parameters imparting causation in the genetic and phenotypic scales (151, 524). However, genetic interactions also play a role in explaining some of this unexplained variance (38, 552).

Causation is important in GWAS interpretation. GWAS have had limited success at associating disease causing SNPs to both renal function and hypertension (112, 385, 388, 497). The gene encoding Tamm-Horsfall glycoprotein (*Umod*), the most abundant mammalian urinary protein, being one exception. In terms of causation the limited success of GWAS in this context can be explained by the observation that renal function (particularly salt handling) itself is implicated in the genesis of hypertension whilst hypertension alone cannot explain progression of kidney disease (as evident from the limited range of antihypertensive therapies for kidney disease). These concepts are explored in the following sections.

1.2 Blood Pressure and the Kidney

Poiseuille's law defines the proportionality between changes in luminal pressure and blood flow. Changes in blood pressure without parallel increases in haemodynamic flow can be interpreted as increases in vascular resistance. This relationship shows that blood pressure homoeostasis requires appropriate regulation of total blood volume or extracellular fluid volume (146). High salt intake increases extracellular fluid volume: the opposite effect is observed under low sodium intake (274). A positive linear association exists between 24-hour sodium excretion and SBP (114, 473). Importantly salt sensitivity of blood pressure is not apparent in all individuals, yet those susceptible show increased mortality rates even in normotension (133, 322, 528, 529). Low sodium diet reduces blood pressure in normotensives and hypertensives (189). Together these data indicate that a population-wide reduction in blood pressure (thus reducing cardiovascular risk) might be achieved by simply reducing salt intake. However, this is vehemently debated (7, 273, 479).

The kidney is the principal regulator of sodium excretion in the body. Guyton and co-workers used a systems analysis approach to model circulatory regulation and proposed the kidney as the dominant regulator of cardiac output (172, 173)[1]. The evidence presented in the following sections supports the tenet that long

[1]One criticism of the Guytonian model is the level of detail on dynamic mechanisms mediating the central control of blood pressure (304). This highlights an important uncertainty and ongoing debate regarding the key events (and organ(s)) initiating hypertension. That is to say, salt driven volume expansion is not necessarily the initiating event; changes in sympathetic tone, for example, might be important (27, 101, 232, 305, 487).

term blood pressure homoeostasis is regulated by the excretion of sodium through vascular and tubular interactions within the kidney.

1.2.1 Renal haemodynamics

The renal arterial system supplies oxygen rich blood, approximately 20% of the cardiac output, through a vast network of arteries and arterioles (269, 352). Since the work of Bowman (40) the injection of fine inks and resins into the renal circulation has provided great insight into the beautifully complex microstructures of the kidney (333, 334). Construction of arterial tree network maps is now becoming possible (118, 368) allowing for microcirculatory mathematical models that are architecturally considerate (79, 206, 264).

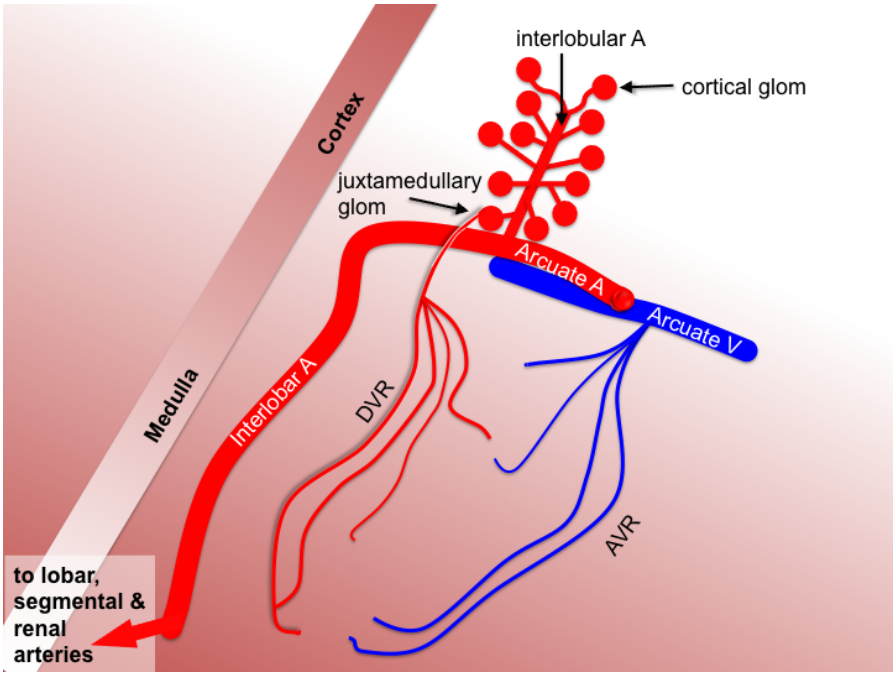

Figure 1.1: Renal Vascular Architecture - Illustration of the renal arterial network leading to the cortical glomeruli (cortical glom) or juxtamedullary glomeruli (juxtamedullary glom) and the vasa recta. DVR: descending vasa recta, AVR: ascending vasa recta, A: artery (red), V: vein (blue)

The major contributories to the renal circulation consist of renal, segmental, lobar, interlobar, arcuate, interlobular and glomerular-supplying afferent arterioles in order of decreasing lumen diameter (Fig.1.1). Not all glomeruli are presumed structurally, or functionally, equivalent. The two acknowledged types of glomeruli are shown in Fig1.1. Cortical (or superficial) glomeruli supply tubules which ascend only to the outer medullary structure (Fig.1.1, as indicated). Glomeruli positioned at the edge of the renal medulla, known as juxtamedullary glomeruli (Fig.1.1, as indicated) supply the descending vasa recta of the medulla and supplying tubules ascending into the deepest sections of the inner medulla. Approximately 10% of juxtamedullary glomeruli can be bypassed to perfuse the vasa recta directly, (61, 63, 450). This may occur in response to altered metabolic demands in a pathophysiological setting (142, 143).

Total renal blood flow (RBF) and glomerular filtration rate (GFR) are autoregulated, that is, maintained constant over a physiological blood pressure range whilst urine flow is not regulated. Typical human values for RBF, GFR and urine flow for a range of blood pressures are given in Fig.1.2. Autoregulation is mediated by multiple vascular (myogenic response) and tubular feedback mechanisms (including tubuloglomerular feedback (TGF) and connecting tubule glomerular feedback (CTGF)).

Arterial resistance is inversely proportional to arterial diameter. Thus the myogenic tone of the renal vasculature increases with decreasing lumen diameter (13, 335) such that afferent arterioles are thought to be the most functionally important for renal autoregulation. It is estimated that up to 80% of total autoregulation occurs in the preglomerular vascular tree (62) protecting the glomeruli as well as pre- and post-glomerular vasculature from mechanical damage (299, 350). Myogenic tone is mediated by smooth muscle cell contractility (92, 196, 320) and regulated differentially in afferent and efferent arterioles which ensures a constant GFR (58, 298, 357, 428). Mechanistically, vascular smooth muscle purinergic P2X1 receptors (216) and transient receptor potential (TRP) channels (102) have been identified as important mediators of the myogenic response.

TGF occurs through purinergic signalling between the proximal convoluted tubule (PCT) and the afferent arteriole (171, 444, 447). Increased PCT sodium reabsorption decreases sodium chloride (NaCl) concentration sensed by the macula densa and therefore decreases afferent arteriole resistance (41, 207, 359). Simultaneously, efferent arteriole constriction will be increased by renin secretion (10, 329, 330).

There are likely multiple molecular mechanisms mediating TGF. Increased luminal NaCl is sensed by macula densa cells provoking the release of ATP through a maxi anion channel (29). ATP activates messangial cell purinergic P2X1 receptors directly (211, 213, 303). The expression pattern (afferent but not efferent

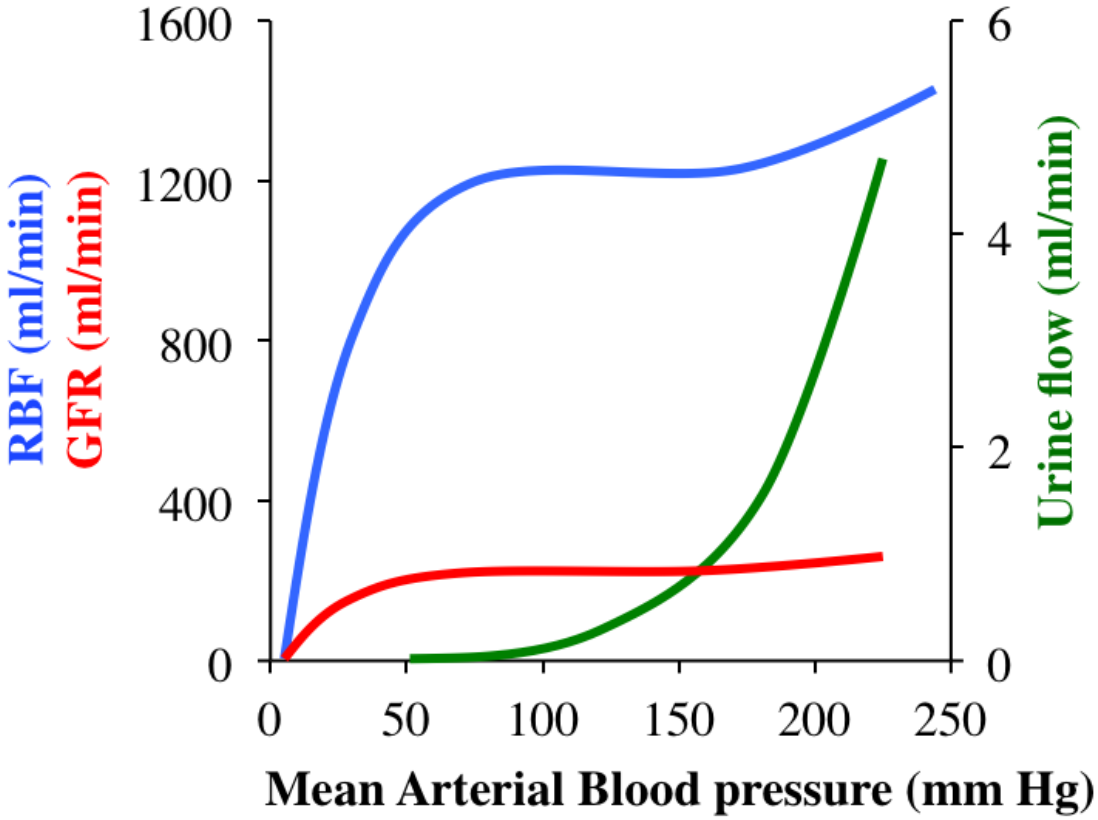

Figure 1.2: Renal Autoregulation - Autoregulation is observed in renal blood flow (RBF) and glomerular filtration rate (GFR) but not urine flow over a physiological mean arterial blood pressure range. Tyical values are given for measurements in dogs. Adapted from the Guyton and Hall Textbook of Medical Physiology, Chapter 26, Figure 26-17.

arteriole) of P2X1 receptors suggests an important role for this receptor subtype in afferent arteriole tone (212). Rapid hydrolysis of ATP to adenosine diphosphate (ADP) also activates P1 receptors (387, 443, 446) which are critical for the TGF mechanism (480, 491). Together adeonisine receptors increase intracellular Ca^{++} levels within extraglomerular mesangial cells. Transmission of intracellular Ca^{++} to the afferent arteriole (to produce constriction) requires gap junction proteins such as connexin 40 (234, 404, 419). Recently a new tubular feedback mechanism has been identified, CTGF, which occurs following increased luminal NaCl in the connecting tubule and mediates prostaglandin and epoxyeicosatrienoic acid release (418, 420).

Dynamic interactions of the renal autoregulatory mechanisms ensures appropriate luminal flow, and therefore concentration, of luminal NaCl as well as protecting the kidney from barotrauma (88, 233, 486, 492, 506, 518, 521).

1.2.2 The pressure-natriuresis mechanism

Stable GFR ensures stable sodium filtrate (453, 458). GFR appears impressively consistent over a wide physiological pressure range, (468). Total RBF is similarly well autoregulated; typical values are given in Fig.1.2. This stability of renal haemodynamics ensures that filtrate of fluid and sodium does not fluctuate with perfusion pressure. This does not hold true for urine flow and sodium excretion. This is the basis of the pressure-natriuresis mechanism as seen in the physiologically normal renal function curve (Fig.1.3A). Pressure-natriuresis is an interaction between vascular and tubular components. Mechanistically, increases in renal perfusion generally increase papillary flow and therefore capillary pressure causes an increase in total kidney interstitial hydrostatic pressure (RIHP) (162, 256, 267, 272). Increased RIHP inhibits total sodium reabsorbption (123, 141, 429). Furthermore osmotic forces ensure that sodium and water are excreted proportionally.

Micropuncture studies have observed increasing natriuresis in accordance with increases in renal perfusion (175, 353, 384). During such pressure increases the renal cortex remains well autoregulated but many studies have observed transmission of pressures directly to the medulla suggesting this is the important region of the kidney mediating this effect (80, 268, 429, 454). This was originally confounded by the contrasting evidence from other studies which have found autoregulation of the renal medulla (76, 87, 476). More recent studies have gone some way to resolving this apparent contradiction: the circulations of the renal cortex and medulla are regulated oppositely by a number of factors. For example, the potent vasoactive peptide endothelin-1 causes constriction in the cortex but dilation in the renal medulla (168). Unique regulation of the medullary circulation involving multiple vascular-tubular interaction supports the assertion that this region plays a critical role in natriuretic responses to changes in renal perfusion pressure (122, 314).

1.2.3 The pressure-natriuresis mechanism in hypertension

Oedema in congestive cardiac failure patients correlates with reduced renal blood flow (preceding an increase in venous pressure), implicating kidney function *per se* in heart failure pathophysiology (325, 525). Such clinical observations emphasise the role of deleterious renal sodium and water handling in cardiovascular disease (436, 453, 458, 490).

All forms of hypertension described to date involve a shift in the pressure-natriuresis relationship (179). In normal physiology Guyton's so called 'infinite gain' of the kidney maintains stable blood pressure within a wide range of dietary salt intakes through appropriate balance of salt excretion and reabsorption. It is thus assumed that hypertension is characterised by any deviation from this process. Fig.1.3 demonstrates the normal relationship and its deviation in hypertension. Normal salt intake confers the standard pressure-natriuresis curve (curve A). A sustained high salt intake shifts the curve leftward: greater sodium excretion occurs and physiologically normal blood pressure is maintained (curve B). In hypertensive individuals pressure-natriuresis is ineffective. That is, blood pressure becomes sensitive to salt intake by insufficient renal salt handling (curve C).

1.2.4 Renal tubular function and syndromes of innaproriate salt reabsorption

The kidneys filter around ∼24,000 mEq/day of sodium from some ∼180L of water, 99% of which is reabsorbed along the nephron. The kidneys show an impressive propensity to retain sodium appropriately for a wide range of salt intakes (see Fig.1.3) when pressure-natriuresis is intact. Fig.1.4 shows the approximate percentages of sodium reabsorption in the major nephron segments; 50% at the proximal convoluted tubule (PCT), 20% at the descending limb (DL) , 20% at the thick ascending limb (TAL) , 5% in the distal convoluted tubule (DCT) and around 4% in the cortical collecting duct (CCD).[1]

The majority of sodium reabsorption is performed by the sodium-hydrogen antiporter 3 (NHE3) in the PCT (125, 449) (Fig.1.4B). Micropuncture studies demonstrate that PCT reabsorption is decreased by 75% in NHE3$^{-/-}$ mice (449). NHE3$^{-/-}$ mice are volume depleted and hypotensive which appears consistent but compensation of renal salt transporters means that total renal sodium excretion is actually more efficient. This is in part because of decreased epithelial sodium

[1]Water homeostasis is mediated by the aquaporin (AQP1-4) family. AQP1 is expressed in the PCT and TAL (364, 445). AQP2-4 are expressed in the CCD and are involved in vasopressin mediated water reabsorption (363). Rare AQP2 mutations cause a diabetes insipidus like phenotype (33, 99, 510).

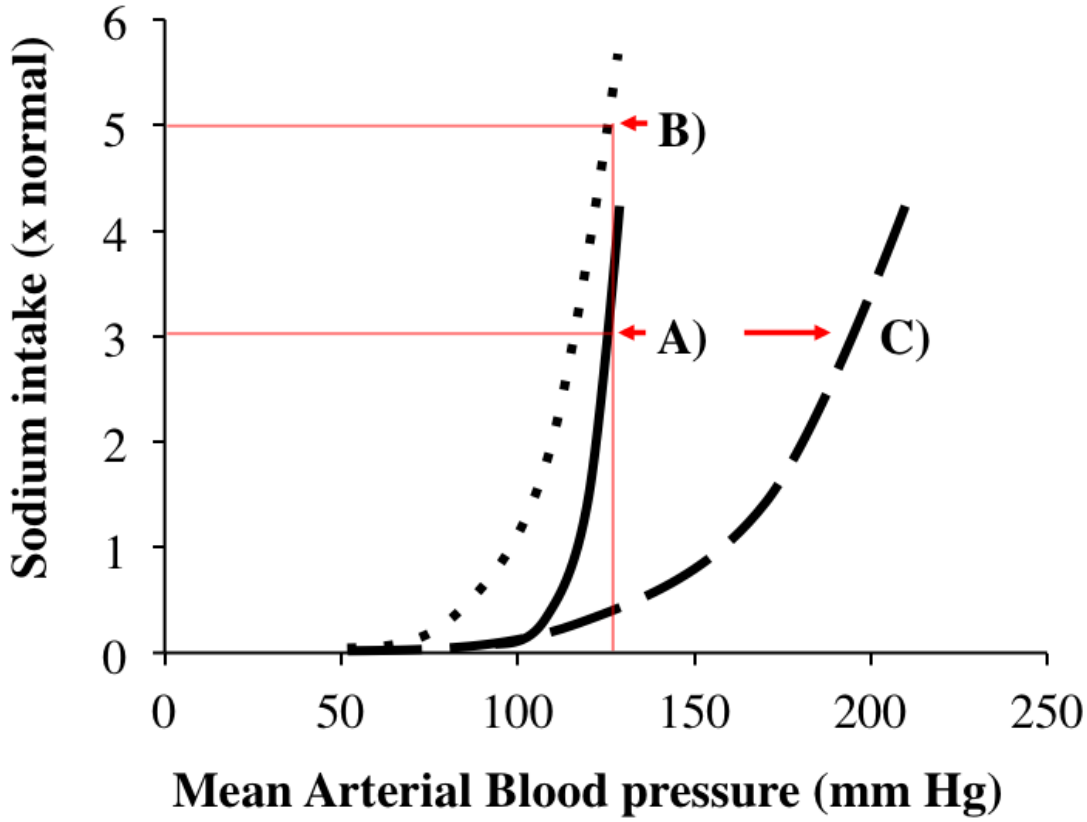

Figure 1.3: The Relationship Between Sodium Intake and Blood Pressure - In Man blood pressure rises minimally with sodium intake according to normal pressure-natriuresis (A). A leftward shift in the curve occurs following sustained sodium intake, the kidneys excrete a greater proportion of salt to ensure blood pressure remains stable (B). A rightward shift in the curve describes impairment of the mechanism, as found in hypertensive individuals (C). Figure adapted from (170).

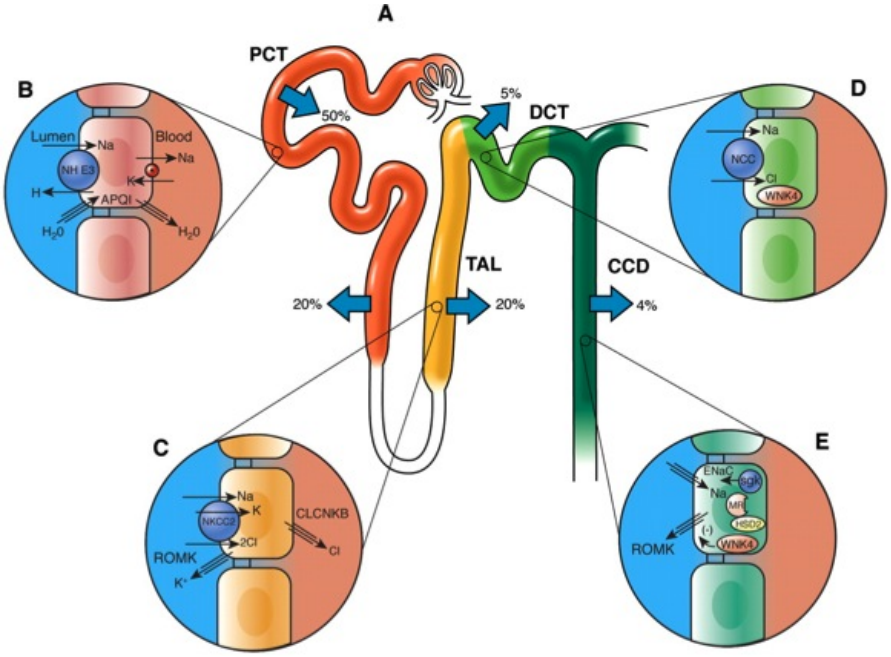

Figure 1.4: Major Renal Sodium Transporters - The percentage of sodium reabsorbed in each major nephron segment (A). The major salt transporters are shown for the proximal tubule (B), thick ascending loop of Henle (C), distal convoluted tubule (D) and the cortical collecting duct (E). From (343)

channel (ENaC) activity and RAS activation increasing sodium reabsorption in the aldosterone sensitive distal nephron (ASDN) (16, 46).

In the loop of Henle (Fig.1.4C) sodium reabsorption is dominated by $Na^+ - K^+ - 2Cl^-$ cotransport (NKCC2) (163). Mice null for either NKCC2 or the renal outer medulla potassium channel (ROMK) are severely volume depleted (300, 484) and reflect the phenotype of Bartter's syndrome sufferers (460).

Gordon's syndrome (pseudohypoaldosteronism type II) is so named because the clinical symptoms are equivalent to those found during chronically low aldosterone (lack of salt wasting and hypokalemia), however aldosterone levels are in fact chronically elevated (538). Gordon's syndrome is caused by of a lack of feedback owing to mutations in with-no-lysine-K (WNK) kinases WNK1 and WNK4 (71, 235, 546) from the thick ascending limb to the CCD (200).

DCT sodium reabsorption is predominantly mediated by the thiazide-sensitive NaCl cotransporter (NCC) (140). Loss of function mutations in the gene encoding NCC, *Slc12a3*, cause Gittleman's syndrome characterised by hypokalemia (causing metabolic alkalosis), hypocalciuria and hypomagnesemia (461). $NCC^{-/-}$ mice have the Gittleman's syndrome phenotype (449). However, much like the increased total sodium reabsorption in the nephron of $NHE3^{-/-}$ (16) $NCC^{-/-}$ display only a mild phenotype indicating a striking redundancy of sodium transport in the kidney (46).

The fine tuning of sodium reabsorption is mediated by ENaC within the connecting tubule and CCD. ENaC consists of α, β and γ subunits all three of which are regulated by aldosterone (310) describing an important arm of sodium regulation by the RAS. Liddle's syndrome is caused by mutations in the β subunit of ENaC (457) preventing ubiquitination by the enzyme NEDD4 (474) resulting in uncontrolled natriuresis.

The identification of mutations in renal sodium transporters as causative in several hypertensive syndromes has highlighted both the role of the kidney in hypertension and the redundancy of sodium transport in the kidney. The effect of these mutations on blood pressure is not equally proportional to their effect on total renal sodium flux.

1.2.5 Hypertension and renal transplantation

Some renal transplantation studies have found that host genotype is the predominant cause of hypertension. For example, renal transplants from Dahl salt sensitive (normotensive) donors into hypertensives does not alleviate hypertension (73). It is not yet clear whether severing of renal innervations during the transplant process plays a critical role (45, 275, 441).

Renal transplant recipients from donors of hypertensive families are susceptible to developing hypertension (167). Hypertensive individuals receiving kidney trans-

plants from normotensive donors achieve long term normotension (89). Blood pressure lowering has been observed in multi-treatment resistant hypertensive patients following bilateral nephrectomy and transplantation from normotensive donors (266). As such, renal transplantation studies have provided significant insight into the role of the kidneys in genetically determined hypertension (165, 422).

Kidneys transplanted from young Milan rats (pre-hypertension) into controls do not cause hypertension whereas hypertensive renal donors instigate hypertension (130). Dahl salt sensitive rats treated with low salt and co-transplanted demonstrate the importance of donor over recipient genetics (90, 190, 337, 423). Spontaneously hypertensive rats maintained chronically normotensive become hypertensive following renal transplantation into normotensive controls. (421). The case is similar for the stroke-prone spnetaneously hypertensive rat (423). Mechanistically, renal transplantation studies have identified renal ANG II receptors as key mediators of hypertension and detrimental cardiovascular consequences (74, 85, 86). These data support the notion that renal allograft genotype, over host genotype, predominate the propensity for hypertension.

Renal transplant studies are also limiting in their interpretation due to immune activation by cross genome implantation (437, 438) typically requiring immune suppression. Over-activation of the renin angiotensin system (RAS) plays a direct role in immune cell activation during inflammation and vascular injury (174, 245, 455) and the use of RAS inhibitors might reduce transplant rejection rates (291, 369, 477). However recent studies suggest that the RAS is neither overly active in transplant recipients (217) nor does its inhibition improve rejection rates (191).

1.3 The Renin Angiotensin System

The renin angiotensin system (RAS) is the dominant hormonal system regulating blood pressure and fluid homeostasis (see Fig1.5). Angiotensinogen (AGT) is cleaved by renin producing angiotensin I (ANG I). This is the rate-limiting step in RAS activation (12). The ubiquitously distributed angiotensin converting enzyme (ACE) rapidly converts inert ANG I to the vasoactive peptide ANG II which regulates blood pressure both directly; due to peripheral vasoconstriction, activation of the sympathetic nervous system, increased sodium reabsorption and indirectly; influencing secretion of aldosterone and vasopressin. RAS blockade has proven integral in the reduction of cardiovascular risk (442). The RAS operates normally through balancing of feedback loops (192).

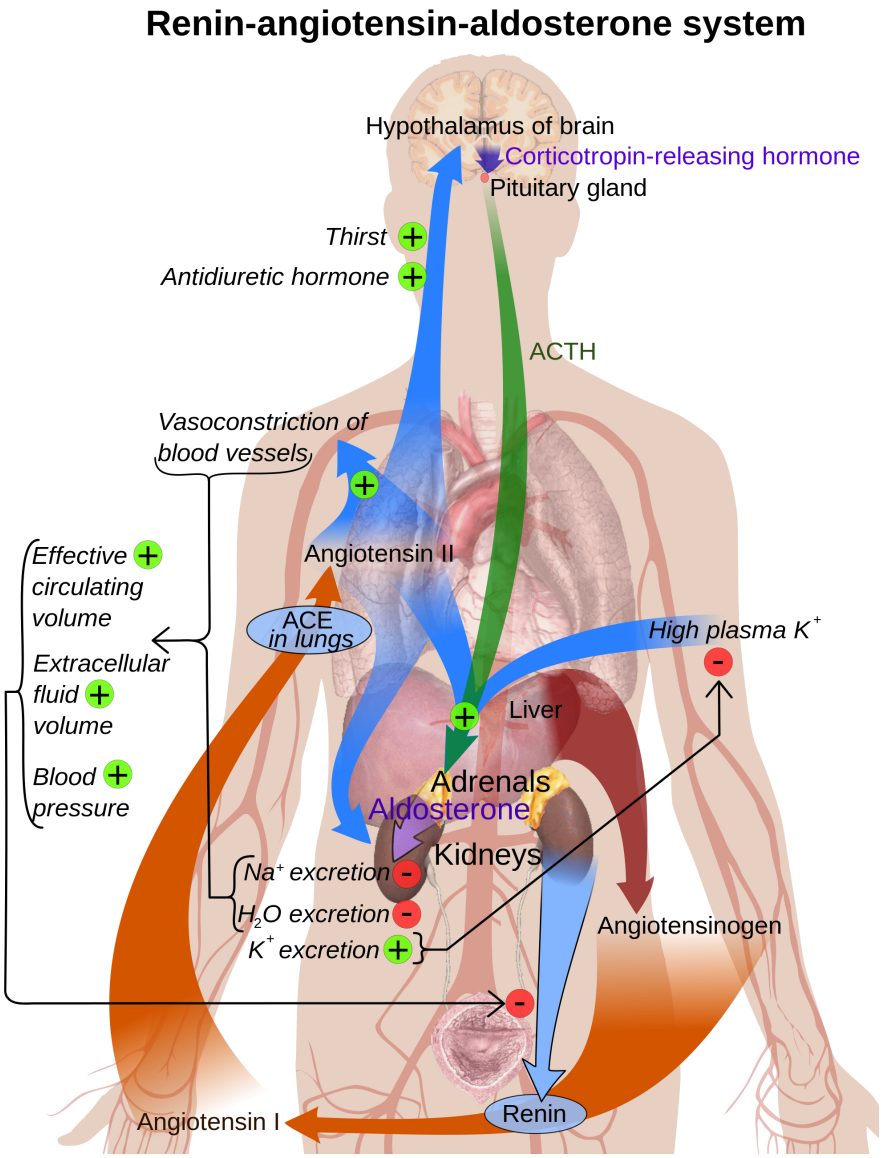

Figure 1.5: Renin Angiotensin System in Man - Adapted from page 866-867 (Integration of Salt and Water Balance) and 1059 (The Adrenal Gland) in (39) `http://en.wikipedia.org/wiki/File:Renin-angiotensin_system_in_man_shadow.svg`)

1.3.1 Angiotensinogen

Plasma angiotensinogen is synthesised predominantly in the liver (526) but to a lesser extent in the peripheral systems potentially moderating local RAS activation (56). Nonetheless, hepatic angiotensinogen is the major preliminary for renal ANG II production (313). Angiotensinogen synthesis is also regulated by various steroid hormones including corticosteroids (265).

1.3.2 Renin

Renin is predominantly synthesised in the juxtaglomerular cells of the kidney (164, 176). Other tissues expressing renin have been identified (164) which release only the inactive form, prorenin (278). In juxtaglomerular cells amino acid cleavage from the c-terminus in the endoplasmic reticulum produces prorenin, which on passing through the golgi apparatus, introduces glycosylation sites for tagging (106, 451). These tags can be identified for storage in granules to be later secreted. Renin is also secreted following synthesis in its inactive form constitutively from juxtaglomerular cells.

Most species studied have a single renin gene. Mice such as C57BL/6 have a single renin gene (Ren1c) whilst other strains such as 129 have two (Ren1d and Ren2) (342). Ren1 controls renin expression in the kidney, whilst Ren2 has relatively lower renal expression but also controls renin expression in the submandibular gland. Appearance of two renin genes is thought to have occurred by a gene duplication event (103). Mice with two renin genes have higher circulating renin activity, higher blood pressure and are salt sensitive compared with single renin gene controls (456, 522).

Increases in arterial pressure typically inhibit renal renin secretion whilst sympathetic innervations increase secretion following a decrease in blood pressure (160, 516). Changes in luminal fluid, sensed by the macula densa can also influence renin secretion levels (64). Specifically it has been shown that adenosine released by the macula densa, in response to a decrease in tubular sodium chloride concentrations, signals renin release from the juxtaglomerular cells (405, 447).

1.3.3 Angiotensin converting enzymes

Angiotensin converting enzyme (ACE) cleaves two c-terminal residues of ANG I to produce the active peptide ANG II (119, 396). ACE is predominantly highly expressed in the lungs (119). Lower expression levels are also found in other tissues including the kidney (119), at decreasing levels throughout the nephron (60) where it is implicated in the regulation of a local intrarenal RAS (see section 1.3.5).

ACE mediates vasoconstriction through ANG II production and reduces vasodilation directly by inactivation of bradykinin (277). Chymases can convert ANG I to ANG II (395) and several non-renin enzymes can produce ANG II directly from angiotensinogen (504).

The ACE homologue ACE2 is found in the testis, kidney and heart (104). ACE2 converts both ANG I to ANG 1-9, which might prevent cardiac hypertrophy (373). ACE2 protects the lungs from acute dysfunction and injury (208). ACE2 also converts ANG II to ANG 1-7 which exerts a tonic vasodilatory effect following binding to the Mas receptor (284, 435). In the kidney ANG 1-7 infusion can initiate natriuresis (182).

1.3.4 Angiotensin II

ANG II is the dominant vasoactive peptide in the RAS. Sodium reabsorption is regulated by the actions of ANG II in the proximal tubule, (75). The G-protein coupled angiotensin receptors AT(1-4)mediate the effects of ANG II with distinct roles (96, 493). The AT1 receptor is dominant in its regulation of physiological and pathophysiological blood pressure regulation (243). Two types of AT1 receptor exist in the rodent, AT1a and AT1b, having high homology with the human receptors (20, 53). AT1a receptors in the proximal tubule regulate blood pressure directly (169). AT2 receptors appear to regulate cell cycle progression (318, 346) and vasodilation through flow mediated kinin release (244). Furthermore, NHE3 is down regulated following ANG II infusion (169, 317). In transgenic *Cyp1a1-ren2.F* rats (see section 1.5) systemic activation of the mouse renin-2 gene results in activation of NCC (11). AT1 receptors in CCD stimulate ENaC (403), additionally to the effects of aldosterone (306).

Degradation of ANG II can also result in physiological effects. Cleavage of ANG II by aminopeptidases produce active peptides such as ANG III (2-8) which is the dominant regulator of vasopressin release by the brain (550)) and ANG IV (3-7), albeit with much reduced potency in comparison with ANG II (159). Cleavage of ANG II by endopeptidases produces ANG 1-7 which produces a tonic vasodilation as described in section 1.3.3. AT3 and AT4 receptors have been also identified with the AT4 receptor showing higher affinity for ANG IV than ANG II. Their function appears to mediate sensory and neuromotor regulation (65, 96, 540).

1.3.5 The intrarenal renin angiotensin system

Many tissue and cell populations communicate locally enabling local physiological regulation. This phenomenon is paracrine signalling and whilst distinct from systemic processes there is often significant endocrine/paracrine overlap. Paracrine

signalling mediates a number of autoregulatory feedback mechanisms in the kidney (198, 357, 358, 440, 447).

The RAS is regulated locally in a number of tissues including those of the cardiovascular system (395). In mice, brain RAS activation regulates systemic blood pressure (340) by a mechanism dependent on sympathetic stimulation and release of vasopressin (293, 475). In the kidney the local RAS regulates the pressure-natriuresis mechanism (356, 360).

Early renal functional studies in dogs indicated functionally important intrarenal regulation of ANG II (19, 259). Localisation of angiotensinogen mRNA to the proximal tubule subsequently provided integral evidence of local regulation (209). This is because angiotensinogen ($\sim$65 kDa) is not easily filtered by glomeruli (347). Urinary angiotensinogen concentration has been proposed as a non-invasive method for the of intrarenal RAS (271).

Counterintuitively, elevated circulating plasma ANG II levels cause a disproportionately higher inter-renal concentration of ANG II (270, 354, 355). Internalisation of ANG II into tubular endosomes by an AT1 receptor dependent mechanism might negate otherwise deleterious consequences of inappropriate activation of the RAS (351, 395).

1.4 The Renin Angiotensin System and Hypertension

As a dominant hormonal system the RAS sets the level of overall pressure-natriuresis. Inappropriate activation is a major factor of hypertension and thus drugs targeting the RAS are integral for hypertensive management (72, 221, 431, 537).

The Framingham study identified a blood pressure QTL, albeit with LOD$\geqslant$2, on chromosome 17 overlapping the ACE locus (286). Polymorphisms in AGT have been associated with hypertension in Japanese and European cohorts (186, 223). The cohorts for heart and ageing research in genomic epidemiology (CHARGE) consortium has confirmed the association between polymorphisms in AGT and hypertension in >80,000 individuals (228, 231). The M*bo*I of the renin gene associates with essential hypertension in Japanese (378), Caucasian (237) and Gulf Arab populations (5, 137). Furthermore renin gene insertion/deletion is associated with hypertension in the Mongolian population (547). An insertion/deletion polymorphism in the ACE gene has been associated with hypertension in a Tunisian cohort (319). Gene-gene interactions are also important: epistasis has been described between pairs of AGT, ACE and AT1 polymorphisms associated with coronary artery disease (498).

1.5 The *Cyp1a1-Ren2* Transgenic Rat

Animal models can provided tractable genetic and physiological dissection of the mechanisms leading to renal injury in hypertension (301). In the study of inappropriately activated RAS, the mouse *Ren2* gene was introduced into the rat genome on the Sprague Dawley background. Presence of this additional gene results in severe hypertension by two months of age (344). Furthermore the highest blood pressure was observed in homozygotes confirming that the absolute magnitude of synthesised renin set the blood pressure (282). Expression of *Ren2* is highest in the adrenal gland, lowest in the kidneys and lungs and overall circulating renin levels are much reduced (117, 282). High adrenal transgene activity might suggest that hypertension in this model is adrenal-dependent (402, 494) but sprionolactone failed to lowering blood pressure (11, 434).

The spontaneous development of hypertension was controlled through fusion of *Ren2* to *Cyp1a1*. Since *Cyp1a1* is not constitutively expressed, and can be reversibly induced by dietary administration of various aryl hydrocarbons such as indole-3-carbinol (I3C), this transgenic rat can provide accurate temporal control over hypertension (240). Mechanistically, I3C actually binds the aryl hydrocarbon receptor which can then bind DNA elements in the *Cyp1a1* promoter and initiate expression (222, 400).

The rise in blood pressure in *Cyp1a1-Ren2* can be titrated to study the organ injury associated with slowly developing (78) or malignant hypertension (240). In the malignant setting (Fig.1.6), vascular injury predominates, with myocycte vacuolation preceding confluent myocyte cell death and microalbuminuria (11). The critical receptor for hypertension appears to be the AT1 receptor since blockade prevents malignancy (11, 331, 332). Renal injury can be attenuated with spironolactone (11, 383). Following induction RBF is initially preserved, but increased vascular resistance coincides with the onset of microalbuminuria,(11), which is indicative of impaired autoregulation and glomerular barotrauma.

Quantitative trait loci (QTL) for cardiovascular mortality have been identified on chromosomes 10 and 17 (241). The chromosome 10 QTL was subsequently captured in reciprocal congenic lines and expression of the ACE gene was found by microarray in a QTL-dependent manner (296). Furthermore histological and functional studies validated ACE as a key modifier of hypertensive organ injury (296). Genetic background also plays a role in hypertension, renal injury and malignancy in the *Cyp1a1-Ren2* transgenic rat identified using strains susceptible (F334 (77)) or relatively resistant (Lewis (26)). Specifically the Lewis background confers some renoprotection whereas the F344 strain is susceptible (240, 296).

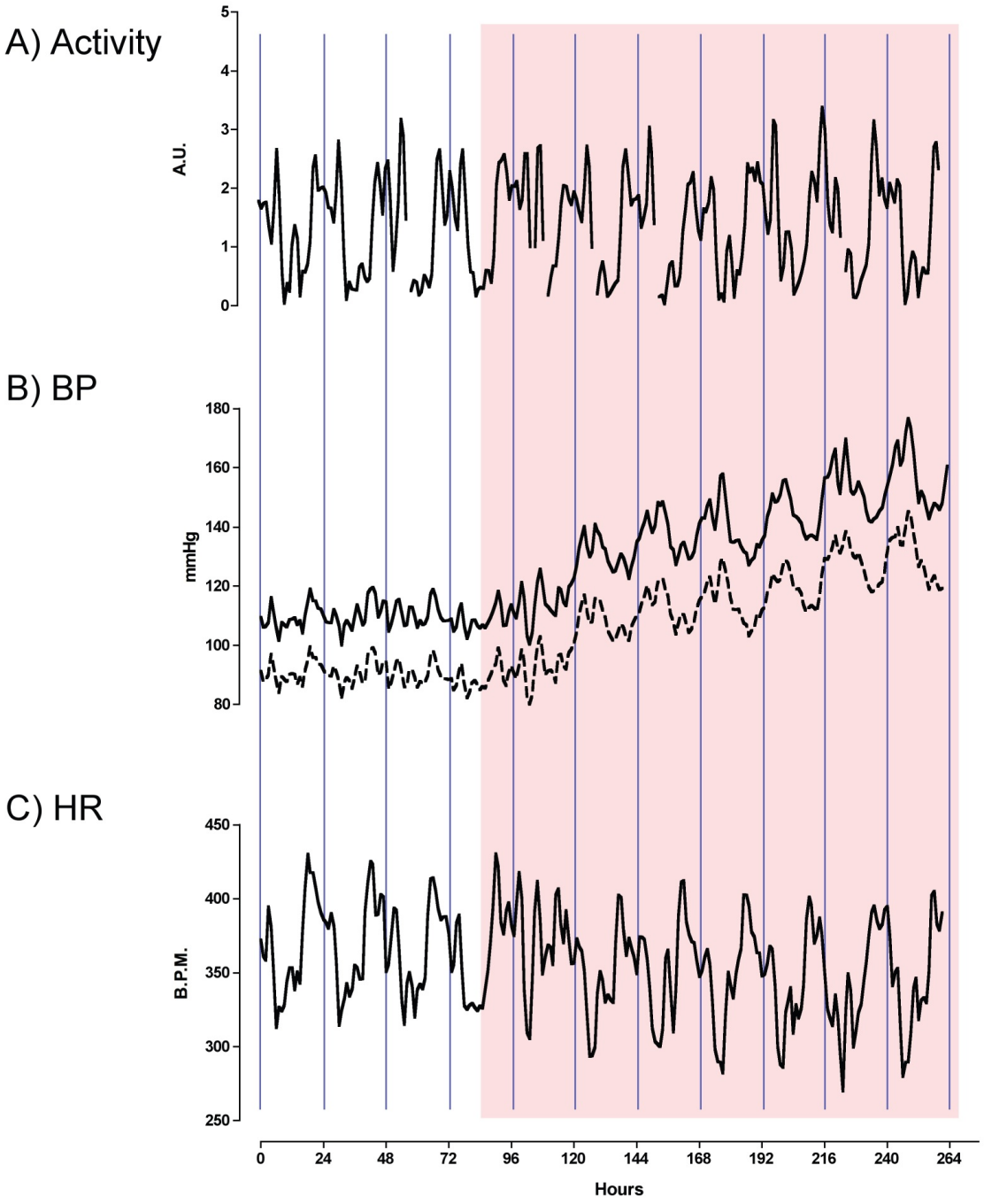

Figure 1.6: Hypertension in the *Cyp1a1-Ren2*.F Transgenic Rat - Telemetric recordings prior to, and during, I3C administration (shaded area) in the *Cyp1a1-Ren2*.F rat. A) locomotor activity; B) Blood pressure; SBP (solid line); DBP (broken line) and C) heart rate (HR). This figure is reproduced from (11) a reprint of this paper is included in Appendix B, section 8.2.

1.6 Hypothesis & Aims

1.6.1 Hypothesis:

Genes differentially expressed in the *Cyp1a1-Ren2* transgenic rat in the normotensive state contain candidates contributing to poor renal function and susceptibility to renal injury in the F344 strain or the relative renoprotection observed on the Lewis background.

1.6.2 Aims

- Identify candidate modifier genes of renal injury using informative inbred susceptible (F344) and protected (Lewis) strains. This aim will be achieved by re-examination of an exon microarray previously published by the Molecular Physiology lab (296)
- Prioritize candidate gene(s) in the normotensive kidney using stratified bioinformatic enrichment analysis
- Determine the renal functional consequence of candidate gene(s) activation in the progression of renal injury in hypertension

1.6.3 Summary of outcome:

Using these approaches two purinergic receptors P2X7 and P2X4 were identified and validated as candidate genes for renal injury susceptibility Gene and protein expression of these P2X receptors were both higher in F344 compared with Lewis. Immunohistochemistry localised P2X7 and P2X4 to the renal vascular endothelium and tubules: preglomerular expression was similar in both strains but became distinct in the renal medulla. Vascular P2X4 receptor function has recently been described (545) whilst little is known about vascular P2X7 receptors.

Renal functional studies examined P2X7 and P2X4 function *in vivo* indicating that F344 showed a significant drop in blood pressure but maintained renal blood flow, indicative of tonic renal vasoconstriction. The Lewis strain did not responded to BBG. When ANG II was infused into F344 rats, there was a modest increase in blood pressure and an impairment of the pressure-natriuresis mechanism but no overt injury. Renal blood oxygenation-level dependent MRI identified a decrease in renal R2* signal following P2X7 and P2X4 antagonism in ANG II infused F344 rats. These results suggest that P2X7/4 receptor activation exerts tonic constriction reducing renal perfusion/oxygenation and therefore pressure-natriuresis. These effects are pro-fibrotic and may underpin susceptibility to renal injury in the earliest, and most poorly understood, stages of kidney disease progression.

2
IDENTIFYING GENETIC MODIFIERS OF RENAL INJURY

2.1 Introduction

Genetic background influences susceptibility to renal injury in the *Cyp1a1-Ren2* transgenic rat (240). The F344 genetic background is susceptible, whilst transgene activation on the Lewis background bestows some protection from renal injury (296). These informative strains have been used to identify QTL for organ injury, (241), and the development of reciprocal congenic lines validated the gene *Ace* as a plausible modifier of renal injury (296). The AT1 receptor antagonist losartan prevents the blood pressure rise on the F344 background but is only partially protective against renal vascular injury (11). This suggests that susceptibility to renal injury in this model is governed by the interplay between multiple pathways. In the present study genome wide expression analysis is used to identify candidate genes and pathways with a focus on normotension.

2.2 Methods

2.2.1 Renal microarray analysis

A previously published Affymetrix microarray (296) was re-mined[1] to identify differentially expressed probe-sets in the kidney of normotensive *Cyp1a1-Ren2* transgenic rats, i.e. rats in which the *Ren2* transgene was silent. The array was performed on four groups of rats (n=4 per group): the two consomic parental strains (F344, Lewis) and the two reciprocal congenic strains (F344-MOD-Lewis, Lewis-MOD-F344) containing a 14Mb region of chromosome 10. This congenic region contained the *Ace* locus and the congenics were included in the present analysis to determine whether cis (or trans) regulation occurred. The 16 CEL intensity files were imported into Bioconductor and arrays normalized by the robust multi-array average (RMA) method. Microarray analysis was performed in collaboration with Jon Manning (CVS Bioinformatics).

[1]Explicitly no new tissue was used in this microarray study

2.2.2 Enrichment analysis

Differentially expressed genes were imported into the web client online version of the multi-database enrichment tool Endeavour (3, 4). The following passage is reproduced from the Endeavour website:

"...identification of key genes involved in health and disease remains a formidable challenge. We develop novel bioinformatics to prioritize candidate genes underlying biological processes or diseases. Currently, our prioritization strategies are based on how similar a candidate gene is to a profile derived from genes already known to be involved in the processes. Data from multiple heterogeneous sources (coding sequence, gene expression, annotation, literature, regulatory information, etc.) are integrated, or fused, into a global ranking of the candidates. Endeavour is a software application for the computational prioritization of candidates genes, based on a set of training genes. It is made up of three stages: training, scoring and fusion. In the first stage, information about the training genes (genes already known to play a role in the process under study) are retrieved from numerous data sources in order to build models. It includes functional annotations, protein-protein interactions, regulatory information, expression data, sequence based data and literature mining data. In the second stage, the models are then used to score the candidate genes and to rank them according to their scores. Lastly, the rankings per data source are fused into a global ranking using order statistics..."

In the present study a list of 157 'training' genes isolated from the rat genome database (280) were selected for their association with blood pressure regulation in the rat and imported into the Endeavour tool. These genes were not tissue specific and assumed no mutual exclusivity with inflammatory, or other disease, processes. The Endeavour method then employed multiple database mining using parallel approaches to enrich the list of differentially regulated genes. These approaches were: i) published literature text mining; ii) protein-protein interactions in the STRING database; iii) transcriptome analysis from the WalkerEtAl database; iv) sequence comparison with BLAST; and v) annotations within Gene Ontology, InterPro, KEGG and Swiss-Prot. Finally, global ranking by Q-statistic generated a list of genes in order of prioritization for the observed phenotype. This approach is known as 'genomic data fusion' (3).

2.2.3 Protein quantification

Kidneys were freshly harvested[1] and snap frozen on dry ice followed by storage at -80C. Whole kidneys were homogenized in ice-cold buffer containing 250mmol/l sucrose and 10mmol/l triethanolamine. Protease inhibitors (Cocktail set III, Calbiochem) and phosphatase/kinase inhibitors (2mmol/l ethylenediaminetetraacetic acid (EDTA), 50mmol/l sodium fluoride (NaF), 25mmol/l sodium glycerophosphate, 5mmol/l pyrophosphate and 1mmol/l sodium orthovanadate) were added and the pH adjusted to 7.6. Following quantification by Bradford assay, protein samples were added to Laemlli buffer and resolved by SDS-PAGE, on a NuPAGE®Tris-Acetate gel (8% Novex®) using a Tris-acetate running buffer (50mmol/l tricine, 50mmol/l Tris base, 0.1% SDS, pH 8.24) NuPAGE®antioxidant was added to the upper chamber. For the P2X4 receptor, 12μg of total protein was loaded; 20μg for P2X7 receptor experiments. Following semi-dry transfer the membrane was incubated overnight at 4C with the primary antibody P2X4 1:2000 (APR-002, Alomone Labs) and P2X7 1:1000 (APR-004, Alomone Labs). A goat-antirabbit horseradish peroxidase (HRP) secondary antibody was then added and the bands visualized by enhanced chemiluminescence (ECL). The autoradiogram was scanned and band intensity (corrected for background) was quantified by densitometry using ImageJ. Values were normalized to the total protein intensity (Coomassie-Blue) at the appropriate molecular weight.

2.2.4 Statistical analysis

Data are presented as mean ± standard error of the mean (SEM). Statistical analysis was performed by the linear models for microarray data (LIMMA) to calculate fold-change and *p-value* statistics from normalized intensities (for microarray analysis) or Mann-Whitney U-test (for Western analysis).

2.3 Results

2.3.1 Differential gene expression

After normalization, 67 probe-sets were differentially regulated on the basis of genetic background: 23 over-expressed and 44 under-expressed (Table 2.1). The congenic strains (F344-MOD-Lewis, Lewis-MOD-F344) had no effect on expression profile in the present setting where transgene activation is not expected: all expression differences were explained by genetic background.

[1]Explicitly the kidneys harvested for protein quantification were not from the same rats as those used in the previously published microarray. These were a new group of animals

(+)			(−)				
Symbol	Chr.	Fold	*p-value*	Symbol	Chr.	Fold	*p-value*
Rpl30	7	7.6798	0.0226	Olr1668	20	-27.2451	0.0123
Akr1c2	17	7.3466	0.0241	Olr1680	20	-24.6268	0.0162
Spta1	13	5.6906	0.009	RGD1309362	18	-13.1217	0.0162
Akr1b8	4	4.6613	0.0178	Pigzl1	11	-6.7012	0.007
LOC361914	2	3.6785	0.0094	Kif5c	3	-6.6248	0.009
Ace	10	3.54	0.0178	Ces1e	19	-5.7903	0.0094
LOC100359585	8	3.386	0.025	Cyp4v3	16	-5.2337	0.0166
Guca2b	5	2.7994	0.0479	Olr1326	8	-5.1722	0.0336
Ypel4	3	2.7596	0.0253	Acsm5	1	-4.7035	0.0178
Rtp4	11	2.6916	0.0241	Hhip	19	-4.6118	0.0166
Clstn2	8	2.5879	0.0253	Hmgcs2	2	-4.2039	0.0336
P2rx4	12	2.5327	0.0162	Cyp2d5	7	-3.8624	0.0289
Klkb1	16	2.4303	0.009	Rdh2	7	-3.4214	0.0162
Exnef	1	2.4073	0.009	LOC302192	9	-3.3622	0.0256
Pigr	13	2.3473	0.0336	Lcn2	3	-3.097	0.0253
P2rx7	12	2.1586	0.0336	Csmd1	16	-3.019	0.0336
Akr1b7	4	2.1071	0.0336	Slc10a2	16	-2.7769	0.0226
Cd59	3	1.854	0.0256	Rxrg	13	-2.6987	0.0336
Fam149a	16	1.7008	0.0336	Cntnap4	19	-2.6686	0.0192
P4ha2	10	1.6668	0.0336	RT1-CE5	20	-2.6679	0.0336
Arl4d	10	1.5187	0.0336	Erc2	16	-2.5297	0.0253
Igfbp4	10	1.4873	0.0336	Ptprq	7	-2.4522	0.0182
Col15a1	5	1.2734	0.0336	RGD1311723	8	-2.4244	0.0372
				Rbp4	1	-2.3816	0.0336
				Abcb10	19	-2.2669	0.0256
				Sult1b1	14	-2.2336	0.0493
				RGD1563120	3	-2.1689	0.045
				Mis18a	11	-2.1532	0.0192
				Slc35f1	20	-2.1291	0.0372
				Tcerg1l	1	-2.0443	0.0253
				Acadsb	1	-1.9181	0.0336
				Rgs7	13	-1.8925	0.0277
				Retsat	4	-1.8721	0.0253
				Gas2	1	-1.8114	0.045
				Ly75	3	-1.74	0.0442
				Slco1a6	4	-1.7194	0.031
				Slc26a11	10	-1.6736	0.0317
				Pfas	10	-1.6633	0.0178

Eps8l2	1	-1.6505	0.0336
Dpp6	4	-1.6382	0.0259
RGD1311575	14	-1.5914	0.0491
RGD1564614	13	-1.5199	0.0344
Cdc42ep2	1	-1.4477	0.0372
Synm	1	-1.4011	0.0442

Table 2.1: Genome wide comparison of gene expression between F344 and Lewis inbred strains listed in order of magnitude of fold change (F344 vs. Lewis, fold $>\pm 1.2$, $p<0.05$).Chr: Chromosome

Ace which was identified previously as a key modifier of renal injury (296) featured as the sixth most highly expressed gene (fold = +3.54, $p<0.05$). This serves to exemplify the notion that that neither fold change or $p-value$ alone capture the collective knowledge of microarray data. Unbiased microarray enrichment methods can illuminate important features within the 67 differentially regulated probe-sets using the collective knowledge of many databases.

2.3.2 Enrichment analysis

Instead of a labour intensive search for functionally important gene(s) in this dataset the Endeavour analysis, as described in the methods section, was used to rank the differentially expressed genes enriched against the training genes of blood pressure regulation. The result for the ten highest globally ranked genes are given in Table 2.2.

Ace was the highest ranked gene, consistent with our previous QTL and congenic studies (296), and was not studied further. The second and third ranked genes were purinergic receptors *P2rx7* and *P2rx4*, respectively. The expression of both was higher in the F344 rats than in the Lewis rats.

Gene	Known Biological Function(s)	Rank	Score	Ratio
Ace (ENSRNOG00000007467)	BP regulation	1	0.019	0.091
P2xr7 (ENSRNOG00000001296)	Ion transport, cell volume, apoptosis	2	0.062	0.182
P2xr4 (ENSRNOG00000001300)	Ion transport, BP regulation, NOS	3	0.118	0.273
Rgs7 (ENSRNOG00000021984)	G-protein signalling	4	0.583	0.364
Erc2 (ENSRNOG00000015148)	Nerve terminal assembly	5	0.674	0.455
Klkb1 (ENSRNOG00000014118)	Proteolysis, coagulation, inflammation	6	0.787	0.545
Kif5c (ENSRNOG00000004680)	Motor axon guidance	7	0.796	0.636
Dpp6 (ENSRNOG00000030547)	Proteolysis	8	0.933	0.727
Pigr (ENSRNOG00000004405)	Antibody receptor	9	0.936	0.818
Rdh2 (ENSRNOG00000029651)	Retinoid metabolism, oxidation reduction	10	0.988	0.909

Table 2.2: Microarray Enrichment analysis. Genes are ranked according to the Q-statistic value (score) derived from multiple-database enrichment

2.3.3 Protein quantification

The P2X4 antibody detect a band of ∼60kDa; the P2X7 antibody detect a band at ∼75kDa. For P2X7 faint bands at ∼165kDa (which appears most distinct in mitochondria/nuclei subfractions when the ∼75kDa is less distinct and therefore might relate to receptor localisation or trafficking (194)) and ∼55kDa (which represent a protease cleavage artefact (515, 533)) were also detected (not shown). No other bands were detected.

The expression pattern of *P2x7* and *P2x4* was confirmed by Western analysis: there was a 7-fold increase in total P2X7 receptor protein ($P<0.05$; Fig2.1A) and a 3-fold increase in P2X4 receptor abundance ($P<0.05$; Fig.2.1B).

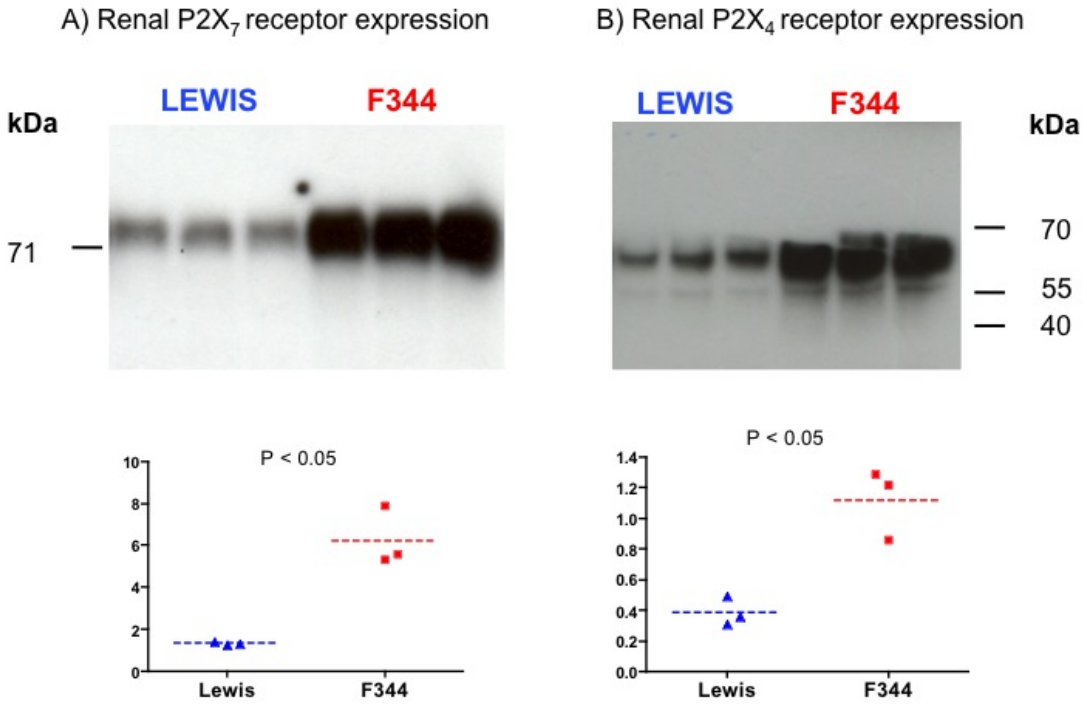

Figure 2.1: P2X7 and P2X4 Receptor Expression in Whole Kidney Homogenates - Western analysis of P2X7 (A) and P2X4 (B) protein abundance. Dashes show mean values but individual animals are also shown for Lewis (triangles) and F344 (squares). Statistical comparisons were made using the Mann-Whitney U test

2.4 Discussion

The method of enrichment analysis presented in this chapter directed focus towards the P2X7 and P2X4 receptors. P2X7 and P2X4 receptor abundance is higher in F344 rats , both in the microarray analysis and at the protein level. Adenosine nucleosides and nucleuotides have been identified as important extracellular messengers (47, 50, 380, 413). In the kidney adenosine and ATP mediate renin secretion as well as vascular and tubular function (15, 211, 218, 358, 447, 507) and their function as autocrine/paracrine signalling networks is supported by the rapid hydrolysis of ATP culminating in a mean plasma half-life <1 sec (341). Purinergic receptors are divided into P1 and P2 families, (371). Most purinergic receptors have been identified in the kidney (16, 66, 501, 503, 513). P1 receptors are further divided into the G_o/G_i protein coupled A1 and A3 subtypes (6, 391) and the G_s protein coupled A2A and A2B subtypes (379, 406). The P2 receptor family are widely expressed, (52), consisting of eight metabotrophic P2Y(1,2,4,6,11,12,13,14) receptors (1, 51) and consisting of seven ioinotropic P2XR(1-7) receptors (371). P2X7 receptors are predominantly associated with inflammatory processes (116) and are most highly expressed on macrophages (533). Loss of endothelial P2X4 receptors has been associated with vascular dysfunction (543). However the P2X1 receptors are the best described functionally in the kidney, regulating microvascular tone (216) and potentially TGF (see section 1.2.1).

Comparison of two distinct inbred rat strains without congenic refinement is arguably one major limitation of this study. Equally, the result that the region of chromosome 12 encoding P2X7 and P2X4 is functionally interesting now provides an avenue for such refined breeding strategies. The microarray presented in this study has been extensively validated by previously (295). Nonetheless a second limitation of the present study was a re-analysis of raw intensity files comparing strains only and most of the differential expression presented was not verified by qRT-PCR, particularly validation was limited to protein abundance of P2X7 and P2X4.

Enrichment analysis found several other potentially relevant genes for renal paracrine signalling. The 4th hit was the regulator of G-protein signalling 7 (*Rgs7*) which interacts with polycystin-1 to promote polycystic kidney disease (PKD) (257). Furthermore P2Y receptors are G-protein coupled and reduced P2X7 expression reduces cyst formation in PKD (67, 197). The 6th hit was the plasma kalikrein (*Klkb1*) involved in inflammation and more highly expressed in F344 rats (336). However these enriched genes scored lower than *P2xr7* and *P2xr4*.

High throughput identification for coding sequences responsible for broad phenotypic differences each have caveats. Ribonucleic acid (RNA) sequencing can be used to identify causative microRNAs and SNPs but statistical methods for quan-

tifying differential expression in both short and long coding sequences is not yet standardised (386, 470). Conversely the Affymetrix microarray used in the present study provides a reliable tool for identifying genome-wide differential expression in protein encoding genes. Thus identifying *P2xr7* and *P2xr4* as pertaining to injury susceptibility must be interpreted as a result based on protein coding regions. Localisation of these receptors within the kidney and the functional consequence of their activation remains to be determined. This is the subject of chapter 3.

Data presented in this chapter have been published (323). A reprint of this paper is included in Appendix B, section 8.2.

3

LOCALISATION AND FUNCTION OF RENAL P2X7 AND P2X4 RECEPTORS

3.1 Introduction

Multiple subtypes of P2X and P2Y receptors are expressed throughout the kidney and extracellular nucleotides regulate renal tubular, endocrine and vascular functions (17, 18, 459). Infusion of ATP into the renal artery increases blood flow (483) and vasodilatation is dependent on production of nitric oxide/prostacyclin by the endothelium (115). Conversely ATP applied *in vitro* to the adventitial surface of the renal microvasculature causes contraction (214) mediated by P2X1 receptors (216) in the vascular smooth muscle (66). In the previous chapter renal microarray did not detect P2X1 expression in either rat strain. However P2X1 is the most extensively described vascular P2X receptor (166, 211, 215) hence immunolocalisation of P2X1 was therefore performed for comparison with P2X4 and P2X7 immunolocalisations. Downstream in all nephron segments studied, luminal increases in ATP activate epithelial P2X receptors in an autocrine/paracrine manner to regulate local homeostatic processes (459).

The previous Chapter identified P2X7 and P2X4 as candidate genes for renal injury in the F344 strain. The experiments presented in the present chapter describe the renal immunolocalisation of these receptors and their functional consequence in renal homeostasis measured by pressure-diuresis.

3.2 Methods

3.2.1 Renal immunolocalisation

Kidneys were freshly harvested and immersion fixed in formalin. After 48 hours kidneys were transferred to 70% ethanol for longer term storage.

Immunohistology was performed by the Shared University Research Facilities (SuRF) paid service. Primary rabbit polyclonal antibodies against the P2X1 (APR-001, Alomone Labs) as well as P2X4 and P2X7 (as described in chapter 2 section 2.2.3) receptors were selected based on supplier reported validation for

use in the rat by immunohistochemistry (Alomone website). Each antibody was optimised in a dilution series (1: 250, 500, 1000, 2000, 4000, 5000 & 7500) using control rat kidney, following heat-induced epitope recovery (HIER) with citrate buffer. The final titers were selected to give minimal background : P2X1 (1: 5000), P2X4 (1: 7500) and P2X7 (1: 2000). All staining was performed on a Leica Bond X immunostaining robot using a refined HRP polymer detection system. Following HIER and blocking in peroxidase, the section was incubated in primary antibody for 2 hours at room temperature. Following two 5 min washes, sections were exposed to anti-rabbit HRP polymer before being washed. Immunopositive staining was visualized with 3,3′-Diaminobenzidine (DAB; Sigma, UK) and counterstaining with haematoxylin.

3.2.2 Renal functional studies

Rats were anaesthetised (Thiobutabarbital 120 mg/kg IP) and prepared surgically for measurement of the pressure-diuresis relationship. The right jugular vein was cannulated and 0.9% NaCl was infused at a rate of 50μl/min/100g during abdominal surgery (to minimize surgical losses) and then at 33μl/min/100g during the post-surgical equilibration (60 minutes) and throughout the experimental protocol. The left femoral artery was cannulated and connected to brass transducer (MLT844; Capto) connected to a Powerlab (AD Instruments, UK). Blood pressure was recorded continuously at 1kHz. A midline laparotomy was performed and a Doppler transit time probe (MA1PRB; Transonic, USA) placed around the left renal artery. Acoustic gel was used to ensure good sonic coupling. Loose silk ties were placed around the superior mesenteric and coeliac arteries: these ligatures were tightened during the experimental procedure to create an acute pressure ramp of two stages above baseline blood pressure. The bladder was catheterised for urine collection under mineral oil with flow rate being determined gravimetrically. The entire procedure was performed under homeostatic temperature control at 37^{o}C. A typical surgical preparation, with complete isolation of the kidney from perirenal adipose is given in Fig.3.1A. Stability of the preparation and step-wise increases in blood pressure following sequential ligation is also shown (Fig.3.1B).

Pressure-diuresis experiments were performed first on a control group of F344 (n=7) and Lewis (n=5) rats and then on a second cohort of F344 (n=5) and Lewis (n=6) rats receiving an IV infusion (50μg/min/100g) of Brilliant Blue G (BBG, Sigma, UK).

3.2.3 Statistical analysis

Data are presented as mean ± standard error of the mean (SEM). Statistical analysis was performed by unpaired t-test unless otherwise stated. Comparisons

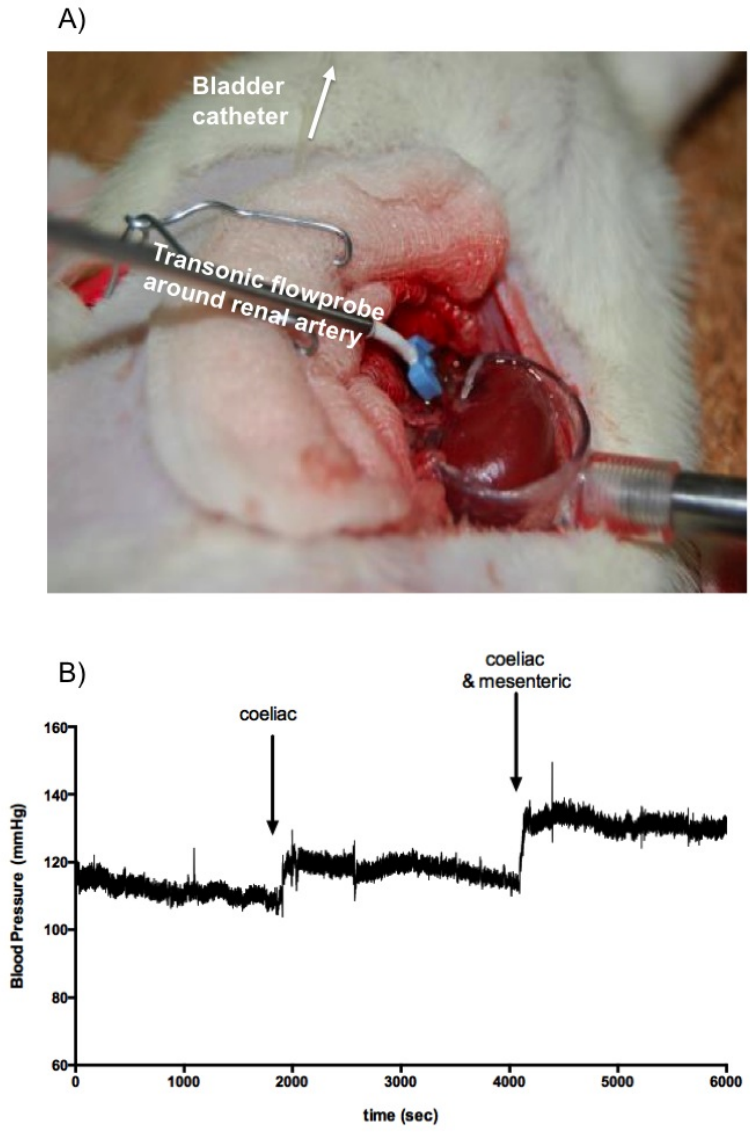

Figure 3.1: Exemplar Surgical Preparation - A) Surgical setup demonstrating isolation of the left kidney from perirenal fat (held in position by a stereotactic perspex cup), measurement of renal blood flow by Transonic flow probe placed around the renal artery and urine collection by bladder catheterisation .B) Typical blood pressure trace over a ∼1.7 hour period is given. Sequential blood pressure increases following ligation of respective arterial beds are indicated.

between groups of the pressure-diuresis relationship were made by linear regression.

3.3 Results

3.3.1 Renal immunolocalisation of P2X7, P2X4 & P2X1

P2X7 localised to the endothelium of the entire preglomerular vasculature (Fig.3.2A-F). Endothelial staining was qualitatively lower in the large to medium arteries of Lewis (Fig.3.2A,C). compared to F344 (Fig.3.2B,D). P2X7 positive staining was also seen in F344 glomeruli (Fig.3.2F) but rarely in vascular myocytes.

Vascular P2X4 immuno-positive endothelial staining was found in the preglomerular vasculature (Fig.3.3A-F). P2X4 receptor staining was also observed in the renal tubules, particular in the F344 strain (Fig.3.3D). In some places this staining was punctate and localized to both the nucleus and cytoplasm (Fig.3.3F). No P2X4 staining was seen in the renal glomerulus (Fig.3.3E,F)

P2X1 receptor expression was limited to the vascular network and not expressed in the renal tubules (Fig.3.4A-F). P2X1 receptor immunopositive staining was observed in the smooth muscle layer of all artery types from lobar to afferent arteriole in both rat strains. P2X1 positive staining appeared qualitatively lower in the F344 strain, particularly in interlobar arteries (Fig.3.4D) and afferent arterioles (Fig.3.4F.)

Postglomerular staining was found in the renal medulla and was architecturally distinct (Fig.3.5). No medullary P2X1 expression was observed. P2X7 expression was found in the renal outer-medullary vasa recta of F344 (Fig.3.5B). P2X4 expression localised to the collecting ducts in F344 (Fig.3.5D). In the Lewis strain P2X7 and P2X4 medullary staining was typically indistinguishable from background (Fig.3.5A and C).

3.3.2 Renal function

3.3.2.1 F344 and Lewis Strains

Compared to Lewis rats, F344 rats had a higher baseline blood pressure (Figure 3.6A) and a lower renal blood flow (Figure 3.6B): renal vascular resistance was significantly higher in F344 rats than in Lewis (31.2±6.1 versus 11.2±2.2 mmHg/ml.min^{-1}; $P<0.05$).

The imposition of a pressure ramp evoked an increase in urine flow rate in both strains of rats (Fig. 3.7A). The slope of the relationship was significantly different from zero in both groups ($P<0.001$) and the gradient was significantly blunted in the F344 strain compared to the Lewis ($P<0.01$). There was no significant

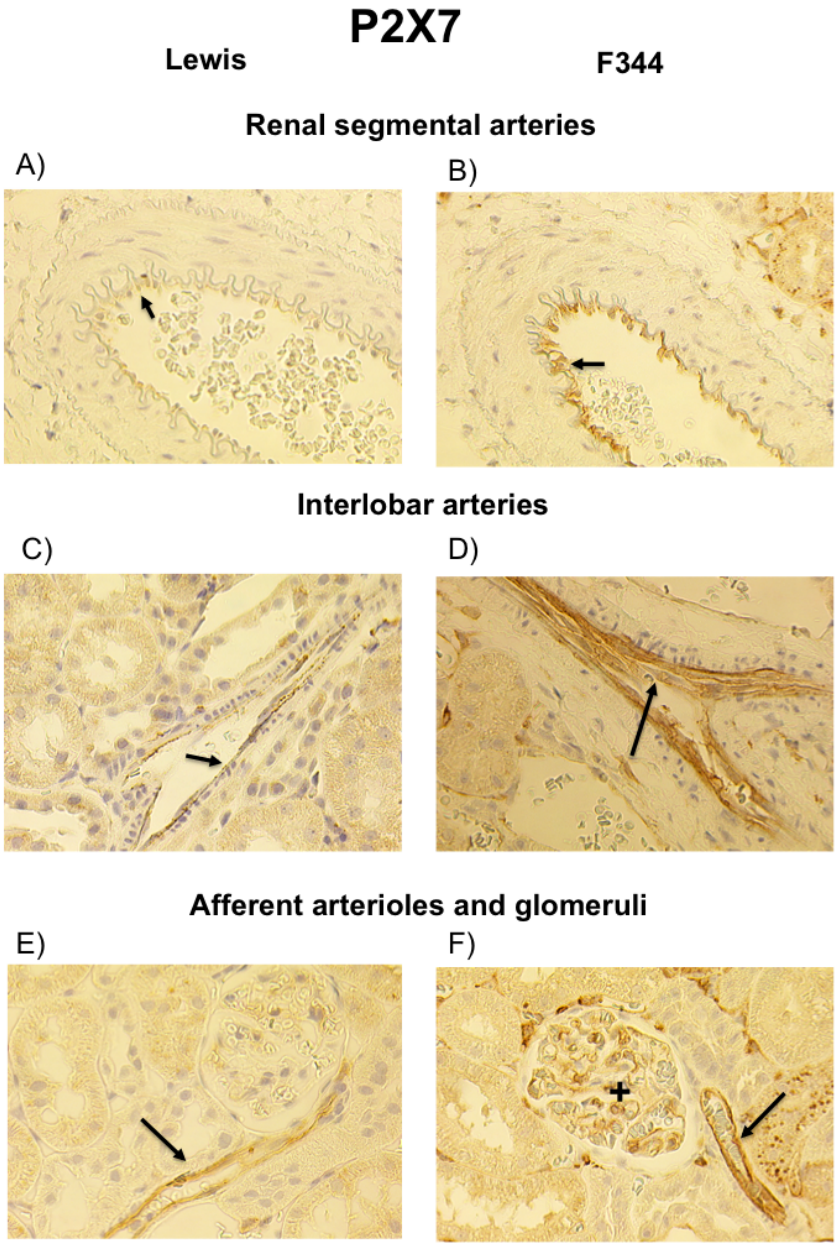

Figure 3.2: Renal P2X7 Localisation - Exemplar images of P2X7 positive staining in large (A, B), intermediate (C, D) and small (E, F) renal arteries. Arrows indicate endothelial staining. Glomerular staining indicated by (+). Images were taken at 400x magnification.

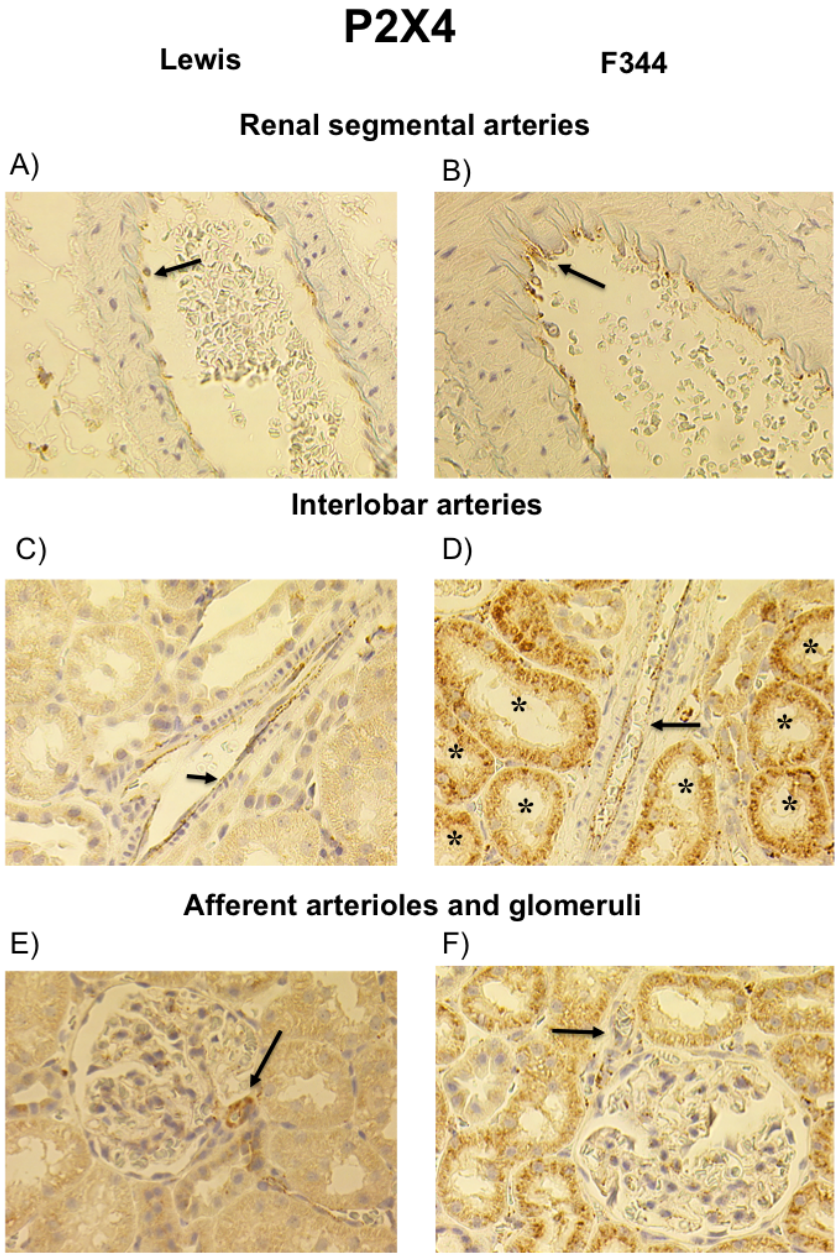

Figure 3.3: Renal P2X4 Localisation - Exemplar images of P2X4 positive staining in large (A, B), intermediate (C, D) and small (E, F) renal arteries. Arrows indicate endothelial staining. Tubule staining indicated by (∗). Images were taken at 400x magnification.

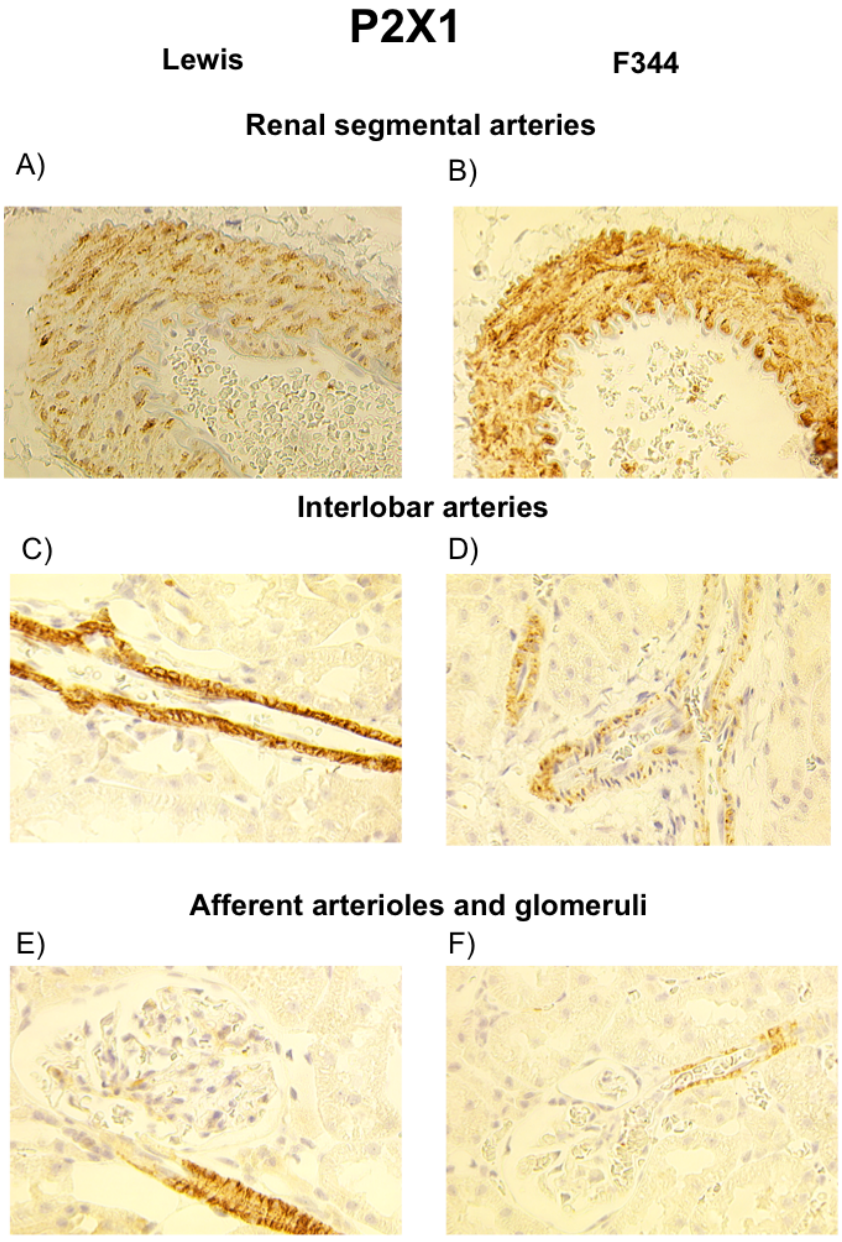

Figure 3.4: Renal P2X1 Localisation - Exemplar images of P2X1 positive staining in large (A, B), intermediate (C, D) and small (E, F) renal arteries. Images were taken at 400x magnification.

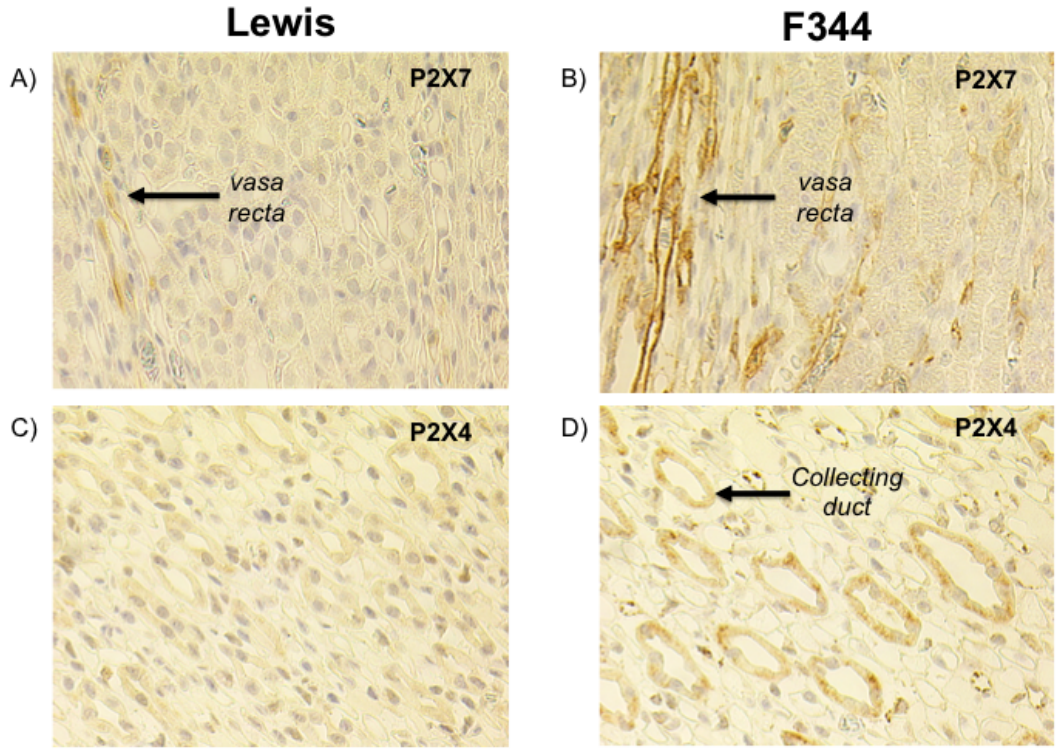

Figure 3.5: Renal Medullary P2X Localisation - P2X7 receptor expression in the renal outermedullary vasa recta in Lewis (A) and F344 (B). Vasa recta staining was almost below detection in Lewis. P2X4 collecting duct expression was comparable to background in Lewis (C) but distinct in F344(D). Images were taken at 400x magnification.

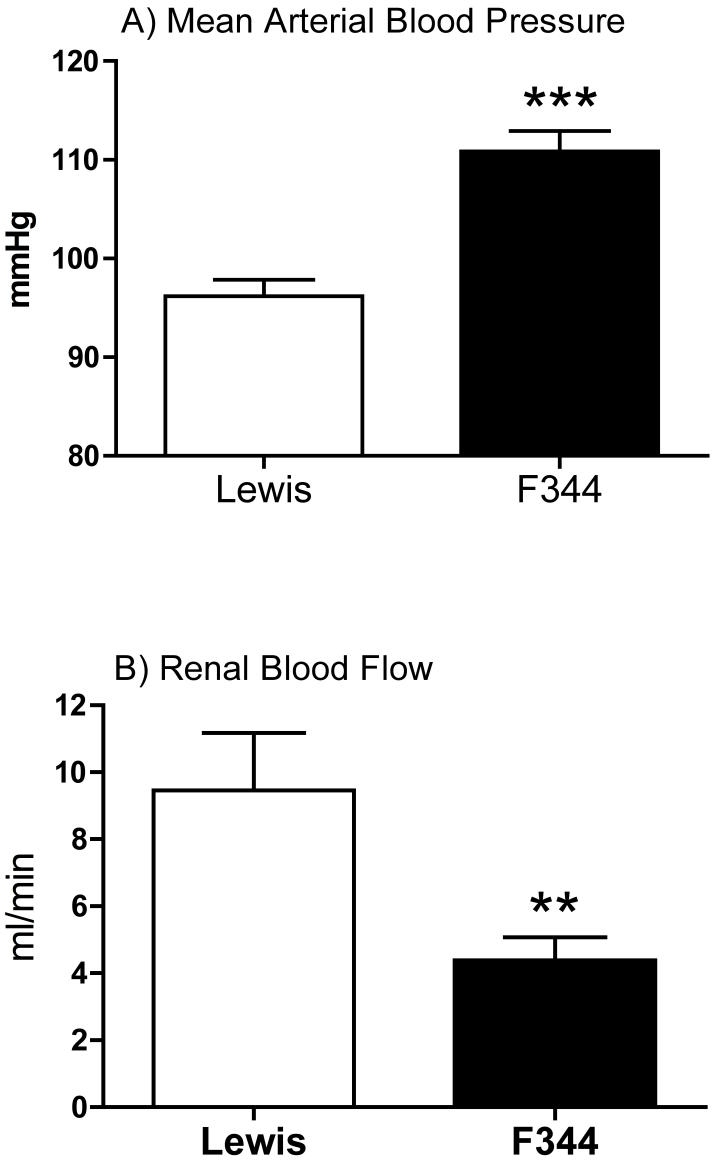

Figure 3.6: Blood Pressure and Renal Haemodynamics in F344 and Lewis strains - A) Mean arterial blood pressure; (B) left renal artery blood flow in Lewis (n = 8; open bars) and F344 (n = 7; black bars) rats. Data are mean ± SEM. Statistical comparisons were made with unpaired t-test. ***P<0.001; **P<0.01.

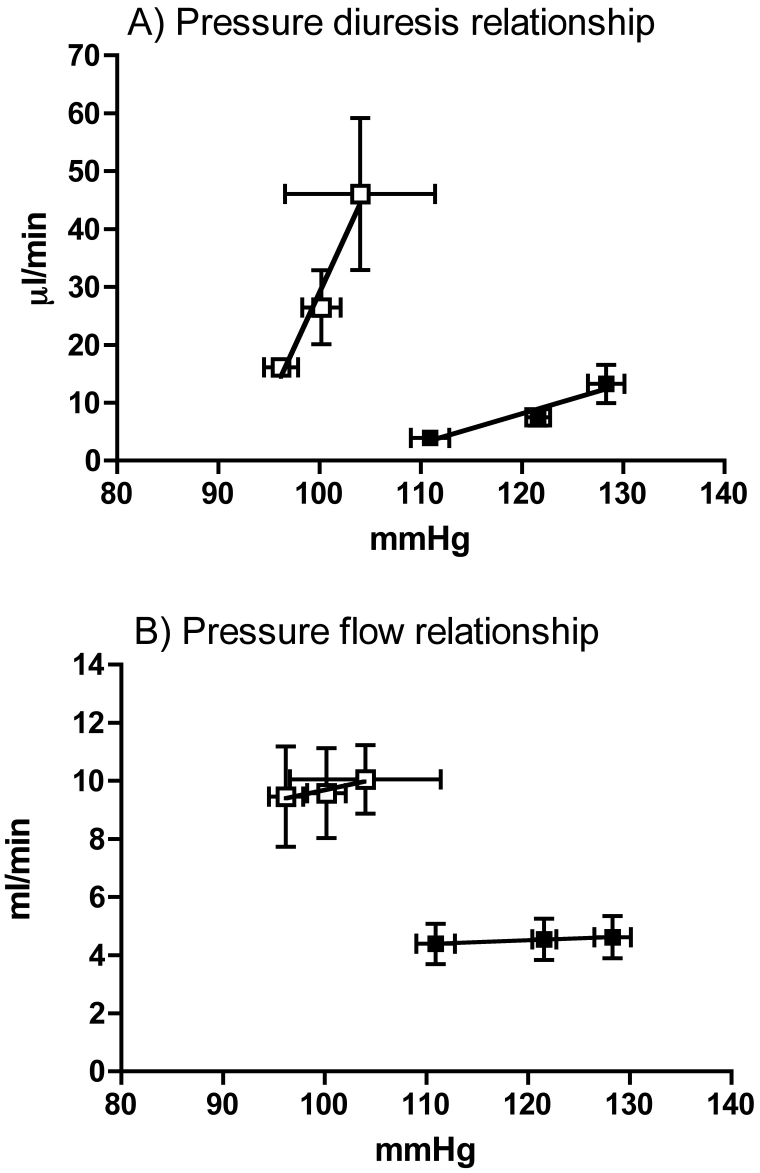

Figure 3.7: Blood Pressure and Flow Relationships in F344 and Lewis strains - (A) Pressure diuresis and (B) pressure flow relationship in Lewis (n = 8; open squares) and F344 (n = 7; black squares) rats. Data are mean±SEM. Statistical test was performed by linear regression analysis

relationship between blood flow and blood pressure in either strain of animals, indicative of intact auto-regulation (Figure 3.7B).

3.3.2.2 Strain dependent responses to BBG

Under baseline (non-ligated) conditions, acute infusion of BBG caused a significant reduction of mean arterial blood pressure in F344 rats but not in Lewis animals (Fig.3.8A). Blood flow through the left renal artery was not significantly affected by BBG in either group (Fig.3.8B). However, BBG caused a significant decrease in renal vascular resistance in F344 rats (Fig.3.8C).

Acute infusion of BBG did not affect the pressure-diuresis relationship in Lewis rats (Figure 3.9A). In F344 rats, BBG caused a significant leftward shift of the pressure-diuresis intercept (Figure 3.9B), reducing the threshold of this response, but did not alter the gradient of the slope. Renal blood flow remained flat over the physiological pressure range studied, indicative of intact autoregulation.

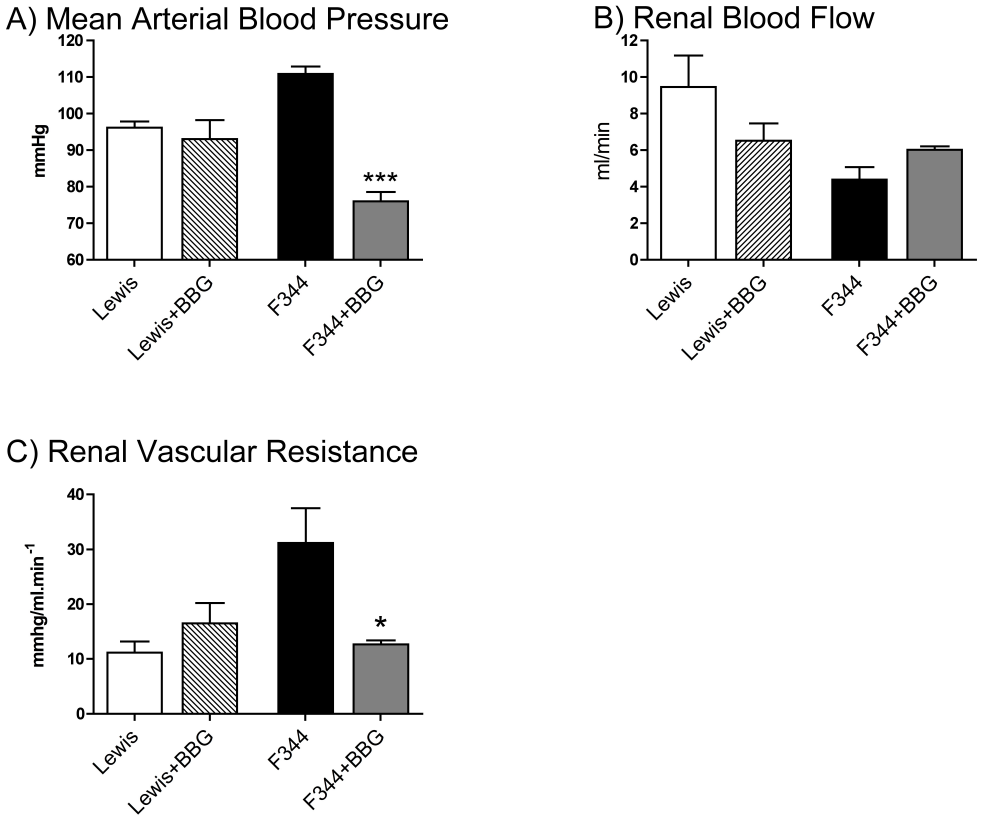

Figure 3.8: Effect of BBG on Blood Pressure, Flow and Renal Vascular Resistance - (A)Mean arterial blood pressure; (B) left renal artery blood flow and (C) renal vascular resistance in the left renal artery measured in Lewis and F344 rats receiving either saline or BBG by intravenous infusion. Data are mean±SEM. Statistical comparisons were made within strain by unpaired t-test. ***P<0.001; *<P0.05. Statistical comparisons were made using one way ANOVA with Bonferroni post-test.

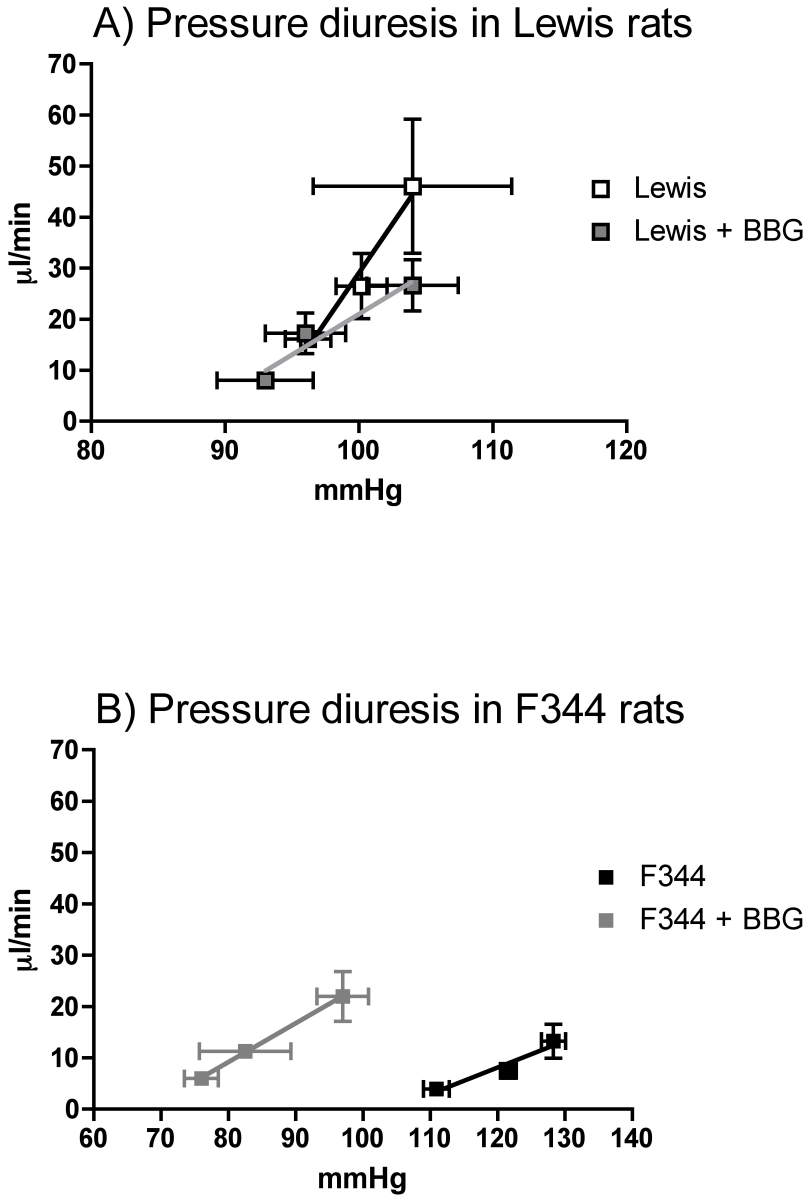

Figure 3.9: Effect of BBG on F344 and Lewis pressure diuresis - The Pressure diuresis relationship measured in (A) Lewis and (B) F344 rats receiving either saline (Lewis: open squares; F344: closed squares) or BBG (Lewis + BBG: grey filled black squares; F344 + BBG: grey squares) by intravenous infusion. Data are mean±SEM. Statistical testing was performed by linear regression analysis.

3.4 Discussion

This study is largely consistent with the published distribution of P2X receptors. mRNA encoding P2Y1, P2Y2, P2X4 and P2X7 receptors have all been identified in human vascular smooth muscle and endothelial cells (416, 522, 544).

P2X1 receptor expression was limited to the vascular smooth muscle of the renal arteries and afferent arteriole. Renal autoregulation is severely attenuated in P2X1 null mice, (166, 212, 215), illustrating the importance of this receptor for renal vascular function. In the present study, renal autoregulation was intact in both strains of rats and there was no evidence linking differential expression of the P2X1 receptor, or indeed P2X4 or P2X7 receptors to the impaired renal vascular function observed in F344 rats.

P2X4 and P2X7 receptors were localised to the endothelium of the pre-glomerular vasculature. Bioinformatic ranking analysis associated increased expression with vascular dysfunction and loss of blood pressure control. Both P2X4 (545) and P2X7 receptors (294) can modulate blood vessel contractility by promoting the release of vasodilators from the endothelium. One interpretation of the present study is that the up-regulation of receptors in F344 rats is a compensatory response to improve poor renal blood flow. Thus acute receptor antagonism *in vivo* should inhibit this tonic vasodilation. There was a trend for this in the Lewis rats but the reduction in blood flow induced by BBG was not statistically different. BBG did induce a significant haemodynamic effect in F344 rats but this was to increase blood flow, rather than to reduce it. One interpretation of this outcome is that in F344 rats P2X4/P2X7 receptor activation induces a tonic vasoconstriction. It is difficult to reconcile such an effect with the predominantly endothelial location of these receptors. However, the endothelium also releases potent vasoconstrictive mediators, including mono- or di-nucleoside polyphosphates such as adenosine 5′tetraphosphate (495) and uridine adenosine tetraphosphate is a partial agonist at the rat P2X4 receptor (536) causing profound vasoconstriction when perfused via the intravascular route into the isolated rat kidney (495). Furthermore, although it is not presently known if there is strain specific (F344 or Lewis) regulation of these receptors nor whether there are any sequence differences which would account for differing responses to antagonism.

P2X4 and P2X7 receptors were also identified in the renal tubule in both strains of rats. Tubular expression of P2X4 receptor is consistent with several previous studies (18). There was some evidence of intracellular, punctate staining, particularly in the Lewis rats. It is possible that this represents expression of P2X4 receptors in intracellular vesicles, which might act as a reservoir for trafficking of receptors to the apical or basolateral membrane or serve as mediators of vacuolar calcium release (464). P2X receptors, including P2X4 have an emerging role in

regulating tubular sodium reabsorption processes (18) but in our studies BBG did not affect urine flow rate.

Pericytes expressing P2X7 receptors have previously been described in the vasa recta (84, 252). Contraction of the vasa recta was attributed to P2X7 receptor expression on these vessels. In the present study however P2X7 expression was found in the vasa recta vessels themselves; although distinction between pericyte and vascular staining in the present study could not be delineated. Functionaly, expression of P2X7 on the vasa recta itself could facilitate constriction (as seen in sephenous vein (57)) ultimately increasing intraluminal vasa recta pressure, and RIHP with consequently reduced solute and sodium excretion as described by the pressure-natriuresis mechanism (see section 1.2.2).

The relationship between P2X7 and P2X4 receptor activation and sodium/water reabsorption is complex, however, and may depend on the local sodium concentration. P2X7 and P2X4 are activated under different conditions, for example P2X7 appears insensitve to ATP concentrations $<100\mu$M (371). Consequently cation currents through P2X7 or P2X4 receptors vary significantly under local ATP concentrations - examples of which have been modelled in Appendix A7 using a model of ligand gated activation of Goldman-Hodgkin-Katz currents fitted to experimental data (Fig.7.2 and 7.1). Simulating activation of these receptors in response to a local ATP concentrations (0.001-0.01 M) , it is clear that the instantaneous calcium influx is higher through P2X4 receptors (Fig,7.3). However sustained activation ultimately leads to longer-term Ca^{++} influx mediated through P2X7 (Fig.7.4). Thus the calcium dynamics mediated by P2X4 and P2X7 receptor activation are distinct and could well indicate distinct roles in vascular contractility not resolved by the present study (371, 414).

An obvious concern in interpreting these results is the selectivity of the antagonist, BBG. This compound is a potent inhibitor of rat P2X7 receptors (IC50=10nM) and although it can also block the P2X4 receptor, its selectivity for P2X7 receptor is 1000-fold greater. BBG has been used previously in vivo to elucidate P2X7 receptor functionality (227, 401). Indeed, chronic administration of BBG reduces renal injury and lowers blood pressure in the Dahl salt sensitive rat (225); P2X7 null mice are similarly protected from the renal injury associated with salt-induced hypertension (226). Nevertheless, BBG may also antagonize rat P2X4 receptors and our infusion protocol could inhibit both P2X receptor subtypes. Furthermore, a number of off-target effects of BBG have been reported (246), which cannot exclude the possibility that P2X7-independent effects also contribute to the haemodynamic actions of BBG observed in the F344 rats.

Altered sodium homoeostasis identified by the pressure-diuresis relationship is a hallmark of hypertension and kidney disease. The work presented in this chapter has focused on strain differences in identifying the cause(s) of impaired

renal function, now the question to be answered is whether the renal vascular expression of P2X7 and P2X4 in the F344 strain pertains impaired renal function during over-activation of the RAS.

Data presented in this chapter have been published (323). A reprint of this paper is included in Appendix B, section 8.2.

4

P2X7 AND P2X4 RECEPTORS IMPAIR PRESSURE NATRIURESIS FOLLOWING CHRONIC ANGIOTENSIN II INFUSION

4.1 Introduction

In the previous chapter P2X7 and P2X4 receptor localisation and function was determined in physiologically normal renal function. The present chapter will now investigate the function of these receptors following chronic over-activation of the RAS. An ANG II infusion model was selected for two reasons; (1) the rise in blood pressure in *Ren2* and *Cyp1a1-Ren2* transgenic rat models is ANG II dependent (279, 331) and (2) ANG II infusion models are well characterised (258). ANG II infusion typically causes injury to the kidney, particularly in vascular smooth muscle cells (258, 496). Injury occurs through mechanical transmission of pressures (2, 229) and indirect activation of paracrine signalling networks (326, 339, 408, 432). The extent, and strain specificity, of renal injury following ANG II infusion was determined by histological scoring as well as qualitative histological analysis.

Distinct renal medullary immunolocalisation of P2X7 (vasa recta) and P2X4 (collecting duct) was identified in the previous chapter. These were quite distinct in F344 but almost undetectable in Lewis rats. The vasa recta is considered the critical site for mediating changes in RIHP resulting in the pressure-natriuresis mechanism (see section 1.2.2 & 1.2.3). However P2X7 is most highly expressed on macrophages (249, 533) and therefore increased renal expression following significant injury may relate to the high expression of the P2X7 receptor on infiltrating macrophages. To investigate the vascular and tubular roles of P2X7 and P2X4, a low dose ANG II infusion was used to blunt the pressure-natriuresis mechanism without confounding factors of significant renal injury. Thus in a separate cohort of F344 rats *in vivo* measurements of both pressure-diuresis and pressure-natriuresis were performed to investigate whether 1) inappropriately activated RAS caused a change in the renal function curve and 2) whether acute infusion of BBG improved the renal function curve.

4.2 Methods

4.2.1 Study 1

4.2.1.1 Angiotensin II infusion model

This study investigated the histological consequences of chronic ANG II infusion in Lewis and F344 rats. Osmotic minipumps (model 2002; Alzet, UK) were surgically implanted under isofluorane anaesthetic. Pumps contained ANG II (A9525, Sigma, UK) continuously infusing at 30ng/min for 14 days (Lewis + ANG II, n =6) and (F344 + ANG II, n=6). On the 14th day tissues were harvested for analysis. The right kidney was removed first and snap frozen on dry ice then stored at -80C prior to Western analysis. The left kidney was immersion fixed in formalin for 48 hours then placed in 70% ethanol for longer term storage.

4.2.1.2 Protein quantification

Kidneys stored at -80C were used for protein quantification: performed by Western analysis as described in chapter 2, section 2.2.3. Control samples (Fig.2.1) were used for comparison with rats receiving 14 day ANG II infusion.

4.2.1.3 Renal injury

Renal injury scoring was performed on hematoxylin and eosin (H&E) stained sections. Injury was determined by severity of sites of vacuolation which were distinguished from sectioning and staining artefact as having well defined edges close to circular, displaced nuclei (these were often close to the vacuole edge and those not obviously micro-capillaries containing red blood cells). Total number of vacuoles counted was normalised to vessel thickness (number of smooth muscle cell nuclei thick) to remove bias from over-selection of any renal arterial bed.

Macrophage staining was performed in collaboration with Dr. Frederick Tam (Imperial College, London). Paraffin embedded kidney sections were dewaxed and boiled for 15 mins in 0.01 M sodium citrate buffer. Peroxidases were blocked with H_2O_2 (0.3% in 50% methanol), washed with phosphate buffered saline (PBS) and incubated with goat serum (20%). Slides were incubated with CD68 antibody (1:500; Serotec, UK) overnight followed by 45 mins incubation with goat anti-mouse secondary antibody (Dako, UK). Finally slides were exposed to biotinylated HRP (Vector Labs, UK) for 30 mins. CD68 positive staining was visualised with DAB and counterstaining with haematoxylin. MΦ positive staining was quantified using the automated detection tool ImmunoRatio (500) and normalised to haematoxylin positive staining within a manually selected region containing individual glomeruli. At least 30 glomeruli were analysed per group. Sections stained

with sirius red and periodic acid-Schiff (PAS) were also included to investigate the extent of glomerular injury.

4.2.1.4 Renal immunolocalisation

Formalin fixed kidneys were used for renal immuolocalisation of P2X7, P2X4 and P2X1: performed as described in chapter 3, section 3.2.1.

4.2.2 Statistical analysis

Data are presented as mean ± SEM. Statistical analysis was performed by ANOVA with Bonferroni post-hoc correction unless otherwise stated.

4.2.3 Study 2

4.2.3.1 Angiotensin II infusion model

This study investigated the effect of ANG II on renal pressure-diuresis and pressure-natriuresis via osmotic minipumps (model 2002; Alzet) implanted under isoflurane anaesthetic. Minipumps infused ANGII (A9525, Sigma) at 30ng/min in F344 rats (n=6) for 13-15 days.

4.2.3.2 Renal functional studies

Renal functional studies were performed as described previously in chapter 3, section 3.2.2. Diuresis (gravimetric) and natriuressis (SmartLyte, Diamond Diagnostics) measurements were made. Data are presented as scatter plots matching blood pressure to either urine flow (pressure-diuresis) or sodium excretion (pressure-natriuresis). Where both measurements could not be made the point does not appear on the scatter plots but was included in statistical analysis as exact co-ordinate matching was not required[1]. Renal functional studies were performed after 13-15 days of ANG II infusion (F344 + ANG II; n=6). A second group receiving chronic ANG II infusion was treated acutely with constant BBG infusion (50μg/min/100g) included in the saline infusate (F344 + ANG II + BBG; n=5).

[1]Several urine samples were over-sampled to the point where urine could not be pipetted without mineral oil contamination and some samples even ran out completely following multiple removals from cold storage (-80C) to measure electrolytes. This was unavoidable due to failure of the original electrolyte machine and multiple replacement parts, then ultimately a replacement machine. As a consequence, although both pressure-diuresis and pressure-natriuresis measurements were performed on the same total animal number, it is clear that the pressure-natriuresis scatter plot has fewer data points.

Control F344 rats from chapter 3 were included where necessary for statistical comparisons.

4.2.4 Statistical analysis

Data are presented as mean±SEM. Statistical analysis was performed by ANOVA with Bonferroni post-hoc correction unless otherwise stated. Comparisons between groups of the pressure-diuresis relationship were made by linear regression.

4.3 Results

4.3.1 Study 1

4.3.1.1 Protein quantification

Western analysis of homogenates indicated that whole kidney P2X4 and P2X7 expression was not upregulated by ANG II infusion (Fig.4.1).

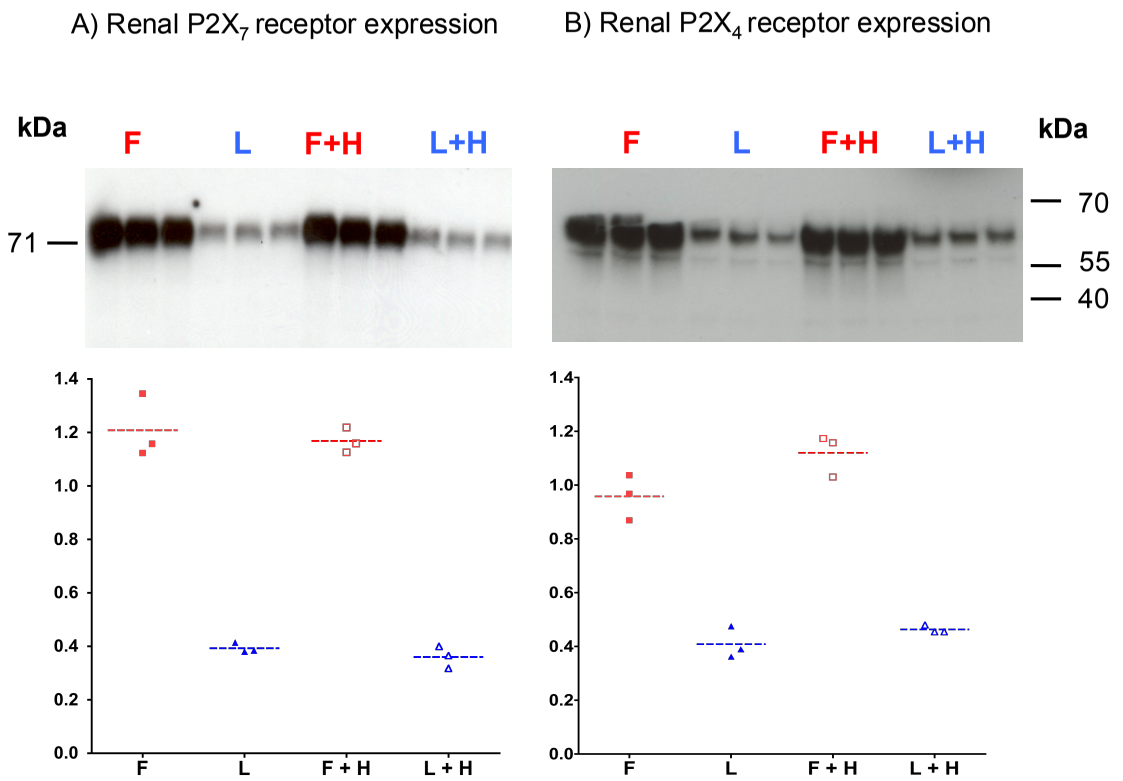

Figure 4.1: P2X7 and P2X4 Receptor Expression Following Chronic ANG II Infusion - Western analysis of P2X7 (A) and P2X4 (B) protein abundance from from whole kidney homogenates. Dashes show mean values but individual anamials are also shown for F344 (F, closed squares), Lewis (L, closed triangles), F344 + ANG II (F+H, open squares) and ; Lewis + ANG II (L+H, open triangles) .

4.3.1.2 Renal immunolocalisation of P2X7, P2X4 & P2X1 following angiotensin II infusion

Renal P2X7 positive staining remained distinct in the endothelium of the entire preglomerular vascular tree (Fig.4.2A-F) and was comparable to the distribution seen in normotension (Fig.3.2A-F). Occasional myocyte staining was evident in the larger renal segmental arteries in the F344 + ANG II group (Fig.4.2B). Glomerular atrophy associated with apparent arteriolopathy was occasionally observed in the F344 +ANG II group (Fig.4.2F).

Preglomerular P2X4 staining remained observable in vascular endothelial cells during hypertension (Fig.4.3A-F). Renal medullary tubule staining was most apparent in the F344 + ANG II group (Fig.4.3D,F) particularly adjacent to the interlobar arteries indicated by (∗).

P2X1 positive staining in hypertension was distinct to the preglomerular arteries (Fig.4.4A-F) as was seen in nornotension (Fig.3.4A-F). No staining was found in the renal tubules.

4.3.1.3 Renal injury

Lewis rats remained protected from renal injury (Fig.4.5A,B). Conversely, ANG II infusion caused a significant increase in myocyte vacuolation in the F344 strain (Fig.4.5A). The extent of renal preglomerular vascular myocyte vacuolation was most prominent in the intermediate arteries of the kidneys in F344 rats (Fig.4.5C).

Renal macrophage staining appeared qualitatively more intense in the F344 + ANG II group (Fig4.6A, indicated with black arrow) however this did not withstand robust statistical testing (Fig4.6D) in part because of the variability observed. Sirius red (Fig.4.6B) and PAS (Fig.4.6C) stained sections indicated that neither fibrosis nor obvious changes to the basement membrane had occurred by low dose ANG II infusion. Macrophage staining was not observed in the preglomerular vasculature.

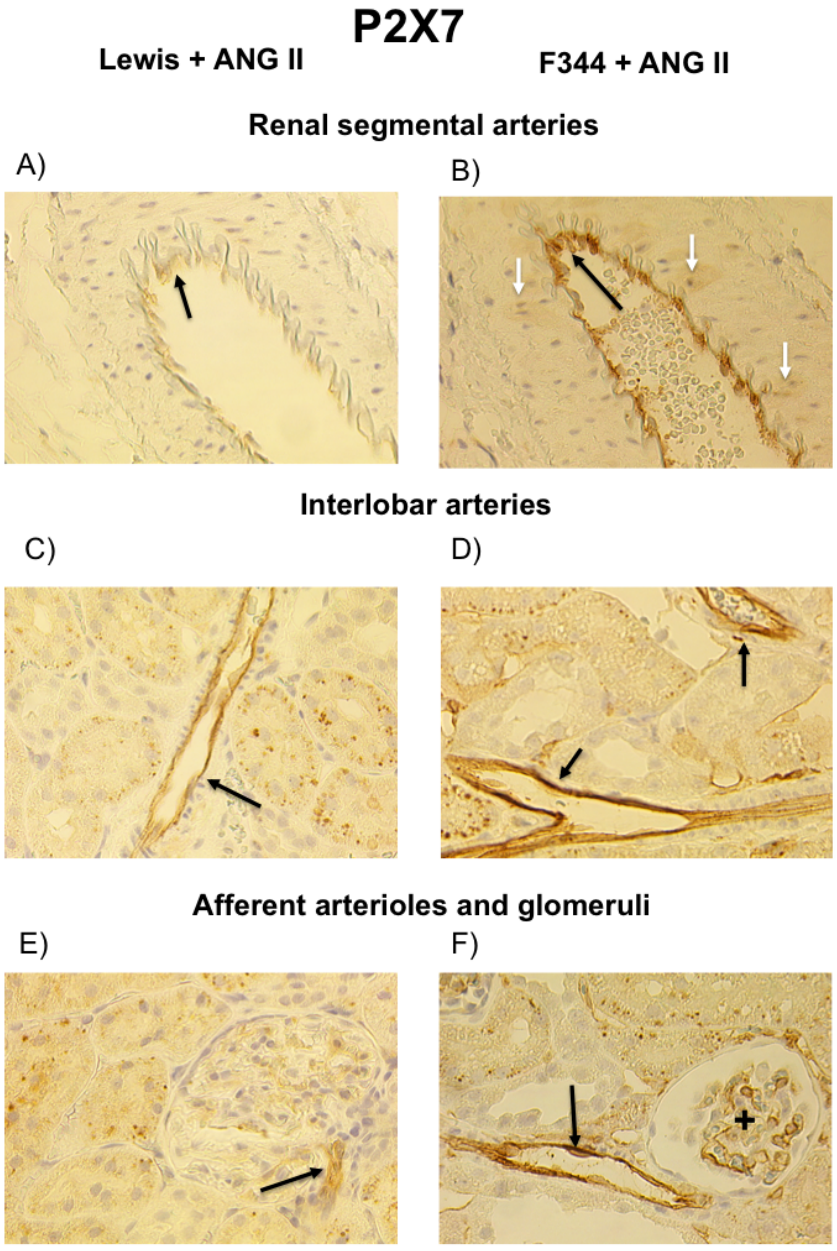

Figure 4.2: Renal P2X7 Localisation Following Chronic ANG II Infusion - Exemplar images of P2X7 positive staining in large (A, B), intermediate (C, D) and small (E, F) renal arteries of hypertensive rats. Black arrows indicate endothelial staining, white arrows indicate smooth muscle cells staining. Glomerular staining indicated by (+). Images were taken at 400x magnification.

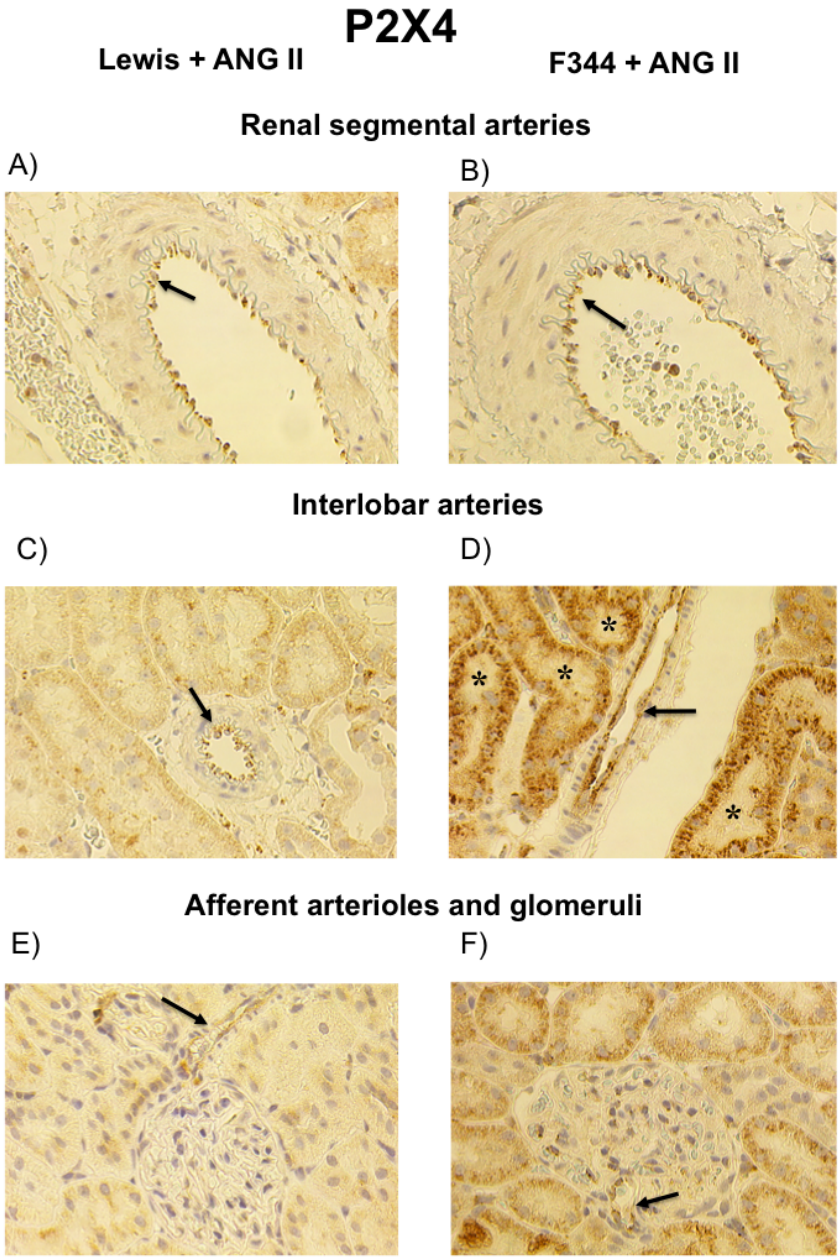

Figure 4.3: Renal P2X4 Localisation Following Chronic ANG II Infusion - Exemplar images of P2X4 positive staining in large (A, B), intermediate (C, D) and small (E, F) renal arteries of hypertensive rats. Arrows indicate endothelial staining. Tubule staining indicated by (∗). Images were taken at 400x magnification.

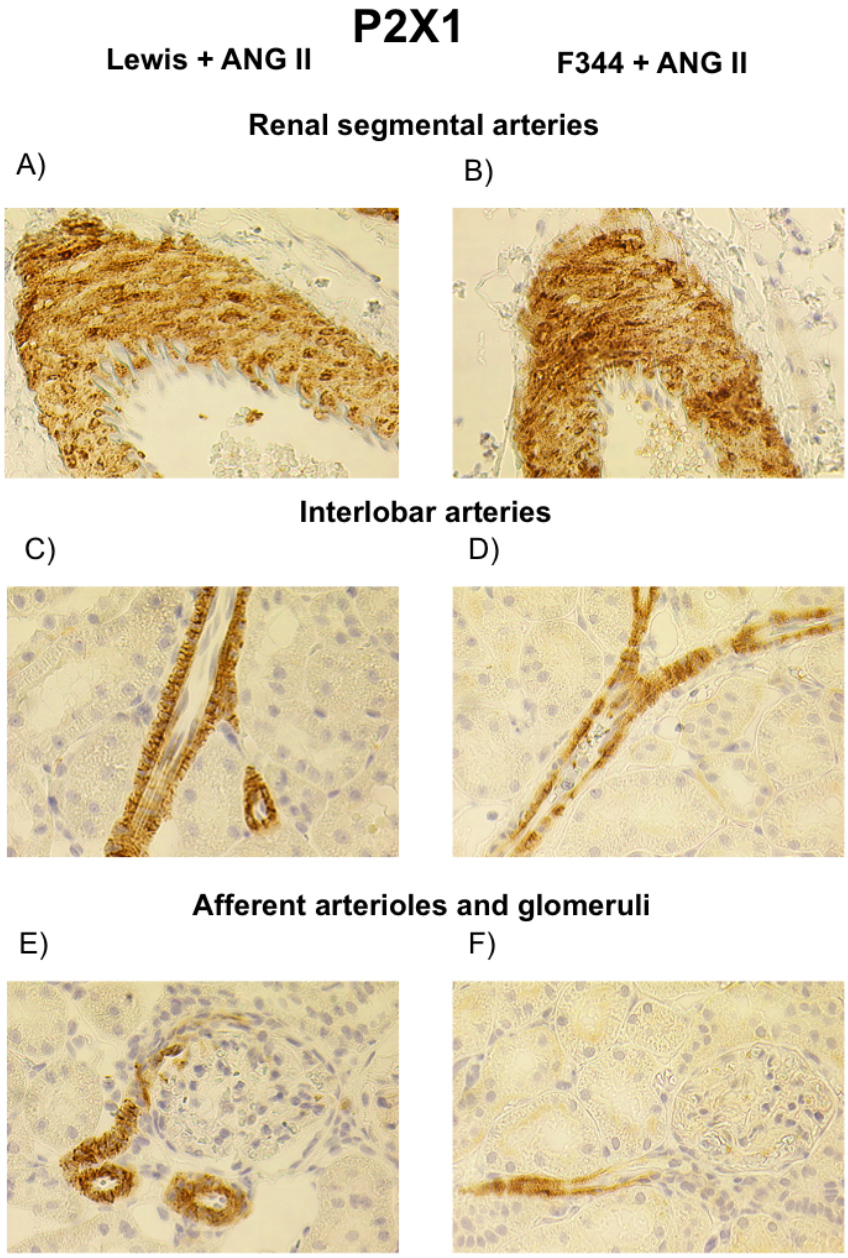

Figure 4.4: Renal P2X1 Localisation Following Chronic ANG II Infusion - Exemplar images of P2X1 positive staining in large (A, B), intermediate (C, D) and small (E, F) renal arteries of hypertensive rats. Images were taken at 400x magnification.

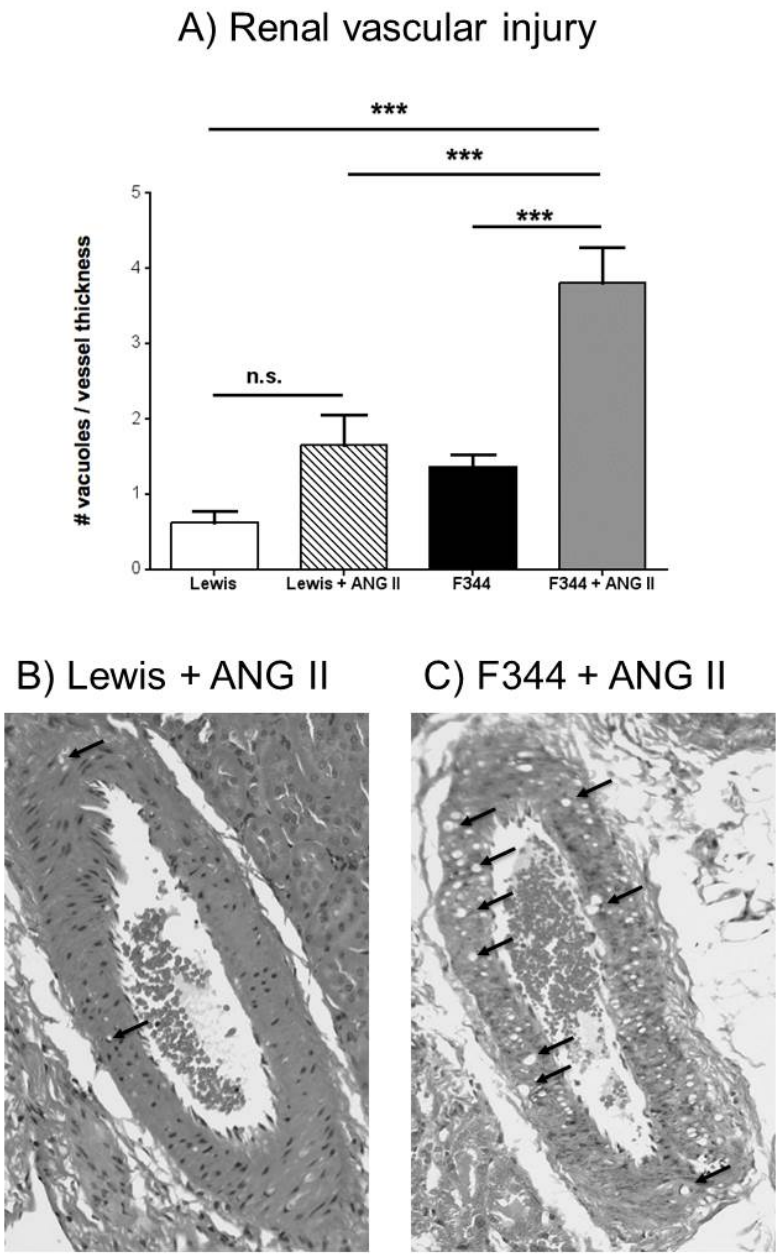

Figure 4.5: Renal Vascular Injury Following Chronic ANG II Infusion - Quantification of renal vascular injury (A). Exemplar renal segmental arteries hypertensive strains are given in the lower panel for Lewis + ANG II (B) and F344 + ANG II (C) respectively. Images were taken at 200x magnification. Arrows indicate distinct sites of vacuolation. Statistical comparisons were made using by ANOVA and post-hoc testing with Bonferonni. ***P<0.001.

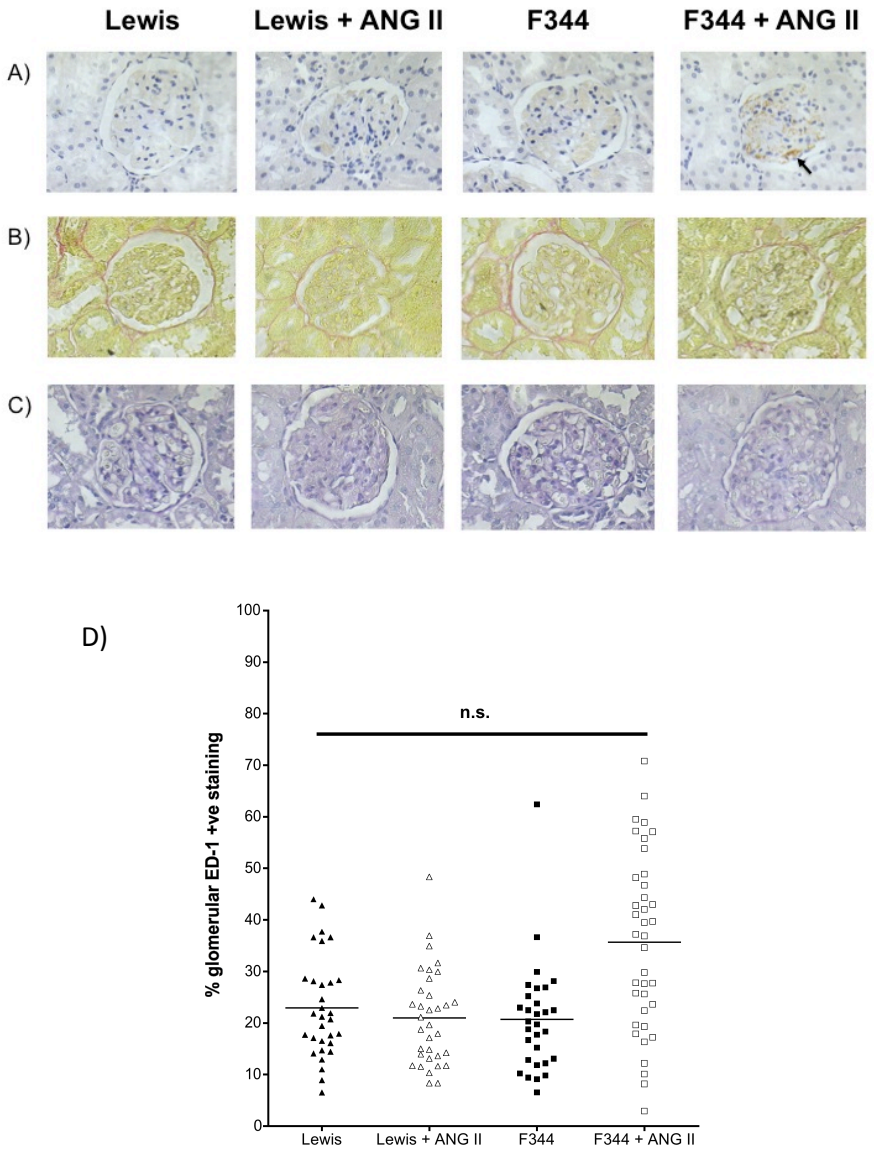

Figure 4.6: Glomerular Injury Following Chronic ANG II Infusion - Glomeruli showing immunopositive staining for MΦ with CD68 antibody (A). Sirius red (B) and periodic acid-Schiff (PAS) (C) stained sections. D) Quantification of glomerular ED-1 positive staining. Images were taken at 400x magnification. Statistical comparisons were made using by ANOVA and post-hoc testing with Bonferonni.

4.3.2 Study 2

4.3.3 Renal functional studies

ANG II infusion over 13-15 days resulted in a significant increase in blood pressure in F344 rats (Fig.4.7A). Acute infusion of BBG lowered blood pressure to a level comparable with controls. Renal blood flow was unchanged by both chronic ANG II infusion or acute BBG (Fig.4.7B).

Acute infusion of BBG caused a significant shift in the ANG II infused pressure-diuresis relationship (Fig.4.8). BBG caused a leftward shift in the curve (apparent in the mean blood pressure drop shown in Fig4.7). Furthermore BBG infusion increased the gradient of slope of the hypertensive pressure-diuresis relationship significantly (linear regression, $P<0.0001$). BBG infusion induced a similarly significant shift in the pressure-natriuresis relationship (Fig.4.9). The gradient of slopes were significantly different between groups (linear regression, $P<0.0001$).

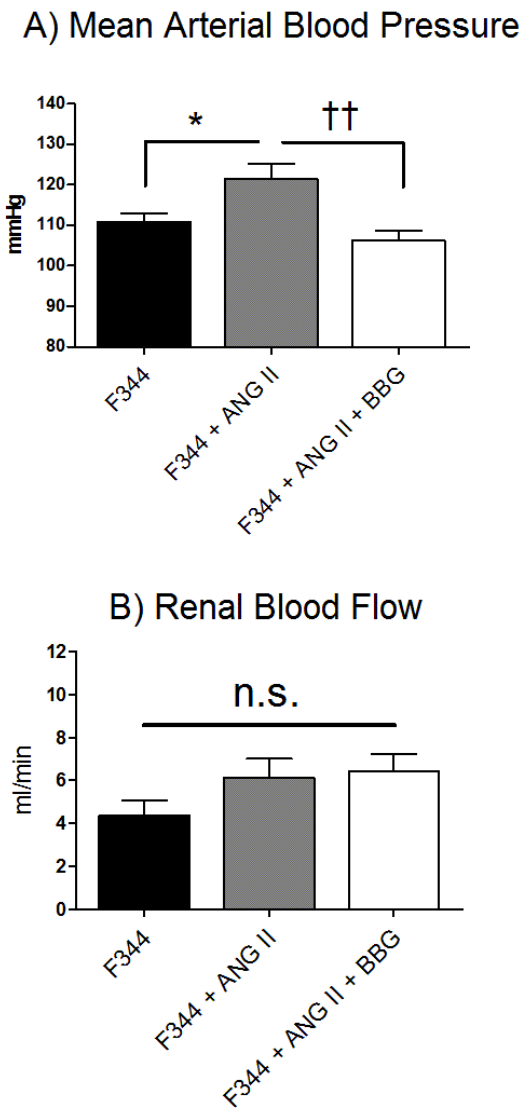

Figure 4.7: Effect of BBG on Blood Pressure and Renal Blood Flow Following Chronic ANG II Infusion - (A) blood pressure and (B) renal blood flow data in F344 (n=7), F344 + ANG II (n=6) and F344 + ANG II + BBG (n=5) groups. Statistical comparisons were made using one way ANOVA with Bonferroni post-test. *P<0.05, ††P<0.01

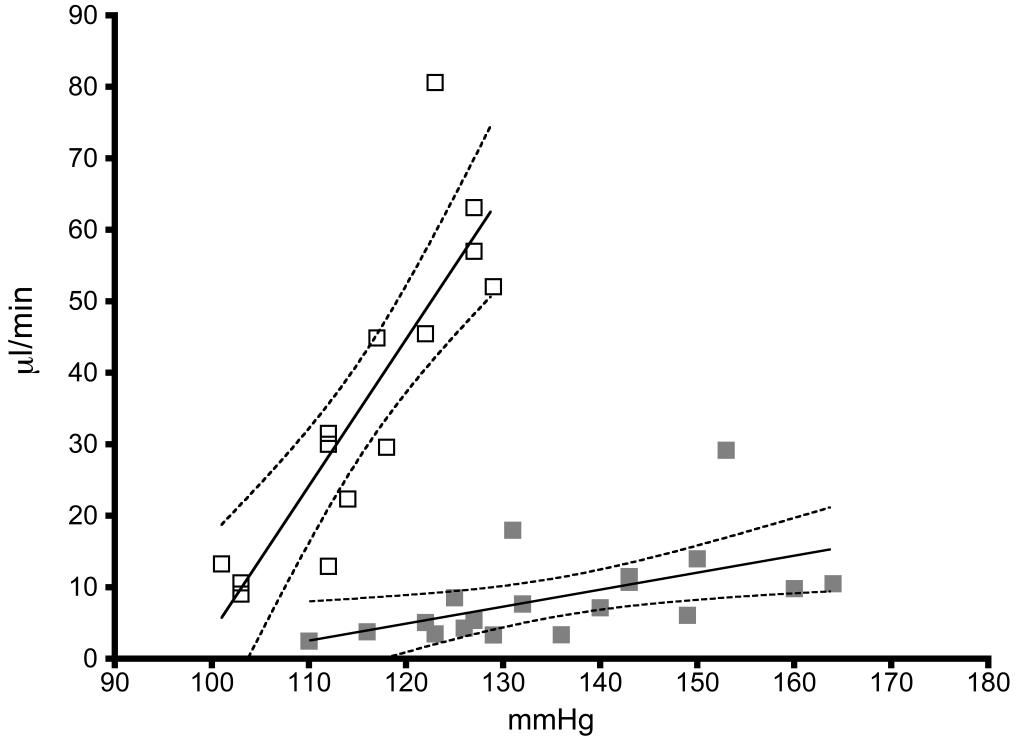

Figure 4.8: Effect of BBG on Pressure-Diuresis Following Chronic ANG II Infusion - Data are presented as scatter plots for the groups; ANG II (■) and ANG II + BBG (□). Solid lines are linear regression best-fits and broken lines are 95% confidence intervals. Statistical testing was performed by linear regression analysis.

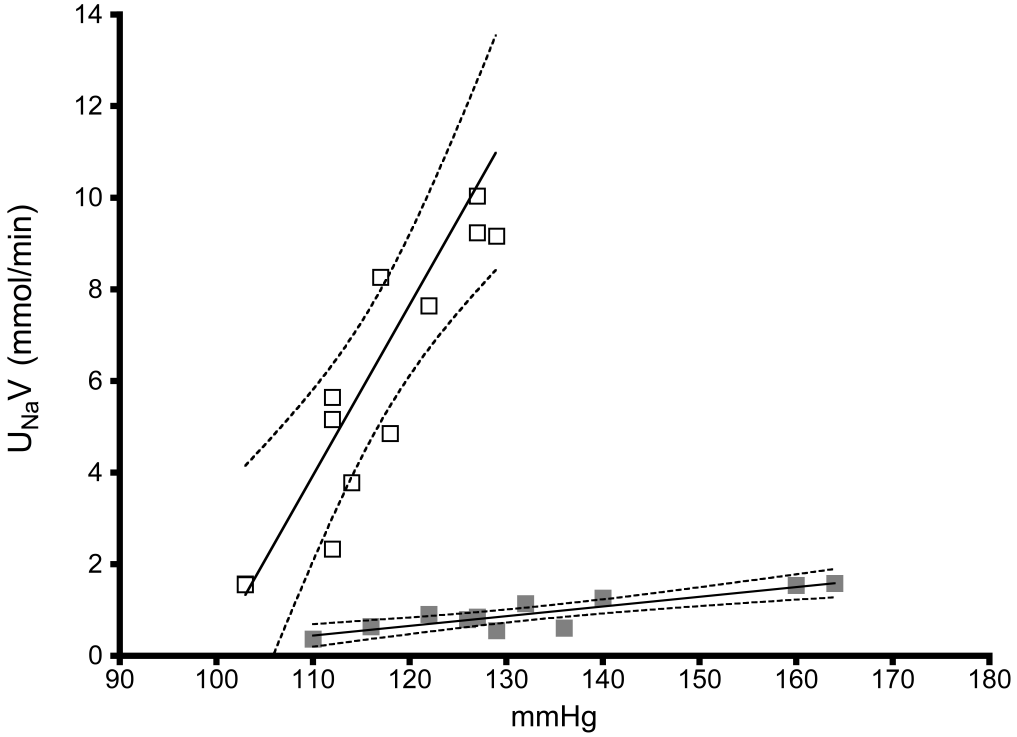

Figure 4.9: Effect of BBG on Pressure-Natriuresis Following Chronic ANG II Infusion - Data are presented as scatter plots for the groups; ANG II (■) and ANG II + BBG (□). Solid lines are linear regression best-fits and broken lines are 95% confidence intervals. Statistical testing was performed by linear regression analysis. Note some data points were omited where both pressure and sodium measurements could not be matched.

4.4 Discussion

4.4.1 Pathogenesis of kidney disease

Kidney injury and declining renal function are diagnostic indicators of kidney disease and present a global health burden with high population prevalence (109, 136, 147, 156, 436). Hypertension is a major risk factor for CKD (348) and progression can be slowed if blood pressure is controlled (185).

Progression of renal injury is characterised by increasing albuminuria (202) which typically precedes the development of hypertension(42, 253, 520). Drugs that reduce albuminuria are considered important treatments for CKD as well as cardiovascular disease in general (98, 514). However, blood pressure transmission to the glomeruli can also initiate renal injury in hypertension (34, 262).

Failure of the myogenic response in the renal afferent arteriole is implicated in the transmission of pressures required for glomerular injury (299, 465). The larger renal arteries also contribute to total resistance (193, 236, 509) hence net loss of renal vascular integrity is causative in the pathophysiology of hypertensive renal injury (260, 285, 374, 466). Preglomerular vascular injury, especially in the renal interlobar artery segments, typically precedes total renal damage and dysfunction, see section 4.4.1 and (11, 374, 509). These studies are consistent with the preglomerular vacuolation seen in the F344 strain following ANG II infusion. However, renal injury and fibrosis can also develop independently of barotrauma and the local actions of agents such as aldosterone (11, 248) and ANG II (339, 408) have been implicated.

Nevertheless, causation between hypertension and CKD is unclear (135) and several other key mechanisms worthy of note have not been studied here. The severity of high blood pressure is moderated by 24 hour variability (393) such that accurate measurement of blood pressure assists risk prediction (139, 184, 452). Temporal measurements of blood pressure can identify individuals with a non dipping night-time blood pressure phenotype, thought to be indicative of impaired renal sodium handling (21, 138), reversible by hydrochlorothiazide diuretics (417, 505). Other likely important mechanisms such as the regulation of salt reabpsorption in a 24 hour period, remain to be uncovered (97, 283, 407).

Low birth weight is also associated with adulthood CKD and more generally cardiovascular disease and morbidity (22, 22, 95, 424). Brenner originally hypothesised that reduced nephron number is a key factor initiating primary hypertension (43) due to hypertrophic compensatory mechanisms following reductions in renal mass either by whole kidney removal or partial ablation (188). This hypothesis is supported by micropuncture studies in 5/6 renal ablated rats which have compensatory and deleterious single nephron hyperfiltration (9, 201). Observations

in patients with primary hypertension found apparent compensation of reduced glomerular number with hypertrophy or oligomeganephronia (251).

The complex pathologies of CKD eventually converge upon a significant inflammatory component (54, 126, 372) characterised by the infiltration, and activation, of inflammatory mediators (37, 499) and immune cells (195, 448, 523). T-cell activation following minor injury can occur by a number of stimuli including oxidative stress, salt imbalances and ANG II (37, 54, 174, 261, 411) promoting macrophage infiltration. Macrophages can themselves cause vasoconstriction and drive blood pressure higher still (302). Multiple P2 receptors are implicated in both pro - as well as anti- inflammatory modulation (116, 219). Thus the kidney is likely the cause of the hypertension that can ultimately deteriorate it (263).

4.4.2 Renal P2X7 and P2X4 receptors in a pre-fibrotic setting

In the kidney P2X7 expression has been best described in the glomeruli and specifically the messangial cell of the *Ren2* transgenic rat (515). Uretral obstruction in the mouse causes significant renal macrophage infiltration and collagen deposition mediated by the P2X7 receptor (158). Loss of P2X7 receptor activity has been associated with reduced cyst development in a *Danio rerio* model of polcystic kidney disease (67) and reduced renal injury in glomerulosclerosis (488). Interactions between P2X7 and P2X4 receptors occur in multiple tissues (83). P2X4 receptors expressed on macrophages might enhance the P2X7 mediated response (247).

Whole protein Western analysis indicated that P2X7 and P2X4 were not regulated by the dose of ANG II infused. This is not surprising because together the renal injury data did not indicate significant fibrosis. Renal injury scored significantly higher in the F344 strain following ANG II infusion and was limited to myocyte vacuoloation and occasional glomerular atrophy. This is consistent with the earliest stages of renal injury in the *Cyp1a1-Ren2*.F rat (11). However, macrophage infiltration into the preglomerular vascular wall was not observed following ANG II infusion in either strain suggesting the vascular injury was minimal. Renal injury scoring also verified that ANG II infusion did not cause renal vascular injury in Lewis rats. Unfortunately the quality of MΦ immunolocalisation was not sufficiently clear to permit individual macrophage counting. Nonetheless it was clear that total CD68 positive staining within the glomerulus did not increase. It remains unclear whether (subject to the large variability) the CD68 positive staining in F344 + ANG II group glomeruli (Fig.4.6A, black arrow) can explain the P2X7 positive staining in glomeruli of this group (Fig.4.2F). Alternatively the increased P2X7 positive staining in the F344 + ANG II group glomeruli might be native tissue expression.

Acute P2X7 and P2X4 antagonism significantly ameliorated the blood pressure rise caused by ANG II infusion. Increases in blood pressure are associated with increases in renal interstitial ATP concentrations (365, 366) which enhances the TGF mechanism (216, 367). Furthermore chronically elevated extracellular ATP is associated with smooth muscle cell hypertrophy and hyperplasia (49, 120, 205, 469, 519). A role for renal purines in regulating renal vascular resistance in ANG II dependent hypertension is well established (131, 132, 177, 178, 183, 527). P2 receptors are implicated in glomerular and vascular injury in ANG II hypertension (161). ANG II infusion markedly decreases renal afferent arteriole calcium influx and vasoconstriction via P2X, but not P2Y, receptors (549).

Pressure-natriuresis in the F344 rat was blunted by ANG II infusion. Activation of the RAS sufficiently alters the renal functional curve inducing salt sensitivity of blood pressure in several animal models (230). Furthermore the pressure-natriuresis mechanism is hypothesised to shift prior to onset of hypertension (80, 180) such that even subpressor infusion of ANG II is sufficient to blunt pressure-natriuresis (398, 462, 508). Thus the dominant functional consequence of P2X7 and P2X4 expression following ANG II infusion in the F344 rat was a blunting of the pressure-natriuresis mechanism.

In conclusion, low dose ANG II infusion in the F344 rat can model the earliest stages of renal dysfunction and injury prior to significant macrophage infiltration and fibrosis. Renal tissue hypoxia is implicated in the earliest stages of CKD progression, with low partial pressure of oxygen (pO_2) eventually causing activation of a pro-fibrotic cascade (128, 390, 535). The next chapter will therefore investigate the role of P2X7 and P2X4 receptors in the control of renal oxygenation during ANG II infusion.

5

P2X7 AND P2X4 RECEPTORS IMPAIR RENAL OXYGENATION AND PERFUSION FOLLOWING CHRONIC ANGIOTENSIN II INFUSION

5.1 Introduction

Under physiological conditions renal pO_2 is thought to have a marked cortico-medullary gradient, with the medulla being poorly oxygenated compared to the cortex (121). Cells of the medulla have a higher anaerobic capacity than those of the cortex and paracrine signalling pathways also provide some resistance against hypoxia (362). Nevertheless, the medulla is susceptible to hypoxic injury and abnormal vascular reactivity can cause hypoperfusion initiating a vicious cycle of microvasculature injury, inflammation and fibrosis (315). Hypertension imposes increased metabolic demand on the kidney which may drive the medulla towards a hypoxic state (44, 108, 127, 128, 129). As such, it has been proposed that hypoxia is a common pathway in the genesis of CKD (375, 390).

Causation relating defects in renal oxygenation to renal disease is implied by immunohistochemical detection of pimonidazole adducts (349), formed when pO_2 is <10 mmHg. This method is, however, insensitive and non-quantitative (430). Oxygen sensitive microelectrodes offer a quantitative and sensitive approach, (121), but measurements made at the electrode tip cannot give insights into the wider distribution of tissue oxygen. Moreover, being invasive, microelectrodes are not usually amenable to longitudinal studies of renal function and local tissue damage (causing release of ATP) can make interpretation difficult.

Blood oxygenation-level dependent (BOLD) magnetic resonance imaging (MRI) is emerging as a technique through which to assess renal oxygen bioavailability (312). The BOLD signal (T2*) is a combination of the spin-spin relaxation rate between local protons (T2) and local field inhomogeneities produced by the paramagnetic property of deoxyhemoglobin as described in Eqn.5.1.

$$\frac{1}{T2^*} = \frac{1}{T2} + \frac{1}{T2'} \tag{5.1}$$

The relaxation rate (R2*=1/T2*) is thus proportional to the level of deoxyhemoglobin and R2* reflects the oxygenation status of red blood cells (377, 409).

R2* can be associated with tissue pO_2 and indeed much of the physiological utility of BOLD MRI rests on the assumption that tissue pO_2 is in responsive equilibrium with red blood cell pO_2. In pigs the spatial gradients of oxygenation observed by BOLD MRI are consistent with those measured in the contralateral kidney by O_2 microelectrodes (397).

BOLD MRI thus provides a unique tool to investigate the regulation of renal oxygenation during the progression of hypertension. In this chapter, Study 1 presents the development of a BOLD MRI acquisition and analysis protocol showing that ANG II infusion caused a transient disturbance in renal oxygenation in F344 rats. Study 2 investigated the effect of P2X7 and P2X4 receptor antagonism on renal oxygenation.

5.2 Methods

5.2.1 MRI scanning protocol

BOLD MRI measurements were performed using a 7 Tesla preclinical MRI scanner (Agilent Technologies, UK). Rats (n=6) were anesthetised with 1.5 - 2 % isoflurane in oxygen-enriched air (0.5 l/min air, 0.5 l/min oxygen). Rectal temperature was maintained at (37^oC). Respiration and ECG were monitored for stability throughout the scanning protocol. A birdcage volume coil (72 mm diameter) and a 4-channel phased array surface coil (Rapid Biomedical GmbH, Germany) were used for radio frequency transmission and signal reception, respectively.

Image acquisition used a multiple echo gradient-recalled BOLD MRI pulse sequence of ten T2*-weighted echoes; TE = 4, 8, 12, 16, 20, 24, 28, 32, 36, 40 ms, TR=100 ms and flip angle of 30^o at an 83 kHz bandwidth. An axial slice through the centre of the right kidney was selected with 50 x 40 mm field of view containing a 192 x 128 acquisition matrix (in-plane resolution = 0.26 x 0.31 mm). A single axial slice, aligned parallel with the renal artery identified by rapid scout scanning (fast gradient echo, 3 slices in coronal orientation), ensured slice position encompassed the most representative section of the kidney regions. Slice thickness was 2 mm with 14 signal averages. Temporal resolution was 3 minutes for each BOLD scan.

5.2.2 Image analysis pipeline

Image analysis procedures were developed and coded in collaboration with Andrew Zammit-Mangion (School of Informatics, University of Edinburgh).

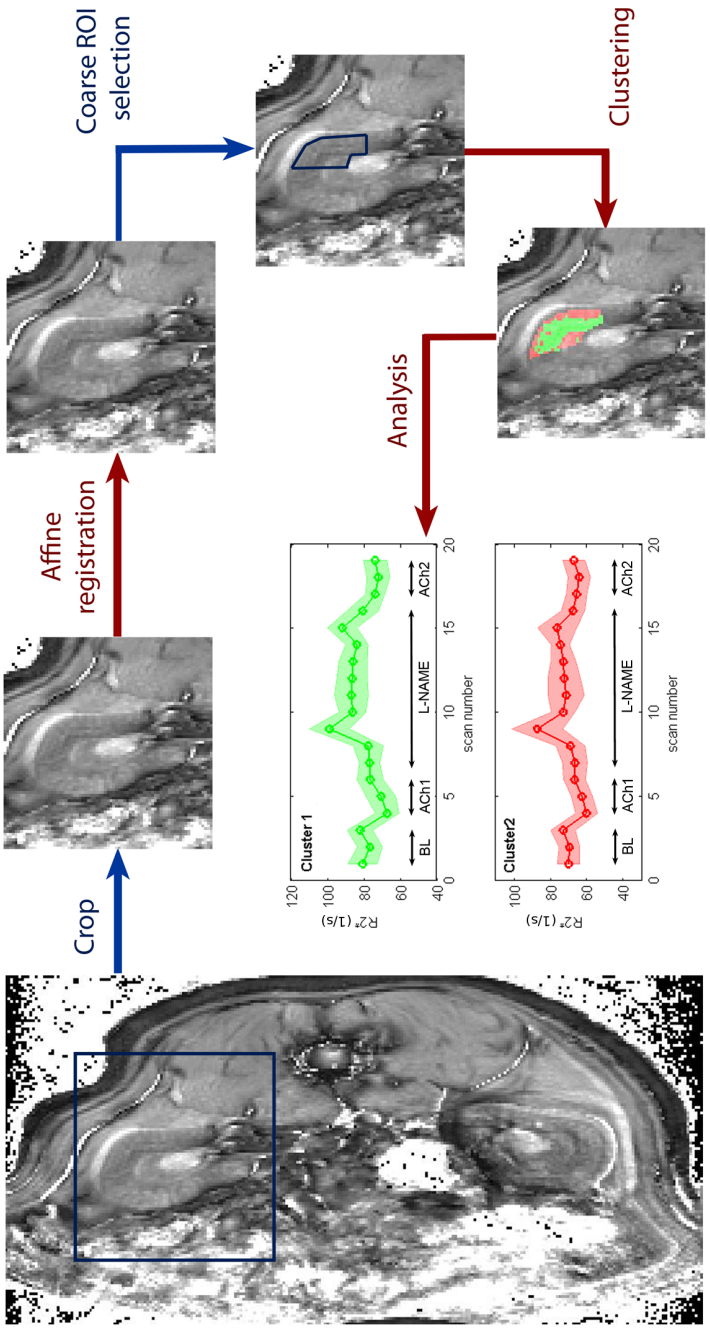

Figure 5.1: Analysis Pipeline of BOLD MRI Data. - Following registration of the images (examplar T2* map is shown), a kidney quadrant was manually selected. The k-means clustering of the data for time series analysis was then performed automatically and two compartments identified with statistically distinct mean R2* time series. For clarity blue arrows indicate manual steps and red arrows automation. ROI, regions of interest; BL, baseline; L-NAME, N-nitro-L-arginine methyl ester hydrochloride.

Although the use of BOLD MRI to rapidly and non-invasively define renal hypoxia is clinically attractive (152), interpretation of images is often challenging. Most post-acquisition analyses rely on manual selection of small regions of interest (ROI) to generate anatomically informative R2* maps. However, kidneys are subject to respiratory and cardiovascular motions that might be difficult to gate against, particularly in experimental models. Unless image registration is employed, time-series data within an individual ROI are unlikely to be acquired from exactly corresponding anatomical regions. The selection of small segments that are well delineated within the cortex and medulla has been advocated (153) but this approach will discard from the analysis biological information contained within the data set. Moreover, this approach is subjective and risks a selection bias towards areas at the extremes of signal intensity (152).

In biomedical research, the use of algorithms that cluster individual data points based on concepts of quantitative "nearness" or "similarity" are more commonly associated with analysis of gene expression data sets (105) but is broadly applicable to large data sets, such as those generated through BOLD MRI. The present method applied k-means clustering as an anatomically unbiased approach to BOLD MRI analysis. The central tenet of this approach is that voxels clustered on quantitative nearness of the R2* signal share a commonality of biological process. Importantly, quantitative similarity does not necessarily equate to close anatomical proximity of voxels or compartmentalization within a given region of the kidney.

5.2.2.1 Image selection and registration

Motion correction was performed by complimentary measures to ensure voxels in different frames overlapped; global registration (consistent over entire image), intensity based registration (using grey-level image values) and rigid registration (only allowing translation and rotation) were used on each rat and on each day separately.

Initial outlier detection was assessed by a Hampel identifier, used to detect scans having an intensity profile significantly different from the median (X0.5) or outside the 90th percentile (X0.9): scan imprecision largely reflected significant motion artefact and these outliers were rejected (Fig.5.2).

Figure 5.2: Statistically Detected BOLD MRI Outlier Scans - (A) Typical BOLD MRI scan of kidney taken from baseline scan rat. (B-G) A range of extreme examples demonstrating outliers detected from a control rats on both baseline days. Outliers detected by Hampel identifier on raw data set. Colour scale indicates relative T2* levels which were binned evenly to map to the colour range.

Rigid registration was performed on the remaining images using an exhaustive search. The third baseline scan was selected and all other scans in the sequence were translated and rotated until the mutual information (gradient^2) was maximised. This improved stability across sequences: 96% of scans required less than one voxel translational correlation or less than 1^o rotation, indicating that rigid registration was sufficient for the present dataset.

5.2.2.2 K-means clustering analysis

Automated image segmentation was performed using a k-means clustering algorithm (with k, the number of clusters). K-means clustering identifies k-clusters within a multi-dimensional space using Euclidean distance (for details, see chapter 9.1 of (36)). Given a set of points, the target of the algorithm is to find k cluster-centres such that the sum of square distances of each point to its closest cluster centre is a minimum. The (local) minimum is searched for in an iterative manner, the two steps of which are i) the association of the points with their closest cluster centres and ii) the updating of the cluster centres such that the sum of square distances to the associated points is minimized. The final cluster configuration can be dependent on the initial cluster configuration. To validate our approach the appropriate number of initial conditions was therefore determined to establish the lowest number insensitive to the starting conditions. The present dataset found 10 random initial conditions to fit this condition, thus the algorithm was run for each scan set and saved the final configuration as that with the lowest sum of intra-cluster distances.

To select the number of clusters (K) a pilot analysis was performed using k=1,2,3,...13 to identify the value of k such that the increase in explained variance of k+1 clusters was 50% of the additional variance explained by the k^{th} cluster. With the use of this approach k=2 was chosen, as the addition of a third cluster did not contribute sufficiently to an increase in explained variance.

5.2.3 Study 1: Validation of renal BOLD MRI clustering analysis

The effect of acetlycholine (5μg/kg, Sigma-Aldrich) on the R2* signal was determined prior to, and following administration of N-Nitro-L-arginine methyl ester hydrochloride (L-NAME; 10mg/kg Sigma-Aldrich). Both compounds were administered via the tail vein in a volume of $\sim$0.15ml. Immediately following injection the catheter was flushed through with a volume of saline equal to the catheter volume. Scans obtained under control conditions (days -6 and -4) were compared statistically and then (consequentally) combined into one control group. On day 0, osmotic minipumps (Model 2002, Alzet, Charles River, UK), adapted for

MRI by replacement of the stainless steel flow moderator with a polyetheretherketone equivalent (part #2496, PEEK, Charles River, UK), containing ANG II (60ng/min) were surgically implanted under isofluorane anesthetic. Rats were scanned again after 3 & 6 days of ANG II infusion (n=6 in each group).

The effect of acetylcholine and L-NAME on blood pressure and renal blood flow were measured in a parallel study using the protocol described above for control rats (n=4) and rats receiving ANG II (60ng/min; ANG II; n=5). Rats were anesthetized (Thiobutabarbital 120 mg/kg IP). The right jugular vein was cannulated for infusion of 0.9% NaCl containing 1% bovine serum albumin. Rats were infused at 100μl/min until a total volume of 1.25ml/100g bwt was reached, then 30μl/min maintenance rate. The left femoral artery was cannulated for blood pressure measurement (MLT844, AD Instruments); a tracheotomy performed to maintain a clear airway. A midline laparotomy was performed and a Doppler transit time probe (MA1PRB; Transonic, USA) placed around the left renal artery. Core body temperature was servo-maintained at 37^{o}C.

5.2.4 Study 2: Effect of P2X7 and P2X4 antagonism on renal BOLD signal

The effect of BBG (40mg/kg, Sigma-Aldrich) on the R2* signal was determined by administered via the tail vein injections. Rats were scanned on day 0 and following the final MRI scan, osmotic minipumps (Model 2002, Alzet, Charles River, UK), adapted for MRI by replacement of the stainless steel flow moderator with a polyetheretherketone equivalent (part #2496, PEEK, Charles River, UK), were implanted subcutaneously containing ANG II (30ng/min; n=6). Rats were scanned again after 14 days of ANG II infusion.

5.2.5 Statistical analysis

Data are presented as mean ± standard error of the mean (SEM). Statistical analysis was performed by ANOVA with Bonferroni post-hoc correction unless otherwise stated. Comparisons between groups of the pressure-diuresis relationship were made by linear regression. Histograms were used to compare signal distributions between Study 1 and Study 2.

5.3 Results

5.3.1 Study 1: Validation of renal BOLD MRI clustering analysis

The clustering approach was used to generate R2* maps within a kidney quadrant in each of six control rats, using the postacquisition pipeline (Fig.5.1). Two compartments of distinct mean R2* intensities were created (cluster 1 = 70.96±1.48; cluster 2 = 79.00±1.50; means±SE; n = 18 scans in 6 rats; P<0.01). Each rat underwent three consecutive baseline scans on control days 6 and 4 and following 3 days of ANG II infusion. In control rats, baseline scans repeated sequentially on separate days or on different rats did not vary significantly for either cluster 1 (Fig.5.3A) or cluster 2 (Fig.5.3B). ANG II infusion did not effect the consistency of consecutive baselines found verifying scan reproducibility. Baseline scans were therefore combined for both groups.

Systemic injection of acetylcholine significantly attenuated the R2* signal (P<0.01, ANOVA) in both clustered compartments (Fig.5.4A), suggesting an increase in pO_2 throughout the kidney. This effect was transient; reaching its nadir in the scan performed 6 min post-injection. In a parallel study, acetylcholine initially caused a rapid fall in mean blood pressure and renal blood flow ((Fig.5.4B & bi). This effect was short lived (<1 min), and during the BOLD MRI scan protocol, renal blood flow was ∼30% higher than at baseline. Importantly, the average renal blood flow remained stable suggesting intact autoregulation. Administration of L-NAME caused a slowly progressive increase in signal intensity in the high R2* compartment (P<0.01, ANOVA) but was without effect in the low R2* compartment (Fig.5.4A). L-NAME also caused a reduction in renal blood flow over this time course (Fig.5.4B & bii). Acetylcholine was again injected. The effect on blood pressure and renal blood flow persisted, but the attenuation of R2* signal by acetylcholine was no longer observed.

Blood pressure and renal blood flow were not significantly affected by 3 day infusion of ANG II. Following 3 days of ANG II infusion, the R2* signal was no longer significantly affected by administration of either acetylcholine or L-NAME (Fig.5.5A). Nevertheless, acetylcholine still induced a transient reduction in renal blood flow and blood pressure (Fig.5.5B) and L-NAME increased renal vascular resistance.

The k-means clustering approach resolved the data into distinct compartments; indeed, convergence is assured by this algorithm, but the magnitude of the difference in intensity between the two compartments was much reduced (cluster 1 = 71.30±2.00; cluster 2 = 72.48±1.27; mean±SE; NS). Critically, baseline means of the two clustered compartments were less distinct during baseline and no longer

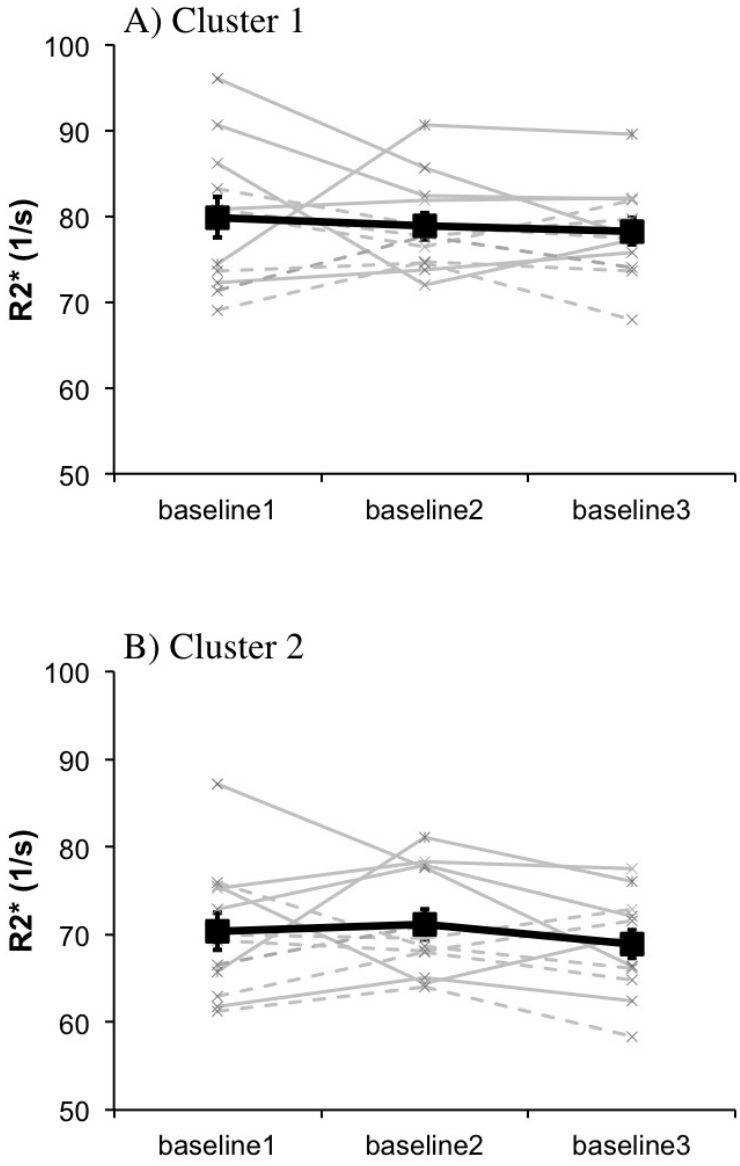

Figure 5.3: Reproducibility of Baseline BOLD MRI Data. - Rats were scanned in triplet (baseline 1, 2, and 3) and in 2 cohorts on day 6 (solid grey lines) or day 4 (broken grey lines). No significant difference between any of these measurements was observed (black line); thus baseline scans were assimilated into one baseline value.

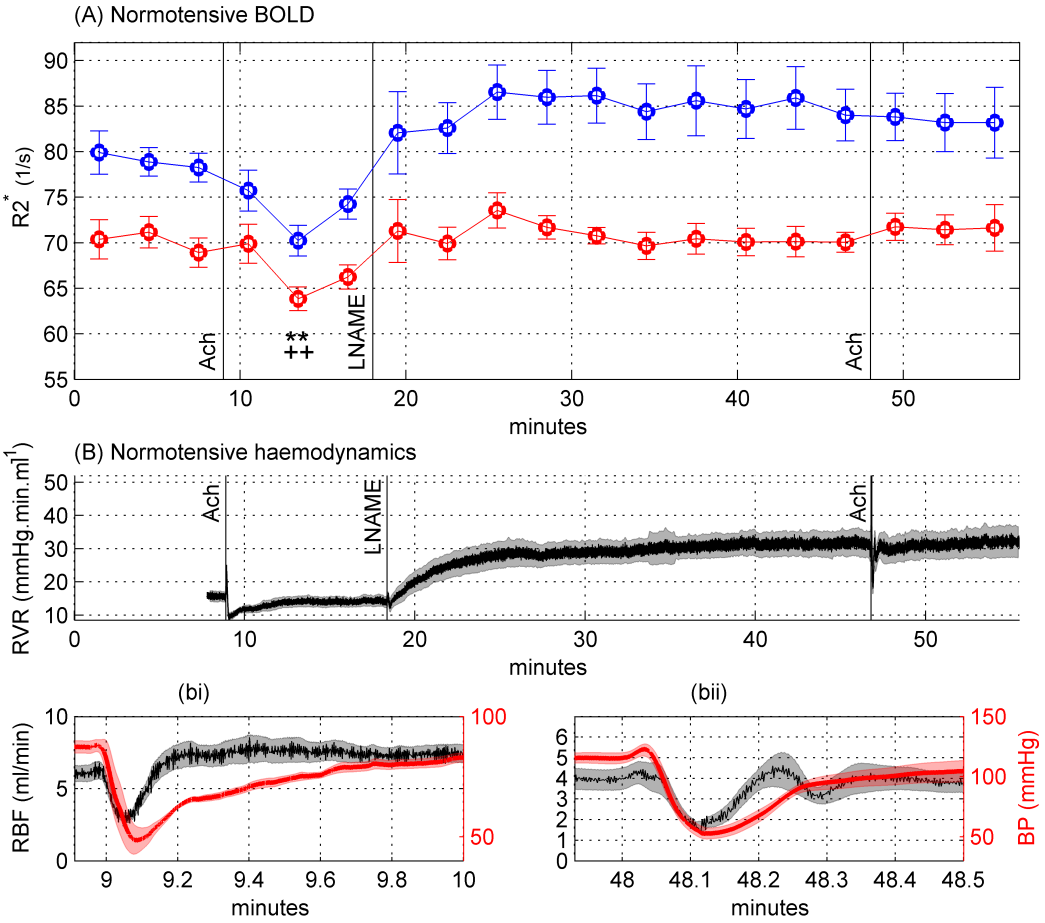

Figure 5.4: Control BOLD MRI and Renal Haemodynamic Data. - Acetylcholine exerts a non-heamodynamic NO-dependent R2* effect in the normotensive kidney. (A) R2* trace measured over scanning protocol. (B) Renal vascular resistance (RVR) haemodynamic study following protocol time course and zoomed in regions around first ACh dose (bi) and ACh following LNAME (bii) where BP (red) and RBF (black). **P<0.01 medulla versus baseline, ††P<0.01 cortex versus baseline

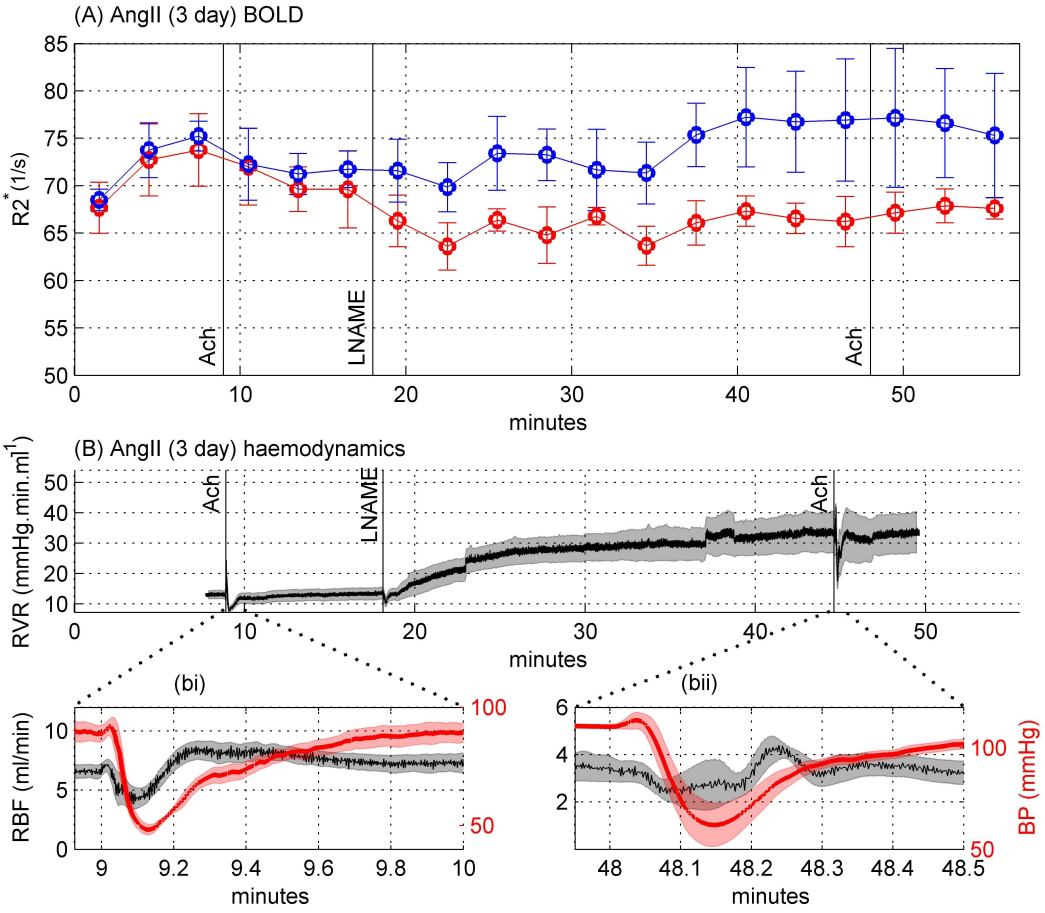

Figure 5.5: Renal BOLD MRI and Haemodynamic Analysis After 3 Day ANG II infusion. - A: R2* trace measured by k-means clustering, red line(cluster 1) and blue line (cluster 2) signal. B: renal vascular resistance (RVR) haemodynamic study following protocol time course and insert showing ACh (bi) or L-NAME (bii) trace with blood pressure (black line) and RBF (red line).

mapped to discrete anatomical regions of the kidney (see Fig.5.6 for example images). This suggests that a short exposure to ANG II disrupts the oxygenation gradient through the kidney, creating areas of high and low pO_2 in both cortex and medulla. As stated previously, the R2* signal actually reflects oxygenation of red blood cells and thus altered patterns of renal perfusion may also account for the disrupted gradient. However this effect appeared transient since rats scanned following 6 days of ANG II infusion, the baseline scan regions became once again more distinct (suggesting a re-establishment of pO_2 gradient in the kidney) whilst the effects of ACh and L-NAME on the R2* signal remained impaired (Fig 5.7).

5.3.2 Study 2: Effect of P2X7 and P2X4 antagonism on renal BOLD signal

In control animals two compartments of distinct mean R2* intensities were created (cluster 1 = 60.21±1.38; cluster 2 = 67.61±1.68; means±SE; n = 18 scans in 6 rats; $P<0.05$). Acute injection of BBG produced no observable effect in normotensive animals (Fig.5.8A). Following 2 week ANG II infusion clustering analysis found distinct clusters (cluster 1 = 65.75±3.20; cluster 2 = 75.56±4.89; means±SE; n = 18 scans in 6 rats; $P<0.01$). Following 2 week ANG II infusion, injection of BBG produced an observable decrease in renal R2*(Fig.5.8B).

The variance of Study 2 was a factor of $\sim 1x10^6$ lower than that observed in Study 1 ($2.44x10^6$ v.s. 0.04; Study 1 v.s. Study 2 respectively). To clarify whether this reduced variability was weighted towards the 'high' or 'low' T2* values it was necessary to construct histograms of both studies. For clarity these hitograms have been overlapped to demonstrate that the reduced variability in fact translated into a reduced number of observed intensities over most of the distribution (Fig.5.9). This might be interpreted as reduced overall T2* signal within Study 2 (compared with Study 1) rather than simply a weighting (or skewed distribution) towards a smaller T2* range.

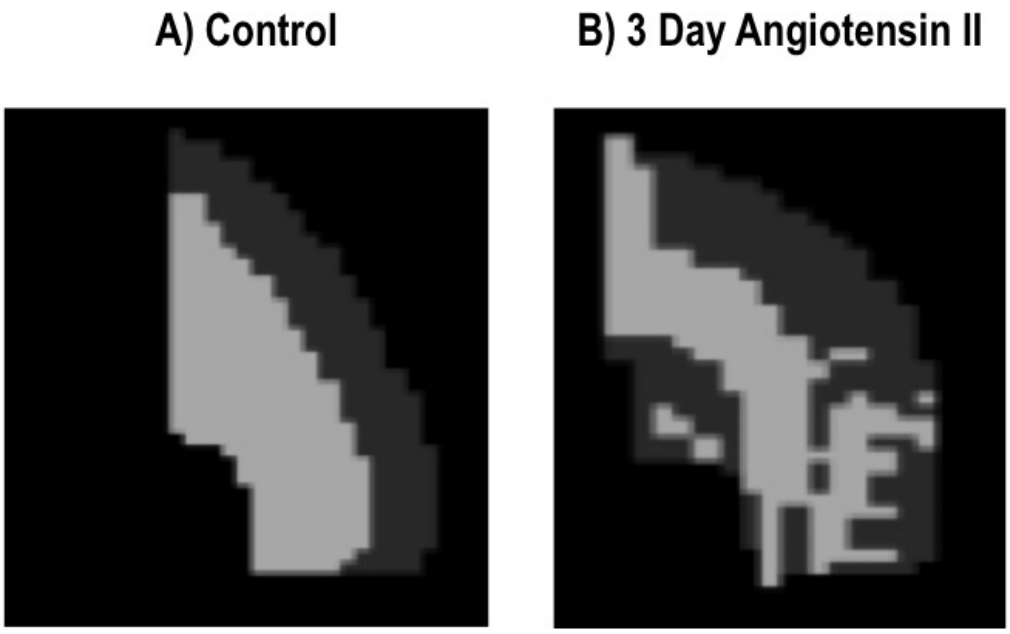

Figure 5.6: Anatomical Heterogeneity of Renal BOLD Signal After 3 Day ANG II Infusion. - Exemplar clustering analysis in manually delineated renal quadrants of rat kidney under control conditions (A) and following ANG II infusion (B). The k-means clustering was used to segment data on a quantitative basis into low (dark grey) and high (light grey) R2* clusters. In control conditions, these clusters mapped to anatomical regions; following ANG II infusion, the spatial relationship between similar R2* values was less well defined

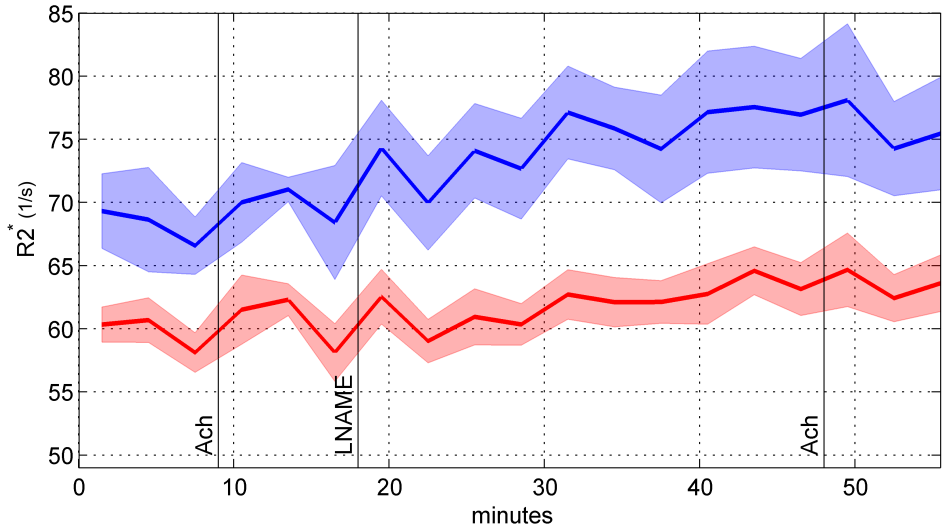

Figure 5.7: Renal BOLD MRI After 6 Day ANG II infusion. - R2* trace measured by k-means clustering, red line(cluster 1) and blue line (cluster 2) signal. Shaded regions for both traces are mean±SEM over the entire trace to highlight the distinct clustering achieved.

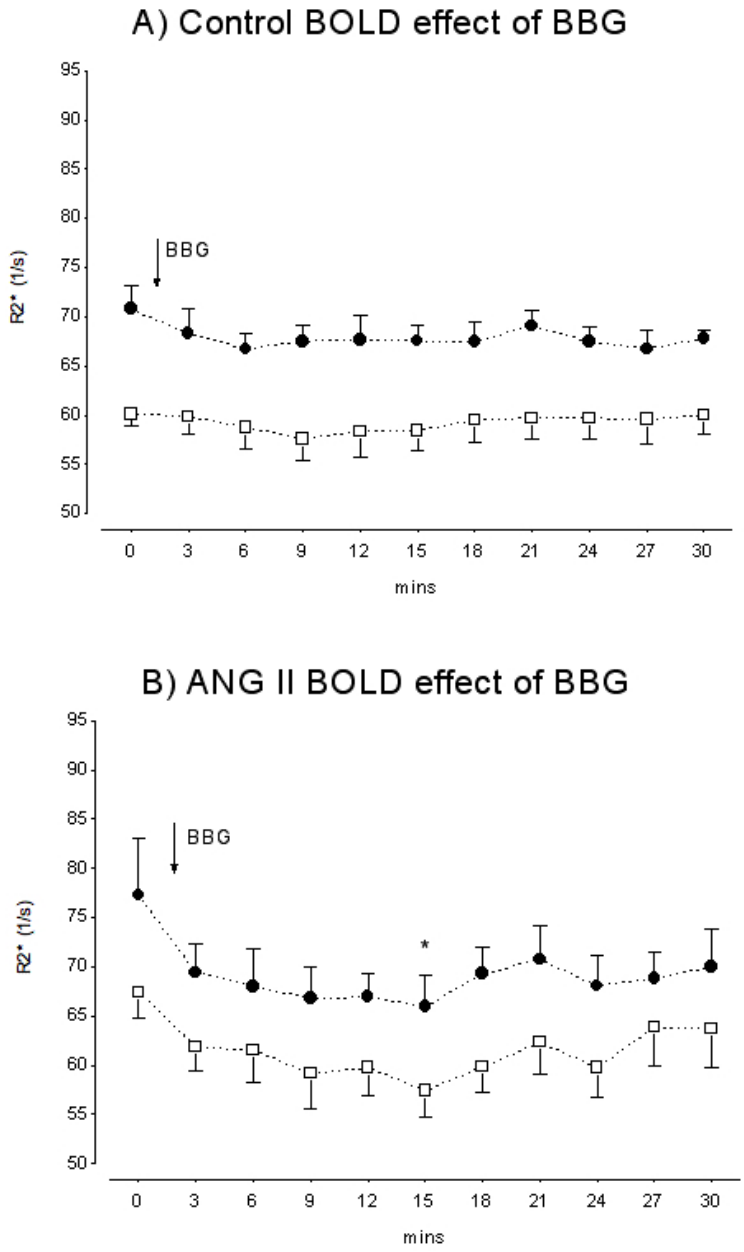

Figure 5.8: R2* Effect of P2X7 and P2X4 Antagonism - (A) Control (B) ANG II infusion. Arrow indicates time point of BBG injection. Data are presented as mean±SE; cluster 1 data (open squares); cluster 2 data (closed circles). Statistical testing performed by 2-way ANOVA with Bonferroni post-hoc testing *P<0.05

Figure 5.9: Histogram of T2* Maps - Control (n=6) and ANG II infused (n=6) rats from Study 1 and Study 2 (19 scans/rat) were used to construct this histogram of T2* maps. Cropped images from the analysis pipeline were selected to ensure most of the signal was from the kidney. X-axis represents the relative bin values in relative (or arbitrary) units, bins were mapped to the distribution data ensuring equivalent bin size was constructed for the two independent data sets, allowing for visual comparison. Y-axis shows number of observations or 'frequency'.

5.4 Discussion

BOLD MRI is an attractive tool for clinical research since it does not require exogenous contrast agents which can be nephrotoxic and has a rapid acquisition time (154). BOLD MRI is increasingly used to quantify renal oxygenation in a variety of disease settings and studies typically focus on the medulla, which is vulnerable to hypoxic insult. Hypoxia of the cortex is also evident in severe renovascular disease (155) and in diabetic and non-diabetic CKD (309) . A global map of renal R2* could therefore be a valuable diagnostic/prognostic tool for ischemic renal disease. However, the relationship between R2* and tissue hypoxia is complex (312). R2* reports oxygenation of the red blood cells and the signal reflecting local perfusion, is also influenced by pH and hydration status. In CKD, BOLD MRI studies have produced conflicting data (328, 541). This partially reflects the complexity of CKD; the future diagnostic utility of renal BOLD MRI is nevertheless contentious (210).

One major challenge for the field is standardization of protocols, particularly for post-processing, that would facilitate meaningful cross-comparison of data sets. Most studies quantify renal oxygenation by measuring R2* signal intensity in small manually selected ROI. A strength of this approach is that the generation of time-series data is based firmly on anatomical knowledge of renal structure. Reliable placement can be difficult, however, and averaging across several ROI can mask the heterogeneity of oxygenation. Importantly, the ROI approach discards from analysis much of the biological information contained within an image and the power of BOLD MRI to assess renal oxygenation on a global scale is often underexploited.

5.4.1 Clustering analysis of renal BOLD MRI data

Data-led segmentation of datasets has previously been used for analysis of brain (55) and kidney (107, 551) MRI. The proposed method here offers two differences. First, each cluster is defined from time series since voxel variation in time is informative and more easily controlled than maps defined in a separate computed tomography scanner where renal orientation might be difficult to replicate. Second, distinct and separate cortical and medullary R2* distributions are not necessary to define by different distribution functions or otherwise. Semi-automated post-acquisition pipeline for analysis of BOLD MRI images using k-means (where k=2) clustering assigned individual voxels into one of two statistically distinct compartments. The advantages of the method are that it: i) does not require user-led selection of small anatomical ROI but rather a gross quadrant of the whole kidney to be segregated into two compartments in a user-independent manner; ii) obviates the need for voxel-tracking through a time-series stack; iii) is anatomically

unbiased, identifying on a global scale clusters of pO_2 homogeneity for each patient or experimental subject.

This study has clinical relevance: a recent study, averaging R2* across multiple ROI, demonstrated cortical hypoxia in a small number of CKD patients (309). The effect size was small and the variation large, suggesting that constraints of statistical power will make comparisons of absolute R2* across patients and between studies difficult (328, 541). Qualitatively, Manotham and colleagues noted that the R2* signal was more heterogeneous and liable to rapid decay in CKD patients than in controls (309). This suggests that global disruption of a spatially constrained pO_2 gradient may be a hallmark of the defects in oxygenation associated with renal injury. The present study partially supports this notion. However the disruption of pO_2 gradient (3 day ANG II) was transient and not observed 3 days later (6 day ANG II). This limits the utility of pO_2 gradient mapping as a diagnostic tool.

Acutely, NO bioavailability was manipulated pharmacologically. The manoeuvres were designed to change whole kidney blood flow, either rapidly and reversibly with acetylcholine, or with sustained effect through nitric oxide synthesis inhibition, without altering autoregulatory capacity (28). Chronically ANG II was infused to cause a change in R2*: over this time frame there would be no major change in renal vascular resistance but an increase in renal tubular sodium reabsorption (11, 508, 548). These complimentary experiments provided the means to dissect the physiologically complex R2* signal, resolving the influence of nitric oxide bioavailability and renal blood flow.

Acute administration of ANG II causes a rapid increase in R2* in healthy subjects, attributed to a fall in renal perfusion (439). Conversely, acute blockade of AT1 receptors increases pO_2 in the renal cortex of CKD patients (309). An increase in cortical oxygenation following AT1 receptor blockade has also been observed in normal (370) and hypertensive rats (531), effects attributed to improved blood flow and efficiency of O_2 usage respectively. In Study 1, a 3-day infusion of ANG II did not increase blood pressure, consistent with previous data (70) and gross renal blood flow was unchanged. Tubular sodium reabsorption is increased within this time-frame (11, 548), and there was evidence for disruption of the regional homogeneity of pO_2. This may reflect a local mismatch of delivery/consumption or a reduction in the efficiency of O_2 utilization, as reported in the ANG II-dependent Goldblatt model (531).

Most MRI scanners are not calibrated directly for pO_2. The absolute R2* value is often therefore less informative for cross-comparison than is the dynamic response to manoeuvres affecting perfusion or sodium transport. In this study, injection of acetylcholine suppressed the R2* signal throughout the kidney. This was probably not dependent on whole kidney perfusion, there being temporal

separation between the reduction in blood flow and the reduction in R2*. The attenuation of R2* was dependent on NO generation, being inhibited by L-NAME, and had a delayed onset, being evident only in the second scan post injection. A previous study also reported no immediate effect of NO on R2* intensity (439).

NO reacts irreversibly with both oxy- and deoxyhaem moieties (113). These reactions are rapid and hemoglobin and deoxyhemoglobin levels should be equivalently affected over each three minute BOLD scan. Reduced R2* therefore might indicate an NO-dependent increase in pO_2 throughout the kidney, most probably reflecting inhibition of tubular sodium transport (145). The effect of acetylcholine was lost following 3 day ANG II infusion. Prolonged exposure to ANG II causes oxidative stress in rats (281) and these data plausibly reflect accumulation of superoxide anion leading to NO deficiency and defects in renal oxygenation (530).

There are two important limitations. First, it was not possible to measure renal blood flow and BOLD signal simultaneously. The invasive surgery required for Doppler measurements of renal arterial blood flow also mean that measurements were not made in the same animals: repeated R2* measurements were instead obtained in a longitudinal study. Second, the BOLD MRI and renal blood flow data were obtained under differing anaesthetic regimens. Maintenance of anaesthesia within the MRI scanner required ECG monitoring under gas anaesthesia (Isoflurane) while stability of renal perfusion following the invasive abdominal surgery is best obtained with a long-lasting barbiturate (517). Renal haemodynamics may be differentially affected by the anaesthetics but it unlikely that this accounts for the temporally distinct dynamic response to acetylcholine of the R2* signal and blood flow.

This study presents the development of an anatomically unbiased method for the assessment of renal function by BOLD MRI, employing signal analysis to remove errors inherent in manual ROI selection. These data indicate that protocols assessing the dynamic response of R2* to acetylcholine can provide information relating to renal NO bioavailability and offer temporal insight into renal oxygenation homeostasis. Data presented in this study have been published (324). A reprint is included in Appendix B, section 8.2.

5.4.2 The effect of P2X7 and P2X4 antagonism on renal oxygenation

Under control conditions acute injection of BBG had no effect on renal R2* signal. This result was surprising because during constant acute infusion BBG caused a significant decrease in blood pressure (Figs.3.8 & 3.9). There are several possible explanations for this; 1) this was a consequence of the lower total dose of BBG injected in the present study, 2) there was activation of an unknown compensatory

mechanism maintaining constant oxygenation while perfusion is significantly reduced or 3) the loss of BOLD MRI signal in the second study reduced the sensitivity of the BOLD signal. Signal intensity was indeed weaker in Study 2 and the distribution of intensities (indicated by the histrogram) was also reduced. Loss of signal might have limited the sensitivity of Study 2 to both the clustering approach and acute pharmacological manoeuvres.

Following ANG II infusion BBG induced a transient decrease in renal R2* signal. This result suggests that P2X7 and P2X4 receptors mediate renal perfusion/oxygenation following over activation of the RAS. Furthermore these data are consistent with the renal functional studies which demonstrated improved pressure-natriuresis following acute BBG infusion in chronically ANG II infused F344 rats (chapter 4, section 4.3.3).

ATP activated P2X receptors are indeed implicated in disease progression (35, 255). Local hypoxia can induce cellular ATP release from several cell types including erythrocytes (31) and endothelial cells (48) where P2X7 and P2X4 receptors are expressed. The present study has demonstrated that P2X7 and P2X4 receptor activation is associated with hypoxia. Eventually this will lead to inflammation and CKD progression (69, 512) suggesting these P2X receptors could be promising therapeutic targets.

6
GENERAL DISCUSSION

The starting point of this research was to mine a renal microarray in order to identify genes contributing to differential susceptibility to hypertensive vascular injury. This result, although limited to protein encoding genes, used an unbiased comparative approach. *Ace* was the top ranked gene by this approach, consistent with previous research published from this laboratory using alternative strategies where both the validity of the microarray and expression of *Ace* was validated (295). The injury susceptible F344 background had higher renal ACE concentration, lower concentration of the anti-inflammatory tetrapeptide N-acetyl-Ser-Asp-Lys-Pro (Ac-SDKP) and showed a greater blood pressure increase following exposure to I3C. All of these differences likely contributed to the modifying effect of *Ace* and this was not investigated further here.

P2x7 and *P2x4* genes were identified as the next top ranking hits for injury susceptibility (Fig.6.1). The molecular physiological approaches described in this thesis provide compelling data for functional expression of these receptors in the renal vasculature. F344 rats had higher expression of P2X7 and P2X4 receptors at the genetic and protein levels. P2X7 and P2X4 receptors were identified on the vascular endothelium. In smooth muscle cells the vascular contractile responses to ATP have been largely attributed to P2X1 receptors (216). In the endothelium P2X4 receptors are the most abundantly expressed, followed by P2X7 ($\sim$50%) and then by P2Y1 and P2Y2 ($\sim$20%) receptors (544). A similar profile is observed in endothelial cells cultured from the mouse pulmonary artery (545) and P2X4 and P2X7 receptors have also been immunolocalised to the endothelium of the larger renal arteries of the rat (287).

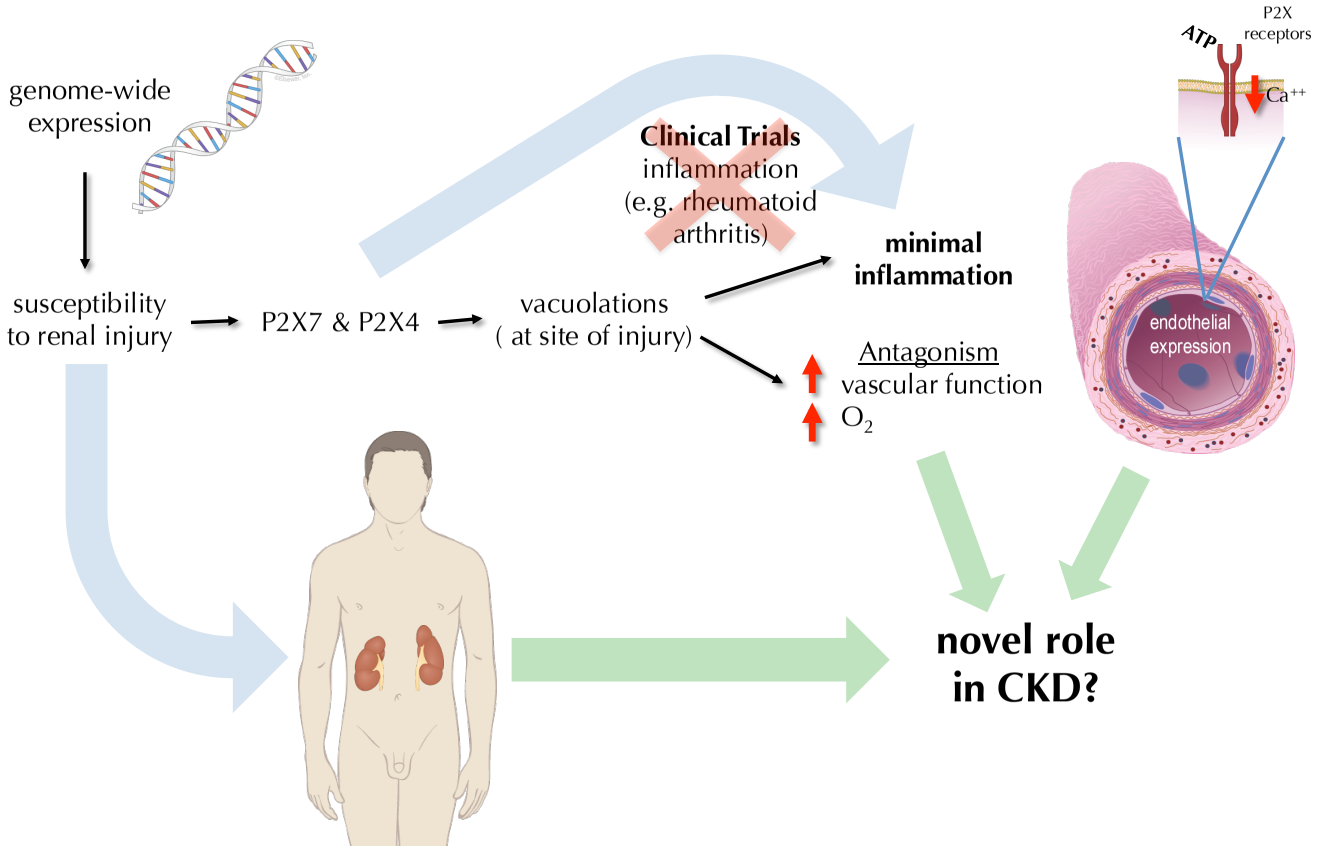

Figure 6.1: Working Hypothesis - P2X7 and P2X4 receptors in CKD.

However, the P2X7 receptor is most highly expressed on macrophages (533). Chronic activation results in the release of interleukin 1 beta (IL-1β) amongst other cytokines (116, 292) and eventually causes cell death. P2X7 facilitates these processes through association of its long c-terminal tail with membrane pores, such as pannexin-1 (399), making it unique amongst the P2X receptor family. P2X4 receptors can also activate pro-inflammatory cascades (247, 502). Acute infusion of BBG, under surgical conditions, was selected over chronic treatment to cause a functional response attributable to the receptors expressed in the vasculature. Using this approach it was identified that P2X7 and P2X4 may contribute to the normal control of renal arterial resistance of the F344 strain. BBG is 1000 times more selective for the P2X7 receptor then P2X4 (227). These receptors therefore cannot be separated pharmacologically with BBG, however, their expression was distinct and appeared on separate cell types of the renal medulla. P2X7 staining was observed in the vasa recta of F344, but not Lewis, rats. One explanation of the renal functional response of F344 to BBG infusion could be a direct consequence of this since the vasa recta plays a key role in the pressure-natriuresis mechanism (80). P2X7-mediated contractions have been also demonstrated in human saphenous veins (57) and indeed the renal vasa recta (84), although contraction of the renal vasa recta was entirely attributed to pericytes. P2X4 was not expressed on the vasa recta. Together these data implicate P2X7 receptors expressed on the vasa recta in mediating the pressure-natriuresis seen in F344 rats.

To investigate the role of blood pressure *per se*, antagonism of P2X7 and P2X4 in the F344 strain was investigated following ANG II infusion. ANG II has been shown to increase expression of P2 receptors (132, 549) however this was not observed here likely because the dose of ANG II selected did not cause overt hypertension or injury. Acute BBG infusion did however significantly improved the pressure-natriuresis relationship of chronically ANG II infused F344 rats.

Further evidence supporting the role of the P2X7 receptor in the functional data described here is found in gene deleted mice: P2X4 deficiency is not protective whilst P2X7 deficiency is. *P2x4*$^{-/-}$ mice have impaired endothelial-dependent vascular function (545). *P2x7*$^{-/-}$ mice infused with deoxycorticosterone acetate (DOCA) salt develop more profound hypertension and renal injury compared to DOCA salt infused controls (226) and are partially protected from experimental glomerulonephritis (488). BBG has also been used to ameliorate renal injury and hypertension in Dahl salt sensitive rats (225). Together these studies implicate P2X7 in the initiation of a cascade of profibrotic events (Fig.6.1).

The encoding gene for P2X7 transcribes a large number of splice variants with reportedly different functionality (467, 542) which may also contribute to contrasting vasoactive effects in different strains of rat as observed here. The P2X7 antibody used in the present study binds to the c-terminal region (epitope: 576-

595) which would exclude the detection of truncated forms of the receptor (311). In humans *P2X4* and *P2X7* are located within 130kb of each other on chromosome 12. These genes can be regulated independently: the endothelial expression of P2X4 receptors in the human aorta is increased following injury; P2X7 receptor expression is not affected (410). It is possible, however, that these receptors have common promotor elements. Physiological interactions between the receptors are postulated (83) and the locus is associated with human disease. For example, a SNP in the first intron of *P2x7* is strongly associated with elevated blood pressure (392) and a loss-of-function SNP in the *P2x7* coding region associates with protection against ischemic stroke (150). Similarly, a loss of function SNP in the P2X4 receptor has been associated with increased pulse pressure (478).

Two separate clinical trials have targeted P2X7 in rheumatoid arthritis (254, 394) and were unsuccessful in ameliorating the symptoms of this disease compared with current treatment (methotrexate). Loss of function receptor variants might explain these observations since stratification was not performed. However, this thesis has also identified a novel vascular role of P2X7. This suggests that targeting P2X7 before the onset of overt inflammation and fibrosis might improve clinical outcomes of CKD (Fig.6.1).

There are at least two broadly important avenues for future research. Firstly refinement of the physiological methods discussed here by both improved pharmacology (using pharmaceutical industry prepared compounds) as well as *in vitro* studies on isolated vascular beds (for example using wire myography for the preglomerular endothelial P2X receptor function) will further refine the molecular mechanism(s) of independent P2X7 and/or P2X4 receptor activation. Secondly, investigating whether P2X receptor sequence differences between the rat strains studied here exist and might account for loss/gain of receptor function will further explain the renal functional data. Furthermore the availability of P2X7 antagonists for human studies presents a strong translational potential for this research.

In conclusion this thesis indicates that P2X7 activation impairs renal perfusion, the pressure-natriuresis response and reduced oxygenation. In combination with the well defined roles of P2X7 on macrophages these data indicate that P2X7 is central to the cascade of pro-fibrotic events (Fig.6.1) and is an attractive target in CKD.

References

[1] Abbracchio, M. P., Burnstock, G., Boeynaems, J.-m., Barnard, E. A., Kennedy, C., Knight, G. E., Fumagalli, M., Gachet, C., Jacobson, K. A., and Weisman, G. A. **International Union of Pharmacology LVIII : Update on the P2Y G Protein-Coupled Nucleotide Receptors : From Molecular Mechanisms and Pathophysiology**. *Pharmacological Reviews*, **58**(3):281–341, 2006. (page 29).

[2] Abu-Amarah, I., Bidani, A. K., Hacioglu, R., Williamson, G. A., and Griffin, K. A. **Differential effects of salt on renal hemodynamics and potential pressure transmission in stroke-prone and stroke-resistant spontaneously hypertensive rats.** *American journal of physiology. Renal physiology*, **289**:F305–13, 2005. (page 47).

[3] Aerts, S., Lambrechts, D., Maity, S., Van Loo, P., Coessens, B., De Smet, F., Tranchevent, L.-C., De Moor, B., et al. **Gene prioritization through genomic data fusion.** *Nature biotechnology*, **24**(5):537–44, 2006. (page 22).

[4] Aerts, S., Vilain, S., Hu, S., Tranchevent, L.-C., Barriot, R., Yan, J., Moreau, Y., Hassan, B. a., and Quan, X.-J. **Integrating computational biology and forward genetics in Drosophila.** *PLoS genetics*, **5**(1):e1000351, 2009. (page 22).

[5] Ahmad, U., Saleheen, D., Bokhari, A., and Frossard, P. M. **Strong association of a renin intronic dimorphism with essential hypertension.** *Hypertension Research*, **28**(4):339–44, 2005. (page 17).

[6] Akbar, M., Okajima, F., Tomura, H., Shimegi, S., and Kondo, Y. **A single species of A1 adenosine receptor expressed in Chinese hamster ovary cells not only inhibits cAMP accumulation but also stimulates phospholipase C and arachidonate release.** *Molecular pharmacology*, **45**(5):1036–42, 1994. (page 29).

[7] Alderman, M. H. and Cohen, H. W. **The IOM Report Fails To Detect Evidence to Support Dietary Sodium Guidelines.** *American journal of hypertension*, **26**(10):1198–200, 2013. (page 4).

[8] Alexander, B. T. **Fetal programming of hypertension.** *Am J Physiol Regul Integr Comp Physiol*, **290**(1):R1–R10, 2006. (page 1).

[9] Anderson, S., Meyer, T. W., Rennke, H. G., Brenner, B. M., Troy, J. L., Degraphenried, R. L., Noddin, J. L., Nunn,

A. W., and Sandstrom, D. **Control of Glomerular Hypertension Limits Glomerular Injury in Rats with Reduced Renal Mass**. *Journal of Clinical Investigation*, **76**:612–619, 1985. (page 62).

[10] Arendshorst, W. J., Brännström, K., and Ruan, X. **Actions of angiotensin II on the renal microvasculature.** *Journal of the American Society of Nephrology : JASN*, **10 Suppl 1**:S149–61, 1999. (page 6).

[11] Ashek, A., Menzies, R. I., Mullins, L. J., Bellamy, C. O. C., Harmar, A. J., Kenyon, C. J., Flatman, P. W., Mullins, J. J., and Bailey, M. a. **Activation of thiazide-sensitive cotransport by angiotensin II in the cyp1a1-Ren2 hypertensive rat.** *PloS one*, **7**(4):e36311, 2012. (pages 16, 18, 19, 21, 62, 63, 82).

[12] Atlas, S. a. **The renin-angiotensin aldosterone system: pathophysiological role and pharmacologic inhibition.** *Journal of managed care pharmacy : JMCP*, **13**(8 Suppl B):9–20, 2007. (page 13).

[13] Aukland, K. **Myogenic mechanisms in the kidney.** *Journal of hypertension. Supplement : official journal of the International Society of Hypertension*, **7**(4):S71–6; discussion S77, 1989. (page 6).

[14] Azizan, E. a. B., Poulsen, H., Tuluc, P., Zhou, J., Clausen, M. V., Lieb, A., Maniero, C., Garg, S., et al. **Somatic mutations in ATP1A1 and CACNA1D underlie a common subtype of adrenal hypertension.** *Nature genetics*, **45**(9):1055–60, 2013. (page 2).

[15] Bailey, M. a., Hillman, K. a., and Unwin, R. J. **P2 receptors in the kidney.** *Journal of the autonomic nervous system*, **81**(1-3):264–70, 2000. (page 29).

[16] Bailey, M. a., Giebisch, G., Abbiati, T., Aronson, P. S., Gawenis, L. R., Shull, G. E., and Wang, T. **NHE2-mediated bicarbonate reabsorption in the distal tubule of NHE3 null mice.** *The Journal of physiology*, **561**(Pt 3):765–75, 2004. (pages 12, 29).

[17] Bailey, M. A. and Shirley, D. G. **Effects of extracellular nucleotides on renal tubular solute transport.** *Purinergic signalling*, **5**:473–80, 2009. (page 31).

[18] Bailey, M. a., Unwin, R. J., and Shirley, D. G. **P2X receptors and kidney function**. *Wiley Interdisciplinary Reviews: Membrane Transport and Signaling*, **1**(4):503–511, 2012. (pages 31, 44, 45).

[19] Bailie, M. D., Rector, F. C., and Seldin, D. W. **Angiotensin II in arterial and renal venous plasma and renal lymph in the dog.** *The Journal of clinical investigation*, **50**(1):119–26, 1971. (page 17).

[20] Balmforth, A. J., Bryson, S. E., Aylett, J., Warbur-

ton, P., Ball, S. G., Pun, K.-t., Middlemiss, D., and Drew, M. **Comparative pharmacology of recombinant rat AT1A , ATIB and human AT1 receptors expressed by transfected COS-M6 cells**. *Br. J. Pharmacol*, **112**:277–281, 1994. (page 16).

[21] Bankir, L., Bochud, M., Maillard, M., Bovet, P., Gabriel, A., and Burnier, M. **Nighttime blood pressure and nocturnal dipping are associated with daytime urinary sodium excretion in African subjects.** *Hypertension*, **51**(4):891–8, 2008. (page 62).

[22] Barker, D. J. P., Osmond, C., Golding, J., Kuh, D., and Wadsworth, M. E. J. **Growth in utero , blood pressure in childhood and adult life , and mortality from cardiovascular disease**. *BMJ*, **298**:564–567, 1989. (page 62).

[23] Barker, D., Gluckman, P., Godfrey, K., Harding, J., Owens, J., and Robison, J. **Fetal nutrition and cardiovascular disease in adult life.** *Lancet*, **341**(8857):1421–2, 1993. (page 1).

[24] Basson, J., Simino, J., and Rao, D. C. **Between candidate genes and whole genomes: time for alternative approaches in blood pressure genetics.** *Current hypertension reports*, **14**(1):46–61, 2012. (page 3).

[25] Bateson, W. and Saunders, E. **Experimental studies in the physiology of heredity**. *Reports to the Evolution Committee of the Royal Society*, **2**:1–55, 80–99, 1905. (page 3).

[26] Baum, A., Pohlmeyer, G., Rapp, K. G., and Deerberg, F. **Lewis rats of the inbred strain LEW/Han: life expectancy, spectrum and incidence of spontaneous neoplasms.** *Experimental and toxicologic pathology : official journal of the Gesellschaft für Toxikologische Pathologie*, **47**(1):11–8, 1995. (page 18).

[27] Beard, D. A. **Tautology vs. Physiology in the Etiology of Hypertension.** *Physiology (Bethesda, Md.)*, **28**(5):270–1, 2013. (page 4).

[28] Beierwaltes, W. H., Sigmon, D. H., and Carretero, O. A. **Endothelium modulates renal blood flow but not autoregulation**. *Am J Physiol Renal Fluid Electrolyte Physiol*, **262**:F943–F949, 1992. (page 82).

[29] Bell, P. D., Lapointe, J.-Y., Sabirov, R., Hayashi, S., Peti-Peterdi, J., Manabe, K.-I., Kovacs, G., and Okada, Y. **Macula densa cell signaling involves ATP release through a maxi anion channel.** *Proceedings of the National Academy of Sciences of the United States of America*, **100**(7):4322–7, 2003. (page 6).

[30] Benediktsson, R., Lindsay, R. S., Noble, J., Seclkl, J. R.,

and Edwards, C. R. W. **Glucocorticoid exposure in utero: new model fro adult hypertension**. *Lancet*, **341**:339–341, 1993. (page 1).

[31] Bergfeld, G. R. and Forrester, T. **Release of ATP from human erythrocytes in response to a brief period of hypoxia and hypercapnia**. *Cardiovascular Res*, **26**:40–47, 1992. (page 84).

[32] Beuschlein, F., Boulkroun, S., Osswald, A., Wieland, T., Nielsen, H. N., Lichtenauer, U. D., Penton, D., Schack, V. R., et al. **Somatic mutations in ATP1A1 and ATP2B3 lead to aldosterone-producing adenomas and secondary hypertension.** *Nature genetics*, **45**(4):440–4, 444e1–2, 2013. (page 2).

[33] Bichet, D. G. **Hereditary polyuric disorders: new concepts and differential diagnosis.** *Seminars in nephrology*, **26**(3):224–33, 2006. (page 9).

[34] Bidani, A. K., Polichnowski, A. J., Loutzenhiser, R., and Griffin, K. a. **Renal microvascular dysfunction, hypertension and CKD progression.** *Current opinion in nephrology and hypertension*, **22**(1):1–9, 2012. (page 62).

[35] Birch, R. E., Schwiebert, E. M., Peppiatt-Wildman, C. M., and Wildman, S. S. **Emerging key roles for P2X receptors in the kidney.** *Frontiers in physiology*, **4**(September):262, 2013. (page 84).

[36] Bishop, C. M. *Pattern Recognition and Machine Learning*. New York: Springer, 2006. (page 70).

[37] Blasi, E. R., Rocha, R., Rudolph, A. E., Blomme, E. a. G., Polly, M. L., and McMahon, E. G. **Aldosterone/salt induces renal inflammation and fibrosis in hypertensive rats.** *Kidney international*, **63**(5):1791–800, 2003. (page 63).

[38] Bloom, J. S., Ehrenreich, I. M., Loo, W. T., Lite, T.-L. V. o., and Kruglyak, L. **Finding the sources of missing heritability in a yeast cross.** *Nature*, **494**(7436):234–7, 2013. (page 4).

[39] Boron, W. F. and Boulpaep, E. L. *Medical Physiology: A Cellular and Molecular Approach*. Elsevier/Saunders, 2003. (page 14).

[40] Bowman, W. **On the Structure and Use of the Malpighian Bodies of the Kidney, with Observations on the Circulation through That Gland**. *Philosophical Transactions of the Royal Society of London*, **132**:57–80, 1842. (page 5).

[41] Braam, B., Mitchell, D., Koomans, H. A., and Navar, L. G. **Relevance of the Tubuloglomerular Feedback Mechanism in Pathophysiology**. *J Am Soc Nephrol*, **4**:1257–1274, 1993. (page 6).

[42] Brantsma, A. H., Bakker, S. J. L., de Zeeuw, D., de Jong, P. E., and Gansevoort, R. T. **Urinary albumin excretion as a predictor of the development of hypertension in the general population.** *Journal of the American Society of Nephrology : JASN*, **17**(2):331–5, 2006. (page 62).

[43] Brenner, B. M., Garcia, D. L., and Anderson, S. **Glomeruli and blood pressure. Less of one, more the other?** *American Journal of Hypertension*, **1**:335–347, 1988. (page 62).

[44] Brezis, M. and Rosen, S. **Hypoxia of the renal medulla - its implications for disease**. *New England Journal of Medicine*, **332**(10):647–655, 1995. (page 65).

[45] Brinkmann, J., Heusser, K., Schmidt, B. M., Menne, J., Klein, G., Bauersachs, J., Haller, H., Sweep, F. C., et al. **Catheter-based renal nerve ablation and centrally generated sympathetic activity in difficult-to-control hypertensive patients: prospective case series.** *Hypertension*, **60**(6):1485–90, 2012. (page 12).

[46] Brooks, H. L., Sorensen, a. M., Terris, J., Schultheis, P. J., Lorenz, J. N., Shull, G. E., and Knepper, M. a. **Profiling of renal tubule Na+ transporter abundances in NHE3 and NCC null mice using targeted proteomics.** *The Journal of physiology*, **530**(Pt 3):359–66, 2001. (page 12).

[47] Burnstock, G. **Purinergic Nerves**. *Pharmacological Reviews*, **24**:508–581, 1972. (page 29).

[48] Burnstock, G. **Release of vasoactive substances from endothelial cells by shear stress and purinergic mechanosensory transduction.** *Journal of anatomy*, **194 (Pt 3**:335–42, 1999. (page 84).

[49] Burnstock, G. **Purinergic Signaling and Vascular Cell Proliferation and Death**. *Arteriosclerosis, Thrombosis, and Vascular Biology*, **22**(3):364–373, 2002. (page 64).

[50] Burnstock, G., Campbell, G., Satchell, D., and Smythe, a. **Evidence that adenosine triphosphate or a related nucleotide is the transmitter substance released by non-adrenergic inhibitory nerves in the gut.** *British journal of pharmacology*, **40**(4):668–88, 1970. (page 29).

[51] Burnstock, G. **Vessel tone and remodeling A channel to neurodegeneration**. *Nature medicine*, **12**(1):16–17, 2006. (page 29).

[52] Burnstock, G. and Knight, G. E. **Cellular distribution and functions of P2 receptor subtypes in different systems.** *International review of cytology*, **240**:31–304, 2004. (page 29).

[53] Burson, J. M., Aguilera, G., Gross, K. W., and Sigmund, C. D. **Differential expression of angiotensin receptor 1A and 1B in mouse.** *The American journal*

of physiology, **267**(2 Pt 1):E260–7, 1994. (page 16).

[54] Cachofeiro, V., Goicochea, M., de Vinuesa, S. G., Oubiña, P., Lahera, V., and Luño, J. **Oxidative stress and inflammation, a link between chronic kidney disease and cardiovascular disease.** *Kidney international. Supplement*, **74**(111):S4–9, 2008. (page 63).

[55] Calhoun, V. D., Adali, T., Pearlson, G. D., and Pekar, J. J. **Spatial and temporal independent component analysis of functional MRI data containing a pair of task-related waveforms.** *Human brain mapping*, **13**(1):43–53, 2001. (page 81).

[56] Campbell, D. J. and Habener, J. F. **Angiotensinogen gene is expressed and differentially regulated in multiple tissues of the rat.** *The Journal of clinical investigation*, **78**(1):31–9, 1986. (page 15).

[57] Cario-Toumaniantz, C., Loirand, G., Ladoux, a., and Pacaud, P. **P2X7 Receptor ActivationInduced Contraction and Lysis in Human Saphenous Vein Smooth Muscle**. *Circulation Research*, **83**(2):196–203, 1998. (pages 45, 87).

[58] Carmines, P. K. and Navar, L. G. **Disparate effects of Ca channel blockade on afferent and efferent arteriolar responses to ANG II**. *Am J Physiol Renal Physiol*, **256**:F1015–F1020, 1989. (page 6).

[59] Carretero, O. a. and Oparil, S. **Essential Hypertension : Part I: Definition and Etiology**. *Circulation*, **101**(3):329–335, 2000. (page 1).

[60] Casarini, D. E., Boim, M. A., Stella, R. C., Krieger-Azzolini, M. H., Krieger, J. E., and Schor, N. **Angiotensin I-converting enzyme activity in tubular fluid along the rat nephron.** *The American journal of physiology*, **272**(3 Pt 2):F405–9, 1997. (page 15).

[61] Casellas, D. and Mimran, a. **Shunting in renal microvasculature of the rat: a scanning electron microscopic study of corrosion casts.** *The Anatomical record*, **201**(2):237–48, 1981. (page 6).

[62] Casellas, D., Moore, L. C., and Moore, C. **Autoregulation of intravascular pressure in preglomerular juxtamedullary vessels**. *Am J Physiol Renal Physiol*, **264**:F315–F321, 1993. (page 6).

[63] Casellas, D. and Mimran, A. **Aglomerular pathways in intrarenal microvasculature of aged rats**. *Am J Anat.*, **156**(2):293–299, 1979. (page 6).

[64] Castrop, H., Hocherl, K., Kurtz, A., Schweda, F., Todorov, V., and Wagner, C. **Physiology of Kidney Renin**. *Physiol Rev*, **90**:607–673, 2010. (page 15).

[65] Chai, S. Y., Fernando, R., Peck, G., Ye, S.-Y., Mendelsohn, F. a. O., Jenkins, T. a., and Albiston, a. L. **The angiotensin IV/AT4 receptor.** *Cellular and molecular life sciences : CMLS*, **61**(21):2728–37, 2004. (page 16).

[66] Chan, C. M., Unwin, R. J., Bardini, M., Oglesby, I. B., Ford, a. P., Townsend-Nicholson, a., and Burnstock, G. **Localization of P2X1 purinoceptors by autoradiography and immunohistochemistry in rat kidneys.** *The American journal of physiology*, **274**(4 Pt 2):F799–804, 1998. (pages 29, 31).

[67] Chang, M.-Y., Lu, J.-K., Tian, Y.-C., Chen, Y.-C., Hung, C.-C., Huang, Y.-H., Chen, Y.-H., Wu, M.-S., Yang, C.-W., and Cheng, Y.-C. **Inhibition of the P2X7 receptor reduces cystogenesis in PKD.** *Journal of the American Society of Nephrology : JASN*, **22**(9):1696–706, 2011. (pages 29, 63).

[68] Cheek, D. B. and Perry, J. W. **A salt wasting syndrome in infancy**. *Archives of Disease in Childhood*, **169**(33):252–256, 1957. (page 2).

[69] Chen, K., Zhang, J., Zhang, W., Zhang, J., Yang, J., Li, K., and He, Y. **ATP-P2X4 signaling mediates NLRP3 inflammasome activation: a novel pathway of diabetic nephropathy.** *The international journal of biochemistry & cell biology*, **45**(5):932–43, 2013. (page 84).

[70] Chin, S. Y., Wang, C.-t., Majid, D. S. A., and Navar, L. G. **Renoprotective effects of nitric oxide in angiotensin II-induced hypertension in the rat**. *Renal Physiology*, **274**:F876–F882, 1998. (page 82).

[71] Choate, K. A., Kahle, K. T., Wilson, F. H., Nelson-Williams, C., and Lifton, R. P. **WNK1, a kinase mutated in inherited hypertension with hyperkalemia, localizes to diverse Cl- -transporting epithelia.** *Proceedings of the National Academy of Sciences of the United States of America*, **100**:663–668, 2003. (page 12).

[72] Chobanian, A. V., Bakris, G. L., Black, H. R., Cushman, W. C., Green, L. A., Izzo, J. L., Jones, D. W., Materson, B. J., et al. **The Seventh Report of the Joint National Committee on Prevention, Detection, Evaluation, and Treatment of High Blood Pressure: the JNC 7 report.** *JAMA : the journal of the American Medical Association*, **289**(19):2560–72, 2003. (page 17).

[73] Churchill, P. C., Churchill, M. C., and Bidani, A. K. **Kidney cross transplants in Dahl salt-sensitive and salt-resistant rats**. *Am J Physiol Heart Circ Physiol*, **262**:H1809–H1817, 1992. (page 12).

[74] Coffman, T. M., Himmelstein, S., Best, C., and Klotman, P. E. **Post-transplant hypertension in the rat: effects of captopril and native nephrectomy.** *Kidney international*, **36**(1):35–40, 1989. (page 13).

[75] Cogan, M. G. **Angiotensin II: a powerful controller of sodium transport in the early proximal tubule**. *Hypertension*, **15**(5):451–458, 1990. (page 16).

[76] Cohen, H. J., Marsh, D. J., and Kayser, B. **Autoregulation in vasa recta of the rat kidney**. *Am J Physiol Renal Fluid Electrolyte Physiol*, **14**(8):F32–F40, 1983. (page 8).

[77] Coleman, G. L., Barthold, S. W., Osbaldiston, G. W., Foster, S. J., and Jonas, A. M. **Pathological Changes During Aging in**. *Journal of Gerontology*, **32**(3):258–278, 1977. (page 18).

[78] Conway, B. R., Rennie, J., Bailey, M. a., Dunbar, D. R., Manning, J. R., Bellamy, C. O., Hughes, J., and Mullins, J. J. **Hyperglycemia and renin-dependent hypertension synergize to model diabetic nephropathy.** *JASN*, **23**(3):405–11, 2012. (page 18).

[79] Cornelissen, A. J. M., Dankelman, J., VanBavel, E., and Spaan, J. a. E. **Balance between myogenic, flow-dependent, and metabolic flow control in coronary arterial tree: a model study.** *American journal of physiology. Heart and circulatory physiology*, **282**(6):H2224–37, 2002. (page 5).

[80] Cowley, A. W. **Long-term control of arterial blood pressure.** *Physiological reviews*, **72**(1):231–300, 1992. (pages 8, 64, 87).

[81] Cowley, A. W. **The genetic dissection of essential hypertension.** *Nature reviews. Genetics*, **7**(11):829–40, 2006. (page 3).

[82] Cowley, A. W., Nadeau, J. H., Baccarelli, A., Berecek, K., Fornage, M., Gibbons, G. H., Harrison, D. G., Liang, M., et al. **Report of the National Heart, Lung, and Blood Institute Working Group on epigenetics and hypertension.** *Hypertension*, **59**(5):899–905, 2012. (page 1).

[83] Craigie, E., Birch, R. E., Unwin, R. J., and Wildman, S. S. **The relationship between P2X4 and P2X7: a physiologically important interaction?** *Frontiers in physiology*, **4**(August):216, 2013. (pages 63, 88).

[84] Crawford, C., Kennedy-Lydon, T. M., Callaghan, H., Sprott, C., Simmons, R. L., Sawbridge, L., Syme, H. M., Unwin, R. J., Wildman, S. S. P., and Peppiatt-Wildman, C. M. **Extracellular nucleotides affect pericyte-mediated regulation of rat in situ vasa recta diameter.** *Acta physiologica (Oxford, England)*, **202**(3):241–51, 2011. (pages 45, 87).

[85] Crowley, S. D., Gurley, S. B., Herrera, M. J., Ruiz, P., Griffiths, R., Kumar, A. P., Kim, H.-S., Smithies, O., Le, T. H., and Coffman, T. M. **Angiotensin II causes hypertension and cardiac hypertrophy through its receptors in the kidney.** *Proceedings of the National Academy of Sciences of the United States of America*, **103**:17985–90, 2006. (page 13).

[86] Crowley, S. D., Gurley, S. B., Oliverio, M. I., Pazmino, A. K., Griffiths, R., Flannery, P. J., Spurney, R. F., Kim, H.-s., et al. **Distinct roles for the kidney and systemic tissues in blood pressure regulation by the renin-angiotensin system**. *Journal of Clinical Investigation*, **115**(4):1–8, 2005. (page 13).

[87] Cupples, W. A. and Marsh, D. J. **Autoregulation of blood flow in renal medulla of the rat: no role for angiotensin II.** *Canadian Journal of Physiology and Pharmacology*, **66**:833–836, 1988. (page 8).

[88] Cupples, W. a., Braam, B., and Cupples, W.A. Braam, B. **Assessment of renal autoregulation.** *American journal of physiology. Renal physiology*, **292**(4):F1105–23, 2007. (page 8).

[89] Curtis, J. J., Luke, R. G., Dustan, H. P., Kashgarian, M., Whelchel, J. D., Jones, P., and Diethelm, A. G. **Remission of essential hypertension after renal transplantation.** *The New England Journal of Medicine*, **309**:1009–1015, 1983. (page 13).

[90] Dahl, L. K., Heine, M., and Thompson, K. **Genetic Influence of the Kidneys on Blood Pressure : Evidence from Chronic Renal Homografts in Rats with Opposite Predispositions to Hypertension**. *Circulation*, **34**:94–101, 1974. (page 13).

[91] Dash, R. K., Qi, F., and Beard, D. a. **A biophysically based mathematical model for the kinetics of mitochondrial calcium uniporter.** *Biophysical journal*, **96**(4):1318–32, 2009. (page 143).

[92] Davis, M. J. and Hill, M. a. **Signaling mechanisms underlying the vascular myogenic response.** *Physiological reviews*, **79**(2):387–423, 1999. (page 6).

[93] Dawber, T. R., Kannel, W. B., Revotskie, N., Stokes, J., Kagan, A., and Gordon, T. **Some Factors Associated With The Development of Coronary Heart Disease**. *Am J Public Health Nations Health*, **49**(10):1349–1356, 1959. (page 3).

[94] Dawber, T. R., Meadors, G. F., and Moore, F. E. **Epidemiological Disease : The Approaches to Heart Framingham Study**. *American Journal of Public Health*, **41**:279–286, 1951. (page 3).

[95] de Boer, M. P., Ijzerman, R. G., de Jongh, R. T., Eringa, E. C., Stehouwer, C. D. a.,

Smulders, Y. M., and Serné, E. H. **Birth weight relates to salt sensitivity of blood pressure in healthy adults.** *Hypertension*, **51**(4):928–32, 2008. (page 62).

[96] De Gasparo, M., Catt, K. J., Inagami, T., and Wright, J. W. **International Union of Pharmacology . XXIII . The Angiotensin II Receptors**. *Pharmacological reviews*, **52**(3):415–472, 2000. (page 16).

[97] de Leeuw, P. W. **Nycthemeral relationship between renal function and sodium homeostasis.** *Current hypertension reports*, **13**(2):136–41, 2011. (page 62).

[98] de Zeeuw, D. **Albuminuria, not only a cardiovascular/renal risk marker, but also a target for treatment?** *Kidney international. Supplement*, **66**(92):S2–6, 2004. (page 62).

[99] Deen, P. M., Verdijk, M. A. J., Knoers, N. V. A. M., Wieringa, B., Monnens, L. A. H., van Os, C. H., and van Oost, B. A. **Requirement of human renal water channel aquaporin-2 for vasopressin-dependent concentration of urine**. *Science*, **264**:92–95, 1994. (page 9).

[100] Deng, A. Y. **Genetic basis of polygenic hypertension.** *Human molecular genetics*, **16 Spec No**(2):R195–202, 2007. (page 3).

[101] Denton, D. A., McKinley, M. J., and Weisinger, R. S. **Hypothalamic integration of body fluid regulation.** *Proceedings of the National Academy of Sciences of the United States of America*, **93**(14):7397–404, 1996. (page 4).

[102] Di, A. and Malik, A. B. **TRP channels and the control of vascular function.** *Current opinion in pharmacology*, **10**(2):127–32, 2010. (page 6).

[103] Dickinson, D. P., Gross, K. W., Piccini, N., and Wilson, C. M. **Evolution and variation of renin genes in mice.** *Genetics*, **108**(3):651–67, 1984. (page 15).

[104] Donoghue, M., Hsieh, F., Baronas, E., Godbout, K., Gosselin, M., Stagliano, N., Donovan, M., Woolf, B., et al. **A Novel Angiotensin-Converting Enzyme-Related Carboxypeptidase (ACE2) Converts Angiotensin I to Angiotensin 1-9**. *Circulation Research*, **87**(5):e1–e9, 2000. (page 16).

[105] Dougherty, E. R., Barrera, J., Brun, M., Kim, S., Cesar, R. M., Chen, Y., Bittner, M., and Trent, J. M. **Inference from clustering with Application to gene-expression microarrays**. *Journal of Computational biology*, **9**(1):105–126, 2002. (page 68).

[106] Dzau, V. J. and Herrmann, H. C. **Hormonal control of angiotensinogen production.** *Life sciences*, **30**(7-8):577–84, 1982. (page 15).

[107] Ebrahimi, B., Gloviczki, M., Woollard, J. R., Crane, J. A., Textor, S. C., and Lerman, L. O. **Compartmental Analysis of Renal BOLD MRI Data: Introduction and Validation**. *Invest Radiol*, **47**(3):175–182, 2012. (page 81).

[108] Eckardt, K.-U., Bernhardt, W. M., Weidemann, A., Warnecke, C., Rosenberger, C., Wiesener, M. S., and Willam, C. **Role of hypoxia in the pathogenesis of renal disease.** *Kidney international. Supplement*, **68**(99):S46–51, 2005. (page 65).

[109] Eckardt, K.-U., Coresh, J., Devuyst, O., Johnson, R. J., Köttgen, A., Levey, A. S., and Levin, A. **Evolving importance of kidney disease: from subspecialty to global health burden.** *Lancet*, **382**(9887):158–69, 2013. (page 62).

[110] Egan, T. M., Samways, D. S. K., and Li, Z. **Biophysics of P2X receptors.** *Pflügers Archiv : European journal of physiology*, **452**(5):501–12, 2006. (page 144).

[111] Ehret, G. B. and Caulfield, M. J. **Genes for blood pressure: an opportunity to understand hypertension.** *European heart journal*, **34**(13):951–61, 2013. (page 1).

[112] Ehret, G. B., Munroe, P. B., Rice, K. M., Bochud, M., Johnson, A. D., Chasman, D. I., Smith, A. V., Tobin, M. D., et al. **Genetic variants in novel pathways influence blood pressure and cardiovascular disease risk.** *Nature*, **478**(7367):103–9, 2011. (page 4).

[113] Eich, R. F., Li, T., Lemon, D. D., Doherty, D. H., Curry, S. R., Aitken, J. F., Mathews, a. J., Johnson, K. a., et al. **Mechanism of NO-induced oxidation of myoglobin and hemoglobin.** *Biochemistry*, **35**(22):6976–83, 1996. (page 83).

[114] Elliott, P., Stamler, J., Nichols, R., Dyer, A. R., Stamler, R., and Kesteloot, H. **Intersalt revisited: further analyses of 24 hour sodium**. *British Medical Journal*, **312**(May):1249–1253, 1996. (page 4).

[115] Eltze, M. and Ullrich, B. **Characterization of vascular P2 purinoceptors in the rat isolated perfused kidney.** *European journal of pharmacology*, **306**(1-3):139–52, 1996. (page 31).

[116] Eltzschig, H. K., Sitkovsky, M. V., and Robson, S. C. **Purinergic signaling during inflammation.** *The New England journal of medicine*, **367**(24):2322–33, 2012. (pages 29, 63, 87).

[117] Engler, S., Paul, M., and Pinto, Y. M. **The TGR(mRen2)27 transgenic rat model of hypertension.** *Regulatory peptides*, **77**:3–8, 1998. (page 18).

[118] Eppel, G. a., Jacono, D. L., Shirai, M., Umetani, K., Evans,

R. G., and Pearson, J. T. **Contrast angiography of the rat renal microcirculation in vivo using synchrotron radiation.** *American journal of physiology. Renal physiology*, **296**(5):F1023–31, 2009. (page 5).

[119] Erdos, E. G. **Angiotensin I converting enzyme**. *Circulation Research*, **36**(2):247–255, 1975. (page 15).

[120] Erlinge, D., Yoo, H., Edvinsson, L., Reis, D. J., and Wahlestedt, C. **Mitogenic effects of ATP on vascular smooth muscle cells vs. other growth factors and sympathetic cotransmitters.** *The American journal of physiology*, **265**(4 Pt 2):H1089–97, 1993. (page 64).

[121] Evans, R. G., Gardiner, B. S., Smith, D. W., and O'Connor, P. M. **Methods for studying the physiology of kidney oxygenation.** *Clinical and experimental pharmacology & physiology*, **35**(12):1405–12, 2008. (page 65).

[122] Evans, R. G., Majid, D. S. A., and Eppel, G. A. **MECHANISMS MEDIATING PRESSURE NATRIURESIS : WHAT WE KNOW AND WHAT WE NEED TO FIND OUT**. *Clinical and Experimental Pharmacology and Physiology*, (December 2004):400–409, 2005. (page 8).

[123] Farrugia, E., Lockhart, J. C., and Larson, T. S. **Relation between vasa recta blood flow and renal interstitial hydrostatic pressure during pressure natriuresis**. *Circulation Research*, **71**(5):1153–1158, 1992. (page 8).

[124] Feinleib, M., Garrison, R. J., Fabsitz, R., Christian, J. C., Hrubec, Z., Borhani, N. O., Kannel, W. B., Rosenman, R., Schwartz, J. T., and Wagner, J. O. **The NHLBI twin study of cardiovascular disease risk factors: methodology and summary of results**. *Am J Epidemiology*, **106**(4):284–295, 1977. (page 1).

[125] Féraille, E. and Doucet, a. **Sodium-potassium-adenosinetriphosphatase-dependent sodium transport in the kidney: hormonal control.** *Physiological reviews*, **81**(1):345–418, 2001. (page 9).

[126] Filiopoulos, V. and Vlassopoulos, D. **Inflammatory syndrome in chronic kidney disease: pathogenesis and influence on outcomes.** *Inflammation & allergy drug targets*, **8**(5):369–82, 2009. (page 63).

[127] Fine, L. G., Bandyopadhay, D., and Norman, J. T. **Is there a common mechanism for the progression of different types of renal diseases other than proteinuria? Towards the unifying theme of chronic hypoxia.** *Kidney international. Supplement*, **75**:S22–6, 2000. (page 65).

[128] Fine, L. G., Orphanides, C., and Norman, J. T. **Progressive renal disease: the chronic**

hypoxia hypothesis. *Kidney international. Supplement*, **65**:S74–8, 1998. (pages 64, 65).

[129] Fine, L. G. and Norman, J. T. **Chronic hypoxia as a mechanism of progression of chronic kidney diseases: from hypothesis to novel therapeutics.** *Kidney international*, **74**(7):867–72, 2008. (page 65).

[130] Fox, U. Bianchi, G. **The primary role of the kidney in causing the blood pressure difference between the Milan hypertensive strain (MHS) and normotensive rats**. *Clin Exp Pharmacol Physiol*, **53**:S71–S74, 1976. (page 13).

[131] Franco, M., Bautista, R., Pérez-Méndez, O., González, L., Pacheco, U., Sánchez-Lozada, L. G., Santamaría, J., Tapia, E., Monreal, R., and Martínez, F. **Renal interstitial adenosine is increased in angiotensin II-induced hypertensive rats.** *American journal of physiology. Renal physiology*, **294**(1):F84–92, 2008. (page 64).

[132] Franco, M., Bautista, R., Tapia, E., Soto, V., Santamaría, J., Osorio, H., Pacheco, U., Sánchez-Lozada, L. G., Kobori, H., and Navar, L. G. **Contribution of renal purinergic receptors to renal vasoconstriction in angiotensin II-induced hypertensive rats.** *American journal of physiology. Renal physiology*, **300**(6):F1301–9, 2011. (pages 64, 87).

[133] Franco, V. and Oparil, S. **Salt sensitivity, a determinant of blood pressure, cardiovascular disease and survival.** *Journal of the American College of Nutrition*, **25**:247S–255S, 2006. (page 4).

[134] Franklin, S. S. and Wong, N. D. **Hypertension and cardiovascular disease: contributions of the Framingham heart study**. *Global Heart*, **8**(1):49–57, 2013. (page 1).

[135] Freedman, B. I. and Sedor, J. R. **Hypertension-associated kidney disease: perhaps no more.** *Journal of the American Society of Nephrology : JASN*, **19**(11):2047–51, 2008. (page 62).

[136] Fried, L. F., Shlipak, M. G., Crump, C., Kronmal, R. a., Bleyer, A. J., Gottdiener, J. S., Kuller, L. H., and Newman, A. B. **Renal insufficiency as a predictor of cardiovascular outcomes and mortality in elderly individuals**. *Journal of the American College of Cardiology*, **41**(8):1364–1372, 2003. (page 62).

[137] Frossard, P. M., Lestringant, G. G., Elishahat, Y. I., John, A., and Obineche, E. N. **An MboI Two-Allele Polymorphism May Implicate the Human Renin Gene in Primary Hypertension**. *Hypertension Research*, **21**(3):221–225, 1998. (page 17).

[138] Fukuda, M. and Kimura, G. **Salt sensitivity and nondippers in chronic kidney dis-**

ease. *Current hypertension reports*, **14**(5):382–7, 2012. (page 62).

[139] Gaborieau, V., Delarche, N., and Gosse, P. **Ambulatory blood pressure monitoring versus self-measurement of blood pressure at home: correlation with target organ damage.** *Journal of Hypertension*, **26**:1919–1927, 2008. (page 62).

[140] Gamba, G., Saltzberg, S. N., Lombardi, M., Miyanoshita, a., Lytton, J., Hediger, M. a., Brenner, B. M., and Hebert, S. C. **Primary structure and functional expression of a cDNA encoding the thiazide-sensitive, electroneutral sodium-chloride cotransporter.** *Proceedings of the National Academy of Sciences of the United States of America*, **90**(7):2749–53, 1993. (page 12).

[141] Garcia-Estañ, J. and Roman, R. J. **Role of renal interstitial hydrostatic pressure in the pressure diuresis response.** *The American journal of physiology*, **256**(1 Pt 2):F63–70, 1989. (page 8).

[142] Gardiner, B. S., Smith, D. W., O'Connor, P. M., and Evans, R. G. **A Mathematical Model of Diffusional Shunting of Oxygen from Arteries to Veins in the Kidney.** *American journal of physiology. Renal physiology*, 2011. (page 6).

[143] Gardiner, B. S., Thompson, S. L., Ngo, J. P., Smith, D. W., Abdelkader, A., Broughton, B. R. S., Bertram, J. F., and Evans, R. G. **Diffusive oxygen shunting between vessels in the preglomerular renal vasculature: anatomic observations and computational modeling.** *American journal of physiology. Renal physiology*, **303**(5):F605–18, 2012. (page 6).

[144] Garrett, M. R., Dene, H., Walder, R., Zhang, Q.-Y., Cicila, G. T., Assadnia, S., Deng, A. Y., and Rapp, J. P. **Genome Scan and Congenic Strains for Blood Pressure QTL Using Dahl Salt-Sensitive Rats**. *Genome Research*, **8**:711–723, 1998. (page 3).

[145] Garvin, J. L., Herrera, M., and Ortiz, P. a. **Regulation of renal NaCl transport by nitric oxide, endothelin, and ATP: clinical implications.** *Annual review of physiology*, **73**:359–76, 2011. (page 83).

[146] Gauer, O. H., Henry, J. P., and Behn, C. **The Regulation of Extracellular Fluid Volume**. *Annual review of physiology*, **32**:547–595, 1970. (page 4).

[147] Gerstein, H. C., Hoogwerf, B., and Rashkow, A. **Albuminuria and Risk of Cardiovascular Events, Death, and Heart Failure in Diabetic and Nondiabetic Individuals**. *JAMA*, **286**(4):421–426, 2001. (page 62).

[148] Geurts, A. M., Cost, G. J., Freyvert, Y., Zeitler, B., Miller, J. C., Choi, V. M.,

Jenkins, S. S., Wood, A., et al. **Knockout rats via embryo microinjection of zinc-finger nucleases.** *Science (New York, N.Y.)*, **325**(5939):433, 2009. (page 2).

[149] Gibson, G. **Rare and common variants: twenty arguments.** *Nature reviews. Genetics*, **13**(2):135–45, 2011. (page 3).

[150] Gidlöf, O., Smith, J. G., Melander, O., Lövkvist, H. k., Hedblad, B., Engström, G., Nilsson, P., Carlson, J., et al. **A common missense variant in the ATP receptor P2X7 is associated with reduced risk of cardiovascular events.** *PloS one*, **7**(5):e37491, 2012. (page 88).

[151] Gjuvsland, A. B., Vik, J. O., Beard, D. a., Hunter, P. J., and Omholt, S. W. **Bridging the genotype-phenotype gap: what does it take?** *The Journal of physiology*, **591**(Pt 8):2055–66, 2013. (page 4).

[152] Gloviczki, M. L., Glockner, J. F., Crane, J. A., McKusick, M. A., Misra, S., Grande, J. P., Lerman, L. O., and Textor, S. C. **Blood oxygen level-dependent magnetic resonance imaging identifies cortical hypoxia in severe renovascular disease.** *Hypertension*, **58**(6):1066–72, 2011. (page 68).

[153] Gloviczki, M. L., Glockner, J. F., Gomez, S. I., Romero, J. C., Lerman, L. O., Mckusick, M., and Textor, S. C. **Comparison of 1.5 and 3T BOLD MR to study oxygenation of kidney cortex and medulla in human renovascular disease**. *Invest Radiol*, **44**(9):566–571, 2009. (page 68).

[154] Gloviczki, M. L., Lerman, L. O., and Textor, S. C. **Blood Oxygen Level-Dependent (BOLD) MRI in Renovascular Hypertension.** *Current hypertension reports*, 2011. (page 81).

[155] Gloviczki, M. L., Lerman, L. O., and Textor, S. C. **Blood oxygen level-dependent (BOLD) MRI in renovascular hypertension.** *Current hypertension reports*, **13**(5):370–7, 2011. (page 81).

[156] Go, A. S., Chertow, G. M., Fan, D., McCulloch, C. E., and Hsu, C.-y. **Chronic kidney disease and the risks of death, cardiovascular events, and hospitalization.** *The New England journal of medicine*, **351**(13):1296–305, 2004. (page 62).

[157] Goldman, B. Y. D. E. **Potential, impedence and rectification in membranes**. *J Gen Physiol*, **27**:37–60, 1943. (page 143).

[158] Gonçalves, R. G., Gabrich, L., Rosário, a., Takiya, C. M., Ferreira, M. L. L., Chiarini, L. B., Persechini, P. M., Coutinho-Silva, R., and Leite, M. **The role of purinergic P2X7 receptors in the inflammation and fibrosis of unilateral ureteral obstruction in mice.**

Kidney international, **70**(9):1599–606, 2006. (page 63).

[159] Goodfriend, T. L. and Peach, M. J. **(DES-Aspartic Acid-1)-Angiotensin II. Evidence and speculation for its role as an important agonist in the renin - angiotensin systemAngiotensin III: (DES-Aspartic Acid-1)-Angiotensin II. Evidence and speculation for its role as an important agonist in th**. *Circulation Research*, **36**(6):38–48, 1975. (page 16).

[160] Gordon, R. D., Küchel, O., Liddle, G. W., and Island, D. P. **Role of the sympathetic nervous system in regulating renin and aldosterone production in man.** *The Journal of clinical investigation*, **46**(4):599–605, 1967. (page 15).

[161] Graciano, M. L., Nishiyama, A., Jackson, K., Seth, D. M., Ortiz, R. M., Prieto-Carrasquero, M. C., Kobori, H., and Navar, L. G. **Purinergic receptors contribute to early mesangial cell transformation and renal vessel hypertrophy during angiotensin II-induced hypertension.** *American journal of physiology. Renal physiology*, **294**(1):F161–9, 2008. (page 64).

[162] Granger, J. P. **Pressure natriuresis. Role of renal interstitial hydrostatic pressure.** *Hypertension*, **19**:I9–I17, 1992. (page 8).

[163] Greger, R. and Plunck, M. **Ion Transport Mechanisms in Thick Ascending Limb of Henle s Loop of Mammalian Nephron**. *Physiological Reviews*, **65**(3):760–797, 1985. (page 12).

[164] Griendling, K. K., Murphy, T. J., and Alexander, R. W. **Molecular biology of the renin-angiotensin system**. *Circulation*, **87**(6):1816–1828, 1993. (page 15).

[165] Grisk, O. and Rettig, R. **Renal transplantation studies in genetic hypertension.** *News in physiological sciences : an international journal of physiology produced jointly by the International Union of Physiological Sciences and the American Physiological Society*, **16**:262–5, 2001. (page 13).

[166] Guan, Z., Osmond, D. A., and Inscho, E. W. **P2X receptors as regulators of the renal microvasculature.** *Trends in pharmacological sciences*, **28**:646–52, 2007. (pages 31, 44).

[167] Guidi, E., Bianchi, G., Rivolta, E., Ponticelli, C., Quarto di Palo, F., Minetti, L., and Polli, E. **Hypertension in man with a kidney transplant: role of familial versus other factors**. *Nephron*, **41**(1):14–21, 1985. (page 12).

[168] Gurbanov, K., Rubinstein, I., Hoffman, A., Abassi, Z., Better, O. S., and Winaver, J. **Differential regulation of renal regional blood flow by endothelin-1**. *Am J Physiol Renal Fluid Electrolyte Physiol*, **271**:F1166–F1172, 1996. (page 8).

[169] Gurley, S. B., Riquier-Brison, A. D. M., Schnermann, J., Sparks, M. a., Allen, A. M., Haase, V. H., Snouwaert, J. N., Le, T. H., et al. **AT1A angiotensin receptors in the renal proximal tubule regulate blood pressure.** *Cell metabolism*, **13**(4):469–75, 2011. (page 16).

[170] Guyton, A. C. **Renal function curve–a key to understanding the pathogenesis of hypertension**. *Hypertension*, **10**(1):1–6, 1987. (page 10).

[171] GUYTON, A. C., LANGSTON, J. B., and NAVAR, G. **THEORY FOR RENAL AUTOREGULATION BY FEEDBACK AT THE JUXTAGLOMERULAR APPARATUS.** *Circulation research*, **15**:SUPPL:187–97, 1964. (page 6).

[172] Guyton, A. **Blood pressure control-special role of the kidneys and body fluids**. *Science*, **252**:1813–1816, 1991. (page 4).

[173] Guyton, A., Coleman, T., and Granger, H. **Circulation: overall regulation.** *Annual review of physiology*, **34**:13–46, 1972. (page 4).

[174] Guzik, T. J., Hoch, N. E., Brown, K. A., McCann, L. A., Rahman, A., Dikalov, S., Goronzy, J., Weyand, C., and Harrison, D. G. **Role of the T cell in the genesis of angiotensin II induced hypertension and vascular dysfunction.** *The Journal of experimental medicine*, **204**(10):2449–60, 2007. (pages 13, 63).

[175] Haas, J. a., Granger, J. P., and Knox, F. G. **Effect of renal perfusion pressure on sodium reabsorption from proximal tubules of superficial and deep nephrons.** *The American journal of physiology*, **250**(3 Pt 2):F425–9, 1986. (page 8).

[176] Hackenthal, E., Paul, M., Ganten, D., and Taugner, R. **Morphology, physiology, and molecular biology of renin secretion.** *Physiological reviews*, **70**(4):1067–116, 1990. (page 15).

[177] Hall, J. E. and Granger, J. P. **Adenosine alters glomerular filtration control by angiotensin II.** *The American journal of physiology*, **250**(5 Pt 2):F917–23, 1986. (page 64).

[178] Hall, J. E., Granger, J. P., and Hester, R. L. **Interactions between adenosine and angiotensin II in controlling glomerular filtration.** *The American journal of physiology*, **248**(3 Pt 2):F340–6, 1985. (page 64).

[179] Hall, J. E., Guyton, A. C., and Brands, M. W. **Pressure-volume regulation in hypertension.** *Kidney international. Supplement*, **55**:S35–41, 1996. (page 9).

[180] Hall, J., Hildebrant, D., and Brands, M. **Abnormal pressure natriuresis. A cause or a consequence of hypertension?** *Hypertension*, **15**:547–559, 1990. (page 64).

[181] Hamm, L. L. and Hering-Smith, K. S. **Pivotal role of the kidney in hypertension.** *The American journal of the medical sciences*, **340**(1):30–2, 2010. (page 2).

[182] Handa, R. K., Ferrario, C. M., and Strandhoy, J. W. **Renal actions of angiotensin-(1-7): in vivo and in vitro studies.** *The American journal of physiology*, **270**(1 Pt 2):F141–7, 1996. (page 16).

[183] Hansen, P. B., Hashimoto, S., Briggs, J., and Schnermann, J. **Attenuated renovascular constrictor responses to angiotensin II in adenosine 1 receptor knockout mice.** *American journal of physiology. Regulatory, integrative and comparative physiology*, **285**(1):R44–9, 2003. (page 64).

[184] Hansen, T. W., Jeppesen, J. r., Rasmussen, S., Ibsen, H., and Torp-Pedersen, C. **Ambulatory blood pressure monitoring and risk of cardiovascular disease: a population based study.** *American journal of hypertension*, **19**(3):243–50, 2006. (page 62).

[185] Hart, P. D. and Bakris, G. L. **Hypertensive nephropathy: prevention and treatment recommendations.** *Expert Opinion On Pharmacotherapy*, **11**:2675–2686, 2010. (page 62).

[186] Hata, A., Namikawa, C., Sasaki, M., Sato, K., Nalamura, T., Tamura, K., and Lalouel, J.-M. **Angiotensinogen as a risk factor for essential hypertension in Japan**. *Journal of Clinical Investigation*, **93**(November 1993):1285–1287, 1994. (page 17).

[187] Havlik, R. J., Garrison, R. J., Feinleib, M., Kannel, W. B., Castelli, W. P., and McNamara, P. M. **Blood pressure aggregation in families.** *American journal of epidemiology*, **110**(3):304–12, 1979. (page 1).

[188] Hayslett, J. P. **Functional adaptation to reduction in renal mass.** *Physiological reviews*, **59**(1):137–64, 1979. (page 62).

[189] He, F. J., Li, J., and Macgregor, G. A. **Effect of longer term modest salt reduction on blood pressure: Cochrane systematic review and meta-analysis of randomised trials.** *BMJ (Clinical research ed.)*, **346**(apr03_3):f1325, 2013. (page 4).

[190] Heller, J., Schubert, G., Havlíckova, J., and Thurau, K. **The role of the kidney in the development of hypertension: a transplantation study in the Prague hypertensive rat.** *Pflügers Archiv : European journal of physiology*, **425**(3-4):208–12, 1993. (page 13).

[191] Hernández, D., Muriel, A., Abraira, V., Pérez, G., Porrini, E., Marrero, D., Zamora, J., González-Posada, J. M., et al. **Renin-angiotensin system blockade and kidney transplantation: a longitudinal cohort study.** *Nephrology, dialy-*

sis, transplantation : official publication of the European Dialysis and Transplant Association - European Renal Association, **27**(1):417–22, 2012. (page 13).

[192] Herrmann, H. C. and Dzau, V. J. **The feedback regulation of angiotensinogen production by components of the renin-angiotensin system**. *Circulation Research*, **52**(3):328–334, 1983. (page 13).

[193] Heyeraas, K. J. and Aukland, K. **Interlobular arterial resistance: influence of renal arterial pressure and angiotensin II.** *Kidney international*, **31**(6):1291–8, 1987. (page 62).

[194] Hiken, J. F. and Steinberg, T. H. **ATP downregulates P2X7 and inhibits osteoclast formation in RAW cells.** *American journal of physiology. Cell physiology*, **287**(2):C403–12, 2004. (page 27).

[195] Hilgers, K. F., Hartner, a., Porst, M., Mai, M., Wittmann, M., Hugo, C., Ganten, D., Geiger, H., Veelken, R., and Mann, J. F. **Monocyte chemoattractant protein-1 and macrophage infiltration in hypertensive kidney injury.** *Kidney international*, **58**(6):2408–19, 2000. (page 63).

[196] Hill, M. a., Zou, H., Potocnik, S. J., Meininger, G. a., and Davis, M. J. **Invited review: arteriolar smooth muscle mechanotransduction: Ca(2+) signaling pathways underlying myogenic reactivity.** *Journal of applied physiology (Bethesda, Md. : 1985)*, **91**(2):973–83, 2001. (page 6).

[197] Hillman, K. A., Woolf, A. S., Johnson, T. M., Wade, A., Unwin, R. J., and Winyard, P. J. D. **The P2X7 ATP receptor modulates renal cyst development in vitro.** *Biochemical and biophysical research communications*, **322**(2):434–9, 2004. (page 29).

[198] Hocher, B., Thöne-Reineke, C., Bauer, C., Raschack, M., and Neumayer, H. H. **The paracrine endothelin system: pathophysiology and implications in clinical medicine.** *European journal of clinical chemistry and clinical biochemistry : journal of the Forum of European Clinical Chemistry Societies*, **35**:175–189, 1997. (page 17).

[199] Hodgkin, A. L. and Katz, B. **The effect of sodium ions on the electrical activity of the giant axon of the squid**. *J. Physiol*, **108**:37–77, 1948. (page 143).

[200] Hoorn, E. J. and Ellison, D. H. **WNK kinases and the kidney**, 2012. (page 12).

[201] Hostetter, T. H., Olson, J. L., Rennke, H. G., Venkatachalam, M. A., and Brenner, B. M. **Hyperfiltration in remnant nephrons : adverse response to renal ablation a potentially**. *Am J Physiol Renal*

Fluid Electrolyte Physiol, **241**:F85–F93, 1981. (page 62).

[202] Hostetter, T. H. **PROGRESSION OF RENAL DISEASE AND RENAL**. *Ann. Rev. Physiol*, **57**:263–278, 1995. (page 62).

[203] Hottenga, J.-J., Boomsma, D. I., Kupper, N., Posthuma, D., Snieder, H., Willemsen, G., and de Geus, E. J. C. **Heritability and stability of resting blood pressure.** *Twin research and human genetics : the official journal of the International Society for Twin Studies*, **8**(5):499–508, 2005. (page 1).

[204] Hubert, H. B., Feinleib, M., McNamara, P. M., and Castelli, W. P. **Obesity as an independent risk factor for cardiovascular disease: a 26-year follow-up of participants in the Framingham Heart Study**. *Circulation*, **67**(5):968–977, 1983. (page 3).

[205] Huwiler, A. and Pfeilschifter, J. **Stimulation by extracellular ATP and UTP of the mitogen-activated protein kinase cascade and proliferation of rat messangial cells**. *Br J Pharmacol*, **113**:1455–1463, 1994. (page 64).

[206] Hyde, E. R., Michler, C., Lee, J., Cookson, A. N., Chabiniok, R., Nordsletten, D. a., and Smith, N. P. **Parameterisation of multi-scale continuum perfusion models from discrete vascular networks.** *Medical & biological engineering & computing*, **51**(5):557–70, 2013. (page 5).

[207] Ichihara, A., Inscho, E. W., Imig, J. D., and Navar, L. G. **Neuronal nitric oxide synthase modulates rat renal microvascular function Neuronal nitric oxide synthase modulates rat renal microvascular function**. *Am J Physiol Renal Physiol*, **724**:F516–F524, 1998. (page 6).

[208] Imai, Y., Kuba, K., Rao, S., Huan, Y., Guo, F., Guan, B., Yang, P., Sarao, R., et al. **Angiotensin-converting enzyme 2 protects from severe acute lung failure.** *Nature*, **436**(7047):112–6, 2005. (page 16).

[209] Ingelfinger, J. R., Zuo, W. M., Fon, E. A., Ellison, K. E., and Dzau, V. J. **In Situ Hybridization Evidence for Angiotensinogen Messenger RNA in the Rat Proximal Tubule. An Hypothesis for the Intrarenal Renin Angiotensin System**. *Journal of Clinical Investigation*, **85**(February):417–423, 1990. (page 17).

[210] Inoue, T., Kozawa, E., Okada, H., and Suzuki, H. **Is there no future for renal BOLD-MRI?** *Kidney international*, **82**(8):934; author reply 935, 2012. (page 81).

[211] Inscho, E. W. **P2 receptors in regulation of renal microvascular function.** *American journal of physiology. Renal physiology*, **280**(6):F927–44, 2001. (pages 6, 29, 31).

[212] Inscho, E. W., Cook, a. K., Imig, J. D., Vial, C., and Evans, R. J. **Renal autoregulation in P2X1 knockout mice.** *Acta physiologica Scandinavica*, **181**(4):445–53, 2004. (pages 8, 44).

[213] Inscho, E. W., Ohishi, K., Cook, a. K., Belott, T. P., and Navar, L. G. **Calcium activation mechanisms in the renal microvascular response to extracellular ATP.** *The American journal of physiology*, **268**(5 Pt 2):F876–84, 1995. (page 6).

[214] Inscho, E. W., Ohishi, K., and Navar, L. G. **Effects of ATP on pre- and postglomerular juxtamedullary microvasculature**. *Am J Physiol Renal Fluid Electrolyte Physiol*, **263**:F886–F893, 2012. (page 31).

[215] Inscho, E. W. **ATP, P2 receptors and the renal microcirculation.** *Purinergic signalling*, **5**:447–60, 2009. (pages 31, 44).

[216] Inscho, E. W., Cook, A. K., Imig, J. D., Vial, C., and Evans, R. J. **Physiological role for P2X1 receptors in renal microvascular autoregulatory behavior**. *Journal of Clinical Investigation*, **112**(12):1895–1905, 2003. (pages 6, 29, 31, 64, 85).

[217] Issa, N., Ortiz, F., Reule, S. a., Kukla, A., Kasiske, B. L., Mauer, M., Jackson, S., Matas, A. J., and Ibrahim, H. N. **The renin-aldosterone axis in kidney transplant recipients and its association with allograft function and structure.** *Kidney international*, pages 1–12, 2013. (page 13).

[218] Jackson, E. K. and Raghvendra, D. K. **The extracellular cyclic AMP-adenosine pathway in renal physiology.** *Annual review of physiology*, **66**:571–99, 2004. (page 29).

[219] Jacob, F., Pérez Novo, C., Bachert, C., and Van Crombruggen, K. **Purinergic signaling in inflammatory cells: P2 receptor expression, functional effects, and modulation of inflammatory responses.** *Purinergic Signalling*, **9**:285–306, 2013. (page 63).

[220] Jacob, H. J., Lazar, J., Dwinell, M. R., Moreno, C., and Geurts, A. M. **Gene targeting in the rat: advances and opportunities.** *Trends in genetics : TIG*, **26**(12):510–8, 2010. (page 2).

[221] Jafar, T. H., Stark, P. C., Schmid, C. H., Landa, M., Maschio, G., de Jong, P. E., de Zeeuw, D., Shahinfar, S., Toto, R., and Levey, A. S. **Progression of Chronic Kidney Disease : The Role of Blood Pressure Control, Proteinuria, and Angiotensin-Converting Ezyme Inhibition. A Patient-Level Meta-Analysis**. *Annals of Internal Medicine*, **139**(4):244–253, 2003. (page 17).

[222] Jellinck, P. H., Forkert, P. G., Riddick, D. S., Okey,

A. B., Michnovicz, J. J., and Bradlow, H. L. **Ah receptor binding properties of indole carbinols and induction of hepatic estradiol hydroxylation.** *Biochemical Pharmacology*, **45**:1129–1136, 1993. (page 18).

[223] Jeunemaitre, X., Soubrier, F., Kotelevtsev, Y. V., Lifton, R. P., Williams, C. S., Charru, a., Hunt, S. C., Hopkins, P. N., Williams, R. R., and Lalouel, J. M. **Molecular basis of human hypertension: role of angiotensinogen.** *Cell*, **71**(1):169–80, 1992. (page 17).

[224] Ji, W., Foo, J. N., O'Roak, B. J., Zhao, H., Larson, M. G., Simon, D. B., Newton-Cheh, C., State, M. W., Levy, D., and Lifton, R. P. **Rare independent mutations in renal salt handling genes contribute to blood pressure variation.** *Nature genetics*, **40**(5):592–9, 2008. (page 3).

[225] Ji, X., Naito, Y., Hirokawa, G., Weng, H., Hiura, Y., Takahashi, R., and Iwai, N. **P2X(7) receptor antagonism attenuates the hypertension and renal injury in Dahl salt-sensitive rats.** *Hypertension research : official journal of the Japanese Society of Hypertension*, (July):1–7, 2011. (pages 45, 87).

[226] Ji, X., Naito, Y., Weng, H., Endo, K., Ma, X., and Iwai, N. **P2X7 deficiency attenuates hypertension and renal injury in deoxycorticosterone acetate-salt hypertension.** *American journal of physiology. Renal physiology*, **303**(8):F1207–15, 2012. (pages 45, 87).

[227] Jiang, L. H., Mackenzie, a. B., North, R. a., and Surprenant, a. **Brilliant blue G selectively blocks ATP-gated rat P2X(7) receptors.** *Molecular pharmacology*, **58**(1):82–8, 2000. (pages 45, 87).

[228] Johnson, A. D., Newton-cheh, C., Chasman, D. I., Ehret, G. B., Rose, L., Rice, K., Verwoert, G. C., Launer, L. J., et al. **Association of hypertension drug target genes with blood pressure and hypertension in 86,588 individuals**. *Hypertension*, **57**(5):903–910, 2011. (page 17).

[229] Johnson, R. J., Alpers, C. E., Yoshimura, a., Lombardi, D., Pritzl, P., Floege, J., and Schwartz, S. M. **Renal injury from angiotensin II-mediated hypertension**. *Hypertension*, **19**(5):464–474, 1992. (page 47).

[230] Johnson, R. J., Herrera-Acosta, J., Schreiner, G. F., and Rodriguez-Iturbe, B. **SUBTLE ACQUIRED RENAL INJURY AS A MECHANISM OF SALT -SENSITIVE HYPERTENSION**. *New England Journal of Medicine*, **346**(12):913–923, 2002. (page 64).

[231] Johnson, T., Gaunt, T. R., Newhouse, S. J., Padmanabhan, S., Tomaszewski, M., Kumari, M., Morris, R. W., Tzoulaki,

I., ET AL. **Blood pressure loci identified with a gene-centric array.** *American journal of human genetics*, **89**(6):688–700, 2011. (page 17).

[232] JULIUS, S. AND NESBITT, S. **Sympathetic overactivity in hypertension. A moving target.** *American journal of hypertension*, **9**(11):113S–120S, 1996. (page 4).

[233] JUST, A. AND ARENDSHORST, W. J. **Dynamics and contribution of mechanisms mediating renal blood flow autoregulation.** *Am J Physiol Regul Integr Comp Physiol*, **285**(3):R619–31, 2003. (page 8).

[234] JUST, A., KURTZ, L., DE WIT, C., WAGNER, C., KURTZ, A., AND ARENDSHORST, W. J. **Connexin 40 mediates the tubuloglomerular feedback contribution to renal blood flow autoregulation.** *Journal of the American Society of Nephrology : JASN*, **20**(7):1577–85, 2009. (page 8).

[235] KAHLE, K. T., WILSON, F. H., LENG, Q., LALIOTI, M. D., O'CONNELL, A. D., DONG, K., RAPSON, A. K., MACGREGOR, G. G., ET AL. **WNK4 regulates the balance between renal NaCl reabsorption and K+ secretion.** *Nature genetics*, **35**:372–376, 2003. (page 12).

[236] KALLSKOG, O., LINDBOM, L. O., ULFENDAHL, H. R., AND WOLGAST, M. **Hydrostatic Pressures within the Vascular Structures of the Rat Kidney**. *Pflugers Archiv*, **363**:205–210, 1976. (page 62).

[237] KANE, P. AND MALLOY, J. **Renin Gene MboI Dimorphism is a Discriminator for Hypertension in dislipidaemic Subjects**. *Hypertension Research*, **22**(4):285–289, 1999. (page 17).

[238] KANNEL, W. B. AND MCGEE, D. L. **Diabetes and cardiovascular risk factors: the Framingham study**. *Circulation*, **59**(1):8–13, 1979. (page 3).

[239] KANNEL, W. B. **Serum Cholesterol, Lipoproteins, and the Risk of Coronary Heart Disease: The Framingham Study**. *Annals of Internal Medicine*, **74**(1):1, 1971. (page 3).

[240] KANTACHUVESIRI, S., FLEMING, S., PETERS, J., PETERS, B., BROOKER, G., LAMMIE, A. G., MCGRATH, I., KOTELEVTSEV, Y., AND MULLINS, J. J. **Controlled hypertension, a transgenic toggle switch reveals differential mechanisms underlying vascular disease.**, 2001. (pages 18, 21).

[241] KANTACHUVESIRI, S., HALEY, C. S., FLEMING, S., KURIAN, K., WHITWORTH, C. E., WENHAM, P., KOTELEVTSEV, Y., AND MULLINS, J. J. **Genetic mapping of modifier loci affecting malignant hypertension in TGRmRen2 rats.** *Kidney international*, **56**:414–20, 1999. (pages 18, 21).

[242] Karlebach, G. and Shamir, R. **Modelling and analysis of gene regulatory networks.** *Nature reviews. Molecular cell biology*, **9**(10):770–80, 2008. (page 3).

[243] Kaschina, E. and Unger, T. **Angiotensin AT1/AT2 receptors: regulation, signalling and function.** *Blood pressure*, **12**(2):70–88, 2003. (page 16).

[244] Katada, J. and Majima, M. **AT(2) receptor-dependent vasodilation is mediated by activation of vascular kinin generation under flow conditions.** *British journal of pharmacology*, **136**(4):484–91, 2002. (page 16).

[245] Kato, S., Luyckx, V. a., Ots, M., Lee, K. W., Ziai, F., Troy, J. L., Brenner, B. M., and MacKenzie, H. S. **Renin-angiotensin blockade lowers MCP-1 expression in diabetic rats.** *Kidney international*, **56**(3):1037–48, 1999. (page 13).

[246] Katrahalli, U., Kalanur, S. S., and Seetharamappa, J. **Interaction of bioactive coomassie brilliant blue g with protein: insights from spectroscopic methods.** *Scientia pharmaceutica*, **78**(4):869–80, 2010. (page 45).

[247] Kawano, A., Tsukimoto, M., Mori, D., Noguchi, T., Harada, H., Takenouchi, T., Kitani, H., and Kojima, S. **Regulation of P2X7-dependent inflammatory functions by P2X4 receptor in mouse macrophages.** *Biochemical and biophysical research communications*, **420**(1):102–7, 2012. (pages 63, 87).

[248] Kawarazaki, W., Nagase, M., Yoshida, S., Takeuchi, M., Ishizawa, K., Ayuzawa, N., Ueda, K., and Fujita, T. **Angiotensin II- and salt-induced kidney injury through Rac1-mediated mineralocorticoid receptor activation.** *Journal of the American Society of Nephrology : JASN*, **23**(6):997–1007, 2012. (page 62).

[249] Ke, H. Z., Qi, H., Weidema, A. F., Zhang, Q., Panupinthu, N., Crawford, D. T., Grasser, W. A., Paralkar, V. M., et al. **Deletion of the P2X7 nucleotide receptor reveals its regulatory roles in bone formation and resorption.** *Molecular endocrinology (Baltimore, Md.)*, **17**:1356–1367, 2003. (page 47).

[250] Kearney, P. M., Whelton, M., Reynolds, K., Muntner, P., Whelton, P. K., and He, J. **Global burden of hypertension: analysis of worldwide data.** *Lancet*, **365**(9455):217–23, 2005. (page 1).

[251] Keller, G., Zimmer, G., Mall, G., Ritz, E., and Amann, K. **Nephron number in patients with primary hypertension.** *The New England journal of medicine*, **348**(2):101–8, 2003. (page 63).

[252] Kennedy-Lydon, T. M., Crawford, C., Wildman, S. S. P.,

and Peppiatt-Wildman, C. M. **Renal pericytes: regulators of medullary blood flow.** *Acta physiologica (Oxford, England)*, **207**(2):212–25, 2013. (page 45).

[253] Kestenbaum, B., Rudser, K. D., Boer, I. H. D., Peralta, C. A., Fried, L. F., Shlipak, M. G., Palmas, W., Stehman-Breen, C., and Siscovick, D. S. **Differences in Kidney Function and Incident Hypertension : The Multi-Ethnic Study of Atherosclerosis**. *Annals of Internal Medicine*, **148**:501–508, 2008. (page 62).

[254] Keystone, E. C., Wang, M. M., Layton, M., Hollis, S., and McInnes, I. B. **Clinical evaluation of the efficacy of the P2X7 purinergic receptor antagonist AZD9056 on the signs and symptoms of rheumatoid arthritis in patients with active disease despite treatment with methotrexate or sulphasalazine**. *Ann Rheum Dis*, **71**:1630–1635, 2012. (page 88).

[255] Khakh, B. S. and North, R. A. **P2X receptors as cell-surface ATP sensors in health and disease.** *Nature*, **442**(7102):527–32, 2006. (page 84).

[256] Khraibi, a. a., Haas, J. a., and Knox, F. G. **Effect of renal perfusion pressure on renal interstitial hydrostatic pressure in rats.** *The American journal of physiology*, **256**(1 Pt 2):F165–70, 1989. (page 8).

[257] Kim, E., Arnould, T., Sellin, L., Benzing, T., Comella, N., Kocher, O., Tsiokas, L., Sukhatme, V. P., and Walz, G. **Interaction between RGS7 and polycystin.** *Proceedings of the National Academy of Sciences of the United States of America*, **96**(11):6371–6, 1999. (page 29).

[258] Kim, S. and Iwao, H. **Molecular and cellular mechanisms of angiotensin II-mediated cardiovascular and renal diseases.** *Pharmacological reviews*, **52**(1):11–34, 2000. (page 47).

[259] Kimbrough, H. M., Vaughan, E. D., Carey, R. M., and Ayers, C. R. **Effect of intrarenal angiotensin II blockade on renal function in conscious dogs**. *Circulation Research*, **40**(2):174–178, 1977. (page 17).

[260] Kimura, K., Tojo, a., Matsuoka, H., and Sugimoto, T. **Renal arteriolar diameters in spontaneously hypertensive rats. Vascular cast study**. *Hypertension*, **18**(1):101–110, 1991. (page 62).

[261] King, M. R., Ismail, A. S., Davis, L. S., and Karp, D. R. **Oxidative stress promotes polarization of human T cell differentiation towards a t helper phenotype**. *Journal of immunology*, **176**:2765–2772, 2006. (page 63).

[262] Klag, M. J., Whelton, P. K., Randall, B. L., Neaton, J. D., Brancati, F. L., Charles, E. F.,

Shulman, N. B., and Stamler, J. **Blood pressure and end-stage renal disease in men**. *New England Journal of Medicine*, **334**(1):13–18, 1996. (page 62).

[263] Klahr, S. **The Kidney in Hypertension – Villain and Victim**. *NEJM*, **320**:731–733, 1989. (page 63).

[264] Kleinstreuer, N., David, T., Plank, M. J., and Endre, Z. **Dynamic myogenic autoregulation in the rat kidney: a whole-organ model.** *American journal of physiology. Renal physiology*, **294**(6):F1453–64, 2008. (page 5).

[265] Klett, C. **Regulation of hepatic angiotensinogen synthesis and secretion by steroid hormones**. *Endocrinology*, **130**(6):3660–3668, 1992. (page 15).

[266] Knepper, M. A., Editor, F., Curtis, J. J., Luke, R. G., and Ritz, E. **Remission of essential hypertension after renal transplantation**. *J Am Soc Nephrol*, **12**:2404–2412, 2000. (page 13).

[267] Knox, F. G., Mertz, J. I., Burnett, J. C., and Haramati, A. **Role of hydrostatic and oncotic pressures in renal sodium reabsorption.** *Circulation Research*, **52**:491–500, 1983. (page 8).

[268] Knox, F. G. and Granger, J. P. **Control of Sodiurn excretion : the kidney produces under pressure**. *Physiology*, **2**:26–29, 1987. (page 8).

[269] Knox, F. G. and Spielman, W. S. **Renal circulation**. In *Hanbook of Physiology, The Cardiovascular System, Peripheral Circulation and Organ Blood Flow*, number 28, chapter 6, pages 183–217. American Physiological Society, 1983. (page 5).

[270] Kobori, H., Nangaku, M., Navar, L. G., and Nishiyama, A. **The Intrarenal Renin-Angiotensin System : From Physiology to the Pathobiology of Hypertension and Kidney Disease**. *Phaarmacological Reviews*, **59**(3):251–287, 2007. (page 17).

[271] Kobori, H., Nishiyama, A., Harrison-Bernard, L. M., and Navar, L. G. **Urinary angiotensinogen as an indicator of intrarenal Angiotensin status in hypertension.** *Hypertension*, **41**(1):42–9, 2003. (page 17).

[272] Komolova, M. and Adams, M. a. **Moment-to-moment characteristics of the relationship between arterial pressure and renal interstitial hydrostatic pressure.** *Hypertension*, **56**(4):650–7, 2010. (page 8).

[273] Kotchen, T. a., Cowley, A. W., and Frohlich, E. D. **Salt in health and disease–a delicate balance.** *The New England journal of medicine*, **368**(13):1229–37, 2013. (page 4).

[274] Kramer, K., Boylan, J., and Keck, W. **Regulation of Total Body Sodium in the Mam-**

malian Organism - Karger Publishers. *Nephron*, **6**:379–387, 1969. (page 4).

[275] Krum, H., Schlaich, M., Whitbourn, R., Sobotka, P. a., Sadowski, J., Bartus, K., Kapelak, B., Walton, A., et al. **Catheter-based renal sympathetic denervation for resistant hypertension: a multicentre safety and proof-of-principle cohort study.** *Lancet*, **373**(9671):1275–81, 2009. (page 12).

[276] Kühn, R., Schwenk, F., Aguet, M., and Rajewsky, K. **Inducible gene targeting in mice.** *Science (New York, N.Y.)*, **269**(5229):1427–9, 1995. (page 2).

[277] Kuoppala, a., Lindstedt, K. a., Saarinen, J., Kovanen, P. T., and Kokkonen, J. O. **Inactivation of bradykinin by angiotensin-converting enzyme and by carboxypeptidase N in human plasma.** *American journal of physiology. Heart and circulatory physiology*, **278**(4):H1069–74, 2000. (page 16).

[278] Kurtz, A. **Renal connexins and blood pressure.** *Biochimica et biophysica acta*, pages 1–6, 2011. (page 15).

[279] Langheinrich, M., Ae, M., Bohm, M., and Pi, Y. M. **Characteristics and Functional Aspects The Hypertensive Ren-2 Transgenic Rat TGR(mRen2)27 in Hypertension Research**. *Internal Medicine*, **7061**:506–512, 1996. (page 47).

[280] Lauledерkind, S. J. F., Hayman, G. T., Wang, S.-J., Smith, J. R., Lowry, T. F., Nigam, R., Petri, V., de Pons, J., et al. **The Rat Genome Database 2013–data, tools and users.** *Briefings in bioinformatics*, **14**(4):520–6, 2013. (page 22).

[281] Laursen, J. B. M., Rajagopalan, S. M., Galls, Z. P., Tarpey, M. M., Freeman, B. A. P., and Harrison, D. G. M. **Role of Superoxide in Angiotensin II-Induced but Not Catecholamine-Induced Hypertension**. *Circulation research*, **95**(3):588–593, 1997. (page 83).

[282] Lee, M. I. N. A. E., Franklin, B., and Ae, M. **Physiological characterization transgenic of the hypertensive**. *Am J Physiol Endocrinol Metab*, **270**:E919–E929, 1996. (page 18).

[283] Leenen, F. H. H., Amin, S., Stewart, A. F. R., and Tesson, F. **Genes and Cardiovascular Function**. In Ostadal, B., Nagano, M., and Dhalla, N. S., editors, *Genes and Cardiovascular Development*, pages 161–175. Springer US, Boston, MA, 2011. (page 62).

[284] Lemos, V. S., Silva, D. M. R., Walther, T., Alenina, N., Bader, M., and Santos, R. A. S. **The Endothelium-Dependent Vasodilator Effect**

of the in the Aorta of Mas - Knockout Mice. *J Cardiovasc Pharmacol*, **46**(3):274–279, 2005. (page 16).

[285] Levy, B., Ambrosio, G., a.R. Pries,, and Struijker-Boudier, H. **Microcirculation in Hypertension: A New Target for Treatment?** *Circulation*, **104**(6):735–740, 2001. (page 62).

[286] Levy, D., Destefano, A. L., Larson, M. G., Donnell, C. J. O., Lifton, R. P., Gavras, H., Cupples, L. A., and Myers, R. H. **Evidence for a Gene Influencing Blood Pressure Genome Scan Linkage Results for Longitudinal Blood Pressure**. *Hypertension*, **36**:477–483, 2000. (page 17).

[287] Lewis, C. and Evans, R. **P2X Receptor Immunoreactivity in Different Arteries from the Femoral , Pulmonary , Cerebral , Coronary and Renal Circulations**. *Journal of Vascular Research*, (38):332–340, 2001. (page 85).

[288] Lifton, R. P., Dluhy, R. G., Powers, M., Rich, G. M., Cook, S., Ulick, S., and Lalouel, J.-M. **A chimaeric 11β-hydroxylase/aldosterone synthase gene causes glucocorticoid-remedial aldosteronism and human hypertension**. *Nature*, **355**:262–265, 1992. (page 2).

[289] Lifton, R. P., Dluhy, R. G., Powers, M., Rich, G. M., Gutkin, M., Fallo, F., Gill, J. R. J., Feld, L., et al. **Hereditary hypertension caused by chimaeric gene duplications and ectopic expression of aldosterone synthase**. *Nature genetics*, **2**:66–74, 1992. (page 2).

[290] Lim, S. S., Vos, T., Flaxman, A. D., Danaei, G., Shibuya, K., Adair-Rohani, H., Amann, M., Anderson, H. R., et al. **A comparative risk assessment of burden of disease and injury attributable to 67 risk factors and risk factor clusters in 21 regions, 1990-2010: a systematic analysis for the Global Burden of Disease Study 2010.** *Lancet*, **380**(9859):2224–60, 2012. (page 1).

[291] Lin, J., Valeri, A. M., Markowitz, G. S., D'Agati, V. D., Cohen, D. J., and Radhakrishnan, J. **Angiotensin converting enzyme inhibition in chronic allograft nephropathy.** *Transplantation*, **73**(5):783–8, 2002. (page 13).

[292] Lister, M. F., Sharkey, J., Sawatzky, D. a., Hodgkiss, J. P., Davidson, D. J., Rossi, A. G., and Finlayson, K. **The role of the purinergic P2X7 receptor in inflammation.** *Journal of inflammation*, **4**:5, 2007. (page 87).

[293] Littlejohn, N. K., Siel, R. B., Ketsawatsomkron, P., Pelham, C. J., Pearson, N. A., Hilzendeger, A. M., Buehrer, B. A., Weidemann, B. J., et al. **Hy-**

pertension in mice with transgenic activation of the brain renin-angiotensin system is vasopressin dependent. *American journal of physiology. Regulatory, integrative and comparative physiology*, **304**(10):R818–28, 2013. (page 17).

[294] Liu, C., Mather, S., Huang, Y., Garland, C. J., and Yao, X. **Extracellular ATP facilitates flow-induced vasodilatation in rat small mesenteric arteries.** *American journal of physiology. Heart and circulatory physiology*, **286**(5):H1688–95, 2004. (page 44).

[295] Liu, X., Bellamy, C. O. C., Bailey, M. A., Mullins, L. J., Dunbar, D. R., Kenyon, C. J., Brooker, G., Kantachuvesiri, S., et al. **Angiotensin-converting enzyme is a modifier of hypertensive end organ damage.** *The Journal of biological chemistry*, **284**:15564–72, 2009. (pages 29, 85).

[296] Liu, X., Bellamy, C. O. C., Mullins, L. J., Dunbar, D., and Mullins, J. J. **The Local Cardiac Renin-Angiotensin Aldosterone System**. *Molecular Physiology*, pages 51–66, 2009. (pages 18, 20, 21, 25).

[297] Longini, I. M., Higgins, M. W., Hinton, P. C., Moll, P. P., and Keller, J. B. **Environmental and genetic sources of familial aggregation of blood pressure in Tecumseh, Michigan**. *Am J Epidemiology*, **120**(1):131–144, 1984. (page 1).

[298] Loutzenhiser, R., Chilton, L., and Trottier, G. **Membrane potential measurements in renal afferent and efferent arterioles : actions of angiotensin II**. *Am J Physiol Renal Physiol*, **273**:F307–F314, 1997. (page 6).

[299] Loutzenhiser, R., Griffin, K., Williamson, G., and Bidani, A. **Renal autoregulation: new perspectives regarding the protective and regulatory roles of the underlying mechanisms.** *American journal of physiology. Regulatory, integrative and comparative physiology*, **290**:R1153–67, 2006. (pages 6, 62).

[300] Lu, M., Wang, T., Yan, Q., Yang, X., Dong, K., Knepper, M. a., Wang, W., Giebisch, G., Shull, G. E., and Hebert, S. C. **Absence of small conductance K+ channel (SK) activity in apical membranes of thick ascending limb and cortical collecting duct in ROMK (Bartter's) knockout mice.** *The Journal of biological chemistry*, **277**(40):37881–7, 2002. (page 12).

[301] Luft, F. C., Mervaala, E., Muller, D. N., Gross, V., Schmidt, F., Park, J. K., Schmitz, C., Lippoldt, a., et al. **Hypertension-Induced End-Organ Damage : A New Transgenic Approach to an Old Problem**. *Hypertension*, **33**(1):212–218, 1999. (page 18).

[302] Machnik, A., Neuhofer, W., Jantsch, J., Dahlmann, A., Tammela, T., Machura, K., Park, J.-K., Beck, F.-X., et al. **Macrophages regulate salt-dependent volume and blood pressure by a vascular endothelial growth factor-C-dependent buffering mechanism.** *Nature medicine*, **15**(5):545–52, 2009. (page 63).

[303] Majid, D. S., Inscho, E. W., and Navar, L. G. **P2 purinoceptor saturation by adenosine triphosphate impairs renal autoregulation in dogs.** *Journal of the American Society of Nephrology : JASN*, **10**(3):492–8, 1999. (page 6).

[304] Malpas, S. **Editorial comment: Montani versus Osborn exchange of views.** *Experimental physiology*, **94**(4):381–2, 2009. (page 4).

[305] Malpas, S. C., Ramchandra, R., Guild, S.-J., McBryde, F., and Barrett, C. J. **Renal sympathetic nerve activity in the development of hypertension.** *Current hypertension reports*, **8**:242–8, 2006. (page 4).

[306] Mamenko, M., Zaika, O., Ilatovskaya, D. V., Staruschenko, A., and Pochynyuk, O. **Angiotensin II increases activity of the epithelial Na+ channel (ENaC) in distal nephron additively to aldosterone.** *The Journal of biological chemistry*, **287**(1):660–71, 2012. (page 16).

[307] Mancia, G., De Backer, G., Dominiczak, A., Cifkova, R., Fagard, R., Germano, G., Grassi, G., Heagerty, A. M., et al. **2007 Guidelines for the management of arterial hypertension: the task force for the management of arterial hypertension of the European Society of Hypertension (ESH) and of the European Society of Cardiology (ESC).** *European heart journal*, **28**(12):1462–536, 2007. (page 1).

[308] Manolio, T. a., Collins, F. S., Cox, N. J., Goldstein, D. B., Hindorff, L. a., Hunter, D. J., McCarthy, M. I., Ramos, E. M., et al. **Finding the missing heritability of complex diseases.** *Nature*, **461**(7265):747–53, 2009. (pages 2, 4).

[309] Manotham, K., Ongvilawan, B., Urusopone, P., Chetsurakarn, S., Tanamai, J., Limkuansuwan, P., Tungsanga, K., and Eiam-Ong, S. **Angiotensin II receptor blocker partially ameliorated intrarenal hypoxia in chronic kidney disease patients: a pre-/post-study**. *Internal Medicine Journal*, **42**(4):e33–e37, 2012. (pages 81, 82).

[310] Masilamani, S., Kim, G. H., Mitchell, C., Wade, J. B., and Knepper, M. a. **Aldosterone-mediated regulation of ENaC alpha, beta, and gamma subunit proteins in rat kidney.** *The*

Journal of clinical investigation, **104**(7):R19–23, 1999. (page 12).

[311] Masin, M., Young, C., Lim, K., Barnes, S. J., Xu, X. J., Marschall, V., Brutkowski, W., Mooney, E. R., Gorecki, D. C., and Murrell-Lagnado, R. **Expression, assembly and function of novel C-terminal truncated variants of the mouse P2X7 receptor: re-evaluation of P2X7 knockouts.** *British journal of pharmacology*, **165**(4):978–93, 2012. (page 88).

[312] Mason, R. P. **Non-invasive assessment of kidney oxygenation: a role for BOLD MRI.** *Kidney international*, **70**(1):10–1, 2006. (pages 65, 81).

[313] Matsusaka, T., Niimura, F., Shimizu, A., Pastan, I., Saito, A., Kobori, H., Nishiyama, A., and Ichikawa, I. **Liver angiotensinogen is the primary source of renal angiotensin II.** *Journal of the American Society of Nephrology : JASN*, **23**(7):1181–9, 2012. (page 15).

[314] Mattson, D. L. **Importance of the renal medullary circulation in the control of sodium excretion and blood pressure**. *Am J Physiol Regul Integr Comp Physiol*, **284**(1):R13–R27, 2003. (page 8).

[315] Mayer, G. **Capillary rarefaction, hypoxia, VEGF and angiogenesis in chronic renal disease.** *Nephrology, dialysis, transplantation : official publication of the European Dialysis and Transplant Association - European Renal Association*, **26**(4):1132–7, 2011. (page 65).

[316] McBride, M. W., Charchar, F. J., Graham, D., Miller, W. H., Strahorn, P., Carr, F. J., and Dominiczak, A. F. **Functional genomics in rodent models of hypertension.** *The Journal of physiology*, **554**(Pt 1):56–63, 2004. (page 3).

[317] McDonough, A. A., Leong, P. K. K., and Yang, L. E. **Mechanisms of pressure natriuresis. How blood pressure regulates renal sodium transport**. *Ann. N.Y. Acad. Sci.*, **986**:669–677, 2003. (page 16).

[318] Meffert, S., Stolf, M., Steckelings, U. M., Bottari, S. P., and Unger, T. **The angiotensin II AT2 receptor inhibits proliferation and promotes differentiation in PC12W cells**. *Molecular and Cellular Endocrinology*, **122**:59–67, 1996. (page 16).

[319] Mehri, S., Mahjoub, S., Hammami, S., Zaroui, A., Frih, A., Betbout, F., Mechmeche, R., and Hammami, M. **Renin-angiotensin system polymorphisms in relation to hypertension status and obesity in a Tunisian population.** *Molecular biology reports*, **39**(4):4059–65, 2012. (page 17).

[320] Meininger, G. A. and Davis, M. J. **Cellular mechanisms involved in the vascular myogenic**

response. *Am J Physiol Heart Circ Physiol*, **263**:H647–H659, 1992. (page 6).

[321] Mendel, G. **Versuche über Plflanzen-hybriden**. *Verhandlungen des naturforschenden Ver-eines in Brünn*, **Bd. IV fu**:3–47, 1866. (page 3).

[322] Meneton, P., Jeunemaitre, X., Wardener, H. E. D. E., and Macgregor, G. A. **Links Between Dietary Salt Intake , Renal Salt Handling , Blood Pressure , and Cardiovascular Diseases**. *Physiol Rev*, **85**:679–715, 2005. (page 4).

[323] Menzies, R. I., Unwin, R. J., Dash, R. K., Beard, D. A., Cowley, A. W., Carlson, B. E., Mullins, J. J., and Bailey, M. A. **Effect of P2X4 and P2X7 receptor antagonism on the pressure diuresis relationship in rats**. *Front. Physiol.*, **4**, 2013. (pages 30, 46).

[324] Menzies, R. I., Zammit-Mangion, A., Hollis, L. M., Lennen, R. J., Jansen, M. a., Webb, D. J., Mullins, J. J., Dear, J. W., Sanguinetti, G., and Bailey, M. a. **An anatomically unbiased approach for analysis of renal BOLD magnetic resonance images.** *American journal of physiology. Renal physiology*, **305**(6):F845–52, 2013. (page 83).

[325] Merrill, A. J. **Edema and decreased renal blood flow in patients with chronic congestive heart failure; evidence of forward failure as the primary cause of edema.** *The Journal of clinical investigation*, **25**(6):389–400, 1946. (page 9).

[326] Mezzano, S. a., Ruiz-Ortega, M., and Egido, J. **Angiotensin II and Renal Fibrosis**. *Hypertension*, **38**(3):635–638, 2001. (page 47).

[327] Miall, W. and Oldham, M. **The hereditary factor in arterial blood-pressure**. *British medical journal*, (5323):75–80, 1963. (page 1).

[328] Michaely, H. J., Metzger, L., Haneder, S., Hansmann, J., Schoenberg, S. O., and Attenberger, U. I. **Renal BOLD-MRI does not reflect renal function in chronic kidney disease.** *Kidney international*, pages 1–6, 2012. (pages 81, 82).

[329] Mitchell, K. D., Braam, B., and Navar, L. G. **Hypertensinogenic mechanisms mediated by renal actions of renin-angiotensin system.** *Hypertension*, **19**(1 Suppl):I18–27, 1992. (page 6).

[330] Mitchell, K. D. and Mullins, J. J. **ANG II dependence of tubuloglomerular feedback responsiveness in hypertensive ren-2 transgenic rats**. *Am J Physiol Renal Physiol*, **268**:F821–F828, 1995. (page 6).

[331] Mitchell, K. D., Bagatell, S. J., Miller, C. S., Mouton, C. R., Seth, D. M., and Mullins, J. J. **Genetic clamping of renin gene expression induces hypertension and elevation of intrarenal Ang II levels of graded severity in Cyp1a1-Ren2 transgenic rats.** *Journal of the renin-angiotensin-aldosterone system : JRAAS*, **7**:74–86, 2006. (pages 18, 47).

[332] Mitchell, K. D. and Mullins, J. J. **Enhanced tubuloglomerular feedback in Cyp1a1-Ren2 transgenic rats with inducible ANG II-dependent malignant hypertension.** *American journal of physiology. Renal physiology*, **289**:F1210–6, 2005. (page 18).

[333] Moffat, D. B. **New ideas on the anatomy of the kidney.** *Journal of clinical pathology*, **34**(11):1197–1206, 1981. (page 5).

[334] Moffat, D. B. and Fourman, J. **The Vascular Pattern of the Rat Kidney.** *Journal of anatomy*, **97**:543–53, 1963. (page 5).

[335] Moore, L. C., Rich, A., and Casellas, D. **Ascending myogenic autoregulation: interactions between tubuloglomerular feedback and myogenic mechanisms.** *Bulletin of mathematical biology*, **56**(3):391–410, 1994. (page 6).

[336] Moreau, M. E., Garbacki, N., Molinaro, G., Brown, N. J., Marceau, F., and Adam, A. **Survey Review The Kallikrein-Kinin System : Current and Future Pharmacological Targets**. *J Pharmacol Sci*, **38**:6–38, 2005. (page 29).

[337] Morgan, D. A., DiBona, G. F., and Mark, A. L. **Effects of interstrain renal transplantation on NaCl-induced hypertension in Dahl rats.** *Hypertension*, **15**:436–42, 1990. (page 13).

[338] Morgan, T. H. **Random Segregation Versus Coupling in Mendelian Inheritance**. *Science*, **34**:384, 1911. (page 3).

[339] Mori, T. and Cowley, A. W. **Role of Pressure in Angiotensin II-Induced Renal Injury Chronic Servo-Control of Renal Perfusion Pressure in Rats**. *October*, pages 752–759, 2004. (pages 47, 62).

[340] Morimoto, S., Cassell, M. D., Beltz, T. G., Johnson, A. K., Davisson, R. L., and Sigmund, C. D. **Elevated blood pressure in transgenic mice with brain-specific expression of human angiotensinogen driven by the glial fibrillary acidic protein promoter.** *Circulation research*, **89**(4):365–72, 2001. (page 17).

[341] Mortensen, S. P., Thaning, P., Nyberg, M., Saltin, B., and Hellsten, Y. **Local release of ATP into the arterial inflow and venous drainage of human skeletal muscle: insight from ATP determination with the intravascular microdialysis**

technique. *The Journal of physiology*, **589**(Pt 7):1847–57, 2011. (page 29).

[342] Mullins, J. J., Burt, D. W., McTurk, P., George, H., and Brammar, W. J. **Molecular cloning of two distinct renin genes from the DBA/2 mouse**. *The EMBO journal*, **1**(11):1461–1466, 1982. (page 15).

[343] Mullins, L. J., Bailey, M. A., and Mullins, J. J. **Hypertension , Kidney , and Transgenics : A Fresh Perspective**. *Physiological Reviews*, pages 709 –746, 2006. (page 11).

[344] Mullins, J J, Peters, J, Ganten, D. **Fulminant hypertension in transgenic rats harbouring the mouse Ren-2 gene**. *Letters to Nature*, **344**:541–544, 1990. (page 18).

[345] Murray, C. J. L., Ezzati, M., Flaxman, A. D., Lim, S., Lozano, R., Michaud, C., Naghavi, M., Salomon, J. a., et al. **GBD 2010: design, definitions, and metrics.** *Lancet*, **380**(9859):2063–6, 2012. (page 1).

[346] Nakajima, M., Hutchinson, H. G., Fujinaga, M., Hayashida, W., Morishita, R., Zhang, L., Horiuchi, M., Pratt, R. E., and Dzau, V. J. **The angiotensin II type 2 (AT2) receptor antagonizes the growth effects of the AT1 receptor: gain-of-function study using gene transfer.** *Proceedings of the National Academy of Sciences of the United States of America*, **92**(23):10663–7, 1995. (page 16).

[347] Nakano, D., Kobori, H., Burford, J. L., Gevorgyan, H., Seidel, S., Hitomi, H., Nishiyama, A., and Peti-Peterdi, J. **Multiphoton imaging of the glomerular permeability of angiotensinogen.** *Journal of the American Society of Nephrology : JASN*, **23**(11):1847–56, 2012. (page 17).

[348] Nakayama, M., Sato, T., Miyazaki, M., Matsushima, M., Sato, H., Taguma, Y., and Ito, S. **Increased risk of cardiovascular events and mortality among non-diabetic chronic kidney disease patients with hypertensive nephropathy: the Gonryo study.** *Hypertension research : official journal of the Japanese Society of Hypertension*, **34**(10):1106–10, 2011. (page 62).

[349] Nangaku, M. **Chronic hypoxia and tubulointerstitial injury: a final common pathway to end-stage renal failure.** *Journal of the American Society of Nephrology : JASN*, **17**(1):17–25, 2006. (page 65).

[350] Navar, L. G. **Renal autoregulation : perspectives from whole kidney and single nephron studies**. *Am J Physiol Renal Physiol*, **234**:F357–F370, 1978. (page 6).

[351] Navar, L. G. **Regulation of Intrarenal Angiotensin II in Hypertension**. *Hypertension*, **39**(2):316–322, 2002. (page 17).

[352] Navar, L. G., Arendshorst, W. J., Pallone, T. L., Inscho, E. W., Imig, J. D., and Bell, P. D. **The Renal Microcirculation**. In *Comprehensive Physiology*, chapter 13, pages 550–683. Wiley Online Library, 2011. (page 5).

[353] Navar, L. G., Bell, P. D., and Burke, T. J. **Autoregulatory responses of superficial nephrons and their association with sodium excretion during arterial pressure alterations in the dog**. *Circulation Research*, **41**(4):487–496, 1977. (page 8).

[354] Navar, L. G., Harrison-Bernard, L. M., Imig, J. D., Wang, C. T., Cervenka, L., and Mitchell, K. D. **Intrarenal angiotensin II generation and renal effects of AT1 receptor blockade.** *Journal of The American Society Of Nephrology*, **10 Suppl 1**:S266–S272, 1999. (page 17).

[355] Navar, L. G., Harrison-Bernard, L. M., Wang, C. T., Cervenka, L., and Mitchell, K. D. **Concentrations and actions of intraluminal angiotensin II.** *Journal of The American Society Of Nephrology*, **10 Suppl 1**:S189–S195, 1999. (page 17).

[356] Navar, L. G., Imig, J. D., Zou, L., and Wang, C. T. **Intrarenal production of angiotensin II.** *Seminars in nephrology*, **17**(5):412–22, 1997. (page 17).

[357] Navar, L. G., Inscho, E. W., Imig, J. D., and Mitchell, K. D. **Heterogeneous activation mechanisms in the renal microvasculature.** *Kidney international. Supplement*, **67**:S17–21, 1998. (pages 6, 17).

[358] Navar, L. G., Inscho, E. W., Majid, D. S. A., Imig, J. D., Harrison-bernard, L. M., and Mitchel, K. D. **Paracrine Regulation of the Renal Microcirculation**. *Physiological Reviews*, **76**(2):425–536, 1996. (pages 17, 29).

[359] Navar, L. G., Inscho, E. W., Majid, S. a., Imig, J. D., Harrison-Bernard, L. M., and Mitchell, K. D. **Paracrine regulation of the renal microcirculation.** *Physiological reviews*, **76**(2):425–536, 1996. (page 6).

[360] Navar, L. G., Paul, R. V., Carmines, P. K., Chou, C. L., and Marsh, D. J. **Intrarenal mechanisms mediating pressure natriuresis: role of angiotensin and prostaglandins.** *Federation proceedings*, **45**(13):2885–91, 1986. (page 17).

[361] Negulyaev, Y. a. and Markwardt, F. **Block by extracellular Mg2+ of single human purinergic P2X4 receptor channels expressed in human embryonic kidney cells.** *Neuroscience letters*, **279**(3):165–8, 2000. (pages 143, 146).

[362] Neuhofer, W. and Beck, F.-X. **Survival in hostile en-**

vironments: strategies of renal medullary cells. *Physiology*, **21**:171–80, 2006. (page 65).

[363] Nielsen, S. **Renal aquaporins: an overview.** *BJU international*, **90 Suppl 3**:1–6, 2002. (page 9).

[364] Nielsen, S., Smith, B. L., Christensen, E. I., Knepper, M. a., and Agre, P. **CHIP28 water channels are localized in constitutively water-permeable segments of the nephron.** *The Journal of cell biology*, **120**(2):371–83, 1993. (page 9).

[365] Nishiyama, A., Majid, D. S. A., Taher, K. A., Miyatake, A., and Navar, L. G. **Relation Between Renal Interstitial ATP Concentrations and Autoregulation-Mediated Changes in Renal Vascular Resistance**. *Circulation Research*, **86**(6):656–662, 2000. (page 64).

[366] Nishiyama, A., Majid, D. S. A., Walker, M., Miyatake, A., and Navar, L. G. **Renal Interstitial ATP Responses to Changes in Arterial Pressure During Alterations in Tubuloglomerular Feedback Activity**. *Hypertension*, **37**(2):753–759, 2001. (page 64).

[367] Nishiyama, A. and Navar, L. G. **ATP mediates tubuloglomerular feedback.** *American journal of physiology. Regulatory, integrative and comparative physiology*, **283**(1):R273–5; discussion R278–9, 2002. (page 64).

[368] Nordsletten, D. A., Blackett, S., Bentley, M. D., Ritman, E. L., Smith, N. P., David, A., Ritman, L., Heart, J. P., Physiol, C., and H, H. **Structural morphology of renal vasculature**. *AJP Heart Circ Physiol*, **291**:H296–H309, 2006. (page 5).

[369] Noris, M., Mister, M., Pezzotta, A., Azzollini, N., Cassis, P., Benigni, A., Gagliardini, E., Perico, N., and Remuzzi, G. **ACE inhibition limits chronic injury of kidney transplant even with treatment started when lesions are established.** *Kidney international*, **64**(6):2253–61, 2003. (page 13).

[370] Norman, J. T., Stidwill, R., Singer, M., and Fine, L. G. **Angiotensin II Blockade Augments Renal Cortical Microvascular pO¡sub¿2¡/sub¿ Indicating a Novel, Potentially Renoprotective Action**. *Nephron Physiology*, **94**(2):p39–p46, 2003. (page 82).

[371] North, R. A. **Molecular physiology of P2X receptors.** *Physiological reviews*, **82**(4):1013–67, 2002. (pages 29, 45, 144).

[372] Oberg, B. P., McMenamin, E., Lucas, F. L., McMonagle, E., Morrow, J., Ikizler, T. A., and Himmelfarb, J. **Increased prevalence of oxidant stress and inflammation in patients with moderate to severe chronic kidney disease**. *Kidney international*, **65**:1009–1016, 2004. (page 63).

[373] Ocaranza, M. P., Lavandero, S., Jalil, J. E., Moya, J., Pinto, M., Novoa, U., Apablaza, F., González, L., et al. **Angiotensin(1-9) regulates cardiac hypertrophy in vivo and in vitro**. *Journal of Hypertension*, **28**(5):1054–1064, 2010. (page 16).

[374] Ochodnický, P., Henning, R. H., Buikema, H. J., de Zeeuw, D., Provoost, A. P., and van Dokkum, R. P. E. **Renal vascular dysfunction precedes the development of renal damage in the hypertensive Fawn-Hooded rat.** *American journal of physiology. Renal physiology*, **298**(3):F625–33, 2010. (page 62).

[375] O'Connor, P. M. and Cowley, A. W. **Modulation of pressure-natriuresis by renal medullary reactive oxygen species and nitric oxide.** *Current hypertension reports*, **12**(2):86–92, 2010. (page 65).

[376] O'Donnell, C. J., Lindpaintner, K., Larson, M. G., Rao, V. S., Ordovas, J. M., Schaefer, E. J., Myers, R. H., and Levy, D. **Evidence for Association and Genetic Linkage of the Angiotensin-Converting Enzyme Locus With Hypertension and Blood Pressure in Men but Not Women in the Framingham Heart Study**. *Circulation*, **97**(18):1766–1772, 1998. (page 2).

[377] Ogawa, S., Lee, T. M., Nayak, A. S., and Glynn, P. **Oxygenation-sensitive contrast in magnetic resonance image of rodent brain at high magnetic fields.** *Magnetic resonance in medicine*, **14**:68–78, 1990. (page 65).

[378] Okura, T., Kitami, Y., and Hiwada, K. **Restriction fragment length polymorphisms of the human renin gene: association study with a family history of essential hypertension.** *Journal of human hypertension*, **7**(5):457–61, 1993. (page 17).

[379] Olah, M. E. **Identification of A2a Adenosine Receptor Domains Involved in Selective Coupling to Gs**. *The Journal of biological chemistry*, **272**(1):337–344, 1997. (page 29).

[380] Olsson, R. A. and Pearson, J. D. **Cardiovascular Purinoceptors**. *Physiological Reviews*, **70**(3), 1990. (page 29).

[381] Omholt, S. W. **From sequence to consequence and back.** *Progress in biophysics and molecular biology*, **111**(2-3):75–82, 2013. (page 4).

[382] Orban, P. C., Chui, D., and Marth, J. D. **Tissue- and site-specific DNA recombination in transgenic mice.** *Proceedings of the National Academy of Sciences of the United States of America*, **89**(15):6861–5, 1992. (page 2).

[383] Ortiz, R. M., Graciano, M. L., Mullins, J. J., and Mitchell, K. D. **Aldosterone receptor antagonism alleviates proteinuria, but not malignant hypertension, in Cyp1a1-Ren2 transgenic rats.** *American journal of physiology. Renal physiology*, **293**(5):F1584–91, 2007. (page 18).

[384] Osborn, J. W. and England, K. **Normalization of arterial pressure after barodenervation: role of pressure natriuresis**. *Am J Physiol Regul Integr Comp Physiol*, **259**:R1172–R1180, 1990. (page 8).

[385] O'Seaghdha, C. M. and Fox, C. S. **Genome-wide association studies of chronic kidney disease: what have we learned?** *Nature reviews. Nephrology*, **8**(2):89–99, 2012. (page 4).

[386] Oshlack, A., Robinson, M. D., and Young, M. D. **From RNA-seq reads to differential expression results.** *Genome biology*, **11**(12):220, 2010. (page 30).

[387] Osswald, H., Hermes, H. H., and Nabakowski, G. **Role of adenosine in signal transmission of tubuloglomerular feedback.** *Kidney international. Supplement*, **12**:S136–42, 1982. (page 8).

[388] Padmanabhan, S., Melander, O., Johnson, T., Di Blasio, A. M., Lee, W. K., Gentilini, D., Hastie, C. E., Menni, C., et al. **Genome-wide association study of blood pressure extremes identifies variant near UMOD associated with hypertension.** *PLoS genetics*, **6**(10):e1001177, 2010. (page 4).

[389] Padmanabhan, S., Newton-Cheh, C., and Dominiczak, A. F. **Genetic basis of blood pressure and hypertension.** *Trends in genetics : TIG*, **28**(8):397–408, 2012. (page 3).

[390] Palm, F. and Nordquist, L. **Renal oxidative stress, oxygenation and hypertension.** *American journal of physiology. Regulatory, integrative and comparative physiology*, **301**(5):R1229–41, 2011. (pages 64, 65).

[391] Palmer, T. M., Gettys, T. W., and Stiles, G. L. **Differential Interaction with and Regulation of Multiple G-proteins by the Rat A3 Adenosine Receptor**. *The Journal of biological chemistry*, **270**(28):16895–16902, 1995. (page 29).

[392] Palomino-Doza, J., Rahman, T. J., Avery, P. J., Mayosi, B. M., Farrall, M., Watkins, H., Edwards, C. R. W., and Keavney, B. **Ambulatory blood pressure is associated with polymorphic variation in P2X receptor genes.** *Hypertension*, **52**(5):980–5, 2008. (page 88).

[393] PARATI, G., POMIDOSSI, G., ALBINI, F., MALASPINA, D., and MANCIA, G. **Relationship of 24-hour blood pressure mean and variability to severity of**

target-organ damage in hypertension. *Journal of hypertension*, **5**(1):93–98, 1987. (page 62).

[394] PARK, W., GUPTA, P., BLOOM, B. J., ISHAQ, S., WEI, N., MEBUS, C. A., STOCK, T. C., AND WANG, X. **Efficacy and Safety of CE-224,535, an Antagonist of P2X7 Receptor, in Treatment of Patients with Rheumatoid Arthritis Inadequately Controlled by Methotrexate**, 2012. (page 88).

[395] PAUL, M., MEHR, A. L. I. P., AND KREUTZ, R. **Physiology of Local Renin-Angiotensin Systems**. *Physiol Rev*, **86**:747–803, 2006. (pages 16, 17).

[396] PEACH, M. J. **Renin-angiotensin system: biochemistry and mechanisms of action.** *Physiological reviews*, **57**(2):313–70, 1977. (page 15).

[397] PEDERSEN, M., DISSING, T. H., MØ RKENBORG, J., STØ DKILDE JØ RGENSEN, H., HANSEN, L. H., PEDERSEN, L. B., GRENIER, N., FRØ KIAER, J. R., PERDERSON, M., AND OTHERS,. **Validation of quantitative BOLD MRI measurements in kidney: application to unilateral ureteral obstruction**. *Kidney International*, **67**(6):2305–2312, 2005. (page 66).

[398] PELAEZ, L. I., MANRIQUEZ, M. C., NATH, K. A., ROMERO, J. C., AND JUNCOS, L. A. **Low-dose angiotensin II enhances pressor responses without causing sustained hypertension.** *Hypertension*, **42**(4):798–801, 2003. (page 64).

[399] PELEGRIN, P. AND SURPRENANT, A. **Pannexin-1 mediates large pore formation and interleukin-1beta release by the ATP-gated P2X7 receptor.** *The EMBO journal*, **25**(21):5071–82, 2006. (page 87).

[400] PELKONEN, O. AND NERBERT, D. W. **Metabolism of Polycyclic Aromatic Hydrocarbons: Etiologic Role in Carcinogenesis**. *Pharmacological Reviews*, **34**:189–222, 1982. (page 18).

[401] PENG, W., COTRINA, M. L., HAN, X., YU, H., BEKAR, L., BLUM, L., TAKANO, T., TIAN, G.-F., GOLDMAN, S. A., AND NEDERGAARD, M. **Systemic administration of an antagonist of the ATP-sensitive receptor P2X7 improves recovery after spinal cord injury.** *Proceedings of the National Academy of Sciences of the United States of America*, **106**(30):12489–93, 2009. (page 45).

[402] PETERS, J., MUNTER, K., BADER, M., HACKENTHAL, E., MULLINS, J. J., AND GANTEN, D. **Increased adrenal renin in transgenic hypertensive rats, TGR(mRen2)27, and its regulation by cAMP, angiotensin II and calcium**. *J. Clin. Invest.*, **91**:742–747, 1993. (page 18).

[403] PETI-PETERDI, J. **Angiotensin II Directly Stimulates ENaC Activity in the Cortical Collect-**

ing Duct via AT1 Receptors. *Journal of the American Society of Nephrology*, **13**(5):1131–1135, 2002. (page 16).

[404] Peti-Peterdi, J. **Calcium wave of tubuloglomerular feedback.** *American journal of physiology. Renal physiology*, **291**(2):F473–80, 2006. (page 8).

[405] Peti-Peterdi, J. and Harris, R. C. **Macula densa sensing and signaling mechanisms of renin release.** *Journal of the American Society of Nephrology : JASN*, **21**(7):1093–6, 2010. (page 15).

[406] Pierce, K. D., Furlong, T. J., Selbie, L. A., and Shine, J. **Molecular cloning and expression of an adenosine A2b receptor from human brain**. *Biochemical and Biophysical Research Communications*, **187**(1):86–93, 1992. (page 29).

[407] Poch, E., Gonzalez, D., Giner, V., Bragulat, E., Coca, a., and de la Sierra, a. **Molecular Basis of Salt Sensitivity in Human Hypertension: Evaluation of Renin-Angiotensin-Aldosterone System Gene Polymorphisms**. *Hypertension*, **38**(5):1204–1209, 2001. (page 62).

[408] Polichnowski, A. J., Lu, L., and Cowley, A. W. **Renal injury in Angiotensin II + L-NAME-induced hypertensive rats is independent of elevated blood pressure.** *American journal of physiology. Renal physiology*, (January), 2011. (pages 47, 62).

[409] Prasad, P. V., Edelman, R. R., and Epstein, F. H. **Noninvasive Evaluation of Intrarenal Oxygenation With BOLD MRI**. *Circulation*, **94**(12):3271–3275, 1996. (page 65).

[410] Pulvirenti, T. J., Yin, J. L., Chaufour, X., McLachlan, C., Hambly, B. D., Bennett, M. R., and Barden, J. a. **P2X (purinergic) receptor redistribution in rabbit aorta following injury to endothelial cells and cholesterol feeding.** *Journal of neurocytology*, **29**(9):623–31, 2000. (page 88).

[411] Rajagopalan, S., Kurz, S., Münzel, T., Tarpey, M., Freeman, B. a., Griendling, K. K., and Harrison, D. G. **Angiotensin II-mediated hypertension in the rat increases vascular superoxide production via membrane NADH/-NADPH oxidase activation. Contribution to alterations of vasomotor tone.** *The Journal of clinical investigation*, **97**(8):1916–23, 1996. (page 63).

[412] Rajasingh, H., Gjuvsland, A. B., Vå ge, D. I., and Omholt, S. W. **When parameters in dynamic models become phenotypes: a case study on flesh pigmentation in the chinook salmon (Oncorhynchus tshawytscha).** *Genetics*, **179**(2):1113–8, 2008. (page 4).

[413] Ralevic, V. and Burnstock, G. **Receptors for purines and pyrimidines.** *Pharmacological reviews*, **50**(3):413–92, 1998. (page 29).

[414] Ramirez, A. N. and Kunze, D. L. **P2X purinergic receptor channel expression and function in bovine aortic endothelium.** *American journal of physiology. Heart and circulatory physiology*, **282**(6):H2106–16, 2002. (page 45).

[415] Rapp, J. P. **Genetic analysis of inherited hypertension in the rat.** *Physiological reviews*, **80**(1):135–72, 2000. (page 3).

[416] Ray, F. R., Huang, W., Slater, M., and Barden, J. a. **Purinergic receptor distribution in endothelial cells in blood vessels: a basis for selection of coronary artery grafts.** *Atherosclerosis*, **162**(1):55–61, 2002. (page 44).

[417] Redon, J. and Lurbe, E. **Nocturnal blood pressure versus nondipping pattern: what do they mean?** *Hypertension*, **51**(1):41–2, 2008. (page 62).

[418] Ren, Y., Garvin, J. L., Liu, R., and Carretero, O. a. **Crosstalk between the connecting tubule and the afferent arteriole regulates renal microcirculation.** *Kidney international*, **71**(11):1116–21, 2007. (page 8).

[419] Ren, Y., Carretero, O. A., and Garvin, J. L. **Role of mesangial cells and gap junctions in tubuloglomerular feedback.** *Kidney international*, **62**:525–531, 2002. (page 8).

[420] Ren, Y., D'Ambrosio, M. a., Garvin, J. L., Wang, H., and Carretero, O. a. **Possible mediators of connecting tubule glomerular feedback.** *Hypertension*, **53**(2):319–23, 2009. (page 8).

[421] Rettig, R., Folberth, C., Stauss, H., Kopf, D., Waldherr, R., and Unger, T. **Role of the kidney in primary hypertension: a renal transplantation study in rats.** *The American journal of physiology*, **258**(3 Pt 2):F606–11, 1990. (page 13).

[422] Rettig, R. and Grisk, O. **The kidney as a determinant of genetic hypertension: evidence from renal transplantation studies.** *Hypertension*, **46**(3):463–8, 2005. (page 13).

[423] Rettig, R., Stauss, H., Folberth, C., Ganten, D., Waldherr, R., and Unger, T. **Hypertension spontaneously transmitted by kidneys from stroke-prone hypertensive rats**. *Am J Physiol Renal Fluid Electrolyte Physiol*, **257**(26):F197–F203, 1989. (page 13).

[424] Rich-Edwards, J. W., Stampfer, M. J., Manson, J. E., Rosner, B., Hankinson, S. E., Colditz, G. a., Willett, W. C., and Hennekens, C. H. **Birth weight and risk of cardiovascular disease in a cohort of women followed up since**

1976. *BMJ*, **315**(7105):396–400, 1997. (page 62).

[425] Riedel, T., Lozinsky, I., Schmalzing, G., and Markwardt, F. **Kinetics of P2X7 receptor-operated single channels currents.** *Biophysical journal*, **92**(7):2377–91, 2007. (pages 143, 145).

[426] Rimoldi, S. F., Scherrer, U., and Messerli, F. H. **Secondary arterial hypertension: when, who, and how to screen?** *European heart journal*, pages 1–12, 2013. (page 1).

[427] Risch, N. and Merikangas, K. **The future of genetic studies of complex human diseases.** *Science (New York, N.Y.)*, **273**(5281):1516–7, 1996. (page 3).

[428] Robertson, C. R., Deen, W. M., Troy, J. L., and Brenner, B. M. **Dynamics of glomerular ultrafiltration and autoregulation in the rat . III . Hemodynamics and autoregulation**. *Am J Physiol*, **223**(5):1191–1200, 1972. (page 6).

[429] Roman, R. J. **Pressure-diuresis in volume-expanded rats. Tubular reabsorption in superficial and deep nephrons**. *Hypertension*, **12**(2):177–183, 1988. (page 8).

[430] Rosenberger, C., Rosen, S., Paliege, A., and Heyman, S. N. **Pimonidazole adduct immunohistochemistry in the rat kidney: detection of tissue hypoxia.** *Methods in molecular biology (Clifton, N.J.)*, **466**:161–74, 2009. (page 65).

[431] Ruggenenti, P., Perna, a., Gherardi, G., Garini, G., Zoccali, C., Salvadori, M., Scolari, F., Schena, F. P., and Remuzzi, G. **Renoprotective properties of ACE-inhibition in non-diabetic nephropathies with non-nephrotic proteinuria.** *Lancet*, **354**(9176):359–64, 1999. (page 17).

[432] Ruiz-Ortega, M., Esteban, V., Suzuki, Y., Ruperez, M., Mezzano, S., Ardiles, L., Justo, P., Ortiz, A., and Egido, J. **Renal expression of angiotensin type 2 (AT2) receptors during kidney damage.** *Kidney international. Supplement*, **64**(86):S21–6, 2003. (page 47).

[433] Sakaki, H., Fujiwaki, T., Tsukimoto, M., Kawano, A., Harada, H., and Kojima, S. **P2X4 receptor regulates P2X7 receptor-dependent IL-1β and IL-18 release in mouse bone marrow-derived dendritic cells.** *Biochemical and biophysical research communications*, **432**(3):406–11, 2013. (page 144).

[434] Sander, M., Bader, M., Djavidani, B., Maser-Gluth, C., Vecsei, P., Mullins, J., Ganten, D., and Peters, J. **The role of the adrenal gland in hypertensive transgenic rat TGR(mRen2)27**. *Endocrinology*, **131**(2):807–814, 1992. (page 18).

[435] Santos, R. A. S., Simoes, A. C., Maric, C., Silva, D. M. R., Machado, R. P., Buhr, I. D., Heringer-walther, S., Pinheiro, S. V. B., et al. **G protein-coupled receptor Mas**. *PNAS*, **100**(14):8258–8263, 2003. (page 16).

[436] Sarnak, M. J., Levey, A. S., Schoolwerth, A. C., Coresh, J., Culleton, B., Hamm, L. L., McCullough, P. a., Kasiske, B. L., et al. **Kidney disease as a risk factor for development of cardiovascular disease: a statement from the American Heart Association Councils on Kidney in Cardiovascular Disease, High Blood Pressure Research, Clinical Cardiology, and Epidemiology and Prevention.** *Circulation*, **108**(17):2154–69, 2003. (pages 1, 9, 62).

[437] Sarwal, M., Chua, M.-s., Kambham, N., Hsieh, S.-c., Satterwhite, T., Masek, M., and Salvatierra, O. **Molecular Heterogeneity in Acute Renal Allograft Rejection Identified by DNA Microarray Profiling**. *NEJM*, **349**:125–138, 2003. (page 13).

[438] Sayegh, M. H. and Turka, L. A. **The role of t-cell costimulatory activation pathways in transplant rejection**. *NEJM*, **338**:1813–1821, 1998. (page 13).

[439] Schachinger, H., Klarhöfer, M., Linder, L., Drewe, J., and Scheffler, K. **Angiotensin II decreases the renal MRI blood oxygenation level-dependent signal.** *Hypertension*, **47**(6):1062–6, 2006. (pages 82, 83).

[440] Schechter, A. N. and Gladwin, M. T. **Hemoglobin and the Paracrine and Endocrine Functions of Nitric Oxide**. *The New England journal of medicine*, **348**(15):1483–1485, 2003. (page 17).

[441] Schlaich, M. P., Sobotka, P. a., Krum, H., Lambert, E., and Esler, M. D. **Renal sympathetic-nerve ablation for uncontrolled hypertension.** *The New England journal of medicine*, **361**(9):932–4, 2009. (page 12).

[442] Schmieder, R. E., Hilgers, K. F., Schlaich, M. P., and Schmidt, B. M. W. **Renin-angiotensin system and cardiovascular risk.** *Lancet*, **369**(9568):1208–19, 2007. (page 13).

[443] Schnermann, J. and Briggs, J. P. **The macula densa is worth its salt.** *The Journal of clinical investigation*, **104**(8):1007–9, 1999. (page 8).

[444] Schnermann, J., Briggs, J. P., and Weber, P. C. **Tubuloglomerular feedback, prostaglandins, and angiotensin in the autoregulation of glomerular filtration rate.** *Kidney international*, **25**(1):53–64, 1984. (page 6).

[445] Schnermann, J., Chou, C. L., Ma, T., Traynor, T., Knepper, M. a., and Verkman, a. S. **Defective proximal tubular fluid reabsorption in transgenic aquaporin-1 null mice.** *Proceedings of the National Academy of Sciences of the United States of America*, **95**(16):9660–4, 1998. (page 9).

[446] Schnermann, J., Osswald, H., and Hermle, M. **Inhibitory Effect of Methylxanthines on Feedback Control of Glomerular Filtration Rate in the Rat Kidney**. *Pflugers Archiv*, **48**:39–48, 1977. (page 8).

[447] Schnermann, J. and Levine, D. Z. **Paracrine factors in tubuloglomerular feedback: adenosine, ATP, and nitric oxide.** *Annual review of physiology*, **65**:501–29, 2003. (pages 6, 15, 17, 29).

[448] Schreiner, G. F., Harris, K. P., Purkerson, M. L., and Klahr, S. **Immunological aspects of acute ureteral obstruction: immune cell infiltrate in the kidney.** *Kidney international*, **34**(4):487–93, 1988. (page 63).

[449] Schultheis, P. J., Clarke, L. L., Meneton, P., Miller, M. L., Soleimani, M., Gawenis, L. R., Riddle, T. M., Duffy, J. J., et al. **Renal and intestinal absorptive defects in mice lacking the NHE3 Na+/H+ exchanger.** *Nature genetics*, **19**(3):282–5, 1998. (pages 9, 12).

[450] Schurek, H. J., Jost, U., Baumgartl, H., and Heckmann, U. **Evidence for a preglomerular oxygen diffusion shunt in rat renal cortex**. *Am J Physiol Renal Physiol*, **259**:F910–F915, 1990. (page 6).

[451] Schweda, F., Friis, U., Wagner, C., Skott, O., and Kurtz, A. **Renin release.** *Physiology (Bethesda, Md.)*, **22**:310–9, 2007. (page 15).

[452] Sega, R., Facchetti, R., Bombelli, M., Cesana, G., Corrao, G., Grassi, G., and Mancia, G. **Prognostic value of ambulatory and home blood pressures compared with office blood pressure in the general population: follow-up results from the Pressioni Arteriose Monitorate e Loro Associazioni (PAMELA) study.** *Circulation*, **111**(14):1777–83, 2005. (page 62).

[453] Selkurt, E. E., Hall, P. W., and Spencer, M. P. **Influence of graded arterial pressure decrement on renal clearance of creatinine, p-aminohippurate and sodium**. *Am J Physiol*, **159**:369–378, 1949. (pages 8, 9).

[454] Selkurt, E. E., Womack, I., and Dailey, W. N. **Mechanism of Natriuresis and Diuresis During Elevated Renal Arterial Pressure.** *The American journal of physiology*, **209**:95–9, 1965. (page 8).

[455] Shao, J., Nangaku, M., Miyata, T., Inagi, R., Yamada,

K., Kurokawa, K., and Fujita, T. **Imbalance of T-cell subsets in angiotensin II-infused hypertensive rats with kidney injury.** *Hypertension*, **42**(1):31–8, 2003. (page 13).

[456] Sharp, M. G., Fettes, D., Brooker, G., Clark, A. F., Peters, J., Fleming, S., and Mullins, J. J. **Targeted Inactivation of the Ren-2 Gene in Mice**. *Hypertension*, **28**(6):1126–1131, 1996. (page 15).

[457] Shimkets, R. A., Warnock, D. G., Bositis, C. M., Nelson-williams, C., Hansson, J. H., Schambelan, M., Gill, J. R., Ulick, S., et al. **Liddles Syndrome : Heritable Human Hypertension Caused by Mutations in the p Subunit of the Epithelial Sodium Channel**. *Cell*, **79**:407–414, 1994. (pages 2, 12).

[458] Shipley, R. E. and Study, R. S. **Changes in renal blood flow, extraction of inulin, glomerular filtration rate, tissue pressure and urine flow with acute alterations of renal artery blood pressure**. *Am J Physiol*, **167**:676–688, 1951. (pages 8, 9).

[459] Shirley, D. G., Bailey, M. A., Scott, S. P., Tam, F. W. K., and Unwin, R. J. **Extracellular Nucleotides and Renal Function**. In *Seldin and Giebisch's The Kidney (Fifth Edition)*, pages 511–537. 2013. (page 31).

[460] Simon, D. B., Karet, F. E., Hamdan, J. M., Di Pietro, A., Sanjad, S. A., and Lifton, R. P. **Bartter's syndrome, hypokalaemic alkalosis with hypercalciuria, is caused by mutations in the Na-K-2Cl cotransporter NKCC2**. *Nature Genetics*, **13**:183–188, 1996. (page 12).

[461] Simon, D. B., Nelson-Williams, C., Johnson, B., Ellison, D., Karet, F. E., Molina, A. M., Vaara, I., Iwata, F., et al. **Gitelman's variant of Bartter's syndrome, inherited hypokalaemic alkalosis, is caused by mutations in the thiazide-sensitive Na-Cl cotransporter**. *Nature Genetics*, **12**:24–30, 1996. (page 12).

[462] Simon, G., Abraham, G., and Cserep, G. **Pressor and subpressor angiotensin II administration. Two experimental models of hypertension.** *American journal of hypertension*, **8**(6):645–50, 1995. (page 64).

[463] Simonetti, G. D., Mohaupt, M. G., and Bianchetti, M. G. **Monogenic forms of hypertension**. *Eur J Pediatr*, **171**(1433-1439):1433–1439, 2012. (page 2).

[464] Sivaramakrishnan, V. and Fountain, S. J. **A mechanism of intracellular P2X receptor activation.** *The Journal of biological chemistry*, **287**(34):28315–26, 2012. (page 44).

[465] Skov, K. and Mulvany, M. J. **Structure of renal afferent ar-**

terioles in the pathogenesis of hypertension. *Acta physiologica Scandinavica*, **181**(4):397–405, 2004. (page 62).

[466] Skov, K., Mulvany, M. J., and Korsgaard, N. **Morphology of renal afferent arterioles in spontaneously hypertensive rats**. *Hypertension*, **20**(6):821–827, 1992. (page 62).

[467] Sluyter, R. **Significance of P2X7 Receptor Variants to Human Health and Disease Significance of P2X7 Receptor Variants to Human Health and Disease**. pages 41–54, 2011. (page 87).

[468] Smith, H. W., Chasis, H., Goldring, W., and Ranges, H. A. **Glomerular dynamics in the normal human kidney**. *Journal of Clinical Investigation*, **19**:751–764, 1940. (page 8).

[469] Solini, A., Iacobini, C., Ricci, C., Chiozzi, P., Amadio, L., Pricci, F., Di Mario, U., Di Virgilio, F., and Pugliese, G. **Purinergic modulation of mesangial extracellular matrix production: role in diabetic and other glomerular diseases.** *Kidney international*, **67**(3):875–85, 2005. (page 64).

[470] Soneson, C. and Delorenzi, M. **A comparison of methods for differential expression analysis of RNA-seq data.** *BMC bioinformatics*, **14**(1):91, 2013. (page 30).

[471] Soto, F., Garcia-Guzman, M., Gomez-Hernandez, J. M., Hollmann, M., Karschin, C., and Stühmer, W. **P2X4: an ATP-activated ionotropic receptor cloned from rat brain.** *Proceedings of the National Academy of Sciences of the United States of America*, **93**(8):3684–8, 1996. (page 144).

[472] Speiser, P. W. and White, P. C. **Congenital adrenal hyperplasia.** *The New England journal of medicine*, **349**(8):776–88, 2003. (page 2).

[473] Stamler, J. **The INTERSALT Study : background, methods, findings, and impliactions**. *Am J Clin Nutr*, **65**:626S–42S, 1997. (page 4).

[474] Staub, O., Dho, S., Henry, P. C., Correa, J., Ishikawa, T., Mcglade, J., and Rotin, D. **WW domains of Nedd4 bind to the proline-rich PY motifs in the epithelial Na + channel deleted in Liddle ' s syndrome**. *The EMBO journal*, **15**(10):2371–2380, 1996. (page 12).

[475] Steckelings, U., Lebrun, C., Qadri, F., Veltmar, A., and Unger, T. **Role of brain angiotensin in cardiovascular regulation.** *Journal of cardiovascular pharmacology*, **19 Suppl 6**:S72–9, 1992. (page 17).

[476] Stern, M. D., Bowen, P. D., Parma, R., Osgood, R. W., Bowman, R. L., and Stein, J. H. **Measurement of renal cortical and medullary blood flow by laser-Doppler spectroscopy in**

the rat. *The American journal of physiology*, **236**(1):F80–7, 1979. (page 8).

[477] Stigant, C. E., Cohen, J., Vivera, M., and Zaltzman, J. S. **ACE inhibitors and angiotensin II antagonists in renal transplantation: an analysis of safety and efficacy.** *American journal of kidney diseases : the official journal of the National Kidney Foundation*, **35**(1):58–63, 2000. (page 13).

[478] Stokes, L., Scurrah, K., Ellis, J. A., Cromer, B. A., Skarratt, K. K., Gu, B. J., Harrap, S. B., and Wiley, J. S. **A loss-of-function polymorphism in the human P2X4 receptor is associated with increased pulse pressure.** *Hypertension*, **58**(6):1086–92, 2011. (page 88).

[479] Strom, B. L., Anderson, C. A. M., and Ix, J. H. **Sodium Reduction in Populations. Insights From the Institute of Medicine Committee**. *JAMA*, **310**(1):31–32, 2013. (page 4).

[480] Sun, D., Samuelson, L. C., Yang, T., Huang, Y., Paliege, a., Saunders, T., Briggs, J., and Schnermann, J. **Mediation of tubuloglomerular feedback by adenosine: evidence from mice lacking adenosine 1 receptors.** *Proceedings of the National Academy of Sciences of the United States of America*, **98**(17):9983–8, 2001. (page 8).

[481] Surprenant, A., Rassendren, F., Kawashima, E., North, R. A., and Buell, G. **The cytolytic P2Z receptor for extracellular ATP identified as a P2X receptor (P2X7)**. *Science*, **272**:735–738, 1996. (page 144).

[482] Syvänen, a. C. **Accessing genetic variation: genotyping single nucleotide polymorphisms.** *Nature reviews. Genetics*, **2**(12):930–42, 2001. (page 3).

[483] Tagawa, H. and Vander, a. J. **Effects of Adenosine Compounds on Renal Function and Renin Secretion in Dogs**. *Circulation Research*, **26**(3):327–338, 1970. (page 31).

[484] Takahashi, N., Chernavvsky, D. R., Gomez, R. a., Igarashi, P., Gitelman, H. J., and Smithies, O. **Uncompensated polyuria in a mouse model of Bartter's syndrome.** *Proceedings of the National Academy of Sciences of the United States of America*, **97**(10):5434–9, 2000. (page 12).

[485] Takahashi, N. and Smithies, O. **Gene targeting approaches to analyzing hypertension.** *Journal of the American Society of Nephrology : JASN*, **10**(7):1598–605, 1999. (page 2).

[486] Takenaka, T., Harrison-Bernard, L. M., Inscho, E. W., Carmines, P. K., and Navar, L. G. **Autoregulation of afferent arteriolar blood flow in juxtamedullary nephrons**.

Am J Physiol Renal Physiol, **267**:F876–F887, 1994. (page 8).

[487] Tarazi, R. C. **Hemodynamic role of extracellular fluid in hypertension**. *Circulation Research*, **38**(6):73–83, 1976. (page 4).

[488] Taylor, S. R. J., Turner, C. M., Elliott, J. I., McDaid, J., Hewitt, R., Smith, J., Pickering, M. C., Whitehouse, D. L., et al. **P2X7 deficiency attenuates renal injury in experimental glomerulonephritis.** *Journal of the American Society of Nephrology : JASN*, **20**(6):1275–81, 2009. (pages 63, 87).

[489] Thomas, K. R. and Capecchi, M. R. **Site-directed mutagenesis by gene targeting in mouse embryo-derived stem cells.** *Cell*, **51**(3):503–12, 1987. (page 2).

[490] Thompson, D. D. and Pitts, R. F. **Effects of Alterations of renal arterial pressure on Sodium and water excretion**. *Am J Physiol*, **168**:490–499, 1951. (page 9).

[491] Thomson, S., Bao, D., Deng, a., and Vallon, V. **Adenosine formed by 5'-nucleotidase mediates tubuloglomerular feedback.** *The Journal of clinical investigation*, **106**(2):289–98, 2000. (page 8).

[492] Thomson, S. C. and Blantz, R. C. **Glomerulotubular balance, tubuloglomerular feedback, and salt homeostasis.** *Journal of the American Society of Nephrology : JASN*, **19**(12):2272–5, 2008. (page 8).

[493] Timmermans, P. B. M. W. M., Wong, P. C., Chiu, A. T., Herblin, W. F., Benfield, P., Carini, D. J., Lee, R. J., Wexler, R. R., Saye, J. A. M., and Smith, R. D. **Angiotensin II Receptors and Angiotensin II Receptor Antagonists**. *Pharmacological reviews*, **45**(2):205–251, 1993. (page 16).

[494] Tokita, Y., Franco-Saenz, R., Mulrow, P. J., and Gantem, D. **Effects of nephrectomy and adrenalectomy on the renin-angiotensin system of transgenic rats TGR(mRen2)27**. *Endocrinology*, **134**:253–257, 1994. (page 18).

[495] Tölle, M., Jankowski, V., Schuchardt, M., Wiedon, A., Huang, T., Hub, F., Kowalska, J., Jemielity, J., et al. **Adenosine 5'-tetraphosphate is a highly potent purinergic endothelium-derived vasoconstrictor.** *Circulation research*, **103**(10):1100–8, 2008. (page 44).

[496] Touyz, R. M. and Schiffrin, E. L. **Signal transduction mechanisms mediating the physiological and pathophysiological actions of angiotensin II in vascular smooth muscle cells.** *Pharmacological reviews*, **52**(4):639–72, 2000. (page 47).

[497] Trudu, M., Janas, S., Lanzani, C., Debaix, H., Schaeffer, C.,

Ikehata, M., Citterio, L., Demaretz, S., et al. **Common noncoding UMOD gene variants induce salt-sensitive hypertension and kidney damage by increasing uromodulin expression**. *Nat Med*, **advance on**, 2013. (page 4).

[498] Tsai, L.-L. and Tsai, Y.-C. **The effect of scheduled forced wheel activity on body weight in male F344 rats undergoing chronic circadian desynchronization.** *International journal of obesity (2005)*, **31**(9):1368–77, 2007. (page 17).

[499] Tummala, P. E., Chen, X.-L., Sundell, C. L., Laursen, J. B., Hammes, C. P., Alexander, R. W., Harrison, D. G., and Medford, R. M. **Angiotensin II Induces Vascular Cell Adhesion Molecule-1 Expression In Rat Vasculature : A Potential Link Between the Renin-Angiotensin System and Atherosclerosis**. *Circulation*, **100**(11):1223–1229, 1999. (page 63).

[500] Tuominen, V. J., Ruotoistenmäki, S., Viitanen, A., Jumppanen, M., and Isola, J. **ImmunoRatio: a publicly available web application for quantitative image analysis of estrogen receptor (ER), progesterone receptor (PR), and Ki-67.** *Breast cancer research : BCR*, **12**(4):R56, 2010. (page 48).

[501] Turner, C. M., Vonend, O., Chan, C., Burnstock, G., and Unwin, R. J. **The Pattern of Distribution of Selected ATP-Sensitive P2 Receptor Subtypes in Normal Rat Kidney : An Immunohistological Study**. *Cells Tissues Organs*, pages 105–117, 2003. (page 29).

[502] Ulmann, L., Hirbec, H., and Rassendren, F. **P2X4 receptors mediate PGE2 release by tissue-resident macrophages and initiate inflammatory pain.** *The EMBO journal*, **29**(14):2290–300, 2010. (page 87).

[503] Unwin, R. J., Bailey, M. a., and Burnstock, G. **Purinergic signaling along the renal tubule: the current state of play.** *News in physiological sciences : an international journal of physiology produced jointly by the International Union of Physiological Sciences and the American Physiological Society*, **18**:237–41, 2003. (page 29).

[504] Urata, H., Nishimura, H., and Ganten, D. **Chymase-Dependent Angistensin II Forming System in Humans**. *American journal of hypertension*, **9**:277–284, 1996. (page 16).

[505] Uzu, T. and Kimura, G. **Diuretics shift circadian rhythm of blood pressure from nondipper to dipper in essential hypertension.** *Circulation*, **100**(15):1635–8, 1999. (page 62).

[506] Vallon, V. **Tubuloglomerular Feedback and the Control of Glomerular Filtration**

Rate. *Physiology*, **18**:169–174, 2003. (page 8).

[507] Vallon, V. and Mu, B. **Adenosine and Kidney Function**. *Physiol Rev*, **86**:901–940, 2006. (page 29).

[508] Van Der Mark, J. and Kline, R. L. **Altered pressure natriuresis in chronic angiotensin II hypertension in rats**. *Am J Physiol Regul Integr Comp Physiol*, **266**:R739–R748, 1994. (pages 64, 82).

[509] Vavrinec, P., Henning, R. H., Goris, M., Vavrincova-Yaghi, D., Buikema, H., and van Dokkum, R. P. E. **Vascular smooth muscle function of renal glomerular and interlobar arteries predicts renal damage in rats.** *American journal of physiology. Renal physiology*, **303**(8):F1187–95, 2012. (page 62).

[510] Verkman, A. S. **Aquaporins in clinical medicine.** *Annual review of medicine*, **63**:303–16, 2012. (page 9).

[511] Viera, A. J. and Neutze, D. M. **Diagnosis of secondary hypertension: an age-based approach.** *American family physician*, **82**(12):1471–8, 2010. (page 1).

[512] Vilaysane, A., Chun, J., Seamone, M. E., Wang, W., Chin, R., Hirota, S., Li, Y., Clark, S. a., et al. **The NLRP3 inflammasome promotes renal inflammation and contributes to CKD.** *Journal of the American Society of Nephrology : JASN*, **21**(10):1732–44, 2010. (page 84).

[513] Vitzthum, H., Weiss, B., Bachleitner, W., Krämer, B. K., and Kurtz, A. **Gene expression of adenosine receptors along the nephron.** *Kidney international*, **65**(4):1180–90, 2004. (page 29).

[514] Vlek, a. L. M., van der Graaf, Y., Spiering, W., Algra, a., and Visseren, F. L. J. **Cardiovascular events and all-cause mortality by albuminuria and decreased glomerular filtration rate in patients with vascular disease.** *Journal of internal medicine*, **264**(4):351–60, 2008. (page 62).

[515] Vonend, O., Turner, C. M., Chan, C. M., Loesch, A., Dell'Anna, G. C., Srai, K. S., Burnstock, G., and Unwin, R. J. **Glomerular expression of the ATP-sensitive P2X receptor in diabetic and hypertensive rat models.** *Kidney international*, **66**(1):157–66, 2004. (pages 27, 63).

[516] Wagner, C. and Kurtz, A. **Regulation of renal renin release**. *Curr Opin Nephrol Hypertens*, **7**:437–441, 1998. (page 15).

[517] Walker, L. A., Buscemi-Bergin, M., and Gellai, M. **Renal hemodynamics in conscious rats: effects of anesthesia, surgery, and recovery.**

Am J Physiol Renal Fluid Electrolyte Physiol, **245**(1):F67–74, 1983. (page 83).

[518] Walker III, M., Harrison-Bernard, L. M., Cook, A. K., and Navar, L. G. **Dynamic interaction between myogenic and TGF mechanisms in afferent arteriolar blood flow autoregulation**. *Am J Physiol Renal Physiol*, **279**:F858–F865, 2000. (page 8).

[519] Wang, D. J., Huang, N. N., and Heppel, L. a. **Extracellular ATP and ADP stimulate proliferation of porcine aortic smooth muscle cells.** *Journal of cellular physiology*, **153**(2):221–33, 1992. (page 64).

[520] Wang, H., Siu, K., Ju, K., Moore, L. C., and Chon, K. H. **Identification of Transient Renal Autoregulatory Mechanisms Using Time-Frequency Spectral Techniques**. *Methods*, **52**(6):1033–1039, 2005. (page 62).

[521] Wang, H., D'Ambrosio, M. a., Garvin, J. L., Ren, Y., and Carretero, O. a. **Connecting tubule glomerular feedback mediates acute tubuloglomerular feedback resetting.** *American journal of physiology. Renal physiology*, **302**(10):F1300–4, 2012. (page 8).

[522] Wang, L., Karlsson, L., Moses, S., Hultgå rdh Nilsson, A., Andersson, M., Borna, C., Gudbjartsson, T., Jern, S., and Erlinge, D. **P2 receptor expression profiles in human vascular smooth muscle and endothelial cells.** *Journal of cardiovascular pharmacology*, **40**(6):841–53, 2002. (pages 15, 44).

[523] Wang, Y., Wang, Y. P., Zheng, G., Lee, V. W. S., Ouyang, L., Chang, D. H. H., Mahajan, D., Coombs, J., et al. **Ex vivo programmed macrophages ameliorate experimental chronic inflammatory renal disease.** *Kidney international*, **72**(3):290–9, 2007. (page 63).

[524] Wang, Y., Gjuvsland, A. B., Vik, J. O., Smith, N. P., Hunter, P. J., and Omholt, S. W. **Parameters in dynamic models of complex traits are containers of missing heritability.** *PLoS computational biology*, **8**(4):e1002459, 2012. (page 4).

[525] Warren, J. V. and Eugene, A. **Fluid dynamics in chronic congestive heart failure**. *JAMA*, **73**:138–147, 1944. (page 9).

[526] Weigand, K., Wernze, H., and Falge, C. **Synthesis of angiotensinogen by isolated rat liver cells and its regulation in comparison to serum albumin**. *Biochemical and Biophysical Research Communications*, **75**(1):102–110, 1977. (page 15).

[527] Weihprecht, H., Lorenz, J. N., Briggs, J. P., and Schnermann, J. **Synergistic effects of angiotensin in the renal microvasculature and adenosine**. *Am J Physiol Renal Fluid*

Electrolyte Physiol, **266**:F227–F239, 1994. (page 64).

[528] Weinberger, M. H. **Salt sensitivity of blood pressure in humans**. *Hypertension*, **27**:481–490, 1996. (page 4).

[529] Weinberger, M. H., Fineberg, N. S., Fineberg, S. E., and Weinberger, M. **Salt Sensitivity, Pulse Pressure, and Death in Normal and Hypertensive Humans**. *Hypertension*, **37**(2):429–432, 2001. (page 4).

[530] Welch, W. J., Blau, J., Xie, H., Chabrashvili, T., and Wilcox, C. S. **Angiotensin-induced defects in renal oxygenation: role of oxidative stress.** *American journal of physiology. Heart and circulatory physiology*, **288**(1):H22–8, 2005. (page 83).

[531] Welch, W. J., Mendonca, M., Aslam, S., and Wilcox, C. S. **Roles of oxidative stress and AT1 receptors in renal hemodynamics and oxygenation in the postclipped 2K,1C kidney.** *Hypertension*, **41**(3 Pt 2):692–6, 2003. (page 82).

[532] welcome trust case Consortium, T. **Genome-wide association study of 14,000 cases of seven common diseases and 3,000 shared controls.** *Nature*, **447**(7145):661–78, 2007. (page 2).

[533] Wewers, M. D. and Sarkar, A. **P2X(7) receptor and macrophage function.** *Purinergic signalling*, **5**(2):189–95, 2009. (pages 27, 29, 47, 87).

[534] White, P. C., Mune, T., and Agarwal, A. K. **11β-hydroxysteroid dehydrogenase and the syndrome of apparent mineralocorticoid excess**. *Endocrine Reviews*, **18**(1):135–156, 1997. (page 2).

[535] Wilcox, C. S. **Oxidative stress and nitric oxide deficiency in the kidney: a critical link to hypertension?** *American journal of physiology. Regulatory, integrative and comparative physiology*, **289**(4):R913–35, 2005. (page 64).

[536] Wildman, S. S., Brown, S. G., King, B. F., and Burnstock, G. **Selectivity of diadenosine polyphosphates for rat P2X receptor subunits.** *European journal of pharmacology*, **367**(1):119–23, 1999. (page 44).

[537] Williams, B., Poulter, N. R., Brown, M. J., Davis, M., McInnes, G. T., Potter, J. F., Sever, P. S., and McG Thom, S. **Guidelines for management of hypertension: report of the fourth working party of the British Hypertension Society, 2004-BHS IV.** *Journal of human hypertension*, **18**(3):139–85, 2004. (page 17).

[538] Wilson, F. H., Disse-Nicodème, S., Choate, K. A., Ishikawa, K., Nelson-Williams, C., Desitter, I., Gunel, M., Milford, D. V., et al. **Human hypertension caused by mutations in WNK kinases.** *Science (New York, N.Y.)*, **293**:1107–1112, 2001. (page 12).

[539] Wolf, P. a., Abbott, R. D., and Kannel, W. B. **Atrial fibrillation as an independent risk factor for stroke: the Framingham Study**. *Stroke*, **22**(8):983–988, 1991. (page 3).

[540] Wright, J. W. and Harding, J. W. **Brain angiotensin receptor subtypes in the control of physiological and behavioral responses.** *Neuroscience and biobehavioral reviews*, **18**(1):21–53, 1994. (page 16).

[541] Xin-Long, P., Jing-Xia, X., Jian-Yu, L., Song, W., and Xin-Kui, T. **A preliminary study of blood-oxygen-level-dependent MRI in patients with chronic kidney disease.** *Magnetic resonance imaging*, **30**(3):330–5, 2012. (pages 81, 82).

[542] Xu, X. J., Boumechache, M., Robinson, L. E., Marschall, V., Gorecki, D. C., Masin, M., and Murrell-Lagnado, R. D. **Splice variants of the P2X7 receptor reveal differential agonist dependence and functional coupling with pannexin-1.** *Journal of cell science*, **125**(Pt 16):3776–89, 2012. (page 87).

[543] Yamamoto, K. and Ando, J. **New Molecular Mechanisms for Cardiovascular Disease: Blood Flow Sensing Mechanism in Vascular Endothelial Cells**. *Journal of Pharmacological Sciences*, **116**(4):323–331, 2011. (page 29).

[544] Yamamoto, K., Korenaga, R., Kamiya, A., Qi, Z. H. I., Sokabe, M., Ando, J., Qi, Z., and Px, J. A. **P2X 4 receptors mediate ATP-induced calcium influx in human vascular endothelial cells**. *Am J Physiol Heart Circ Physiol*, **279**:H285–H292, 2000. (pages 44, 85, 144).

[545] Yamamoto, K., Sokabe, T., Matsumoto, T., Yoshimura, K., Shibata, M., Ohura, N., Fukuda, T., Sato, T., et al. **Impaired flow-dependent control of vascular tone and remodeling in P2X4-deficient mice.** *Nature medicine*, **12**(1):133–7, 2006. (pages 20, 44, 85, 87).

[546] Yang, S.-S., Hsu, Y.-J., Chiga, M., Rai, T., Sasaki, S., Uchida, S., and Lin, S.-H. **Mechanisms for hypercalciuria in pseudohypoaldosteronism type II-causing WNK4 knock-in mice.** *Endocrinology*, **151**:1829–1836, 2010. (page 12).

[547] Ying, C.-Q., Wang, Y.-H., Wu, Z.-L., Fang, M.-W., Wang, J., Li, Y.-S., Zhang, Y.-H., and Qiu, C.-C. **Association of the renin gene polymorphism, three angiotensinogen gene polymorphisms and the haplotypes with essential hypertension in the Mongolian population.** *Clinical and experimental hypertension (New York, N.Y. : 1993)*, **32**(5):293–300, 2010. (page 17).

[548] Zhao, D., Seth, D. M., and Navar, L. G. **Enhanced dis-**

tal nephron sodium reabsorption in chronic angiotensin II-infused mice. *Hypertension*, **54**(1):120–6, 2009. (page 82).

[549] Zhao, X., He, G., Chen, Y.-R., Pandian, R. P., Kuppusamy, P., and Zweier, J. L. **Endothelium-derived nitric oxide regulates postischemic myocardial oxygenation and oxygen consumption by modulation of mitochondrial electron transport.** *Circulation*, **111**(22):2966–72, 2005. (pages 64, 87).

[550] Zini, S., Fournie-Zaluski, M. C., Chauvel, E., Roques, B. P., Corvol, P., and Llorens-Cortes, C. **Identification of metabolic pathways of brain angiotensin II and III using specific aminopeptidase inhibitors: predominant role of angiotensin III in the control of vasopressin release.** *Proceedings of the National Academy of Sciences of the United States of America*, **93**(21):11968–73, 1996. (page 16).

[551] Zöllner, F. G., Sance, R., Rogelj, P., Ledesma-Carbayo, M. J., Rø rvik, J., Santos, A., and Lundervold, A. **Assessment of 3D DCE-MRI of the kidneys using non-rigid image registration and segmentation of voxel time courses.** *Computerized medical imaging and graphics : the official journal of the Computerized Medical Imaging Society*, **33**(3):171–81, 2009. (page 81).

[552] Zuk, O., Hechter, E., Sunyaev, S. R., and Lander, E. S. **The mystery of missing heritability: Genetic interactions create phantom heritability.** *Proceedings of the National Academy of Sciences of the United States of America*, **109**(4):1193–8, 2012. (page 4).

7
Appendix A: Computational Models of P2X4 and P2X7

During my PhD I spent several months working at the NIH Systems Biology Centre Virtual Physiological Rat Project (VPR; `http://virtualrat.org/`) within the Medical College of Wisconsin under the supervision of the VPR investigators Drs. Dan Beard, Brian Carlson and Allen Cowley Jr. The intention of this work was to develop a quantitative understanding of the electrophysiological events mediated by P2X7 and P2X4 receptor activation that might delineate their function. This was deemed necessary because the alternative experimental approaches such as high affinity pharmacology and/or gene deletion in the F344 rat were financially impractical. Thus computational modelling (using literature mined experimental data to guide model parameters) was used to investigate demonstrates the similarities (and distinctions) between P2X7 and P2X4 activation by ATP which could be functionally important in terms of their vascular expression. These data are discussed in the context of the renal functional data (chapter 3, section 3.4).

7.1 Modelling P2X Receptor Electrophysiology

P2X4 and P2X7 channels are ATP gated ion channels. A computational model utilising channel activation by ligand binding affinities was designed using a ligand binding affinity framework (91). The Goldman-Hodgkin-Katz flux equation provide the means to model Na^+, Ca^{2+} and K^+ currents through P2X receptors (157, 199). Model fitness was tested against experimentally determined single channel patch-clamp voltage-current relationships of P2X7 (425) and P2X4 (361) receptors respectively.

Two dimensionless values of ATP-dependent activity inside, α_{in} , or outside, α_{out}, the membrane are determined from the Hill equation for a given ATP concentration, [ATP]. This relationship is described in Eqn.7.1 where K is the dissociation constant and n is the Hill coefficient. The dimensionless value $\alpha_{0_{out}/0_{in}}$ represents the initial activity in either the extracellular or intracellular space respectively.

$$\alpha_{out/in} = \alpha_{0_{out}/0_{in}} \left(\frac{[ATP]^n}{K^n + [ATP]^n} \right) \tag{7.1}$$

The open probability for each ion , equates to a factor of the ion specific activity, the relative permeability for each cation and maximal permeabilities for each receptor shown in Eqn.7.2, where subscript S indicates one of the three ions Na^+, Ca^{2+} or K^+. The cation permeability of P2X7 and P2X2 do not differ significantly (481). Permeability ratios established in experiments of P2X2 receptors were therefore used to parameterise the P2X7 model. Relative permeabilities for P2X4 were taken from (471). It is worthy of note that sustained receptor activation changes these permeabilities (see Fig. 1D of (110)). This is not addressed since the present model was focused on identifying cation permeabilities pertaining to altered contractile function, not the permeability of large molecules. Nonetheless this is a limiting factor of these P2X7 and P2X4 models.

$$P_{Sout/in} = P_S P2X_\phi . \alpha_{out/in} . P_0 P2X_\phi \tag{7.2}$$

P2X channel fluxes were constructed from the Goldman HodgkinKatz flux equation as shown in Eqn.7.3. Symbols are given for membrane potential (Vm), ionic valence (zs), Faradays constant (F), the gas constant (R) and temperature (T).

$$J_{P2X_{\phi S}} = \frac{z_s V_m F}{RT} \left(\frac{P_{Sin}[ATP] exp(-\frac{z_s V_m F}{RT}) - P_{Sout}[ATP]}{exp(\frac{z_s V_m F}{RT}) - 1} \right) \tag{7.3}$$

Total current for the individual channels was then calculated by Na^+, Ca^{2+} influx and K^+ efflux.The resulting, P2X4 channel current is given in Eqn.7.4. For time-dependent simulations the exponential factor $e^{-0.009359.t}$ for time, $t = 0 - 300$ seconds, was included. The factor 0.009359 was established by curve fitting experimental data from Fig. 6 of (544). The importance of this decay can be seen by blocking the P2X7 receptor which causes no sustained calcium influx over time (see Fig.1 in (433)).

$$I_{P2X4} = A_m (F z_s) J_{P2X4_S} . e^{-0.009359.t} \tag{7.4}$$

P2X7 current, Eqn. 7.5, specifically calcium influx, is highly sustained following activation by ATP, (110, 371), this is reflected in the exponential decay factor for time-dependent simulations.

$$I_{P2X7} = A_m (F z_s) J_{P2X7_S} . e^{-0.0009359.t} \tag{7.5}$$

The solutions to Eqns.7.4 and 7.5 provided the final P2X individual channel current models for total current as well as Na^+, Ca^{2+} and K^+ individually for simulations.

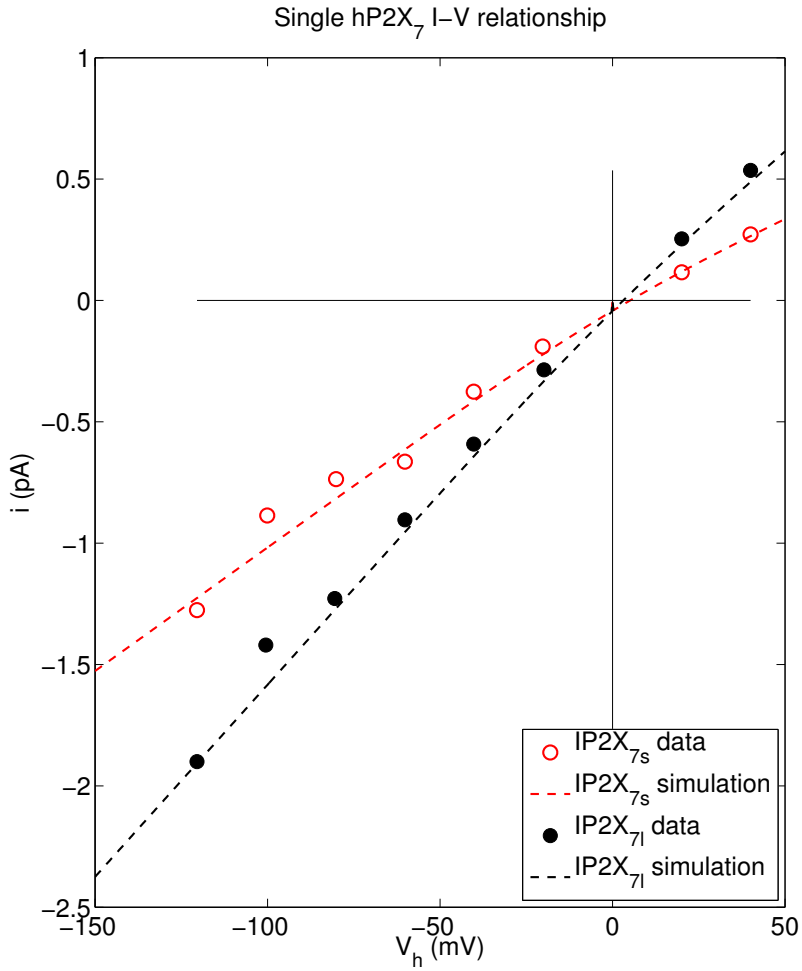

Figure 7.1: Human P2X7 Receptor Voltage-Current Relationship - Experimental and simulation data of voltage current relationships of the P2X7 receptor. Experimental data for long openings (black circles) and short openings (red open circles); silumation results for short openings (red broken line) or long openings (black broken line). Experimental data from (425).

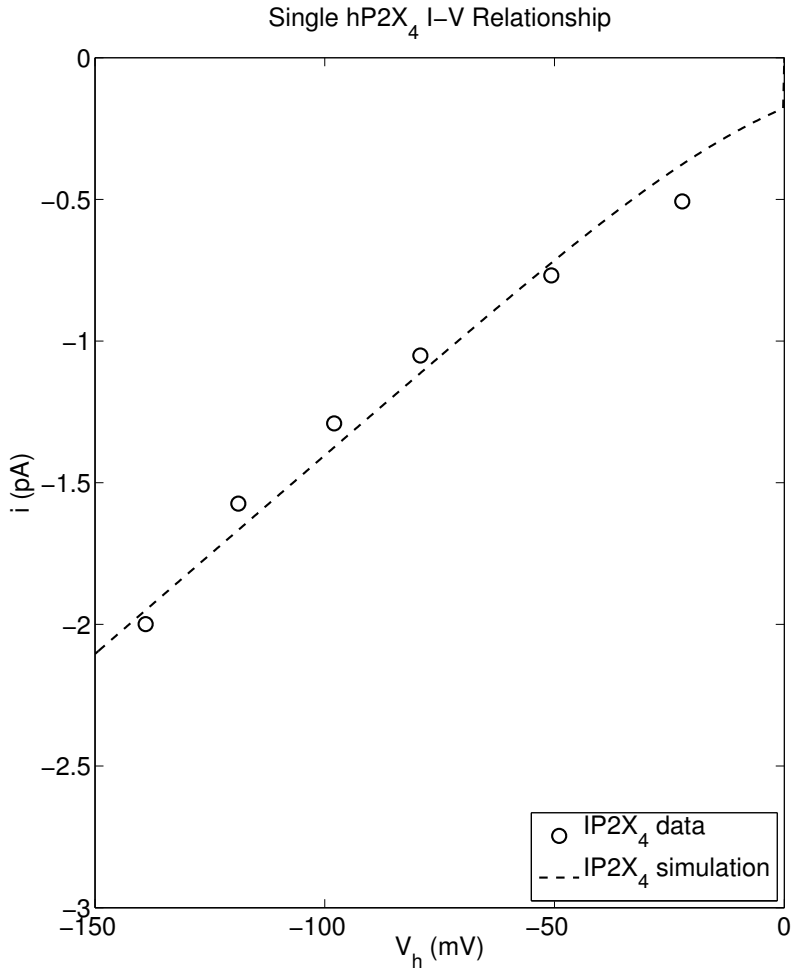

Figure 7.2: Human P2X4 Receptor Voltage-Current Relationship - Experimental and simulation data of voltage current relationships of the P2X4 receptor. Experimental data (open black circles); silumation result (broken black line). Experimental data from (361).

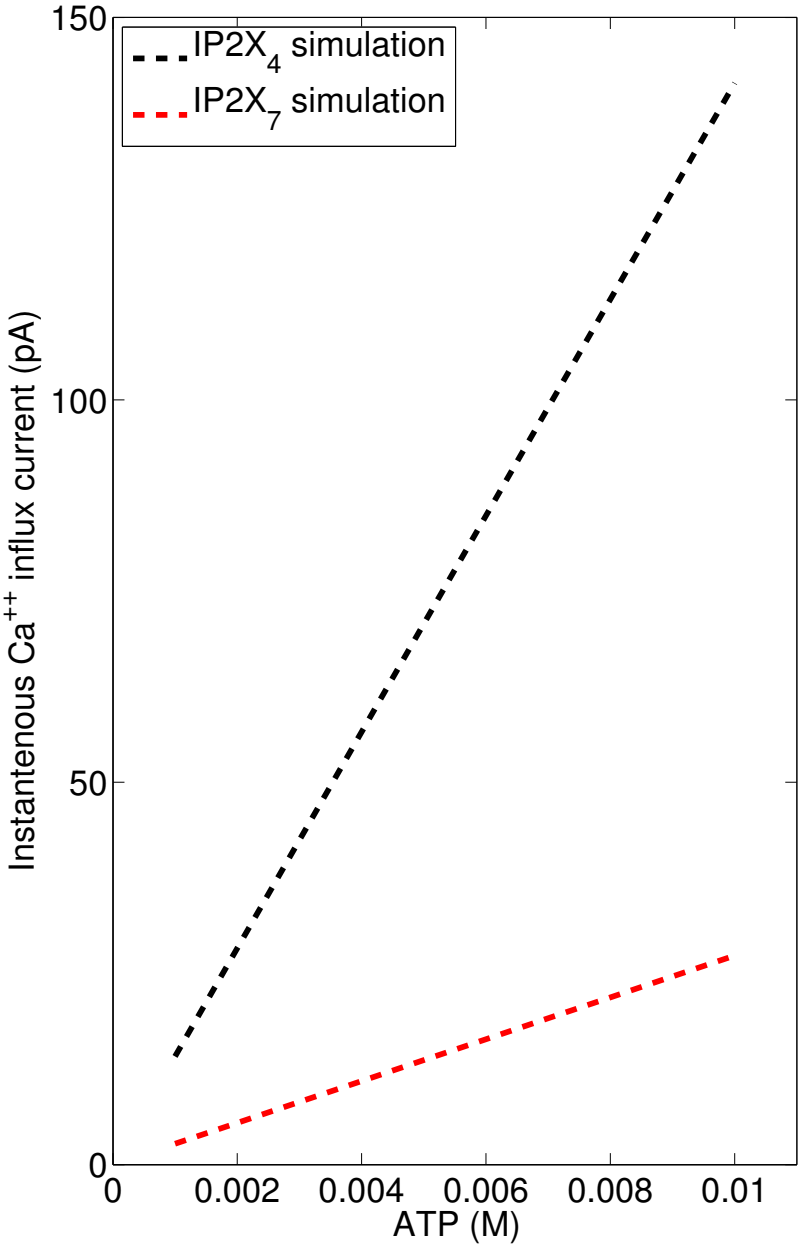

Figure 7.3: Calcium Currents Mediated by P2X7 and P2X4 Receptors - Simulation of endothelial P2X4 and P2X7 currents under a range of local ATP concentrations (0.001-0.01M). Simulation for P2X4 (black broken line) and P2X7 (red broken line).

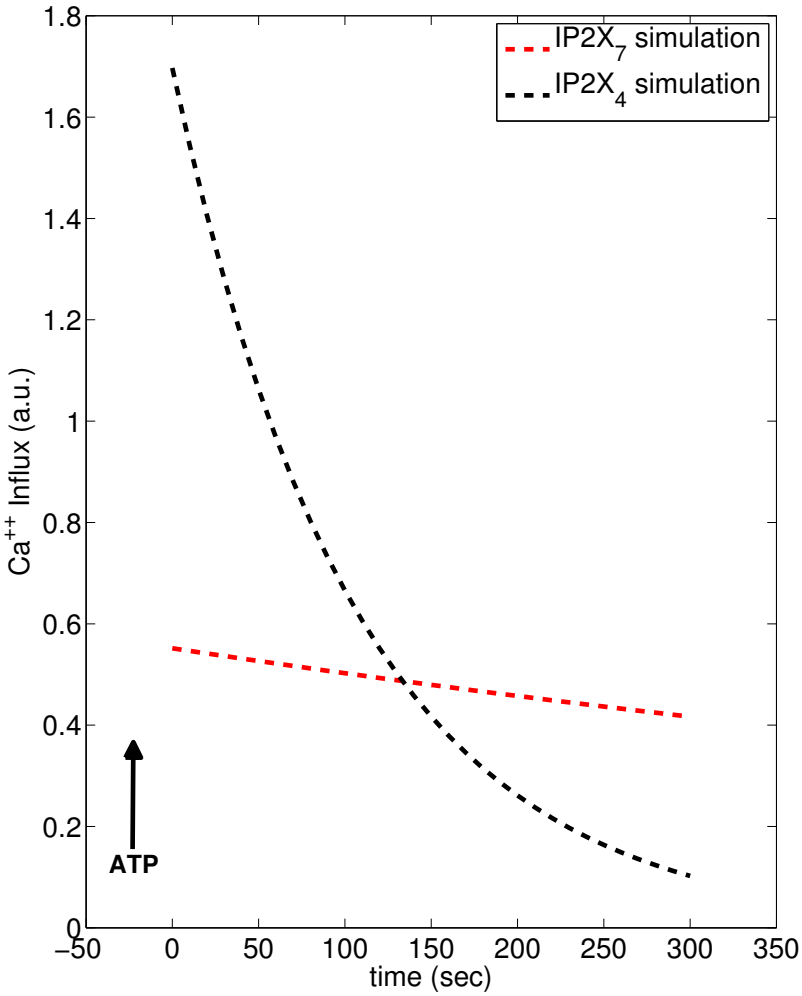

Figure 7.4: Time Dependent Calcium Currents Mediated by P2X7 and P2X4 Receptors - Simulation of endothelial P2X4 and P2X7 currents in response to a local ATP concentration of 200μM. Simulation for P2X4 (black broken line) and P2X7 (red broken line). Arrow indicates simulated application of ATP, activating P2X4 and P2X7 receptors, leading to decay of calcium influx begining at time (t=0).

7.2 Model Code

```
close all
clear all
tic

%     voltage-current experimental patch-clamp data
%     ---------------------------------------------
    % P2X7 which has two open states long/short
    [Header, P2X7] =  Irreg_HD_Load('VI_P2X7_fig4c.txt');
         Vh_short= P2X7(:,1);
         I_short = P2X7(:,2);
         Vh_long= P2X7(:,3);
         I_long = P2X7(:,4);

     %P2X4
      [Header Data] =  Irreg_HD_Load('VI_P2X4_fig1c.txt');
      Vp2x4 = Data(:,1);
      Ip2x4 = Data(:,2);


%     Parameters
%     ----------
    % Universal constants
    F = 96485.3399;                 % Faraday constant     (C/mole)
    R = 8314.472;                   % Gas constant         ...
        ((C*mV)/(K*mole))
    T = 293;                        % Temperature          (K)
    RT = R*T;                       % RT term              ...
        ((C*mV)/mole)
    FRT = F/RT;                     % F/RT term            (1/mV)

   % Membrane properties
    C_m = 25;                       % Total membrane ...
        capacitance (pF)
    A_m = C_m/1e6;                  % Area scaled by ...
        capacitance (cm^2)
   % Ionic valences
    z_K = 1;                        % Potassium valence ...
                (unitless)
    z_Na = 1;                       % Sodium valence ...
                  (unitless)
    z_Ca = 2;                       % Calcium valence ...
                 (unitless)

 V_m = -150:.25:50; %membrane potential range

```

```
 %P2X4 and P2X7 channel permeabilities
%     ------------------------------------------
    % P2X7 channel

    PNa_P2X = 4.2e-4;
    PK_P2X = 1.05*PNa_P2X;
    PCa_P2X = 2.7*PNa_P2X;

    PNa_P2X4 = 4.2e-4;
    PK_P2X4 = .99*PNa_P2X4;
    PCa_P2X4 =4.2*PNa_P2X4;


%% P2X4 (SINGLE CHANNEL) model
% I-V data from Negulyaev and Markwardt Neurosc. Lett. 279 ...
    2000 165-168
%% P2X4
 for i = 1:length(V_m);
ATP = 0.1e-3;
alpha_out_0 = .001; % External cation activity coefficient ...
    (unitless)
alpha_in_0 = 40;    % Internal cation activity coefficient ...
    (unitless)
n =1.4;             % Hill coefficient (cooperativity) for ...
    ligand binding

% Incorporate ligand binding to the channel
% The flux/current through the ion channel obeyes the ...
    Goldman-Hodzkin-Katz
% equation.
pK = 5; K = 10^-pK;
Po_P2X4 = .26;

% Compute calcium uniporter fluxes from the calcium uniporter ...
    model
alpha_out4 = alpha_out_0*(ATP^n/(K^n + ATP^n));
alpha_in4 = alpha_in_0*(ATP^n/(ATP^n + ATP^n));

%openings
Po_Na_out4 = PNa_P2X4*alpha_out4*Po_P2X4;
Po_Na_in4 = PNa_P2X4*alpha_in4*Po_P2X4;

Po_K_out4 = PK_P2X4*alpha_out4*Po_P2X4;
Po_K_in4 = PK_P2X4*alpha_in4*Po_P2X4;

Po_Ca_out4 = PCa_P2X4*alpha_out4*Po_P2X4;
Po_Ca_in4 = PCa_P2X4*alpha_in4*Po_P2X4;

%
```

```
82 dPhi_Na4 = z_Na*FRT*V_m(i);
83 dPhi_K4 = z_K*FRT*V_m(i) ;
84 dPhi_Ca4 = z_Ca*FRT*V_m(i);
85
86 if (V_m(i) == 0)
87      fluxNa4 = -(Po_Na_in4*ATP - Po_Na_out4*ATP);
88      fluxK4 =  -(Po_K_in4*ATP - Po_K_out4*ATP);
89      fluxCa4 = -(Po_Ca_in4*ATP - Po_Ca_out4*ATP);
90 else
91
92 fluxNa4 = ...
       dPhi_Na4*(Po_Na_in4*ATP*exp(-dPhi_Na4)-Po_Na_out4*ATP)...
93     /(exp(-dPhi_Na4)-1);
94 fluxK4 = dPhi_K4*(Po_K_in4*ATP*exp(-dPhi_K4)-Po_K_out4*ATP)...
95     /(exp(-dPhi_K4)-1);
96 fluxCa4 = ...
       dPhi_Ca4*(Po_Ca_in4*ATP*exp(-dPhi_Ca4)-Po_Ca_out4*ATP)...
97     /(exp(-dPhi_Ca4)-1);
98
99 INa_P2X4 = z_Na*F*fluxNa4;
100 IK_P2X4 = z_K*F*fluxK4 ;
101 ICa_P2X4 = z_Ca*F*fluxCa4 ;
102
103 IP2X4(i) = (INa_P2X4 - IK_P2X4+ ICa_P2X4);
104
105 %Calcium current equation for time-dependent model for t = 0:300
106 % exponential decay curve modeled on experimental data from:
107 % Yamamoto et al. AJP Heart Circ 279: H285-H292, 2000
108 %ICa_P2X4 = z_Ca*F*fluxCa4*(exp(-0.009359*t))
109
110 end
111 end
112
113   figure(3)
114   set(gca,'FontSize',18)
115    plot(Vp2x4,Ip2x4,'o','MarkerEdgeColor','k',...
116        'MarkerSize',10,'LineWidth',1.5)
117     hold on
118     plot(V_m, IP2X4, '--k','LineWidth',1.5)
119      xlabel('V_{h} (mV)','FontSize',18)
120        ylabel('i (pA)','FontSize',18)
121      xlim([-150 0])
122     ylim([-3 0])
123
124    legend('IP2X_{4} data','IP2X_{4} simulation', ...
          'Location','SouthEast')
125 title('Single hP2X_4 I-V Relationship')
126
127
```

```
%% P2X7 (SINGLE CHANNEL)
% I-V data from Riedel et. al  Biophys J 92 2007 2377-2391

for i = 1:length(V_m);
     ATP1 = .57e-3; %(M)

%approx alpha (cation activity) by the concentration - OK for small concs.
alpha_out_0 = 4.5; % External cation activity coefficient (unitless)
alpha_in_0 = 11.5;  % Internal cation activity coefficient (unitless)
ns =1.4;           % Hill coefficients (cooperativity) for ligand binding
nl = 1.1;

pK_s = 5; K_s = 10^-pK_s;
pK_l =  3.93; K_l = 10^-pK_l;

Po_P2Xs = 0.28;
Po_P2Xl = .18;


Salpha_out = alpha_out_0*(ATP1^ns/(K_s^ns + ATP1^ns));
Salpha_in = alpha_in_0*(ATP1^ns/(ATP1^ns + ATP1^ns ));

Lalpha_out = alpha_out_0*(ATP1^nl/(K_l^nl + ATP1^nl));
Lalpha_in = alpha_in_0*(ATP1^nl/(ATP1^nl + ATP1^nl ));

%Short openings
sPo_Na_out = PNa_P2X *Salpha_out*Po_P2Xs;
sPo_Na_in = PNa_P2X*Salpha_in*Po_P2Xs;

sPo_K_out = PK_P2X *Salpha_out*Po_P2Xs;
sPo_K_in = PK_P2X*Salpha_in*Po_P2Xs;

sPo_Ca_out = PCa_P2X *Salpha_out*Po_P2Xs;
sPo_Ca_in = PCa_P2X*Salpha_in*Po_P2Xs;

%Long openings
lPo_Na_out = PNa_P2X *Lalpha_out*Po_P2Xl;
lPo_Na_in = PNa_P2X*Lalpha_in*Po_P2Xl;

lPo_K_out = PK_P2X *Lalpha_out*Po_P2Xl;
lPo_K_in = PK_P2X*Lalpha_in*Po_P2Xl;

lPo_Ca_out = PCa_P2X *Lalpha_out*Po_P2Xl;
lPo_Ca_in = PCa_P2X*Lalpha_in*Po_P2Xl;

```

```
173
174 dPhi_Na = z_Na*FRT*V_m(i);
175 dPhi_K = z_K*FRT*V_m(i) ;
176 dPhi_Ca = z_Ca*FRT*V_m(i);
177
178 if (V_m(i) == 0)
179       sfluxNa = -(sPo_Na_in*ATP1 - sPo_Na_out*ATP1);
180       sfluxK = -(sPo_K_in*ATP1 - sPo_K_out*ATP1);
181       sfluxCa = -(sPo_Ca_in*ATP1 - sPo_Ca_out*ATP1);
182
183       lfluxNa = -(lPo_Na_in*ATP1 - lPo_Na_out*ATP1);
184       lfluxK = -(lPo_K_in*ATP1 - lPo_K_out*ATP1);
185       lfluxCa = -(lPo_Ca_in*ATP1 - lPo_Ca_out*ATP1);
186 else
187
188 sfluxNa = ...
       dPhi_Na*(sPo_Na_in*ATP1*exp(-dPhi_Na)-sPo_Na_out*ATP1)...
189      /(exp(-dPhi_Na)-1);
190 sfluxK = dPhi_K*(sPo_K_in*ATP1*exp(-dPhi_K)-sPo_K_out*ATP1)...
191      /(exp(-dPhi_K)-1);
192 sfluxCa = ...
       dPhi_Ca*(sPo_Ca_in*ATP1*exp(-dPhi_Ca)-sPo_Ca_out*ATP1)...
193      /(exp(-dPhi_Ca)-1);
194
195 lfluxNa = ...
       dPhi_Na*(lPo_Na_in*ATP1*exp(-dPhi_Na)-lPo_Na_out*ATP1)...
196      /(exp(-dPhi_Na)-1);
197 lfluxK = dPhi_K*(lPo_K_in*ATP1*exp(-dPhi_K)-lPo_K_out*ATP1)...
198      /(exp(-dPhi_K)-1);
199 lfluxCa = ...
       dPhi_Ca*(lPo_Ca_in*ATP1*exp(-dPhi_Ca)-lPo_Ca_out*ATP1)...
200      /(exp(-dPhi_Ca)-1);
201
202
203 INa_P2Xs = z_Na*F*sfluxNa;
204 IK_P2Xs = z_K*F*sfluxK ;
205 ICa_P2Xs = z_Ca*F*sfluxCa ;
206
207 INa_P2Xl = z_Na*F*lfluxNa;
208 IK_P2Xl = z_K*F*lfluxK ;
209 ICa_P2Xl = z_Ca*F*lfluxCa ;
210
211 IP2X_long(i) = INa_P2Xs - IK_P2Xs + ICa_P2Xs;
212 IP2X_short(i) = INa_P2Xl - IK_P2Xl + ICa_P2Xl;
213
214 %Calcium current equation for time-dependent model for t = 0:300
215 % P2X7 mediated Ca-influx is highly sustained following ATP
216 %ICa_td = (ICa_P2Xs + ICa_P2Xl)*exp(-0.0009359*t);
217 end
```

```
218  end
219     % P2X7
220     p2x7 = figure(1);
221    plot(Vh_short,I_short,'o','MarkerEdgeColor','r',...
222         'MarkerSize',10,'LineWidth',1.5)      % Plot simulation ...
                curve
223          set(gca,'FontSize',18)
224     hold on
225     plot(V_m, IP2X_short, '--r','LineWidth',1.5)
226     plot(Vh_long, I_long, 'o',...
227     'MarkerEdgeColor','k',...
228                  'MarkerFaceColor','k',...
229               'MarkerSize',10)
230       plot(V_m, IP2X_long , '--k','LineWidth',1.5)
231           ylabel('i (pA)','FontSize',18)
232      xlabel('V_{h} (mV)','FontSize',18)
233    %  plot a cross-hair to indicate zero-zero crossing
234     x = [0 0 0 0 0 0 0 0];
235     y = [0 0 0 0 0 0 0 0];
236     plot(x,I_long, 'k')
237     plot(Vh_long, y, 'k')
238      xlim([-150 50])
239     legend('IP2X_{7s} data','IP2X_{7s} simulation','IP2X_{7l} ...
           data',...
240          'IP2X_{7l} simulation', 'Location','SouthEast')
241 title('Single hP2X_7 I-V relationship')
242 toc
```

8
Appendix B: Peer Reviewed Work

8.1 Personal Grants, Awards & Meetings

- **University of Edinburgh Innovation Initiative Grant.** This grant funded equipment necessary to perform the surgical pressure-diuresis/natriuresis studies presented in this thesis

- **American Physiological Society International Early Career Travel Award.** I was selected for this was award from an international cohort of early career researchers at the Experimental Biology 2012 meeting (San Diego) and provided financial support for conference attendance. I gave an oral presentation (Renal Purinergic Club) and a poster presentation on pressure-diuresis in renal injury susceptible rats.

8.2 Thesis Papers

verte

OPEN ACCESS Freely available online

PLoS one

Activation of Thiazide-Sensitive Co-Transport by Angiotensin II in the *cyp1a1-Ren2* Hypertensive Rat

Ali Ashek[1], Robert I. Menzies[1], Linda J. Mullins[1], Christopher O. C. Bellamy[3], Anthony J. Harmar[1], Christopher J. Kenyon[1], Peter W. Flatman[2], John J. Mullins[1], Matthew A. Bailey[1]*

1 University/British Heart Foundation Centre for Cardiovascular Science, The University of Edinburgh, Edinburgh, United Kingdom, **2** Centre for Integrative Physiology, The University of Edinburgh, Edinburgh, United Kingdom, **3** Department of Pathology, Edinburgh New Royal Infirmary, Edinburgh, United Kingdom

Abstract

Transgenic rats with inducible expression of the mouse *Ren2* gene were used to elucidate mechanisms leading to the development of hypertension and renal injury. *Ren2* transgene activation was induced by administration of a naturally occurring aryl hydrocarbon, indole-3-carbinol (100 mg/kg/day by gastric gavage). Blood pressure and renal parameters were recorded in both conscious and anesthetized (butabarbital sodium; 120 mg/kg IP) rats at selected time-points during the development of hypertension. Hypertension was evident by the second day of treatment, being preceded by reduced renal sodium excretion due to activation of the thiazide-sensitive sodium-chloride co-transporter. Renal injury was evident after the first day of transgene induction, being initially limited to the pre-glomerular vasculature. Mircoalbuminuria and tubuloinsterstitial injury developed once hypertension was established. Chronic treatment with either hydrochlorothiazide or an AT1 receptor antagonist normalized sodium reabsorption, significantly blunted hypertension and prevented renal injury. Urinary aldosterone excretion was increased ~20 fold, but chronic mineralocorticoid receptor antagonism with spironolactone neither restored natriuretic capacity nor prevented hypertension. Spironolactone nevertheless ameliorated vascular damage and prevented albuminuria. This study finds activation of sodium-chloride co-transport to be a key mechanism in angiotensin II-dependent hypertension. Furthermore, renal vascular injury in this setting reflects both barotrauma and pressure-independent pathways associated with direct detrimental effects of angiotensin II and aldosterone.

Citation: Ashek A, Menzies RI, Mullins LJ, Bellamy COC, Harmar AJ, et al. (2012) Activation of Thiazide-Sensitive Co-Transport by Angiotensin II in the *cyp1a1-Ren2* Hypertensive Rat. PLoS ONE 7(4): e36311. doi:10.1371/journal.pone.0036311

Editor: Michael Bader, Max-Delbrück Center for Molecular Medicine (MDC), Germany

Received January 16, 2012; **Accepted** April 2, 2012; **Published** April 27, 2012

Funding: This work was supported by the British Heart Foundation (www.BHF.org.uk); the Wellcome Trust (www.wellcome.ac.uk); and the European Commission FP7: Euratrans (www.euratrans.eu). The funders had no role in study design, data collection and analysis, decision to publish, or preparation of the manuscript.

Competing Interests: The authors have declared that no competing interests exist.

* E-mail: matthew.bailey@ed.ac.uk

Introduction

Hypertension is a major world health problem associated with a substantial cost, in terms of patient mortality/morbidity and economic burden. Tremendous strides have been made in this field and there are several treatments for reducing blood pressure in most patients. Nevertheless, basic research to establish causal pathways may lead to more effective management of existing hypertension or importantly provide a foundation for life-style advice in the pre-hypertensive phase. This endeavor is facilitated by the use of appropriate animal models. One such model is the *cyp1a1-Ren2* transgenic rat (TGR) in which hypertension can be reversibly induced, without surgical intervention, by dietary administration of the non-toxic, naturally occurring (for example in brassicas) aryl hydrocarbon, indole-3-carbinol (I3C) [1]. An advantage of this model is that changing the dose of I3C administered can alter the severity of hypertension. This allows, for instance, the generation of a slowly-developing hypertension, analogous to chronic infusion of subpressor doses of angiotensin II [2,3] or malignant hypertension (MH), characterized by rapidly accelerating blood pressure and injury to target organs [4].

In the *cyp1a1-Ren2* rat, a transgene has been integrated into the Y chromosome. This transgene places mouse *Ren2* cDNA expression under the control of an inducible cytochrome p450-1a1 promotor [1]. Expression of *Ren2*, primarily in the liver, leads to increased circulating renin levels, activation of the renin-angiotensin-aldosterone system and a rise in blood pressure. This rise in pressure is accompanied by a sustained elevation of circulating renin. Intrarenal synthesis of angiotensin II [5,6], promoted by elevated renin and pro-renin receptor expression [7], contributes to the pathology of hypertension in the *cyp1a1-Ren2* rat, and the model is therefore complementary to approaches using chronic infusion of angiotensin II, in which renin activity is suppressed.

The current study was designed to resolve key mechanisms leading to hypertension in the *cyp1a1-Ren2* TGR and focuses on sodium transport in the distal convoluted tubule. Several lines of evidence led us to hypothesize that hypertension in the TGR model originates in the kidney and reflects an impaired ability to excrete sodium. First, dietary sodium loading exacerbates hypertension [5]. Second, renal blood flow is attenuated [4], pressure natriuresis is impaired [8] and tubuloglomerular feedback is activated [9], whilst third, the systemic hormonal profile of elevated angiotensin II and aldosterone would reduce natriuretic capacity by effects on the tubule epithelium [10,11,12,13] and medullary *vasa recta* [14]. Our hypothesis is further supported by the observation that manoeuvers improving renal blood flow and/

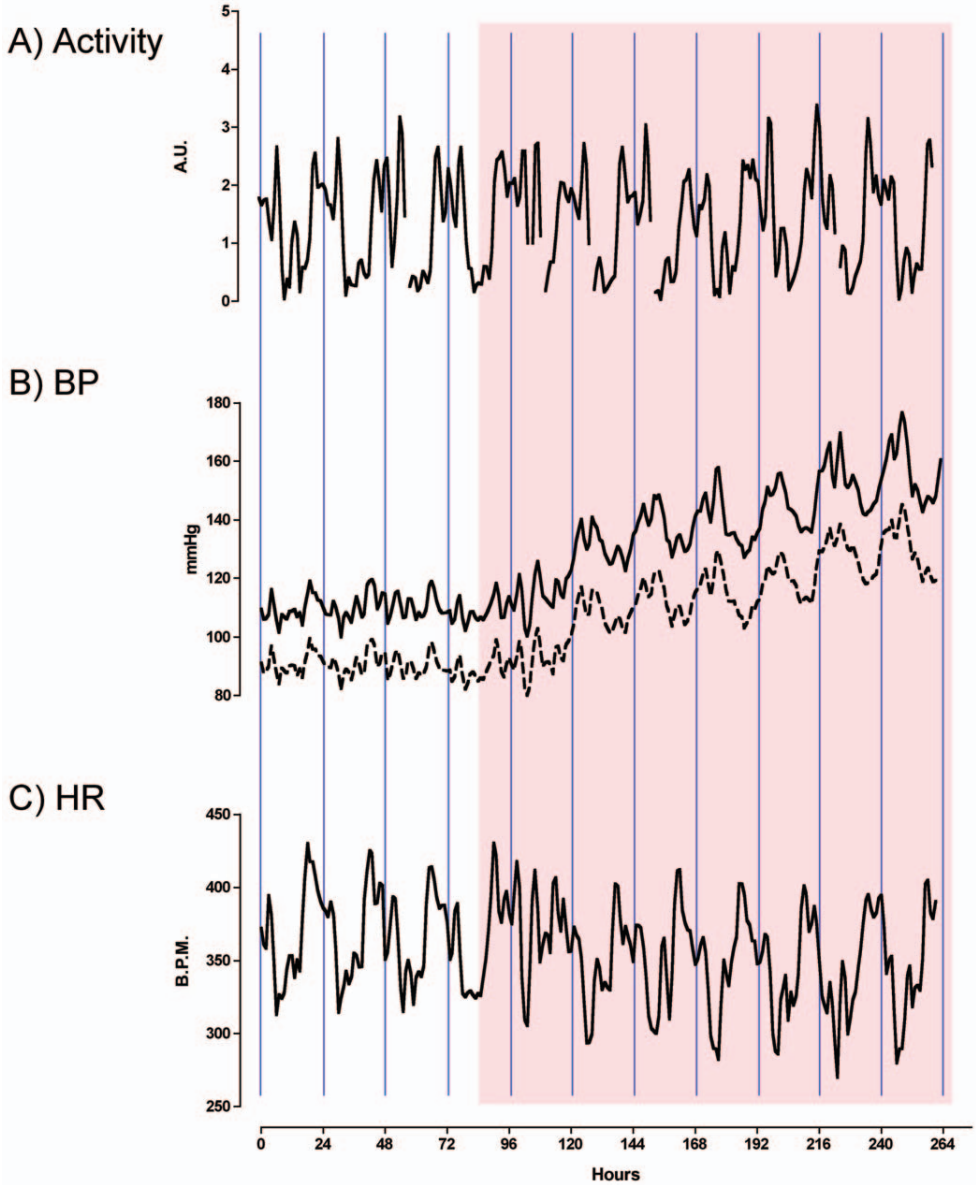

Figure 1. Telemetry data from *Cyp1a1-Ren2* transgenic rats. Recordings were made in rats (n = 5) over a baseline period and following 7 consecutive days of indole-3-carbinol administration (I3C; Shaded area). A) locomotor activity; B) Blood pressure (BP), with systolic as a solid line and diastolic as a dashed line and C) HR. Data are hourly means, smoothed with a 5-point rolling average and shown without error bars for clarity. The vertical lines represent the midnight time point. I3C was administered at 10am.
doi:10.1371/journal.pone.0036311.g001

or sodium excretion blunt the hypertensive response to *Ren2* activation [15,16].

We find that induction of hypertension in the *cyp1a1-Ren2* TGR causes sustained activation of the thiazide-sensitive co-transporter by angiotensin II in the distal tubule. Renal injury is predominantly vascular, precedes the development of hypertension and may involve mineralocorticoid-dependent pathways.

Results

Systolic blood pressure and diastolic blood pressure increased significantly during the 24 hours following the second dose of I3C (Figure 1). Over the experimental time-course, systolic increased proportionally more than diastolic blood pressure and pulse pressure was therefore increased. Heart rate fell significantly during the period of transgene induction, consistent with an intact baroreceptor reflex. The day-night cycle of locomotor activity was unaffected by RAAS activation. The statistically significant periodicity of blood pressures, heart rate and activity was approximately circadian during the baseline period. Analysis was performed on de-trended data from the hypertensive period and persistency of circadian rhythmicity was observed.

Activation of the cyp1a1-Ren2 transgene promotes anti-natriuresis

Under anaesthesia, we observed a progressive increase in mean arterial blood pressure (Figure 2A, ANOVA $P<0.001$) with

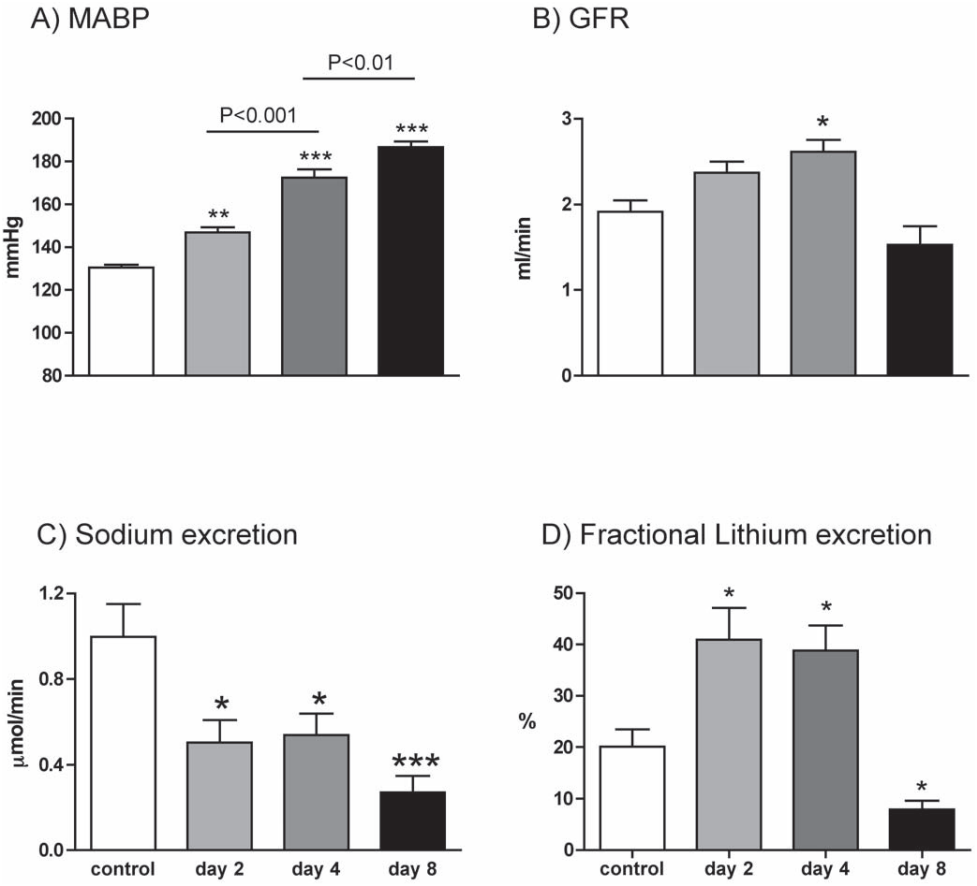

Figure 2. Renal function in anaethetized rats. A) mean arterial blood pressure (MABP); B) glomerular filtration rate (GFR); C) urinary sodium excretion and D) the fractional excretion of lithium. Measurements were made in *cyp1a1-Ren2* transgenic rats, on either day 2 (n = 9), 4 (n = 9) or 8 (n = 9) in the induction regimen. Non-induced rats (n = 8) served as control. Data are mean ± SE. Statistical comparisons were made using ANOVA with Bonferroni post-test. ***P<0.001, **P<0.01, *P<0.05 versus the control group.
doi:10.1371/journal.pone.0036311.g002

repeated doses of I3C, with a small but significant rise being observed on day 2 of *Ren2* induction. Glomerular filtration rate rose significantly, at least until day 4 (Figure 2B; ANOVA P<0.01) but then fell back to control levels. Effective renal plasma flow (Table 1) was stable. In consequence, filtration fraction was elevated only on day 4 and renal vascular resistance only on day 8(Table 1). Transgene induction reduced natriuretic capacity (Figure 2C; ANOVA P<0.001), with sodium excretion falling to ~50% of control values by day 2. There was a significant linear trend toward hypokalaemia (P<0.05), despite which fractional potassium excretion remained robust (Table 1).

Fractional sodium excretion fell (Table 1) with transgene induction, indicating a tubular origin for the antinatriuresis. We attempted to localize this effect by measuring the fractional excretion of lithium excretion (Figure 2D). This was initially elevated (ANOVA P<0.01), indicating diminution of proximal tubular reabsorption and localizing the antinatriuretic effect to more distal nephron segments.

In conscious rats, sodium intake (initially 2.38±0.11 mmol/24 h), declined over the induction period but this was not statistically significant until the final day (1.38±0.17 mmol/24 h; P<0.01). Body weight was found not to change significantly, with end-weight being 96.5±1.2% of start weight. 24 h urinary aldosterone excretion was increased ~20 fold over the induction period (Figure 3 ANOVA P<0.001) and we therefore focused our experiments on the aldosterone-sensitive distal nephron (ASDN). Sodium-chloride co-transport (NCC, *Slc12a3*) and the epithelial sodium channel (ENaC, *Scnn1*) account for the majority of sodium transport in the ASDN and the contribution of each was assessed pharmacologically. At baseline, thiazide-sensitive transport was responsible for the reabsorption of ~5% of the filtered sodium load. This increased progressively during *Ren2*-transgene induction (Figure 4A; ANOVA P<0.01), as did abundance of total NCC protein relative to GAPDH (Figure 4B; ANOVA P<0.001). A positive correlation (Pearson r = 0.60; P<0.01) was observed between NCC protein abundance and thiazide-sensitive sodium reabsorption. An amiloride-sensitive pathway reabsorbed ~2% of the filtered sodium in non-induced rats. There was a slight initial increase in both amiloride-sensitive sodium reabsorption (Figure 4C) and in the abundance of αENaC relative to GAPDH (Figure 4D). Although neither reached statistical significance, both sets of data suggest a similar trend- a transient rise, with both back to baseline by day 8.

The role of NCC-mediated sodium reabsorption was assessed by chronically administering thiazide during transgene induction. The blood pressure increase was significantly attenuated (Figure 4E), but still remained significantly higher than control animals. The partial rescue of the hypertensive phenotype was associated with a large increase in fractional sodium excretion (Figure 4F). An acute bolus of hydrochlorothiazide produced no

Table 1. Renal data and plasma electrolytes in *cyp1a1-Ren2* transgenic rats before and after the induction of hypertension.

	Control	Day 2	Day 4	Day 8	ANOVA
n	8	9	9	8	
Body weight (g)	324±14	318±16	343±13	305±13	NS
FE_{Na} (%)	0.39±0.06	0.16±0.03**	0.15±0.03**	0.09±0.02**	<0.001
FE_K (%)	38.0±4.5	30.3±2.9	31.7±2.2	30.0±9.4	NS
V (µl/min)	9.8±0.7	13.6±3.5	13.2±1.0	9.3±2.0	NS
P_{Na} (mmol/l)	135.9±0.4	134.3±0.7	134.0±0.6	132.6.3±1.7	=0.059
P_K (mmol/l)	4.23±0.06	4.10±0.12	4.03±0.11	3.87±0.09	NS
Hct (%)	46.5±1.0	48.3±0.5	48.7±1.0	52.0±1.1**	<0.01
eRPF (ml/min)	6.7 ± 0.6	8.3±0.8	7.2±0.4	7.6±1.0	NS
RBF (ml/min)	12.7±0.7	16.0±1.3	14.0±0.7	16.1±2.1	NS
FF (%)	28.4±1.6	29.8±2.2	37.0±2.0**	20.0±1.5*	<0.01
RVR (mmHg.ml.min−1)	10.5±0.6	9.7±0.8	12.4±0.6	14.4±1.3*	<0.01

Data are mean± SE. Comparisons were made using one-way ANOVA (P value shown in column), with Bonferroni post-hoc test: * = P<0.05, ** = P<0.01. FE_{Na} and FE_K indicates the fractional excretion of sodium and potassium; V is urine flow rate; P_{Na} and P_K are the plasma concentration of sodium and potassium; Hct is hematocrit; eRPF and RBF are effective renal plasma and blood flow, respectively; FF is filtration fraction and RVR is renal vascular resistance.
doi:10.1371/journal.pone.0036311.t001

further natriuretic effect (data not shown), confirming that NCC blockade was complete at the chronic infusion level.

Activation of the cyp1a1-Ren2 transgene causes microvascular injury

Modest albuminuria developed over the experimental time-course (Figure 5; ANOVA P<0.001) and kidneys were therefore examined for microvascular injury. An ordered categorical scoring of microvascular injury indicated a significant (X^2 analysis; P = 0.028) contingency between the duration of transgene induction and microvascular injury. After 1 day of treatment, medial myocyte vacuolation was evident in arcuate and the larger interlobular arteries, indicative of vasospasm (Figure 6A). There was also rare focal medial myocyte cell death (Figure 6B). No such injury was observed in the control group. In rats studied at day 4, vascular damage was both more prevalent and severe, with foci of confluent medial myocyte death, apoptotic nuclear fragments and hemorrhage into the necrotic foci (Figure 6C). There was low-grade mononuclear cell infiltration into the perivascular adventitia. By day 8, the destructive vascular injury was more extensive still (Figure 6D), and fibroid necrosis was also evident in smaller interlobular arteries and afferent arterioles, consistent with our previous data [4]. Areas of tubulointerstitial injury were also observed, which were small and localized mainly in the cortex. There was no histological evidence of malignant phase hypertension, such as "onion-skinning" of the renal arterioles.

Effect of spironolactone or losartan on blood pressure, renal function an microvascular injury

Chronic administration of losartan blunted the hypertensive response to transgene induction (Figure 7A), increased fractional sodium excretion (*Ren2* induction alone = 0.15±0.03% versus co-administration of losartan = 0.40±0.04; P<0.01) and normalized thiazide-sensitive sodium reabsorption (Figure 7B). Kidneys from three of these rats were examined histologically and there was no evidence of hypertensive vascular injury. Spironolactone had no antihypertensive effect (Figure 7A) and nor did it have any effect on thiazide-sensitive sodium reabsorption (Figure 7B). Mineralocorticoid receptor blockade did, however, prevent the development of albuminuria during transgene induction (albumin excretion in mg/24 h) *Ren2* induction alone = 1.16±0.12; *Ren2* induction with co-administration of spironolactone = 0.18±0.07; P<0.01). Kidneys from five spironolactone treated rats were examined histologically: in two cases there was no evidence of vascular injury; in the other three, variable fibroid necrosis was observed.

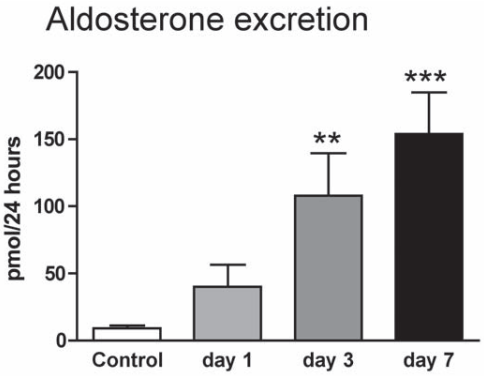

Figure 3. 24-hour urinary excretion of aldosterone. Urine was collected from conscious *cyp1a1-Ren2* transgenic rats (n = 8) maintained in individual metabolism cages, over consecutive days of transgene induction. Data are mean ± SE. Statistical comparisons were made using ANOVA with Bonferroni post-test. ***P<0.001, **P<0.01 versus the control day.
doi:10.1371/journal.pone.0036311.g003

Discussion

In this study we investigated the early renal adaptation to RAAS activation in the *cyp1a1-Ren2* TGR. We show that the early phase of hypertension, characterized in this model by circulating angiotensin II in the high physiological range [5], is associated with impaired natriuresis due to activation of the thiazide-sensitive sodium-chloride cotransporter, with little contribution from amiloride-sensitive sodium transport.

Hypertension, sodium reabsorption and thiazide-sensitive co-transport

The synergistic effect of angiotensin II and sodium intake on blood pressure has long been known but underlying mechanisms are not fully understood. Angiotensin II promotes sodium retention and volume expansion, particularly if sodium intake is high [17,18,19]. However, a strong correlation between sodium balance and blood pressure is not a consistent feature [19,20], perhaps because increased renal arterial pressure can stimulate natriuresis [21]. Sustained hypertension may also reflect salt-induced sensitization of the sympathetic nervous system [22] and vascular smooth muscle [23] to angiotensin II.

Previous studies in *cyp1a1-Ren2* TGR have demonstrated that hypertension is associated with enhanced sodium reabsorption [6] and the rise in blood pressure is aggravated by dietary sodium-loading [5]. In the current study, sodium intake was lower by ~10% over days 1–4 of transgene induction and reduced by 40% by the final day. This might contribute to a reduced sodium excretion, particularly in rats studied after 8 days of hypertension.

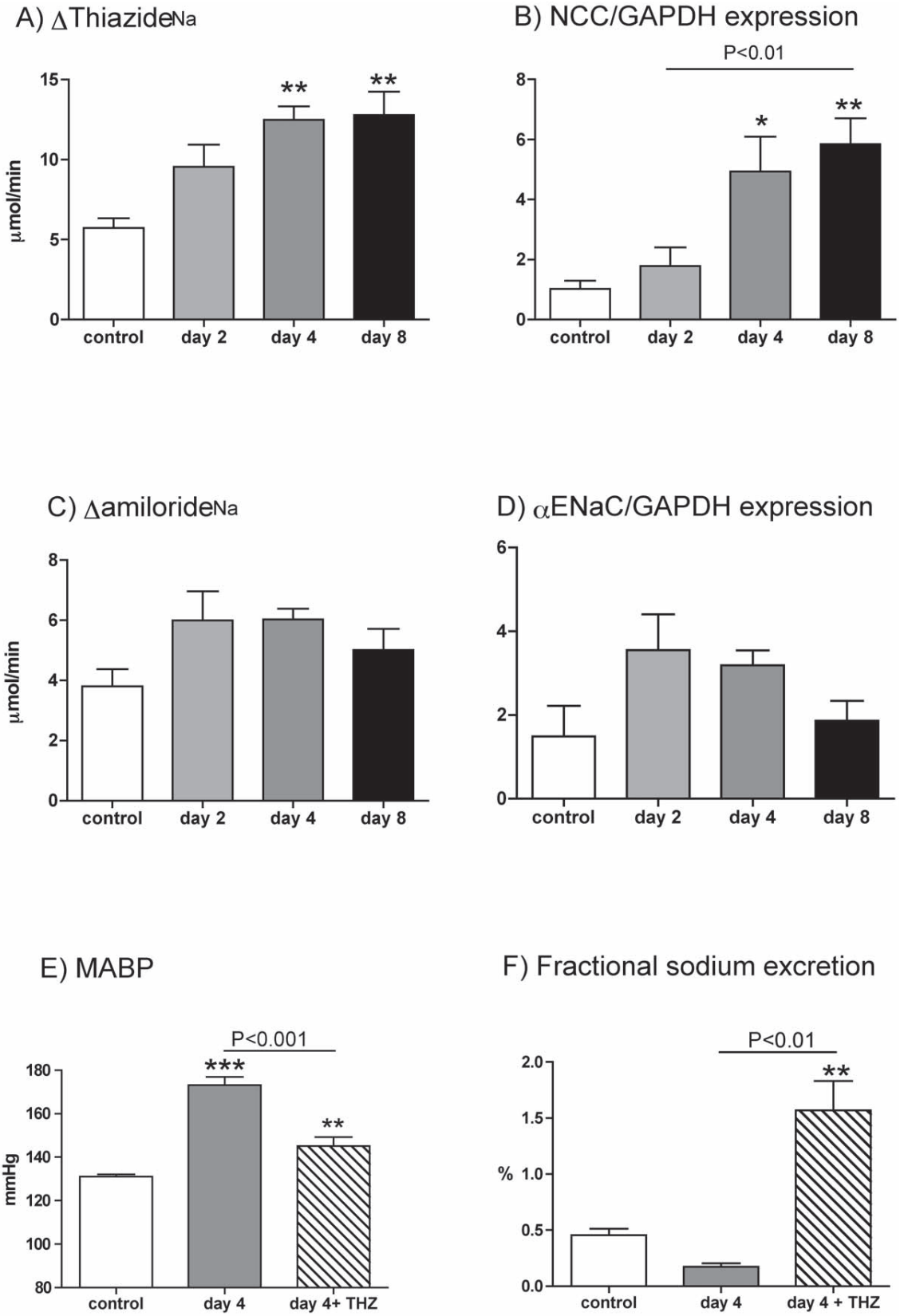

Figure 4. Sodium transport pathways in the aldosterone-sensitive distal nephron. A) hydrochlorthiazide-sensitive sodium reabsorption ($\Delta thiazide_{Na}$); B) the expression of the thiazide-sensitive co-transporter protein (NCC) in whole kidney extracts, normalized to that of GAPDH; C)

amiloride-sensitive sodium reabsorption ($\Delta amiloride_{Na}$); D) the expression of the α subunit of the epithelial sodium channel (αENaC) normalized to that of GAPDH. Measurements were made in *cyp1a1-Ren2* transgenic rats, on either day 2 (n = 9), 4 (n = 9) or 8 (n = 9) in the induction regimen. Non-induced rats (n = 8) served as control. E) mean arterial blood pressure (MABP) and F) fractional sodium excretion. Measurements were made in *cyp1a1-Ren2* transgenic rats receiving either vehicle (grey bar) or hydrochrorothaizide (hatched bar) by minipump. Data are mean ± SE. Statistical comparisons were made using ANOVA with Bonferroni post-test. $P<0.001$, $^{**}P<0.01$, $^{*}P<0.05$ versus the control group.
doi:10.1371/journal.pone.0036311.g004

Nevertheless, body weight was stable and in the cross-sectional studies plasma sodium was not changed. In this setting we observed an impaired capacity to excrete an intravenous saline load. In the proximal tubule, angiotensin II exerts a biphasic effect on sodium transport, becoming inhibitory at high concentrations [24,25]. In our study, the increase in fractional lithium excretion observed at days 2 and 4 indicates a *reduction* in proximal tubule sodium reabsorption [26] and localizes the antinatriuresis to more distal nephron segments. Since mice infused chronically with angiotensin II display increased sodium reabsorption in the ASDN [27], we probed the function of this region with inhibitors of the major pathways for sodium transport, ENaC and NCC. Both angiotensin II and aldosterone can stimulate ENaC activity [13,28] but we found the amiloride-sensitive pathway small and not greatly influenced by transgene induction. There was perhaps a trend towards an increase in both amiloride-sensitive transport and αENaC protein abundance but this normalized by day 8. Our protocol ultimately causes malignant hypertension after ~14 days [4]. In contrast, when induction is aimed at producing a non-malignant stable hypertension, chronic amiloride treatment causes a transiently negative sodium balance and abolishes hypertension in *cyp1a1-Ren2* TGR [3], even though ENaC mRNA levels do not change. It is plausible that that modest increases in angiotensin II activate existing pools of ENaC and the resulting increase in blood pressure is amiloride-sensitive. However, when angiotensin II levels are increased further, a sustained increase in NCC activity is observed. The increased sodium reabsorption in the DCT would reduce sodium delivery to the collecting duct and thereby limit amiloride-sensitive sodium transport. Under such circumstances, hypertension would be expected to be mainly thiazide-sensitive (Figure 4E). The thiazide-resistant component in the present study was small (Figure 4E) and may be due to the transiently increased ENaC activity, uncovered when NCC is inhibited.

Thiazides are considered to be selective inhibitors of transport by NCC, but recently it has been shown that they also inhibit sodium reabsorption through *Slc4A8* in the collecting duct [29].

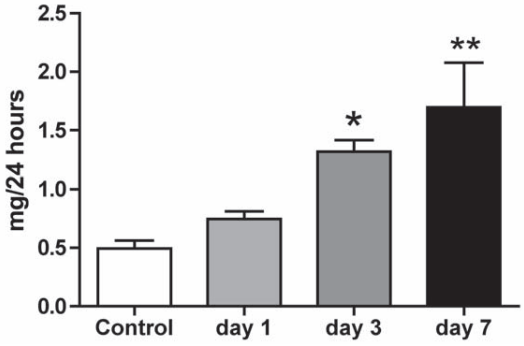

Figure 5. 24-hour urinary excretion of albumin. Urine was collected from conscious *cyp1a1-Ren2* transgenic rats (n = 8) maintained in individual metabolism cages, over consecutive days of transgene induction. Data are mean ± SE. Statistical comparisons were made using ANOVA with Bonferroni post-test. $^{**}P<0.01$, $^{*}P<0.05$ versus the control day.
doi:10.1371/journal.pone.0036311.g005

However, the strong positive correlation between NCC abundance and thiazide-sensitive sodium reabsorption suggests that transport through *Slc4A8* plays only a minor role in our studies.

In order to be physiologically active, NCC must be phosphorylated on threonine and serine residues in a regulatory domain in the N-terminus [30,31], and it must be correctly trafficked to the apical membrane of the DCT. In our study, we did not measure NCC phosphorylation or define localization to a specific subcellular compartment. Measurements of NCC phosphorylation are increasingly used as a surrogates for those of transport, yet evidence suggests that although phosphorylation is necessary, it is not sufficient, to explain transport activation in cation-chloride cotransporters [32]. Thus, we consider that the increase in total NCC expression, which paralleled the blood pressure rise, was more than sufficient to account for the increased thiazide-sensitive sodium reabsorption observed.

Previous studies have shown that both angiotensin II and aldosterone can independently increase NCC-mediated sodium transport in the DCT [12,33,34,35,36]. Our data show that the activation of NCC occurs via AT1R as losartan caused a natriuresis and fully normalized NCC activity. In contrast, spironolactone, at levels sufficient to achieve complete mineralocorticoid receptor blockade [37], had no effect on thiazide-sensitive sodium reabsorption or blood pressure. MR activation does not therefore appear to be major factor in our model, consistent with some previous studies [3,6,27], but contrasting with others [38]. It is also reported that hypertension *per se* reduces NCC expression in the apical membrane of the DCT [39]. We cannot discount a countervailing influence of hypertension on NCC activity, but our data indicate that the overall outcome was an angiotensin II-mediated increase in thiazide-sensitive sodium transport.

Chronic infusion of either hydrochlorothiazide or losartan was an effective antihypertensive measure. Both treatments also increased fractional sodium excretion, implying that renal sodium retention is a key hypertensive mechanism in this model. In support of this hypothesis, reciprocal transplantation studies in AT1AR null and wild-type mice show that renal AT1R mediate the chronic hypertensive effects of angiotensin II infusion by promoting renal sodium reabsorption [40]. However, in our study there was a trend towards volume contraction as blood pressure rose, suggesting that the effects of angiotensin II and dietary salt on blood pressure do not necessarily reflect volume expansion here [19,20]. Indeed, other studies indicate that the antihypertensive effect of thiazide diuretics in angiotensin II-dependent hypertension is not exclusively related to depletion of plasma volume [19] and thiazides might have beneficial effects on vascular resistance [41].

Renal microvascular injury

The afferent arteriole, glomerulus and post-glomerular structures were relatively protected from injury throughout the experiment: mild albuminuria developed by day 4 and was further increased coincident with raised renal vascular resistance. Our data suggest that protection from barotrauma reflects maintenance of efficient autoregulation [42]. In contrast, injury to the larger pre-glomerular resistance arteries was evident on the

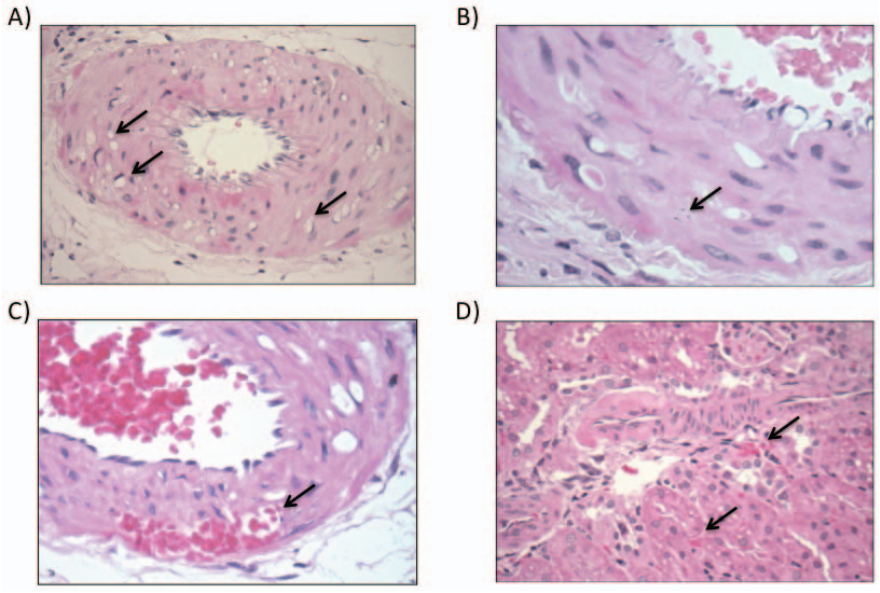

Figure 6. Temporal progression of microvascular injury in kidneys from *cyp1a1-Ren2* transgenic rats. (A) After 1 day of transgene activation myocycte vacuolation was observed in the media of the larger arteries (indicated by arrow). (B) After 3 days apoptotic nuclear fragments were observed (arrow) and (C) there were areas of hemorrhage into necrotic foci. (D) After 7 days, vasculopathy was more extensive still and there were foci of tubulointerstitial injury.
doi:10.1371/journal.pone.0036311.g006

second day, before elevation of blood pressure into the hypertensive range. Renal injury was consistent with vasospasm, and might reflect damaging intermittent surges in systolic blood pressure [43]. These were not visualized in our telemetry analysis but data were only acquired hourly for short periods.

Pressure-independent renal injury, involving both angiotensin II and aldosterone [44,45,46] is also possible. The extent of pressure-independent renoprotection following RAAS inhibition is contentious [47] as AT1R blockade has exacerbated organ damage in some clinical trials [48]. Animal models suggest that transmission of high pressure to the kidney drives vascular remodeling and injury in angiotensin II-dependent hypertension [49,50]. Our data show a protective effect of AT1R blockade, perhaps partially due to losartan's antihypertensive effect. However, chronic thiazide therapy, which caused a similar fall in blood pressure, did not abolish vascular injury, supporting a direct role for angiotensin II in end-organ injury. The beneficial effects of spironolactone were more clearly independent of blood pressure. Experimental and clinical data suggest that aldosterone, some of which may be synthesized in the kidney itself [51], is directly fibrogenic [52] and can damage renal structures [53]. Aldosterone-induced podocyte injury [54], for example, may explain the beneficial effect of spironolactone on the albuminuria seen here.

Concluding Remarks

Renal, vascular and endocrine measurements have established distinctive aetiologies of hypertensive and renovascular disease following the conditional over-expression of renin in *cyp1a1-Ren2* TGR. Our data show that angiotensin II, aldosterone and sodium status act in concert to cause hypertension and renal impairment and underscore the key role of thiazide-sensitive sodium transport in the long-term regulation of blood pressure. Approximately 1/3rd of the blood pressure rise was resistant to thiazide or losartan treatment. A similar proportion of hypertension persists in AT1R null mice infused with angiotensin II [46], pointing to non-renal, non-AT1R-mediated mechanisms. These may involve direct, detrimental actions of renin on vascular function [55], sensitization of the vasculature to vasoactive agents [23] and activation of the sympathetic nervous system [56].

Materials and Methods

Ethics Approval

Experiments were performed under a UK Home Office Project License and protocols were approved by The University of Edinburgh. All surgery was performed under anaesthesia (details are given under relevant sections, below) and all efforts were made to minimize suffering.

Experiments were performed on male *cyp1a1-Ren2 TGR* on a Fischer (F344) background, from a colony maintained in the university's animal house. Rats, aged 12–14 weeks, were given free access to water and commercial rat chow, containing 0.3% sodium by weight (Special Diet Services, UK) and were maintained under controlled conditions of temperature (21±1°C), humidity (50±10%) and light/dark (light 7am–7pm).

Blood pressure measurement in conscious rats

Radiotelemetry devices (Model TA 11PAC20, Data Sciences, UK) were implanted into the thoracic aorta of *Cyp1a1-Ren2* TGR (n = 5) under ketamine/medetomidine anaesthetic, with buprenorphine used as a reversal agent and analgesic. After recovery, one-week equilibration was given during which restoration of the circadian rhythms for blood pressures, activity and heart rate was confirmed. Experimental data were then recorded and decoded using Art 4.0 software (Data Sciences, UK).

Baseline readings were taken over four consecutive days and, on day 5, the *cyp1a1-Ren2* transgene was induced by administering the naturally occurring xenobiotic, indole-3-carbinol (I3C; 100 mg/kg/day in vegetable oil), by gastric gavage at 10am; this was repeated on the following 6 days. Data were obtained on the hour, processed to means, smoothed using a 5-point rolling average and

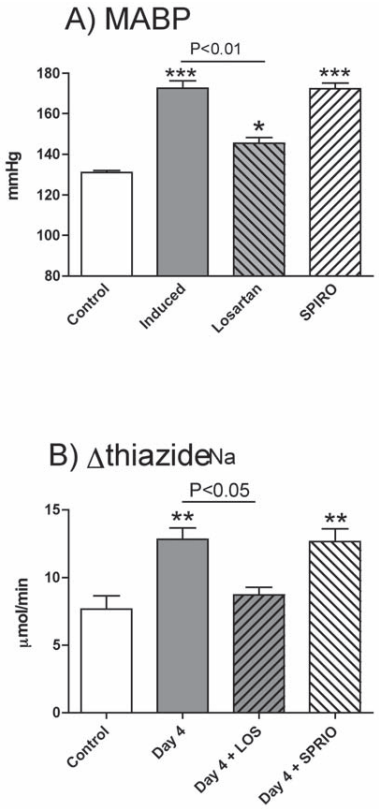

Figure 7. Contributions to hypertension of AT1 and mineralocorticoid receptors. A) Mean arterial blood pressure (MABP) and B) hydrochlorthiazide-sensitive sodium reabsorption ($\Delta thiazide_{Na}$) in *cyp1a1-Ren2* transgenic rats. Measurements were made in cyp1a1-Ren2 transgenic rats, anaesthetized on day 4 of the experimental regimen. The first control group (n = 6; open bars) received vehicle, the second control group (n = 8; grey bars) received I3C to induce the Ren2 transgene. Experimental groups received I3C and either losartan (n = 6; grey hatched bars) or spironolactone (n = 6; open hatched bars). Data are means ± SE and statistical comparisons were made using ANOVA with Bonferroni post-test. ***P<0.001, **P<0.01, *P<0.05 versus the non-induced control group and other comparisons as stated.
doi:10.1371/journal.pone.0036311.g007

used to observe circadian patterns in blood pressure, activity and heart rate (for Figure 1). To analyze statistically periodicity, hourly means were smoothed by 3rd order local polynomial regression, de-trended and analyzed using the χ^2-periodogram algorithm [57].

Renal function in anaesthetized rats

Separate cohorts of *cyp1a1-Ren2* TGRs received I3C for either 1, 3 or 7 days; the control group (n = 8) received an equivalent volume of vegetable oil over a 7-day period. Time-points are designated as control (n = 8), day 2 (n = 9); day 4 (= 9) and day 8 (n = 9). In each group, mean arterial blood pressure and renal function were measured twenty-four hours after the final gavage treatment, as follows. Following thiobutabarbital anaesthesia (Inactin, 120 mg/kg IP; Sigma Aldrich UK), a cannula was inserted into the right jugular vein through which a solution, containing (in mmol/l): 120 NaCl, 10 LiCl, 15 $NaHCO_3$ and 5 KCl, was infused (1 ml/h/100 g IV). The infusate also contained 0.5% p-amino hippuric acid (PAH) and 0.5% FITC-inulin. A cannula, containing heparin-saline, was placed in the right carotid artery for collection of blood and measurement of mean arterial blood pressure. The bladder was catheterized for collection of urine and a tracheostomy was performed to maintain a clear airway.

One hour after the completion of surgery, rats underwent the following protocol: three consecutive collections of urine were made, each of 60 minutes. A sample (75 μl) of arterial blood was drawn at the start and then after each urine collection period for the measurement of haematocrit, FITC-inulin and PAH.

After the first urine collection, amiloride was administered (2 mg/kg bolus; 2 mg/kg/h infusion). After the second urine collection, hydrochlorothiazide was administered (2 mg/kg bolus; 2 mg/kg/h infusion) alongside the amiloride. The drugs were delivered in a DMSO vehicle (2% v:v), which, in a separate group of rats (n = 7), had no effect on renal function or blood pressure (data not shown). Finally, a 1 ml sample of arterial blood was taken for measurement of plasma electrolytes and the kidneys frozen at −80°C and used for Western blot. Animals were then killed by an overdose of anaesthetic.

Analysis & calculations

The concentration of Na, K and Li in plasma and urine was measured using ion-selective electrodes (Roche ISE, model 9180). The effect of amiloride on sodium excretion was taken as the difference between excretion rates in the first and second urine collections; that of hydrochlorothiazide was taken as the difference between excretion rates in the second and third urine collections.

FITC-inulin and PAH concentrations were measured as described [4]. The clearance of PAH was taken as effective renal plasma flow and used to calculate renal blood flow. Renal vascular resistance was taken as the quotient of arterial blood pressure and renal blood flow. Lithium clearance was used as an index of fluid delivery to the end of the proximal tubule [26].

Urine collection in conscious rats

Cyp1a1-Ren2 transgenic rats (n = 8) were housed individually in metabolism cages with free access to powdered rat chow and water. Rats were acclimatized and after a 4-day control period, I3C was administered on each of 7 consecutive days, as described above. Urine was collected every 24-hours. Albumin was measured using commercial assays (Alpha Laboratories Ltd., UK), aldosterone by ELISA [58].

Interventional studies

Hydrochlorothiazide (4 mg/kg/d; n = 6), spironolactone (20 mg/kg/d; n = 6) or losartan (10 mg/kg/d, n = 6) were administered by osmotic minipump (Alzet, Model 2ML1, Charles River UK), implanted on day 0 under isofluorane anaesthesia. A control group of rats (n = 6) received vehicle (50% DMSO, 50% saline) alone. After implant, the *Ren2* transgene was induced over a period of three days before being anesthetized for renal function studies, as described. A three-day induction was selected as a time-point at which significant changes to tubular function were not associated with a decline in renal haemodynamics or major destructive vascular lesions.

Western blot analysis

Total protein was extracted from one kidney by homogenization and differential centrifugation in ice-cold buffer, containing 250 mM sucrose, 10 mM triethanolamine and 2% protease inhibitor cocktail, pH 7.6 (Pierce Protein Research, Thermoscientific, UK). Protein solubilized in sample buffer (50 μg of total protein per lane) was separated by SDS-PAGE and blotted to PVDF membrane by semi-dry transfer. Immunoblotting was

performed using polyclonal antibodies against NCC (Chemicon, UK; 1:2500) and αENaC (Upstate, NY, USA; 1:2000) and horseradish peroxide-conjugated secondary antibodies. Immunodetection was quantified by densitometry using ImageJ after treatment of the blots with ECL reagents. Equal loading of total protein was confirmed in the GAPDH (R&D Systems, UK; 1:5000) immunoblot.

Histopathologic analysis

Kidneys were immersion-fixed in 10% neutral buffered formalin for 48 h followed by paraffin embedding. Four-micron sections were examined blind by a Consultant Pathologist (C.O.B.). Kidneys from at least three rats per experimental group were examined. For each, 2 complete hemisections of the left kidney were blocked and all vascular profiles in each hemisection examined at 4 different levels in the block. Two were stained with hematoxylin and eosin and two with Periodic Acid Schiff, giving 8 levels per case. Analysis of microvascular injury was performed using an ordered categorical scale according the presence of destructive microvascular arterial or arteriolar lesions characterized by intramural necrosis and/or fibrinoid change. A score of "one" indicates non-confluent necrosis and isolated myocyte death; "two" indicates a single foci of necrosis per section; "three" indicates 2–3 foci; and "four" indicates >3 foci of destructive vascular lesions. Undamaged sections were scored zero.

Statistics

Data are presented as mean ± SE. Comparisons were made using either one- or two-way analysis of variance, as appropriate: post-hoc comparisons were made using the Holm-Sidak test. For scoring of microvascular injury, contingency tables were generated for X^2 analysis.

Acknowledgments

We thank Gillian Brooker for expert technical assistance. Ali Ashek received a University of Edinburgh PhD Studentship; Robert Menzies holds a 4-year PhD studentship from the British Heart Foundation Centre of Research Excellence (CoRE) Award to The University of Edinburgh.

Author Contributions

Conceived and designed the experiments: AA AJH CJK PWF JJM MAB. Performed the experiments: AA RIM LJM COCB MAB. Analyzed the data: AA RIM COCB CJK PWF MAB. Wrote the paper: PWF MAB.

References

1. Kantachuvesiri S, Fleming S, Peters J, Peters B, Brooker G, et al. (2001) Controlled hypertension, a transgenic toggle switch reveals differential mechanisms underlying vascular disease. J Biol Chem 276: 36727–36733.
2. Peters B, Grisk O, Becher B, Wanka H, Kuttler B, et al. (2008) Dose-dependent titration of prorenin and blood pressure in Cyp1a1ren-2 transgenic rats: absence of prorenin-induced glomerulosclerosis. J Hypertens 26: 102–109.
3. Schluter T, Rohsius R, Wanka H, Schmid C, Siepelmeyer A, et al. (2010) Amiloride lowers arterial pressure in cyp1a1ren-2 transgenic rats without affecting renal vascular function. J Hypertens 28: 2267–2277.
4. Liu X, Bellamy CO, Bailey MA, Mullins LJ, Dunbar DR, et al. (2009) Angiotensin-converting enzyme is a modifier of hypertensive end organ damage. J Biol Chem 284: 15564–15572.
5. Huskova Z, Vanourkova Z, Erbanova M, Thumova M, Opocensky M, et al. (2010) Inappropriately high circulating and intrarenal angiotensin II levels during dietary salt loading exacerbate hypertension in Cyp1a1-Ren-2 transgenic rats. J Hypertens 28: 495–509.
6. Ortiz RM, Graciano ML, Mullins JJ, Mitchell KD (2007) Aldosterone receptor antagonism alleviates proteinuria, but not malignant hypertension, in Cyp1a1-Ren2 transgenic rats. Am J Physiol Renal Physiol 293: F1584–F1591.
7. Prieto MC, Williams DE, Liu L, Kavanagh KL, Mullins JJ, et al. (2011) Enhancement of renin and prorenin receptor in collecting duct of Cyp1a1-Ren2 rats may contribute to development and progression of malignant hypertension. Am J Physiol Renal Physiol 300: F581–F588.
8. Erbanova M, Thumova M, Huskova Z, Vaneckova I, Vanourkova Z, et al. (2009) Impairment of the autoregulation of renal hemodynamics and of the pressure-natriuresis relationship precedes the development of hypertension in Cyp1a1-Ren-2 transgenic rats. J Hypertens 27: 575–586.
9. Mitchell KD, Mullins JJ (2005) Enhanced tubuloglomerular feedback in Cyp1a1-Ren2 transgenic rats with inducible ANG II-dependent malignant hypertension. Am J Physiol Renal Physiol 289: F1210–F1216.
10. McDonough AA (2010) Mechanisms of proximal tubule sodium transport regulation that link extracellular fluid volume and blood pressure. Am J Physiol Regul Integr Comp Physiol 298: R851–R861.
11. Silva GB, Garvin JL (2008) Angiotensin II-dependent hypertension increases Na transport-related oxygen consumption by the thick ascending limb. Hypertension 52: 1091–1098.
12. Wang T, Giebisch G (1996) Effects of angiotensin II on electrolyte transport in the early and late distal tubule in rat kidney. Am J Physiol 271: F143–F149.
13. Beutler KT, Masilamani S, Turban S, Nielsen J, Brooks HL, et al. (2003) Long-term regulation of ENaC expression in kidney by angiotensin II. Hypertension 41: 1143–1150.
14. Pallone TL, Zhang Z, Rhinehart K (2003) Physiology of the renal medullary microcirculation. Am J Physiol Renal Physiol 284: F253–F266.
15. Honetschlagerova Z, Z ZH, Vanourkova Z, Sporkova A, Kramer HJ, et al. (2011) Renal mechanisms contributing to the antihypertensive action of soluble epoxide hydrolase inhibition in Ren-2 transgenic rats with inducible hypertension. J Physiol 589: 207–219.
16. Patterson ME, Mouton CR, Mullins JJ, Mitchell KD (2005) Interactive effects of superoxide anion and nitric oxide on blood pressure and renal hemodynamics in transgenic rats with inducible malignant hypertension. Am J Physiol Renal Physiol 289: F754–F759.
17. Ando K, Sato Y, Fujita T (1990) Salt sensitivity in hypertensive rats with angiotensin II administration. Am J Physiol 259: R1012–R1016.
18. Kanagy NL, Pawloski CM, Fink GD (1990) Role of aldosterone in angiotensin II-induced hypertension in rats. Am J Physiol 259: R102–R109.
19. Ballew JR, Fink GD (2001) Characterization of the antihypertensive effect of a thiazide diuretic in angiotensin II-induced hypertension. J Hypertens 19: 1601–1606.
20. Hu L, Catanzaro DF, Pitarresi TM, Laragh JH, Sealey JE (1998) Identical hemodynamic and hormonal responses to 14-day infusions of renin or angiotensin II in conscious rats. J Hypertens 16: 1285–1298.
21. Hall JE (1986) Control of sodium excretion by angiotensin II: intrarenal mechanisms and blood pressure regulation. Am J Physiol 250: R960–R972.
22. Fink GD (1997) Long-term sympatho-excitatory effect of angiotensin II: a mechanism of spontaneous and renovascular hypertension. Clin Exp Pharmacol Physiol 24: 91–95.
23. Csiky B, Simon G (1997) Synergistic vascular effects of dietary sodium supplementation and angiotensin II administration. Am J Physiol 273: H1275–H1282.
24. Harris PJ, Young JA (1977) Dose-dependent stimulation and inhibition of proximal tubular sodium reabsorption by angiotensin II in the rat kidney. Pflugers Arch 367: 295–297.
25. Hiranyachattada S, Harris PJ (1996) Modulation by locally produced luminal angiotensin II of proximal tubular sodium reabsorption via an AT1 receptor. Br J Pharmacol 119: 617–618.
26. Thomsen K, Shirley DG (1997) The validity of lithium clearance as an index of sodium and water delivery from the proximal tubules. Nephron 77: 125–138.
27. Zhao D, Seth DM, Navar LG (2009) Enhanced distal nephron sodium reabsorption in chronic angiotensin II-infused mice. Hypertension 54: 120–126.
28. Peti-Peterdi J, Warnock DG, Bell PD (2002) Angiotensin II directly stimulates ENaC activity in the cortical collecting duct via AT(1) receptors. J Am Soc Nephrol 13: 1131–1135.
29. Leviel F, Hubner CA, Houillier P, Morla L, El Moghrabi S, et al. (2011) The Na+-dependent chloride-bicarbonate exchanger SLC4A8 mediates an electroneutral Na+ reabsorption process in the renal cortical collecting ducts of mice. J Clin Invest 120: 1627–1635.
30. Pacheco-Alvarez D, Cristobal PS, Meade P, Moreno E, Vazquez N, et al. (2006) The Na^+:Cl^- cotransporter is activated and phosphorylated at the amino-terminal domain upon intracellular chloride depletion. J Biol Chem 281: 28755–28763.
31. Rafiqi FH, Zuber AM, Glover M, Richardson C, Fleming S, et al. (2010) Role of the WNK-activated SPAK kinase in regulating blood pressure. EMBO Mol Med 2: 63–75.
32. Hannemann A, Flatman PW (2011) Phosphorylation and transport in the Na-K-2Cl cotransporters, NKCC1 and NKCC2A, compared in HEK-293 cells. PLoS One 6: e17992.
33. Velazquez H, Bartiss A, Bernstein P, Ellison DH (1996) Adrenal steroids stimulate thiazide-sensitive NaCl transport by rat renal distal tubules. Am J Physiol 270: F211–219.
34. Sandberg MB, Maunsbach AB, McDonough AA (2006) Redistribution of distal tubule Na+-Cl− cotransporter (NCC) in response to a high-salt diet. Am J Physiol Renal Physiol 291: F503–508.

35. Vallon V, Schroth J, Lang F, Kuhl D, Uchida S (2009) Expression and phosphorylation of the Na^+-Cl^- cotransporter NCC in vivo is regulated by dietary salt, potassium, and SGK1. Am J Physiol Renal Physiol 297: F704–F712.
36. van der Lubbe N, Lim CH, Fenton RA, Meima ME, Jan Danser AH, et al. (2011) Angiotensin II induces phosphorylation of the thiazide-sensitive sodium chloride cotransporter independent of aldosterone. Kidney Int 79: 66–76.
37. de Gasparo M, Joss U, Ramjoue HP, Whitebread SE, Haenni H, et al. (1987) Three new epoxy-spirolactone derivatives: characterization in vivo and in vitro. J Pharmacol Exp Ther 240: 650–656.
38. Talati G, Ohta A, Rai T, Sohara E, Naito S, et al. (2010) Effect of angiotensin II on the WNK-OSR1/SPAK-NCC phosphorylation cascade in cultured mpkDCT cells and in vivo mouse kidney. Biochem Biophys Res Commun 393: 844–888.
39. Lee DH, Riquier AD, Yang LE, Leong PK, Maunsbach AB, et al. (2009) Acute hypertension provokes acute trafficking of distal tubule Na-Cl cotransporter (NCC) to subapical cytoplasmic vesicles. Am J Physiol Renal Physiol 296: F810–F818.
40. Crowley SD, Gurley SB, Herrera MJ, Ruiz P, Griffiths R, et al. (2006) Angiotensin II causes hypertension and cardiac hypertrophy through its receptors in the kidney. Proc Natl Acad Sci U S A 103: 17985–17990.
41. Ellison DH, Loffing J (2009) Thiazide effects and adverse effects: insights from molecular genetics. Hypertension 54: 196–202.
42. Bidani AK, Griffin KA, Williamson G, Wang X, Loutzenhiser R (2009) Protective importance of the myogenic response in the renal circulation. Hypertension 54: 393–398.
43. Young JH, Klag MJ, Muntner P, Whyte JL, Pahor M, et al. (2002) Blood pressure and decline in kidney function: findings from the Systolic Hypertension in the Elderly Program (SHEP). J Am Soc Nephrol 13: 2776–2782.
44. Maitland K, Bridges L, Davis WP, Loscalzo J, Pointer MA (2006) Different effects of angiotensin receptor blockade on end-organ damage in salt-dependent and salt-independent hypertension. Circulation 114: 905–911.
45. Rocha R, Stier CT, Jr., Kifor I, Ochoa-Maya MR, Rennke HG, et al. (2000) Aldosterone: a mediator of myocardial necrosis and renal arteriopathy. Endocrinology 141: 3871–3878.
46. Crowley SD, Zhang J, Herrera M, Griffiths R, Ruiz P, et al. (2011) Role of AT1 receptor-mediated salt retention in angiotensin II-dependent hypertension. Am J Physiol Renal Physiol 301: F1124–F1130.
47. Bidani AK, Griffin KA (2004) Pathophysiology of hypertensive renal damage: implications for therapy. Hypertension 44: 595–601.
48. Granger CB, McMurray JJ, Yusuf S, Held P, Michelson EL, et al. (2003) Effects of candesartan in patients with chronic heart failure and reduced left-ventricular systolic function intolerant to angiotensin-converting-enzyme inhibitors: the CHARM-Alternative trial. Lancet 362: 772–776.
49. Mori T, Cowley AW, Jr. (2004) Role of pressure in angiotensin II-induced renal injury: chronic servo-control of renal perfusion pressure in rats. Hypertension 43: 752–759.
50. Polichnowski AJ, Cowley AW, Jr. (2009) Pressure-induced renal injury in angiotensin II versus norepinephrine-induced hypertensive rats. Hypertension 54: 1269–1277.
51. Nishikawa T, Suematsu S, Saito J, Soyama A, Ito H, et al. (2005) Human renal mesangial cells produce aldosterone in response to low-density lipoprotein (LDL). J Steroid Biochem Mol Biol 96: 309–316.
52. Brem AS, Morris DJ, Ge Y, Dworkin LD, Tolbert E, et al. (2010) Direct Fibrogenic Effects of Aldosterone on Normotensive Kidney: An Effect Modified by 11B-HSD Activity. Am J Physiol Renal Physiol 298: F1178–F1187.
53. Hollenberg NK (2004) Aldosterone in the development and progression of renal injury. Kidney Int 66: 1–9.
54. Shibata S, Nagase M, Yoshida S, Kawachi H, Fujita T (2007) Podocyte as the target for aldosterone: roles of oxidative stress and Sgk1. Hypertension 49: 355–364.
55. Cherney DZ, Lai V, Scholey JW, Miller JA, Zinman B, et al. (2010) Effect of direct renin inhibition on renal hemodynamic function, arterial stiffness, and endothelial function in humans with uncomplicated type 1 diabetes: a pilot study. Diabetes Care 33: 361–365.
56. Rauch AL, Campbell WG, Jr. (1988) Synthesis of catecholamines in the hypothalamus and brainstem in one-kidney, one clip and two-kidney, one clip hypertension in rabbits. J Hypertens 6: 537–541.
57. Sheward WJ, Naylor E, Knowles-Barley S, Armstrong JD, Brooker GA, et al. (2010) Circadian control of mouse heart rate and blood pressure by the suprachiasmatic nuclei: behavioral effects are more significant than direct outputs. PLoS One 5: e9783.
58. Al-Dujaili EA, Mullins LJ, Bailey MA, Kenyon CJ (2009) Development of a highly sensitive ELISA for aldosterone in mouse urine: validation in physiological and pathophysiological states of aldosterone excess and depletion. Steroids 74: 456–462.

frontiers in
PHYSIOLOGY

ORIGINAL RESEARCH ARTICLE
published: 25 October 2013
doi: 10.3389/fphys.2013.00305

Effect of $P2X_4$ and $P2X_7$ receptor antagonism on the pressure diuresis relationship in rats

Robert I. Menzies[1]*, Robert J. Unwin[2], Ranjan K. Dash[3], Daniel A. Beard[3], Allen W. Cowley Jr.[3], Brian E. Carlson[3], John J. Mullins[1] and Matthew A. Bailey[1]*

[1] *University/British Heart Foundation Centre for Cardiovascular Science, The University of Edinburgh, Edinburgh, UK*
[2] *Centre for Nephrology, University College London Medical School, London, UK*
[3] *Department of Physiology, Medical College of Wisconsin, Milwaukee, WI, USA*

Edited by:
Bellamkonda K. Kishore, University of Utah Health Sciences, USA

Reviewed by:
Lisa M. Harrison-Bernard, Louisiana State University, USA
William J. Welch, Georgetown University, USA

Correspondence:
Robert I. Menzies, Centre for Cardiovascular Science, Queen's Medical Research Institute, The University of Edinburgh, Edinburgh EH16 4TJ, UK
e-mail: r.menzies@sms.ed.ac.uk;
Matthew A. Bailey, Centre for Cardiovascular Science, The Queen's Medical Research Institute, The University of Edinburgh, 47, Little France Crescent, Edinburgh EH16 4TJ, UK
e-mail: matthew.bailey@ed.ac.uk

Reduced glomerular filtration, hypertension and renal microvascular injury are hallmarks of chronic kidney disease, which has a global prevalence of ∼10%. We have shown previously that the Fischer (F344) rat has lower GFR than the Lewis rat, and is more susceptible to renal injury induced by hypertension. In the early stages this injury is limited to the pre-glomerular vasculature. We hypothesized that poor renal hemodynamic function and vulnerability to vascular injury are causally linked and genetically determined. In the present study, normotensive F344 rats had a blunted pressure diuresis relationship, compared with Lewis rats. A kidney microarray was then interrogated using the Endeavour enrichment tool to rank candidate genes for impaired blood pressure control. Two novel candidate genes, *P2rx7* and *P2rx4*, were identified, having a 7- and 3- fold increased expression in F344 rats. Immunohistochemistry localized $P2X_4$ and $P2X_7$ receptor expression to the endothelium of the pre-glomerular vasculature. Expression of both receptors was also found in the renal tubule; however there was no difference in expression profile between strains. Brilliant Blue G (BBG), a relatively selective $P2X_7$ antagonist suitable for use *in vivo*, was administered to both rat strains. In Lewis rats, BBG had no effect on blood pressure, but *increased* renal vascular resistance, consistent with inhibition of some basal vasodilatory tone. In F344 rats BBG caused a significant reduction in blood pressure and a *decrease* in renal vascular resistance, suggesting that $P2X_7$ receptor activation may enhance vasoconstrictor tone in this rat strain. BBG also reduced the pressure diuresis threshold in F344 rats, but did not alter its slope. These preliminary findings suggest a physiological and potential pathophysiological role for $P2X_7$ in controlling renal and/or systemic vascular function, which could in turn affect susceptibility to hypertension-related kidney damage.

Keywords: purinergic, ATP, kidney disease, renal injury, renal vascular resistance

INTRODUCTION

Kidney injury and declining renal function are diagnostic indicators of kidney disease and present a global health burden with high population prevalence (Eckardt et al., 2013). Genetic, epigenetic and environmental factors determine susceptibility to renal injury and the development of chronic kidney disease. Hypertension is a major risk factor for kidney disease (Nakayama et al., 2011) and progression can be slowed if blood pressure is controlled (Hart and Bakris, 2010). Nevertheless, renal injury and fibrosis develop independently of barotrauma and the local actions of agents such as aldosterone (Ashek et al., 2012; Kawarazaki et al., 2012) and angiotensin II (Mori and Cowley, 2004; Polichnowski et al., 2011) have been implicated.

We have previously used the *Cyp1a1-Ren2* transgenic rat to investigate pathways leading to renal injury. In these rats, blood pressure is increased by dietary administration of the non-toxic aryl hydrocarbon, indole-3-carbinol (Kantachuvesiri et al., 2001). The rise in blood pressure can be titrated to study the organ injury associated with slowly developing (Conway et al., 2012) or malignant hypertension (Kantachuvesiri et al., 2001). In the malignant setting, vascular injury predominates, with myocyte vacuolation preceding confluent myocyte cell death and microalbuminuria (Ashek et al., 2012).

Genetic background influences susceptibility to renal injury in several rat models (Churchill et al., 1997; Schulz and Kreutz, 2012), the *Cyp1a1-Ren2* transgenic rat being no exception (Kantachuvesiri et al., 2001). Here, the Fischer (F344) strain is susceptible while *Cyp1a1-Ren2* transgenic rats on the Lewis background are protected from renal injury. We have used these informative strains to identify Quantitative Trait Loci for organ injury (Kantachuvesiri et al., 1999) and the development of reciprocal congenic lines enabled us to validate *Ace*, the gene encoding Angiotensin Converting Enzyme, as a plausible modifier of renal injury (Liu et al., 2009). Although the angiotensin receptor antagonist losartan prevents the blood pressure rise in this model, it is only partially protective against renal vascular injury (Ashek et al., 2012). This suggests that susceptibility to renal injury in this model is governed by the interplay between multiple

pathways. We hypothesized that genes differentially expressed in the *Cyp1a1-Ren2* transgenic rat in the normotensive state would contain candidates contributing to poor renal function and susceptibility to renal injury in the F344 strain or the relative renoprotection observed on the Lewis background.

In the present study we compared the pressure diuresis relationship between the differentially susceptible F344 and Lewis rats. This response being blunted in F344 animals, we re-mined a renal exon-microarray (Liu et al., 2009) identifying the genes encoding the $P2X_4$ receptor and $P2X_7$ receptor as candidates for altered vascular function in F344 rats.

MATERIALS AND METHODS

MICROARRAY ANALYSIS

A previously published Affymetrix microarray (Liu et al., 2009) was re-mined to identify differentially expressed probe-sets in the kidney of normotensive *Cyp1a1-Ren2* transgenic rats, i.e., rats in which the *Ren2* transgene was silent. The array was performed on four groups of rats ($n = 4$ per group): the two consomic parental strains (F344, Lewis) and the two reciprocal congenic strains (F344-MOD-Lewis, Lewis-MOD-F344) containing a 14 Mb region of chromosome 10. This congenic region contained the *Ace* locus and the congenics were included in the present analysis to determine whether cis (or trans) regulation occurred. The 16 CEL intensity files were imported into Bioconductor and arrays normalized by the Robust Multi-array Average (RMA) method. The Linear Models for Microarray Data (LIMMA) algorithm was used to calculate fold-change and *p*-value statistics from the normalized intensities.

Differentially expressed genes were imported into the web client online version of the multi-database enrichment tool Endeavour (Aerts et al., 2006, 2009). A list of 157 "training" genes isolated from the rat genome database (Laulederkind et al., 2002) was also imported. The "training" genes used in this study were selected for their association with blood pressure regulation in the rat. They were not tissue specific and assumed no mutual exclusivity with inflammatory, or other disease, processes. The Endeavour method then employed multiple database mining using parallel approaches to enrich the list of differentially regulated genes. These approaches were: (i) published literature text mining; (ii) protein-protein interactions in the STRING database; (iii) transcriptome analysis from the WalkerEtAl database; (iv) sequence comparison with BLAST; and (v) annotations within Gene Ontology, InterPro, KEGG, and Swiss-Prot. Finally, global ranking by Q-statistic generated a list of genes in order of prioritization for the observed phenotype, known as "genomic data fusion."

ANIMALS

*E*xperiments were performed on male F344 and Lewis rats (Charles River, UK). All rats had access to food and water (Special Diet Services, Witham, Essex, UK) *ad libitum*. Procedures were performed in accordance with the UK Home Office Animals (Scientific Procedures) Act of 1986 after ethical review by The University of Edinburgh.

For Western analysis and immunohistochemistry, F344 and Lewis rats ($n = 3$ per genotype) were killed by decapitation. The kidneys were rapidly excised and the left kidney was snap frozen and stored at −80C for subsequent extraction of total protein. The right kidney was immersion fixed in 10% buffered formalin, transferring to 70% ethanol after 48 h. These kidneys were then paraffin embedded and transverse sections taken for IHC.

IMMUNOHISTOCHEMISTRY

Primary rabbit polyclonal antibodies against the $P2X_1$ (APR-001, Alomone Labs), $P2X_4$ (APR-002, Alomone Labs), and $P2X_7$ (APR-004, Alomone Labs) receptors were selected based on published validation for use in the rat. Each antibody was then optimized in a dilution series (1:250, 500, 1000, 2000, 4000, 5000, and 7500) using control rat kidney, following heat-induced epitope recovery (HIER) with citrate buffer. The final titers were selected to give minimal background: $P2X_1$ (1:5000), $P2X_4$ (1:7500), and $P2X_7$ (1:2000). All staining was performed on a Leica Bond × immunostaining robot using a refined HRP polymer detection system. Briefly, after HIER and blocking in Peroxidase, the section was incubated in primary antibody for 2 h at room temperature. Following two 5 min washes, sections were exposed to anti-rabbit HRP polymer before being washed. Immunopositive staining was visualized with 3,3′-diaminobenzidine and counterstaining with hematoxylin.

WESTERN BLOT

Whole kidneys were homogenized in ice-cold buffer containing 250 mmol/l sucrose and 10 mmol/l triethanolamine. Protease inhibitors (Cocktail set III, Calbiochem) and phosphatase/kinase inhibitors (2 mmol/l EDTA, 50 mmol/l NaF, 25 mmol/l sodium glycerophosphate, 5 mmol/l pyrophosphate, and 1 mmol/l sodium orthovanadate) were added and the pH adjusted to 7.6. Following quantification by Bradford assay, protein samples were added to Laemlli buffer and resolved by SDS-PAGE, on a NuPAGE Tris-Acetate gel (8% NovexTM) using a Tris-acetate running buffer (50 mmol/l tricine, 50 mmol/l Tris base, 0.1% SDS, pH 8.24) NuPAGE antioxidant was added to the upper chamber. For the $P2X_4$ studies, 12 μg of total protein was loaded; 20 μg for $P2X_7$ receptor experiments. Following semi-dry transfer the membrane was incubated overnight at 4C with the primary antibody ($P2X_4$ 1:2000; $P2X_7$ 1:1000; Alomone as described above). A goat-antirabbit HRP secondary antibody was then added and the bands visualized by ECL. The $P2X_4$ antibody detected a band of ∼60 kDa; the $P2X_7$ antibody detect a band at ∼75 kDa. The autoradiogram was scanned and band intensity (corrected for background) was quantified by densitometry using ImageJ. Values were normalized to the total protein intensity (Coomasie-Blue) at the appropriate molecular weight.

RENAL FUNCTIONAL STUDIES

Rats were anaesthetized (Thiobutabarbital 120 mg/kg IP) and prepared surgically for measurement of the pressure-diuresis relationship. The right jugular vein was cannulated and 0.9% NaCl was infused at a rate of 50 μl/min/100 g during abdominal surgery

(to replace surgical losses) and then at 33 μl/min/100 g during the post-surgical equilibration (60 min) and throughout the experimental protocol. The left femoral artery was cannulated and connected to brass transducer (MLT844; Capto) connected to a Powerlab (AD Instruments, UK). Blood pressure was recorded continuously at 1 kHz. A midline laparotomy was performed and a Doppler transit time probe (MA1PRB; Transonic, USA) placed around the left renal artery. Acoustic gel was used to ensure good sonic coupling. Loose silk ties were placed around the superior mesenteric and coeliac arteries: these ligatures were tightened during the experimental procedure to create an acute pressure ramp of two stages above baseline blood pressure. The bladder was catheterized for urine collection under mineral oil with flow rate being determined gravimetrically. The entire procedure was performed under homeostatic temperature control at 37°C.

Pressure-diuresis experiments were performed first on a control group of F344 ($n = 7$) and Lewis ($n = 5$) rats and then on a second cohort of F344 ($n = 5$) and Lewis ($n = 6$) rats receiving an IV infusion (50 μg/min/100 g) of Brilliant Blue G (BBG, Sigma, UK).

STATISTICAL ANALYSIS

Data are presented as mean ± s.e.m. or as individual data with median. Statistical analysis was performed by Mann-Whitney *U*-test (for Western analysis) or by unpaired *t*-test (physiological data). Comparisons between groups of the pressure-diuresis relationship were made by linear regression.

RESULTS

PRESSURE DIURESIS RELATIONSHIP

Compared to Lewis rats, F344 rats had a higher baseline blood pressure (**Figure 1A**) and a lower renal blood flow (**Figure 1B**): renal vascular resistance was significantly higher in F344 rats than in Lewis (**Figure 1C**). The imposition of a pressure ramp evoked an increase in urine flow rate in both strains of rats (**Figure 2A**). The slope of the relationship was significantly different from zero in both groups ($P < 0.001$) but was blunted in the F344 strain compared to the Lewis ($P < 0.01$). There was no significant relationship between blood flow and blood pressure in either strain of animals, indicative of intact auto-regulation (**Figure 2B**).

RENAL MICROARRAY ANALYSIS

After normalization, 67 probe-sets were differentially regulated on the basis of genetic background: 23 over-expressed and 44 under-expressed (**Table 1**). Endeavour analysis was used to rank the differentially expressed genes enriched against the training genes of blood pressure regulation. The ten highest globally ranked genes are given in **Table 2**. *Ace* was the highest ranked gene, consistent with our previous QTL and congenic studies (Liu et al., 2009), and was not studied further. The 2nd and 3rd ranked genes were *P2rx7* and *P2rx4*, respectively. The expression of both was higher in the F344 rats than in the Lewis rats. This was confirmed by Western analysis: there was a 7-fold increase in total $P2X_7$ receptor protein ($P < 0.05$; **Figure 3A**) and a 3-fold increase in $P2X_4$ receptor abundance ($P < 0.05$; **Figure 3B**).

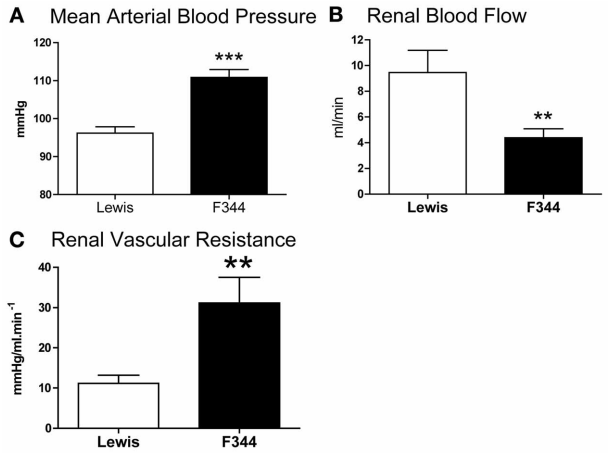

FIGURE 1 | (A) Mean arterial blood pressure; **(B)** left renal artery blood flow and **(C)** renal vascular resistance in the left renal artery measured in Lewis ($n = 8$; open bars) and F344 ($n = 7$; black bars) rats. Data are mean ± *SE*. Statistical comparisons were made with unpaired *t*-test. $^{***}P < 0.001$; $^{**}P < 0.01$.

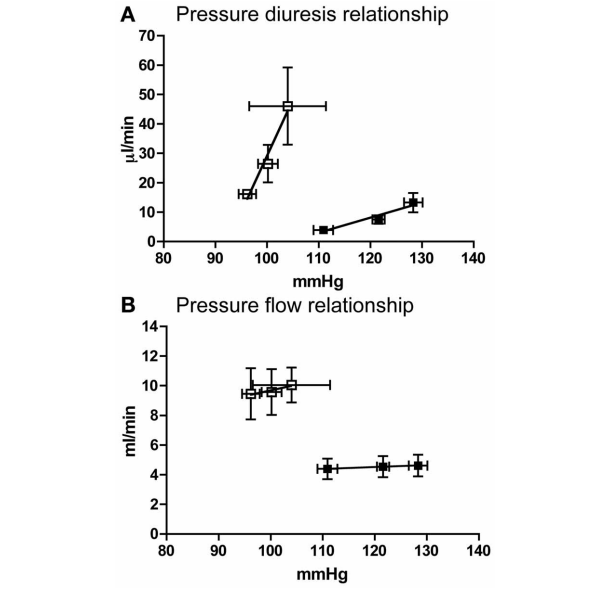

FIGURE 2 | (A) Pressure diuresis and **(B)** pressure flow relationship in Lewis ($n = 8$; open squares) and F344 ($n = 7$; black squares) rats. Data are mean ± *SE*. Statistical test was performed by linear regression analysis.

RENAL LOCALIZATION OF $P2X_{1,4,\text{ and }7}$ RECEPTORS

We observed no differences between strains in the distribution of immunostaining for the P2X receptors. Renal vascular $P2X_4$ immuno-positive staining was restricted to the endothelium throughout the preglomerular vasculature (**Figure 4A**). $P2X_4$ receptor staining was observed in the renal tubules of both strains. In some places this staining was punctate and localized to both the nucleus and cytoplasm (**Figure 4B**).

Table 1 | Genome wide comparison of gene expression between F344 and Lewis inbred strains listed in order of magnitude of fold change (F344 vs. Lewis, fold > ± 1.2, $p < 0.05$).

Over expressed genes (+)			Under expressed genes (−)		
Symbol	**Fold**	***p*-value**	**Symbol**	**Fold**	***p*-value**
Rpl30	+7.6798	0.0226	*Olr1668*	−27.2451	0.0123
Akr1c2	+7.3466	0.0241	*Olr1680*	−24.6268	0.0162
Spta1	+5.6906	0.0090	*RGD1309362*	−13.1217	0.0162
Akr1b8	+4.6613	0.0178	***Pigzl1***	**−6.7012**	**0.007**
LOC361914	+3.6785	0.0094	***Kif5c***	**−6.6248**	**0.009**
Ace	**+3.5400**	**0.0178**	*Ces1e*	−5.7903	0.0094
LOC100359585	+3.3860	0.0250	*Cyp4v3*	−5.2337	0.0166
Guca2b	+2.7994	0.0479	*Olr1326*	−5.1722	0.0336
Ypel4	+2.7596	0.0253	*Acsm5*	−4.7035	0.0178
Rtp4	+2.6916	0.0241	*Hhip*	−4.6118	0.0166
Clstn2	+2.5879	0.0253	*Hmgcs2*	−4.2039	0.0336
P2rx4	**+2.5327**	**0.0162**	*Cyp2d5*	−3.8624	0.0289
Klkb1	**+2.4303**	**0.0090**	***Rdh2***	**−3.4214**	**0.0162**
Exnef	+2.4073	0.0090	*LOC302192*	−3.3622	0.0256
Pigr	**+2.3473**	**0.0336**	*Lcn2*	−3.097	0.0253
P2rx7	**+2.1586**	**0.0336**	*Csmd1*	−3.019	0.0336
Akr1b7	+2.1071	0.0336	*Slc10a2*	−2.7769	0.0226
Cd59	+1.8540	0.0256	*Rxrg*	−2.6987	0.0336
Fam149a	+1.7008	0.0336	*Cntnap4*	−2.6686	0.0192
P4ha2	+1.6668	0.0336	*RT1-CE5*	−2.6679	0.0336
Arl4d	+1.5187	0.0336	***Erc2***	**−2.5297**	**0.0253**
Igfbp4	+1.4873	0.0336	*Ptprq*	−2.4522	0.0182
Col15a1	+1.2734	0.0336	*RGD1311723*	−2.4244	0.0372
			Rbp4	−2.3816	0.0336
			Abcb10	−2.2669	0.0256
			Sult1b1	−2.2336	0.0493
			RGD1563120	−2.1689	0.045
			Mis18a	−2.1532	0.0192
			Slc35f1	−2.1291	0.0372
			Tcerg1l	−2.0443	0.0253
			Acadsb	−1.9181	0.0336
			Rgs7	**−1.8925**	**0.0277**
			Retsat	−1.8721	0.0253
			Gas2	−1.8114	0.045
			Ly75	−1.74	0.0442
			Slco1a6	−1.7194	0.031
			Slc26a11	−1.6736	0.0317
			Pfas	−1.6633	0.0178
			Eps8l2	−1.6505	0.0336
			Dpp6	**−1.6382**	**0.0259**
			RGD1311575	−1.5914	0.0491
			RGD1564614	−1.5199	0.0344
			Cdc42ep2	−1.4477	0.0372
			Synm	−1.4011	0.0442

*Genes identified by enrichment analysis (**Table 2**) shown in bold font.*

Vascular $P2X_7$ receptor staining was observed in the endothelium of the pre-glomerular arteries, including the afferent arterioles of both rat strains (**Figures 4B,C**). Staining was also observed in the glomerulus (**Figure 4C**). In the larger arteries, occasional expression in the vascular smooth muscle was observed but in a given vessel this was limited to a small number of myocytes (**Figure 4D**).

As shown by the low magnification image, $P2X_1$ receptor expression was limited to the vascular network and not expressed in the renal tubules (**Figure 4E**). $P2X_1$ receptor immunopositive staining was observed in the smooth muscle layer of all artery types from lobar to afferent arteriole in both rat strains.

EFFECT OF INFUSION OF BRILLIANT BLUE G

Under baseline (non-ligated) conditions, acute infusion of BBG caused a significant reduction of mean arterial blood pressure in F344 rats but not in Lewis animals (**Figure 5A**). Blood flow through the left renal artery was not significantly affected by BBG in either group (**Figure 5B**). However, BBG caused a significant *decrease* in renal vascular resistance in F344 rats (**Figures 5C, 6B**).

Acute infusion of BBG did not affect the pressure-diuresis relationship in Lewis rats (**Figure 6A**). In F344 rats, BBG caused a significant leftward shift of the pressure-diuresis intercept (**Figure 6B**), reducing the threshold of this response, but did not alter the gradient of the slope. There was no significant relationship between blood flow and blood pressure in either strain (data not shown).

DISCUSSION

F344 rats are susceptible to renal vascular injury whereas Lewis rats are relatively protected (Liu et al., 2009). We find that normotensive F344 rats have a blunted pressure diuresis relationship, which would impair blood pressure control and may underpin the susceptibility to vascular injury observed in this strain. At a genetic level, we identified increased renal expression of $P2X_4$ and $P2X_7$ receptors, which may contribute to impaired vascular function in F344 rats, compared to the Lewis strain.

Multiple subtypes of P2X and P2Y receptors are expressed throughout the kidney and extracellular nucleotides regulate renal tubular, endocrine, and vascular functions (Bailey and Shirley, 2009; Bailey et al., 2012; Shirley et al., 2013). Purinergic control of renal vascular tone is complex and the net vasoactive effect depends upon the route of administration/physiological source of the extracellular nucleotide. Thus, ATP applied *in vitro* to the adventitial surface of the renal microvasculature causes contraction (Inscho et al., 1992) mediated by $P2X_1$ receptors (Inscho et al., 2003) in the vascular smooth muscle (Chan et al., 1998). In contrast, infusion of ATP into the renal artery increases blood flow (Tagawa and Vander, 1970) and the vasodilatation is dependent on production of nitric oxide/prostacyclin by the endothelium (Eltze and Ullrich, 1996). The P2 receptor subtype(s) that mediate the vasodilatory response to ATP is not resolved and may vary in different vascular beds. mRNA encoding $P2Y_1$, $P2Y_2$, $P2X_4$, and $P2X_7$ receptors have all been identified in human arterial endothelial cells (Yamamoto et al., 2000; Ray et al., 2002). $P2X_4$ receptors are the most abundantly expressed, followed by $P2X_7$ (∼50%) and then by $P2Y_1$ and $P2Y_2$ (∼20%) receptors (Yamamoto et al., 2000). A similar profile is observed in endothelial cells cultured from the mouse pulmonary artery (Yamamoto et al., 2006) and $P2X_4$ and

Table 2 | Global prioritization by the Endeavour enrichment method.

Gene	Known biological function(s)	Global prioritization		
		Rank	Score	Rank ratio
Ace (ENSRNOG00000007467)	BP regulation	1	0.0187	0.0909
P2rx7(ENSRNOG00000001296)	Ion transport, cell volume, apoptosis	2	0.0624	0.182
P2rx4 (ENSRNOG00000001300)	Ion transport, BP regulation, NOS	3	0.118	0.273
Rgs7 (ENSRNOG00000021984)	G-protein signaling	4	0.583	0.364
Erc2 (ENSRNOG00000015148)	Nerve terminal assembly	5	0.674	0.455
Klkb1 (ENSRNOG00000014118)	Proteolysis, coagulation, inflammation	6	0.787	0.545
Kif5c (ENSRNOG00000004680)	Motor axon guidance	7	0.796	0.636
Dpp6 (ENSRNOG00000030547)	Proteolysis	8	0.933	0.727
Pigr (ENSRNOG00000004405)	Antibody receptor	9	0.936	0.818
Rdh2 (ENSRNOG00000029651)	Retinoid metabolism, oxidation reduction	10	0.988	0.909

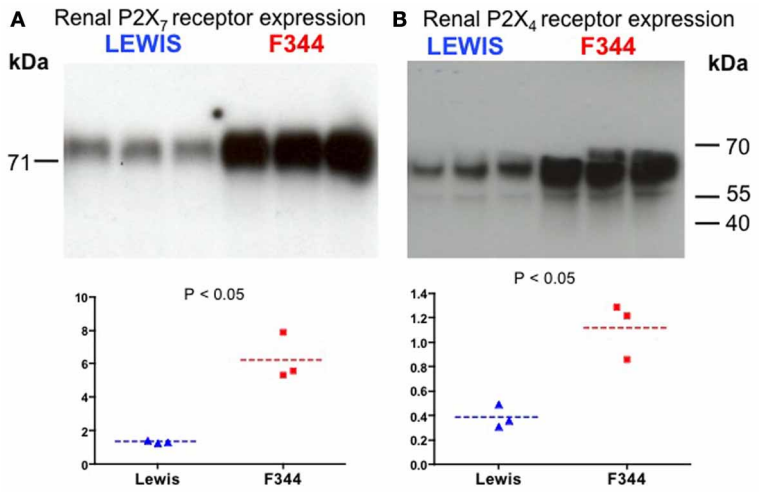

FIGURE 3 | Western blot analysis of (A) $P2X_7$ receptor and (B) P2X4 receptor expression in whole kidney homogenates. The top panels show the blot performed in Lewis and F344 rats ($n = 3$ in each). The bottom panels show the blot intensity (normalized to protein loading) quantified by densitometry.

$P2X_7$ receptors have also been immunolocalized to the endothelium of the larger renal arteries of the rat (Lewis and Evans, 2001).

Our studies are largely consistent with this distribution of P2X receptors. $P2X_1$ receptor expression was limited to the vascular smooth muscle of the renal arteries and afferent arteriole. Renal autoregulation is severely attenuated in $P2X_1$ null mice, (Inscho et al., 2004; Guan et al., 2007; Inscho, 2009), illustrating the importance of this receptor for renal vascular function. In the present study, renal autoregulation was intact in both strain of rats and we find no evidence linking differential expression of the $P2X_1$ receptor, or indeed P2X4 or P2X7 receptors to the impaired renal vascular function observed in F344 rats.

We did find increased abundance of $P2X_4$ and $P2X_7$ receptor, both in the microarray analysis and at the protein level. In humans the encoding genes, *P2RX4* and *P2RX7*, are located within 130 kb of each other on chromosome 12. These genes can be regulated independently: the endothelial expression of $P2X_4$ receptors in the human aorta is increased following injury; $P2X_7$ receptor expression is not affected (Pulvirenti et al., 2000). It is possible, however, that these receptors have common promotor elements. Physiological interactions between the receptors are postulated (Craigie et al., 2013) and the locus is associated with human disease. For example, a single nucleotide polymorphism (SNP) in the first intron of *P2RX7* is strongly associated with elevated blood pressure (Palomino-Doza et al., 2008) and a loss-of-function SNP in the *P2RX7* coding region associates with protection against ischemic stroke (Gidlöf et al., 2012). Similarly, a loss of function SNP in the $P2X_4$ receptor has been associated with increased pulse pressure (Stokes et al., 2011).

Consistent with the previous studies described, we localized $P2X_4$ and $P2X_7$ receptors to the endothelium of the preglomerular vasculature. Our bioinformatic ranking analysis associated increased expression with vascular dysfunction and loss of blood pressure control. Both $P2X_4$ (Yamamoto et al., 2006) and $P2X_7$ receptors (Liu et al., 2004) can modulate blood vessel contractility by promoting the release of vasodilators from the endothelium. One interpretation of our data is that

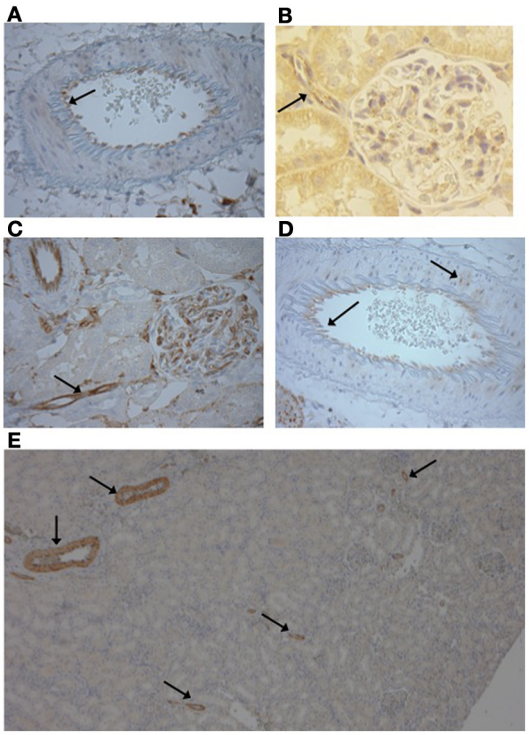

FIGURE 4 | (A) Vascular $P2X_4$ receptors were expressed in the endothelium (Image from F344 rat ×400) and **(B)** the afferent arteriole (Image Lewis rat ×500). **(C)** $P2X_7$ receptors were stained in the endothelium of the preglomerular vasculature, including the afferent arteriole (arrow) and cells of the glomerulus (Image F344 rat, ×400). **(D)** Occasional smooth muscle staining of $P2X_7$ was observed (arrow; Lewis rat, ×400). **(E)** $P2X_1$ immunopositive staining was only observed in the vasculature and was limited to the smooth muscle layer of large and small diameter vessels (F344 rat, ×50).

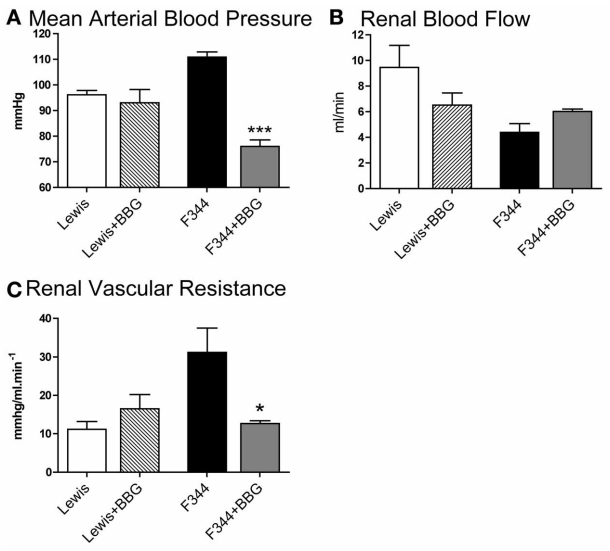

FIGURE 5 | (A) Mean arterial blood pressure; **(B)** left renal artery blood flow and **(C)** renal vascular resistance in the left renal artery measured in Lewis and F344 rats receiving either saline or Brilliant Blue G by intravenous infusion. Data are mean ± *SE*. Statistical comparisons were made within strain by unpaired *t*-test. $^{***}P < 0.001$; $^{*}P < 0.05$. Statistical comparisons were made using one way ANOVA with Bonferroni post-test.

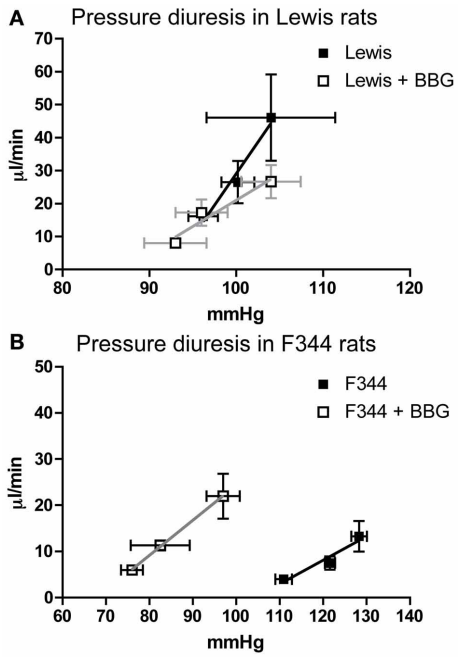

FIGURE 6 | The Pressure diuresis relationship measured in (A) Lewis and (B) F344 rats receiving either saline (closed symbols) or Brilliant Blue G (open symbols) by intravenous infusion. Data are mean ± *SE*. Statistical test was performed by linear regression analysis.

the up-regulation of receptors in F344 rats is a compensatory response to improve poor renal blood flow. Thus, acute receptor antagonism *in vivo* should inhibit this tonic vasodilation. There was a trend for this in the Lewis rats but the reduction in blood flow induced by BBG was not statistically different. BBG did induce a significant hemodynamic effect in F344 rats but this was to increase blood flow, rather than to reduce it. One interpretation of this outcome is that in F344 rats $P2X_4/P2X_7$ receptor activation induces a tonic vasoconstriction. It is difficult to reconcile such an effect with the predominantly endothelial location of these receptors. However, the endothelium also releases potent vasoconstrictive mediators, including mono- or di-nucleoside polyphosphates such as adenosine 5′ tetraphosphate (Tolle et al., 2008) and uridine adenosine tetraphosphate is a partial agonist at the rat $P2X_4$ receptor (Wildman et al., 1999) and causes a profound vasoconstriction when perfused via the intravascular route into the isolated rat kidney (Tolle et al., 2008).

An obvious concern in interpreting these results is the selectivity of the antagonist, BBG. This compound is a potent inhibitor of rat $P2X_7$ receptors ($IC_{50} = 10$ nM) and although it can also block the $P2X_4$ receptor, its selectivity for $P2X_7$ receptor is 1000-fold greater. BBG has been used previously *in vivo* to elucidate $P2X_7$ receptor functionality (Jiang et al., 2000; Peng et al., 2009). Indeed, chronic administration of BBG reduces renal injury and lowers blood pressure in the Dahl salt sensitive rat

(Ji et al., 2012a); $P2X_7$ null mice are similarly protected from the renal injury associated with salt-induced hypertension (Ji et al., 2012b). Nevertheless, BBG may also antagonize rat $P2X_4$ receptors and our infusion protocol could inhibit both P2X receptor subtypes. Furthermore, a number of off-target effects of BBG have been reported (Katrahalli et al., 2010), so we cannot exclude the possibility that $P2X_7$-independent effects also contribute to the hemodynamic actions of BBG observed in the F344 rats.

$P2X_4$ and $P2X_7$ receptors were also identified in the renal tubule in both strains of rats. Tubular expression of $P2X_4$ receptor is consistent with several previous studies (Bailey et al., 2012). We found some evidence of intracellular, punctate staining, particularly in the Lewis rats. It is possible that this represents expression of $P2X_4$ receptors in intracellular vesicles, which might act as a reservoir for trafficking of receptors to the apical or basolateral membrane or serve as mediators of vacuolar calcium release (Sivaramakrishnan and Fountain, 2012). P2X receptors, including $P2X_4$ can regulate tubular sodium reabsorption processes (Bailey et al., 2012) but in our studies BBG did not affect urine flow rate. The relationship between $P2X_4$ receptor activation and sodium/water reabsorption is complex, however, and may depend on the local sodium concentration.

In summary, $P2X_7$ and $P2X_4$ receptors are expressed in the vascular endothelium and may contribute to the normal control of renal arterial resistance. Both receptors are attractive candidate genes for impaired renal vascular function and susceptibility to kidney injury. However, their respective roles are not easy to define: the present findings are consistent with a predominant vasoconstrictor effect of $P2X_7$ and vasodilator effect of $P2X_4$, but the relationship is likely to be more complex than this simple dichotomy suggests. For example, endothelial $P2X_7$ receptors can mediate the release of factors that modulate the inflammatory state of the vessel wall (Wilson et al., 2007). Moreover, the encoding gene for $P2X_7$ transcribes a large number of splice variants with reportedly different functionality (Sluyter and Stokes, 2011; Xu et al., 2012), which may also contribute to contrasting vasoactive effects in different strains of rat as observed here.

AUTHOR CONTRIBUTIONS

Performing experiments: Robert I. Menzies, Data analysis: Robert I. Menzies, Matthew A. Bailey, Data interpretation: Robert I. Menzies, John J. Mullins, Robert J. Unwin, Matthew A. Bailey, Discussion of data and manuscript: all authors, Writing of paper: all authors

ACKNOWLEDGMENTS

This research was supported by a British Heart Foundation Center of Research Excellence (CoRE) PhD studentship (Robert I. Menzies) and a Kidney Research UK grant (Matthew A. Bailey). We thank Jon Manning for bioinformatic support and Jessica Ivy for assistance with the Western analysis. We acknowledge K.U. LEUVEN RESEARCH & DEVELOPMENT, Groot Begijnhof, Benedenstraat 59, B-3000 Leuven, Belgium and Flanders Interuniversity Institute for Biotechnology vzw, Rijvisschestraat 120, B-9052 Zwijnaarde, Belgium as the providers of the Endeavour online bioinformatics tool.

REFERENCES

Aerts, S., Lambrechts, D., Maity, S., Van Loo, P., Coessens, B., De Smet, F., et al. (2006). Gene prioritization through genomic data fusion. *Nat. Biotechnol.* 24, 537–544. doi: 10.1038/nbt1203

Aerts, S., Vilain, S., Hu, S., Tranchevent, L. C., Barriot, R., Yan, J. K., et al. (2009). Integrating computational biology and forward genetics in drosophila. *PLoS Genet.* 5:e1000351. doi: 10.1371/journal.pgen.1000351

Ashek, A., Menzies, R. I., Mullins, L. J., Bellamy, C. O. C., Harmar, A. J., Kenyon, C. J., et al. (2012). Activation of thiazide-sensitive cotransport by angiotensin II in the cyp1a1-Ren2 hypertensive rat. *PLoS ONE* 7:e36311. doi: 10.1371/journal.pone.0036311

Bailey, M. A., and Shirley, D. G. (2009). Effects of extracellular nucleotides on renal tubular solute transport. *Purinergic Signal.* 5, 473–480. doi: 10.1007/s11302-009-9149-z

Bailey, M. A., Unwin, R. J., and Shirley, D. G. (2012). P2X receptors and kidney function. *WIREs Membr. Transp. Signal.* 1, 503–511. doi: 10.1002/wmts.40

Chan, C. M., Unwin, R. J., Bardini, M., Oglesby, I. B., Ford, A. P., Townsend-Nicholson, A., et al. (1998). Localization of P2X1 purinoceptors by autoradiography and immunohistochemistry in rat kidneys. *Am. J. Physiol.* 274, F799–F804.

Churchill, P. C., Churchill, M. C., Bidani, A. K., Griffin, K. A., Picken, M., Pravenec, M., et al. (1997). Genetic susceptibility to hypertension-induced renal damage in the rat. Evidence based on kidney-specific genome transfer. *J. Clin. Invest.* 100, 1373–1382. doi: 10.1172/JCI119657

Conway, B. R., Rennie, J., Bailey, M. A., Dunbar, D. R., Manning, J. R., Bellamy, C. O., et al. (2012). Hyperglycemia and renin-dependent hypertension synergize to model diabetic nephropathy. *J. Am. Soc. Nephrol.* 23, 405–411. doi: 10.1681/ASN.2011060577

Craigie, E., Birch, R. E., Unwin, R. J., and Wildman, S. S. (2013). The relationship between P2X4 and P2X7: a physiologically important interaction. *Front. Physiol.* 4:216. doi: 10.3389/fphys.2013.00216

Eckardt, K. U., Coresh, J., Devuyst, O., Johnson, R. J., Kottgen, A., Levey, A. S., et al. (2013). Evolving importance of kidney disease: from subspecialty to global health burden. *Lancet* 382, 158–169. doi: 10.1016/S0140-6736(13)60439-0

Eltze, M., and Ullrich, B. (1996). Characterization of vascular P2 purinoceptors in the rat isolated perfused kidney. *Eur. J. Pharmacol.* 306, 139–152. doi: 10.1016/0014-2999(96)00244-0

Gidlöf, O., Smith, J. G., Melander, O., Lövkvist, H., Hedblad, B., Engström, G., et al. (2012). A common missense variant in the ATP receptor P2X7 is associated with reduced risk of cardiovascular events. *PLoS ONE* 7:e37491. doi: 10.1371/journal.pone.0037491

Guan, Z., Osmond, D. A., and Inscho, E. W. (2007). P2X receptors as regulators of the renal microvasculature. *Trends Pharm. Sci.* 28, 646–652. doi: 10.1016/j.tips.2007.09.010

Hart, P. D., and Bakris, G. L. (2010). Hypertensive nephropathy: prevention and treatment recommendations. *Expert Opin. Pharmacother.* 11, 2675–2686. doi: 10.1517/14656566.2010.485612

Inscho, E. W. (2009). ATP, P2 receptors and the renal microcirculation. *Purinergic Signal.* 5, 447–460. doi: 10.1007/s11302-009-9147-1

Inscho, E. W., Cook, A. K., Imig, J. D., Vial, C., and Evans, R. J. (2003). Physiological role for P2X1 receptors in renal microvascular autoregulatory behavior. *J. Clin. Invest.* 112, 1895–1905.

Inscho, E. W., Cook, A. K., Imig, J. D., Vial, C., and Evans, R. J. (2004). Renal autoregulation in P2X1 knockout mice. *Acta Physiol. Scand.* 181, 445–453. doi: 10.1111/j.1365-201X.2004.01317.x

Inscho, E. W., Ohishi, K., and Navar, L. G. (1992). Effects of ATP on pre- and postglomerular juxtamedullary microvasculature. *Am. J. Physiol.* 263, F886–F893.

Ji, X., Naito, Y., Hirokawa, G., Weng, H., Hiura, Y., Takahashi, R., et al.

(2012a). P2X(7) receptor antagonism attenuates the hypertension and renal injury in Dahl salt-sensitive rats. *Hypertens. Res.* 35, 173–179. doi: 10.1038/hr.2011.153

Ji, X., Naito, Y., Weng, H., Endo, K., Ma, X., and Iwai, N. (2012b). P2X7 deficiency attenuates hypertension and renal injury in deoxycorticosterone acetate-salt hypertension. *Am. J. Physiol. Renal Physiol.* 303, F1207–F1215. doi: 10.1152/ajprenal.00051.2012

Jiang, L. H., Mackenzie, A. B., North, R. A., and Surprenant, A. (2000). Brilliant blue G selectively blocks ATP-gated rat P2X(7) receptors. *Mol. Pharm.* 58, 82–88.

Kantachuvesiri, S., Fleming, S., Peters, J., Peters, B., Brooker, G., Lammie, A. G., et al. (2001). Controlled hypertension, a transgenic toggle switch reveals differential mechanisms underlying vascular disease. *J. Biol. Chem.* 276, 36727–36733. doi: 10.1074/jbc.M103296200

Kantachuvesiri, S., Haley, C. S., Fleming, S., Kurian, K., Whitworth, C. E., Wenham, P., et al. (1999). Genetic mapping of modifier loci affecting malignant hypertension in TGR(mRen2) rats. *Kidney Int.* 56, 414–420. doi: 10.1046/j.1523-1755.1999.00571.x

Katrahalli, U., Kalanur, S. S., and Seetharamappa, J. (2010). Interaction of bioactive coomassie brilliant blue g with protein: insights from spectroscopic methods. *Sci. Pharm.* 78, 869–880. doi: 10.3797/scipharm.1008-15

Kawarazaki, W., Nagase, M., Yoshida, S., Takeuchi, M., Ishizawa, K., Ayuzawa, N., et al. (2012). Angiotensin II- and salt-induced kidney injury through Rac1-mediated mineralocorticoid receptor activation. *J. Am. Soc. Nephrol.* 23, 997–1007. doi: 10.1681/ASN.2011070734

Laulederkind, S. J. F., Hayman, G. T., Wang, S.-J., Lowry, T. F., Nigam, R., Petri, V., et al. (2002). "Exploring genetic, genomic and phenotypic data at the rat genome database." *Curr. Protoc. Bioinformatics* 40, 1.14.1–1.14.27. doi: 10.1002/0471250953.bi0114s40

Lewis, C. J., and Evans, R. J. (2001). P2X receptor immunoreactivity in different arteries from the femoral, pulmonary, cerebral, coronary and renal circulations. *J. Vasc. Res.* 38, 332–340. doi: 10.1159/000051064

Liu, C., Mather, S., Huang, Y., Garland, C. J., and Yao, X. (2004). Extracellular ATP facilitates flow-induced vasodilatation in rat small mesenteric arteries. *Am. J. Physiol. Heart Circ. Physiol.* 286, H1688–H1695. doi: 10.1152/ajpheart.00576.2003

Liu, X., Bellamy, C. O., Bailey, M. A., Mullins, L. J., Dunbar, D. R., Kenyon, C. J., et al. (2009). Angiotensin-converting enzyme is a modifier of hypertensive end organ damage. *J. Biol. Chem.* 284, 15564–15572. doi: 10.1074/jbc.M806584200

Mori, T., and Cowley, A. W. (2004). Role of pressure in angiotensin II-induced renal injury - Chronic servo-control of renal perfusion pressure in rats. *Hypertension* 43, 752–759. doi: 10.1161/01.HYP.0000120971.49659.6a

Nakayama, M., Sato, T., Miyazaki, M., Matsushima, M., Sato, H., Taguma, Y., et al. (2011). Increased risk of cardiovascular events and mortality among non-diabetic chronic kidney disease patients with hypertensive nephropathy: the Gonryo study. *Hypertens. Res.* 34, 1106–1110. doi: 10.1038/hr.2011.96

Palomino-Doza, J., Rahman, T. J., Avery, P. J., Mayosi, B. M., Farrall, M., Watkins, H., et al. (2008). Ambulatory blood pressure is associated with polymorphic variation in P2X receptor genes. *Hypertension* 52, 980–985. doi: 10.1161/HYPERTENSIONAHA.108.113282

Peng, W., Cotrina, M. L., Han, X., Yu, H., Bekar, L., Blum, L., et al. (2009). Systemic administration of an antagonist of the ATP-sensitive receptor P2X7 improves recovery after spinal cord injury. *Proc. Natl. Acad. Sci. U.S.A.* 106, 12489–12493. doi: 10.1073/pnas.0902531106

Polichnowski, A. J., Lu, L. M., and Cowley, A. W. (2011). Renal injury in angiotensin II plus L-NAME-induced hypertensive rats is independent of elevated blood pressure. *Am. J. Physiol. Renal Physiol.* 300, F1008–F1016. doi: 10.1152/ajprenal.00354.2010

Pulvirenti, T. J., Yin, J. L., Chaufour, X., Mclachlan, C., Hambly, B. D., Bennett, M. R., et al. (2000). P2X (purinergic) receptor redistribution in rabbit aorta following injury to endothelial cells and cholesterol feeding. *J. Neurocytol.* 29, 623–631. doi: 10.1023/A:1010828302936

Ray, F. R., Huang, W., Slater, M., and Barden, J. A. (2002). Purinergic receptor distribution in endothelial cells in blood vessels: a basis for selection of coronary artery grafts. *Atherosclerosis* 162, 55–61. doi: 10.1016/S0021-9150(01)00681-5

Schulz, A., and Kreutz, R. (2012). Mapping genetic determinants of kidney damage in rat models. *Hypertens. Res.* 35, 675–694. doi: 10.1038/hr.2012.77

Shirley, D. G., Bailey, M. A., Wildman, S. S. P., Tam, F. W. K., and Unwin, R. J. (2013). "Chapter 18: Extracellular Nucleotides and Renal Function," in *Seldin and Giebisch's The Kidney: Physiology and Pathophysiology, 5th Edn.*, eds R. J. Alpern, M. J. Caplan, and O. W. Moe (Academic Press), 511–537. doi: 10.1016/B978-0-12-381462-3.00018-5. ISBN: 978-0-12-381462-3

Sivaramakrishnan, V., and Fountain, S. J. (2012). A Mechanism of Intracellular P2X Receptor Activation. *J. Biol. Chem.* 287, 28315–28326. doi: 10.1074/jbc.M112.372565

Sluyter, R., and Stokes, L. (2011). Significance of P2X7 receptor variants to human health and disease. *Recent Pat. DNA Gene Seq.* 5, 41–54. doi: 10.2174/187221511794839219

Stokes, L., Scurrah, K., Ellis, J. A., Cromer, B. A., Skarratt, K. K., Gu, B. J., et al. (2011). A loss-of-function polymorphism in the human P2X4 receptor is associated with increased pulse pressure. *Hypertension* 58, 1086–1092. doi: 10.1161/HYPERTENSIONAHA.111.176180

Tagawa, H., and Vander, A. J. (1970). Effects of adenosine compounds on renal function and renin secretion in dogs. *Circ. Res.* 26, 327–338. doi: 10.1161/01.RES.26.3.327

Tolle, M., Jankowski, V., Schuchardt, M., Wiedon, A., Huang, T., Hub, F., et al. (2008). Adenosine 5'-tetraphosphate is a highly potent purinergic endothelium-derived vasoconstrictor. *Circ. Res.* 103, 1100–1108. doi: 10.1161/CIRCRESAHA.108.177865

Wildman, S. S., Brown, S. G., King, B. F., and Burnstock, G. (1999). Selectivity of diadenosine polyphosphates for rat P2X receptor subunits. *Eur. J. Pharmacol.* 367, 119–123. doi: 10.1016/S0014-2999(98)00976-5

Wilson, H. L., Varcoe, R. W., Stokes, L., Holland, K. L., Francis, S. E., Dower, S. K., et al. (2007). P2X receptorcharacterization and IL-1/IL-1Ra release from human endothelial cells. *Br. J. Pharmacol.* 151, 115–127. doi: 10.1038/sj.bjp.0707213

Xu, X. J., Boumechache, M., Robinson, L. E., Marschall, V., Gorecki, D. C., Masin, M., et al. (2012). Splice variants of the P2X7 receptor reveal differential agonist dependence and functional coupling with pannexin-1. *J. Cell. Sci.* 125, 3776–3789. doi: 10.1242/jcs.099374

Yamamoto, K., Korenaga, R., Kamiya, A., Qi, Z., Sokabe, M., and Ando, J. (2000). P2X(4) receptors mediate ATP-induced calcium influx in human vascular endothelial cells. *Am. J. Physiol. Heart Circ. Physiol.* 279, H285–H292.

Yamamoto, K., Sokabe, T., Matsumoto, T., Yoshimura, K., Shibata, M., Ohura, N., et al. (2006). Impaired flow-dependent control of vascular tone and remodeling in P2X4-deficient mice. *Nat. Med.* 12, 133–137. doi: 10.1038/nm1338

Conflict of Interest Statement: The authors declare that the research was conducted in the absence of any commercial or financial relationships that could be construed as a potential conflict of interest.

Received: 06 June 2013; accepted: 03 October 2013; published online: 25 October 2013.

*Citation: Menzies RI, Unwin RJ, Dash RK, Beard DA, Cowley AW Jr., Carlson BE, Mullins JJ and Bailey MA (2013) Effect of $P2X_4$ and $P2X_7$ receptor antagonism on the pressure diuresis relationship in rats. Front. Physiol. **4**:305. doi: 10.3389/fphys.2013.00305*

This article was submitted to Renal and Epithelial Physiology, a section of the journal Frontiers in Physiology.

Am J Physiol Renal Physiol 305: F845–F852, 2013.
First published July 17, 2013; doi:10.1152/ajprenal.00113.2013.

An anatomically unbiased approach for analysis of renal BOLD magnetic resonance images

Robert I. Menzies,[1] Andrew Zammit-Mangion,[2] Lyam M. Hollis,[1] Ross J. Lennen,[1] Maurits A. Jansen,[1] David J. Webb,[1] John J. Mullins,[1] James W. Dear,[1] Guido Sanguinetti,[2] and Matthew A. Bailey[1]

[1]*University/British Heart Foundation Centre for Cardiovascular Science, The University of Edinburgh, Edinburgh, United Kingdom; and* [2]*School of Informatics, The University of Edinburgh, Edinburgh, United Kingdom*

Submitted 28 February 2013; accepted in final form 8 July 2013

Menzies RI, Zammit-Mangion A, Hollis LM, Lennen RJ, Jansen MA, Webb DJ, Mullins JJ, Dear JW, Sanguinetti G, Bailey MA. An anatomically unbiased approach for analysis of renal BOLD magnetic resonance images. *Am J Physiol Renal Physiol* 305: F845–F852, 2013. First published July 17, 2013; doi:10.1152/ajprenal.00113.2013.—Oxygenation defects may contribute to renal disease progression, but the chronology of events is difficult to define in vivo without recourse to invasive methodologies. Blood oxygen level-dependent magnetic resonance imaging (BOLD MRI) provides an attractive alternative, but the R2* signal is physiologically complex. Postacquisition data analysis often relies on manual selection of region(s) of interest. This approach excludes from analysis significant quantities of biological information and is subject to selection bias. We present a semiautomated, anatomically unbiased approach to compartmentalize voxels into two quantitatively related clusters. In control F344 rats, low R2* clustering was located predominantly within the cortex and higher R2* clustering within the medulla (70.96 ± 1.48 vs. 79.00 ± 1.50; 3 scans per rat; $n = 6$; $P < 0.01$) consistent anatomically with a cortico-medullary oxygen gradient. An intravenous bolus of acetylcholine caused a transient reduction of the R2* signal in both clustered segments ($P < 0.01$). This was nitric oxide dependent and temporally distinct from the hemodynamic effects of acetylcholine. Rats were then chronically infused with angiotensin II (60 ng/min) and rescanned 3 days later. Clustering demonstrated a disruption of the cortico-medullary gradient, producing less distinctly segmented mean R2* clusters (71.30 ± 2.00 vs. 72.48 ± 1.27; $n = 6$; NS). The acetylcholine-induced attenuation of the R2* signal was abolished by chronic angiotensin II infusion, consistent with reduced nitric oxide bioavailability. This global map of oxygenation, defined by clustering individual voxels on the basis of quantitative nearness, might be more robust in defining deficits in renal oxygenation than the absolute magnitude of R2* in small, manually selected regions of interest defined exclusively by anatomical nearness.

k-means; acetylcholine; angiotensin II; nitric oxide; hypoxia

RENAL TISSUE HYPOXIA IS IMPLICATED in the pathogenesis of chronic kidney disease (CKD), with low partial pressure of oxygen (P_{O_2}) causing activation of a profibrotic cascade (27). Even under physiological conditions, the P_{O_2} within the kidney is thought to have a marked cortico-medullary gradient, with the medulla being poorly oxygenated (9). Cells of the medulla have a higher anaerobic capacity than those of the cortex and paracrine signaling pathways also provide some resistance against hypoxia (25). Nevertheless, the medulla is susceptible to hypoxic injury and chronic hypoperfusion, which can initiate a vicious cycle of microvasculature injury, inflammation, and fibrosis (21).

A causal link between defects in renal oxygenation and renal disease is supported by immunohistochemical detection of pimonidazole adducts (24), formed when P_{O_2} is <10 mmHg. This method is, however, insensitive and nonquantitative (30). O_2-sensitive microelectrodes offer a quantitative and sensitive approach (10), but measurements made at the electrode tip cannot give global insights into the distribution of oxygen. Moreover, being invasive, microelectrodes are not usually amenable to longitudinal studies of renal function.

Blood oxygen level-dependent magnetic resonance imaging (BOLD MRI) is emerging as a technique through which to assess renal oxygen bioavailability (20). BOLD imaging exploits the paramagnetic properties of deoxyhemoglobin, generating images based on the dephasing of spin relaxation rate from an applied electromagnetic field pulse. This relaxation rate (R2* = 1/T2*) is proportional to the level of deoxyhemoglobin, and the R2* reflects the oxygenation status of red blood cells. This can be associated with tissue P_{O_2} and indeed much of the physiological utility of BOLD MRI rests on the assumption that tissue P_{O_2} is in responsive equilibrium with red blood cell P_{O_2}. In pigs the spatial gradients of oxygenation observed by BOLD MRI are consistent with those measured in the contralateral kidney by O_2 microelectrodes (28).

Although the use of BOLD MRI to rapidly and noninvasively define renal hypoxia is clinically attractive (14), interpretation of images is often challenging. Most postacquisition analyses rely on manual selection of small regions of interest (ROI) to generate anatomically informative R2* maps. However, kidneys are subject to respiratory and cardiovascular motions that might be difficult to gate against, particularly in experimental models. Unless image registration is employed, time-series data within an individual ROI are unlikely to be acquired from exactly corresponding anatomical regions. The selection of small segments that are well delineated within the cortex and medulla has been advocated (12), but this approach will discard from the analysis biological information contained within the data set. Moreover, this approach is subjective and risks a selection bias towards areas at the extremes of signal intensity (14).

In biomedical research, the use of algorithms that cluster individual data points based on concepts of quantitative "nearness" or "similarity" are more commonly associated with analysis of gene expression data sets (6) but are broadly applicable to large data sets, such as those generated through BOLD MRI. The present study applied *k*-means clustering as an anatomically unbiased approach to BOLD MRI analysis. The central tenet of this approach is that voxels clustered on

Address for reprint requests and other correspondence: M. Bailey, Univ./British Heart Foundation Centre for Cardiovascular Science The Univ. of Edinburgh, Queen's Medical Research Centre, 47 Little France Crescent, Edinburgh EH16 4TJ, UK (e-mail: matthew.bailey@ed.ac.uk).

quantitative nearness of the R2* signal share a commonality of biological process. Importantly, quantitative similarity does not necessarily equate to close anatomical proximity of voxels or compartmentalization within a given region of the kidney.

We employed two complementary strategies to affect R2* in an acute and chronic time frame. Acutely, we manipulated pharmacologically nitric oxide bioavailability. The maneuvers were designed to change whole kidney blood flow, either rapidly and reversibly with acetylcholine, or with sustained effect through nitric oxide synthesis inhibition, without altering autoregulatory capacity (2). To cause a chronic change in R2* we infused angiotensin II: over this time frame we anticipated no major change in renal vascular resistance but an increase in renal tubular sodium reabsorption (1, 32, 38). These complimentary experiments provided the means to dissect the physiologically complex R2* signal, resolving the influence of nitric oxide bioavailability and renal blood flow.

METHODS

All experiments were performed under a UK Home Office license following ethical approval by The University of Edinburgh. Male F344/IcoCrl rats (Charles River), aged 12–16 wk, were given free access to water and commercial rat chow (0.3% sodium by weight; Special Diet Services) and housed under controlled conditions of temperature (24 ± 1°C), humidity (50 ± 10%), and light/dark (light 7 AM-7 PM) during the experiments.

BOLD MRI. Measurements were performed using a 7 Tesla preclinical MRI scanner (Agilent Technologies). Rats (n = 6) were anesthetized with 1.5 - 2% isoflurane in oxygen-enriched air (0.5 l/min air and 0.5 l/min oxygen). Rectal temperature was maintained at (37°C). Respiration and ECG were monitored for stability throughout the scanning protocol. A birdcage volume coil (72-mm diameter) and a 4-channel phased array surface coil (Rapid Biomedical) were used for radio frequency transmission and signal reception, respectively.

Image acquisition used a multiple echo gradient-recalled BOLD MRI pulse sequence of ten images weighted in T2*; TE = 4, 8, 12, 16, 20, 24, 28, 32, 36, and 40 ms; TR = 100 ms and flip angle of 30° at an 83 kHz bandwidth. An axial slice through the centre of the right kidney was selected with 50 × 40 mm field of view containing a 192 × 128 acquisition matrix (in-plane resolution = 0.26 × 0.31 mm). A single axial slice, aligned parallel with the renal artery identified by rapid scout scanning (fast gradient echo, 3 slices in coronal orientation), ensured slice position encompassed the most representative section of the kidney regions. Slice thickness was 2 mm with 14 signal averages. Temporal resolution was 3 min for each BOLD scan.

Scans obtained under control conditions (*days 6* and *4*) were compared statistically and then combined into one group. On *day 0*, osmotic minipumps (model 2002; Alzet, Charles River, UK), adapted for MRI by replacement of the stainless steel flow moderator with a polyetheretherketone equivalent (part no. 2496, PEEK, Charles River, UK), containing angiotensin II (60 ng/min) were surgically implanted under isofluorane anesthetic. Rats were scanned again after 3 days of angiotensin II infusion.

Image selection and registration. Motion correction was performed by complimentary measures to ensure voxels in different frames overlapped; global registration (consistent over entire image), intensity-based registration (using grey-level image values), and rigid registration (only allowing translation and rotation) were used on each rat and on each day separately.

Initial outlier detection was assessed by a Hampel identifier, used to detect scans having an intensity profile significantly different from the median ($X_{0.5}$) or outside the 90th percentile ($X_{0.9}$): scan imprecision largely reflected significant motion artefact and these outliers were rejected.

Rigid registration was performed on the remaining images using an exhaustive search. The third baseline scan was selected and all other scans in the sequence were translated and rotated until the mutual information (gradient^2) was maximized. This improved stability across sequences: 96% of scans required less than one voxel transla-

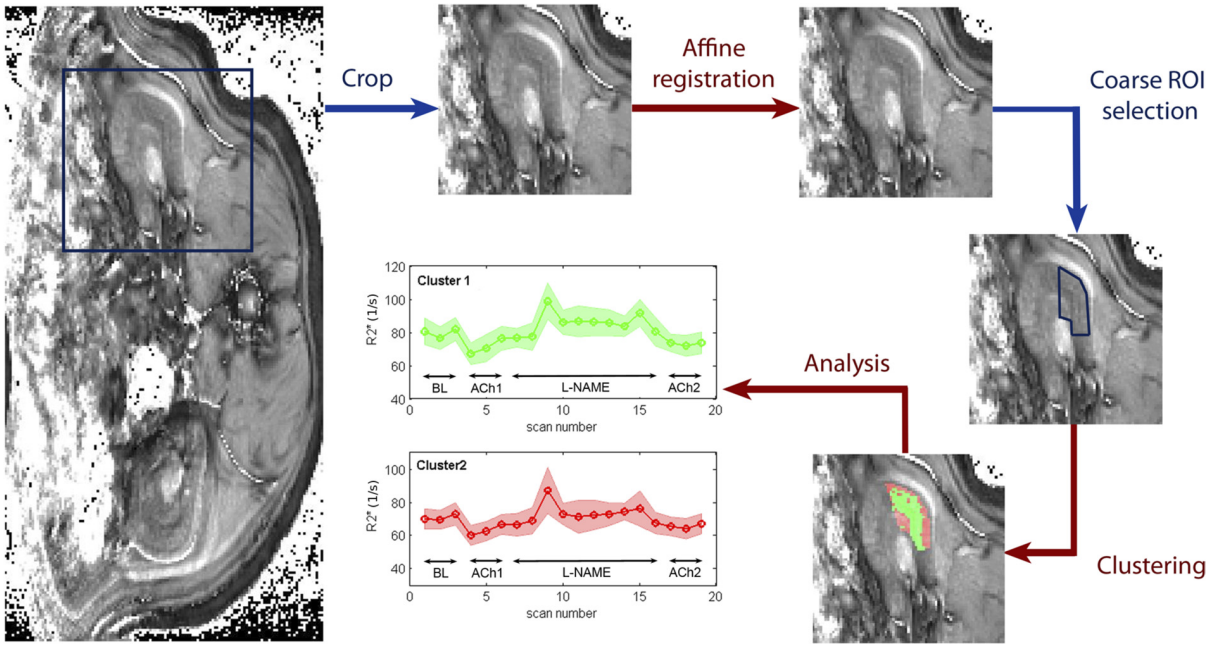

Fig. 1. Analysis pipeline of blood oxygen level-dependent magnetic resonance imaging (BOLD MRI) data. Following registration of the images, a kidney quadrant was manually selected. The *k*-means clustering of the data for time series analysis was then performed automatically, using the MATLAB code provided (https://github.com/andrewzm/BOLD_Kidney) and two compartments identified with statistically distinct mean R2* time series. For clarity blue arrows indicate manual steps and red arrows automation. ROI, regions of interest; BL, baseline; L-NAME, N^{ω}-nitro-L-arginine methyl ester hydrochloride.

tional correlation or less than 1° rotation, indicating that rigid registration was sufficient for the present dataset.

k-Means clustering analysis. Automated image segmentation was performed using a *k*-means clustering algorithm (with *k*, the number of clusters). The *k*-means clustering identifies *k*-clusters within a multi-dimensional space using Euclidean distance (for details, Ref. 3, chapter 9.1). Given a set of points, the target of the algorithm is to find k cluster-centers such that the sum of square distances of each point to its closest cluster centre is a minimum. The (local) minimum is searched for in an iterative manner, the two steps of which are *1*) the association of the points with their closest cluster centers, and *2*) the updating of the cluster centers such that the sum of square distances to the associated points is minimized. The final cluster configuration can be dependent on the initial cluster configuration. To validate our approach, the appropriate number of initial conditions was therefore determined to establish the lowest number insensitive to the starting conditions. The present dataset found 10 random initial conditions to fit this condition, thus for each scan set we ran the algorithm and saved the final configuration as that with the lowest sum of intracluster distances.

To select the number of clusters (*k*), we performed pilot analysis using $k = 1, 2, 3\ldots13$ to identify the value of *k* such that the increase in explained variance of $k + 1$ clusters was <50% of the additional variance explained by the *k*th cluster. With the use of this approach $k = 2$ was chosen, as the addition of a third cluster did not contribute sufficiently to an increase in explained variance. Each time series required ~50 ms to converge run in MATLAB on a standard desktop computer.

Pharmacological protocol. The effect of acetylcholine (5 μg/kg; Sigma-Aldrich) on the R2* signal was determined before and following administration of N^{ω}-nitro-L-arginine methyl ester hydrochloride (L-NAME; 10 mg/kg; Sigma-Aldrich). Both compounds were administered via the tail vein in a volume of ~0.15 ml. Immediately following injection, the catheter was flushed through with a volume of saline equal to the catheter volume. The potential effects of water loading must be considered (15). However, in the present study, the volume of saline injected for each animal over ~1 h did not exceed 0.95 ml in total.

Measurement of blood pressure and renal blood flow. The effects of acetylcholine and the nitric oxide synthase inhibitor L-NAME on blood pressure and renal blood flow were measured in a parallel study using the protocol described above. Renal blood flow data are normalized to total kidney weight. Control rats ($n = 4$) and rats receiving angiotensin II (60 ng/min; $n = 5$) were anesthetized (120 mg/kg ip thiobutabarbital). The right jugular vein was cannulated for infusion of 0.9% NaCl containing 1% bovine serum albumin. Rats were infused at 100 μl/min until a total volume of 1.25 ml/100 g body wt was reached and then 30 μl/min maintenance rate. The left femoral artery was cannulated for blood pressure measurement (MLT844; AD Instruments); a tracheotomy was performed to maintain a clear airway. A midline laparotomy was performed, and a Doppler transit time probe (MA1PRB; Transonic) was placed around the left renal artery. Core body temperature was servo-maintained at 37°C.

Statistics. Data are presented as means ± SE. Statistical analysis was performed by repeated-measures ANOVA, unless otherwise stated. Post hoc significance testing was performed by the Bonferroni method unless otherwise stated.

RESULTS

Postacquisition generation of R2 maps.* The clustering approach was used to generate R2* maps within a kidney quadrant in each of six control rats, using the postacquisition pipeline shown in Fig. 1. Two compartments of distinct mean R2* intensities were created (*cluster 1* = 70.96 ± 1.48; *cluster 2* 79.00 ± 1.50; means ± SE; $n = 18$ scans in 6 rats; $P < 0.01$). Each rat underwent three consecutive baseline scans on control *days 6* and *4* and following 3 days of angiotensin II infusion. In control rats, baseline scans repeated sequentially on separate days or on different rats did not vary significantly for either *cluster 1* (Fig. 2*A*) or *cluster 2* (Fig. 2*B*). Consecutive baseline scan reproducibility was also observed following chronic angiotensin II infusion. Baseline scans were therefore combined for both groups.

In control rats, the cluster having a low R2* mean ("higher" oxygenation) had anatomical coordinates that largely overlaid regions of the renal cortex and the higher R2* mean ("lower" oxygenation) lay within regions of the renal medulla. Thus, in the control setting, regions of quantitative oxygen homogeneity were also spatially proximate, mapping to distinct anatomical regions of the kidney. The spatial oxygenation gradient established here is consistent with that reported using ROI selection and with direct P_{O_2} measurement by microelectrodes.

Nitric oxide bioavailability and renal R2.* Systemic injection of acetylcholine significantly attenuated the R2* signal ($P < 0.01$, ANOVA) in both clustered compartments (Fig. 3*A*), suggesting an increase in P_{O_2} throughout the kidney. This effect was transient; reaching its nadir in the scan performed 6 min postinjection. In a parallel study, acetylcholine initially caused a rapid fall in mean arterial pressure and renal blood flow. This effect was short lived (<1 min), and during the BOLD MRI scan protocol, renal blood flow was ~30% higher than at baseline (Fig. 3*B*). Importantly, the average renal blood

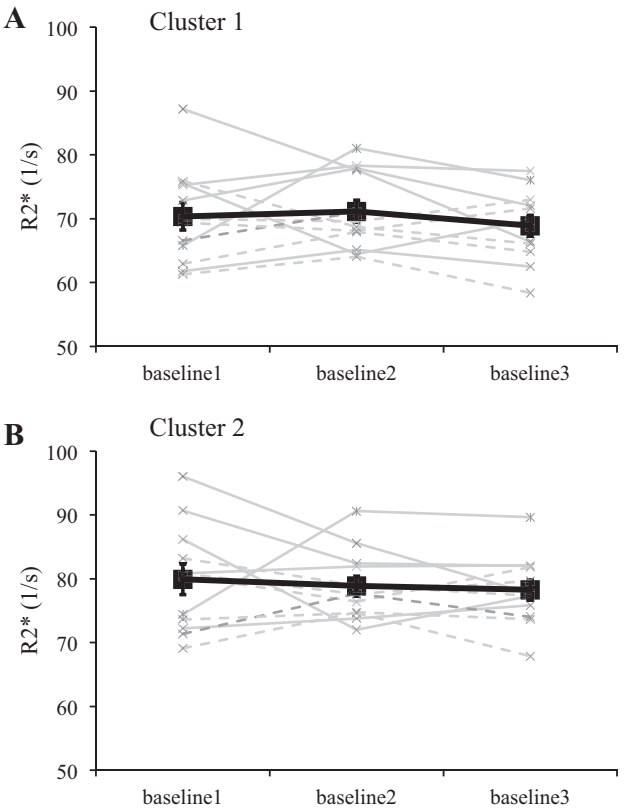

Fig. 2. Reproducibility of baseline BOLD MRI data. Rats were scanned in triplet (baseline 1, 2, and 3) and in 2 cohorts on *day 6* (solid grey lines) or *day 4* (broken grey lines). No significant difference between any of these measurements was observed (black line); thus baseline scans were assimilated into one baseline value.

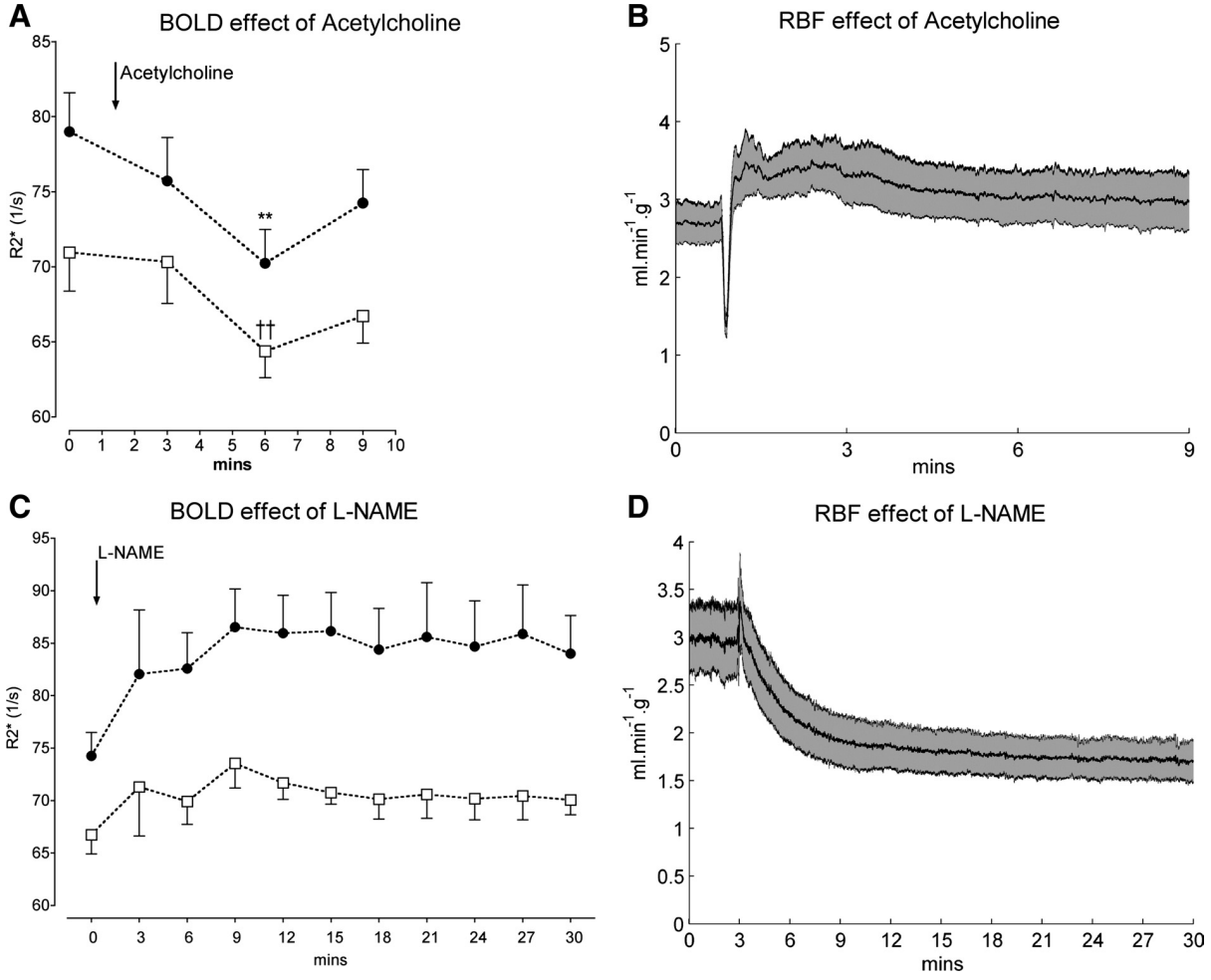

Fig. 3. Renal BOLD-MRI and hemodynamic analysis in control rats. Effect of systemic acetylcholine on R2* signal (*A*) and renal blood flow (RBF; *B*) in the left renal artery. Effect of L-NAME on R2* signal (*C*) and RBF (*D*). For renal BOLD data in *A* and *C*: □, *cluster 1* data; ●, *cluster 2* values. $^{**}P < 0.01$ and $^{*}P < 0.05$.

flow for the entire period remained unchanged (Table 1) suggesting intact autoregulation.

Administration of L-NAME caused a slowly progressive increase in signal intensity in the high R2* compartment ($P < 0.01$, ANOVA) but was without effect in the low R2* compartment (Fig. 3*C*). This is consistent with previous observations showing no effect of nitric oxide synthesis inhibition on R2* intensity in cortical ROI (29). L-NAME also caused a reduction in renal blood flow over this time course (Fig. 3*D*). The effects of L-NAME on both R2* and renal vascular resistance reached steady state after ~20 min in general agreement with the reported inhibitory effect on nitric oxide bioavailability (16). Acetylcholine was again injected. The effect on blood pressure and renal blood flow persisted, but the attenuation of R2* signal by acetylcholine was no longer observed (data not shown).

Effect of chronic angiotensin II infusion. Angiotensin II was infused by osmotic minipump over a 3-day period and BOLD-

Table 1. *Mean arterial blood pressure and left renal artery blood flow in control rats or rats receiving a chronic infusion of angiotensin II*

	Baseline	ACh1	L-NAME	ACh2
BP, mmHg				
Control	89 ± 2	89 ± 1	114 ± 4*	113 ± 4
Angiotensin II	90 ± 3	91 ± 3	110 ± 2*	109 ± 2
RBF, ml·min^{-1}·g kidney wt^{-1}				
Control	2.70 ± 0.3	3.04 ± 0.4	1.73 ± 0.2*	1.74 ± 0.2
Angiotensin II	3.19 ± 0.4	3.41 ± 0.5	1.63 ± 0.2*	1.60 ± 0.2

Mean arterial blood pressure (BP) and left renal artery blood flow (RBF) in control rats ($n = 4$) or rats receiving a chronic infusion of angiotensin II (60 ng/min) for 3 days ($n = 5$). Data are means ± SE and taken during steady state at baseline and during injection of acetylcholine (ACh), either before or after administration of N^{ω}-nitro-L-arginine methyl ester hydrochloride (L-NAME). $^{*}P < 0.05$, baseline vs. L-NAME.

MRI scans were once again obtained. Blood pressure and renal blood flow were not significantly affected by this infusion (Table 1). The *k*-means clustering approach resolved the data into distinct compartments; indeed, convergence is assured by this algorithm, but the magnitude of the difference in intensity between the two compartments was much reduced (*cluster 1* = 71.30 ± 2.00; *cluster 2* = 72.48 ± 1.27; mean ± SE; NS). Critically, baseline means of the two clustered compartments were less distinct during baseline and no longer mapped to discrete anatomical regions of the kidney (see Fig. 5 for example images). This suggests that a short exposure to angiotensin II disrupts the oxygenation gradient through the kidney, creating areas of high and low Po_2 in both cortex and medulla. As stated previously, the R2* signal actually reflects oxygenation of red blood cells and thus altered patterns of renal perfusion may also account for the disrupted gradient. Following angiotensin II infusion, the R2* was no longer significantly affected by administration of either acetylcholine or L-NAME (Fig. 4*A*). Nevertheless, acetylcholine still induced a transient reduction in renal blood flow and blood pressure (Fig. 4, *B* and *C*) and L-NAME significantly increased renal vascular resistance.

DISCUSSION

BOLD MRI is an attractive tool for clinical research since it does not require exogenous contrast agent and has a rapid acquisition time (14). BOLD MRI is increasingly used to quantify renal "oxygenation" in a variety of disease settings, and studies typically focus on the medulla, which is vulnerable to hypoxic insult. Hypoxia of the cortex is also evident in severe renovascular disease (13) and in diabetic and nondiabetic CKD (19). A global map of renal R2* could therefore be a valuable diagnostic/prognostic tool for ischemic renal disease. However, the relationship between R2* and tissue hypoxia is complex (20). R2* reports oxygenation of the red blood

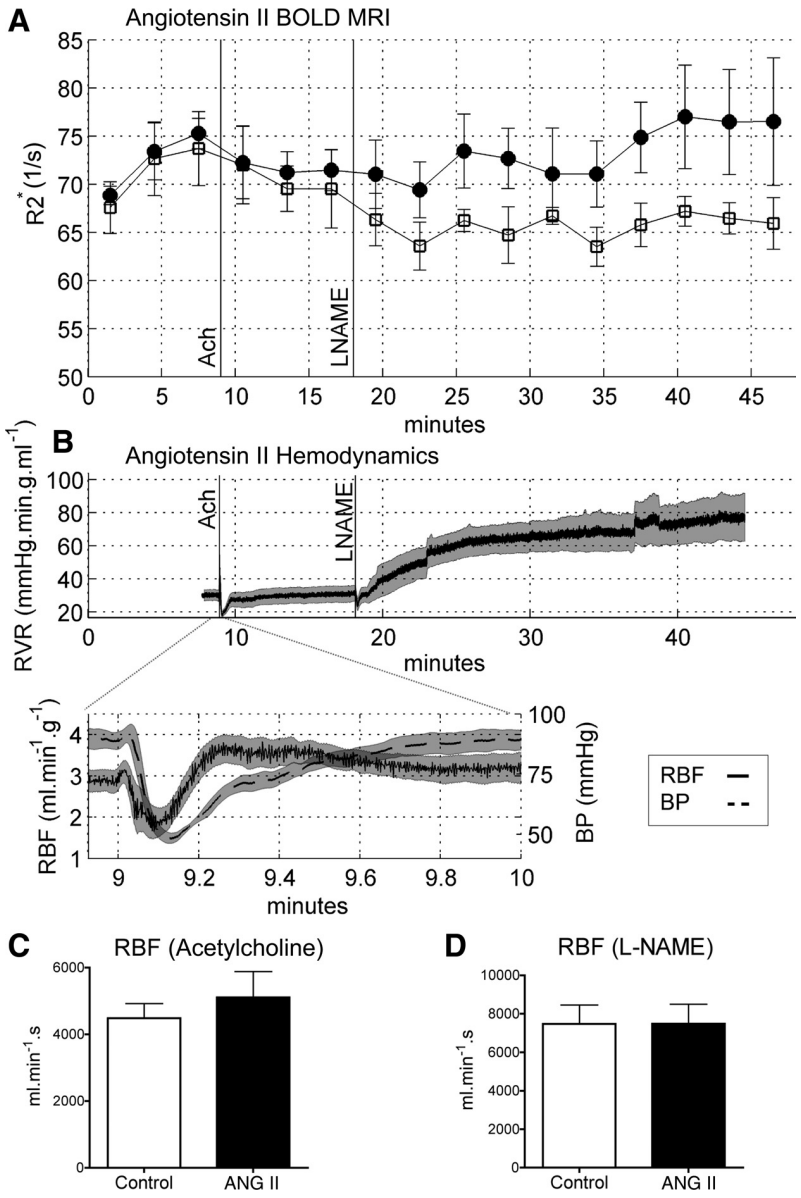

Fig. 4. Renal BOLD-MRI and hemodynamic analysis in rats after angiotensin II infusion. *A*: R2* trace measured by *k*-means clustering, open squares (*cluster 1*) and circles (*cluster 2*) signal. *B*: renal vascular resistance (RVR) hemodynamic study following protocol time course and insert showing ACh trace with BP (broken line) and RBF (solid line). Area under the curve analysis for RBF following injection of ACh (*C*) OR L-NAME (*D*).

cells, and the signal reflecting local perfusion is also influenced by pH and hydration status. In CKD, BOLD MRI studies have produced conflicting data (22, 37). This partially reflects the complexity of CKD; the future diagnostic utility of renal BOLD MRI is nevertheless contentious (17).

One major challenge for the field is standardization of protocols, particularly for postprocessing, that would facilitate meaningful cross-comparison of data sets. Most studies quantify renal oxygenation by measuring R2* signal intensity in small manually selected ROI. A strength of this approach is that the generation of time-series data are based firmly on anatomical knowledge of renal structure. Reliable placement can be difficult, however, and averaging across several ROI can mask the heterogeneity of oxygenation. Importantly, the ROI approach discards from analysis much of the biological information contained within an image and the power of BOLD MRI to assess renal oxygenation on a global scale is often underexploited.

Data-led segmentation of datasets has previously been used for analysis of brain (4) and kidney (7, 39). MRI and our work complements the recent compartmentalization approach to analysis of Ebrahimi et al. (7). Our method has two main differences. First, our cluster is defined from time series since voxel variation in time is informative and more easily controlled than maps defined in a separate computed tomography scanner where renal orientation might be difficult to replicate. Second, we were not able to resolve distinct and separate cortical and medullary R2* distributions and therefore assume no anatomically defined distribution functions. We have incorporated this approach, developing a semi-automated postacquisition pipeline for analysis of BOLD MRI images: *k*-means (where $k = 2$) clustering was used to assign individual voxels into one of two statistically distinct compartments. The advantages of the method are that it: *1*) does not require user-led selection of small anatomical ROI but rather a gross quadrant of the whole kidney to be segregated into two compartments in a user-independent manner; *2*) obviates the need for voxel-tracking through a time-series stack; and *3*) is anatomically unbiased, identifying on a global scale clusters of Po_2 homogeneity for each patient or experimental subject. The analysis pipeline is shown in Fig. 1 and our MATLAB code is available freely (https://github.com/andrewzm/BOLD_Kidney).

In control rats, the clustering analysis delineated compartments that largely mapped to discrete anatomical regions of the kidney (Fig. 5). The low R2* cluster was located predominantly in the cortex, and the high R2* cluster localized primarily to the outer medulla. Under control conditions the clustering approach supports the notion of a cortico-medullary Po_2 gradient and perhaps offers little interpretive gain over ROI selection. However, the clustering analysis indicated a dissipation of the cortex-to-medulla renal Po_2 gradient following angiotensin II infusion (Fig. 5). This global map of oxygenation captures nuances of regional gradients.

This has clinical relevance: a recent study, averaging R2* across multiple ROI, demonstrated cortical hypoxia in a small number of CKD patients (19). The effect size was small and the variation large, suggesting that constraints of statistical power will make comparisons of absolute R2* across patients and between studies difficult (22, 37). Qualitatively, Manotham et al. (19) noted that the R2* signal was more heterogeneous and liable to rapid decay in CKD patients than in controls. We suggest that this global disruption of a spatially constrained Po_2 gradient may be a hallmark of the defects in renal oxygenation associated with renal injury.

Acute administration of angiotensin II causes a rapid increase in R2* in healthy subjects, attributed to a fall in renal perfusion (31). Conversely, acute blockade of AT_1 receptors increases Po_2 in the renal cortex of CKD patients (19). An increase in cortical oxygenation following AT_1 receptor blockade has also been observed in normal (26) and hypertensive rats (34), effects attributed to improved blood flow and efficiency of O_2 usage respectively. In our study, a 3-day infusion of angiotensin II did not increase blood pressure, consistent with previous data (5), and gross renal blood flow was unchanged. Tubular sodium reabsorption is increased within this timeframe (1, 38), and we found evidence for disruption of the regional homogeneity of Po_2. This may reflect a local mismatch of delivery/consumption or a reduction in the efficiency of O_2 utilization, as reported in the angiotensin II-dependent Goldblatt model (36).

Most MRI scanners are not calibrated directly for Po_2. The absolute R2* value is often therefore less informative for cross-comparison than is the dynamic response to maneuvers affecting perfusion or sodium transport. In this study, injection

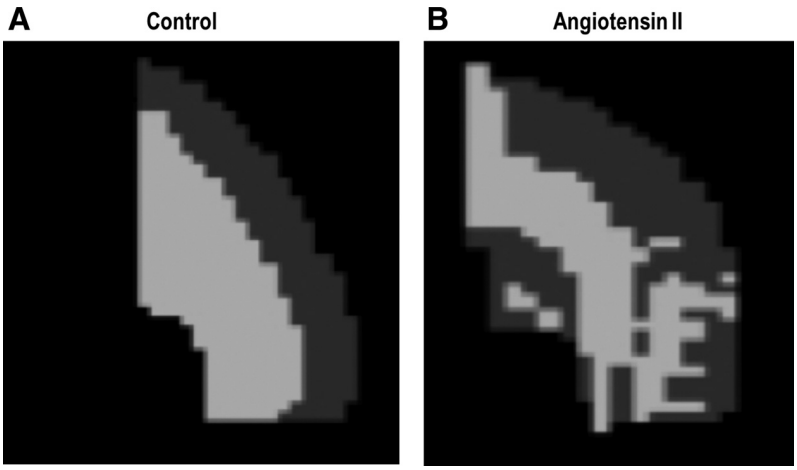

Fig. 5. Anatomical heterogeneity of renal R2* signal following chronic angiotensin II infusion. Exemplar clustering analysis in manually delineated renal quadrants of rat kidney under control conditions (*A*) and following angiotensin II infusion (*B*). The *k*-means clustering was used to segment data on a quantitative basis into low (dark grey) and high (light grey) R2* clusters. In control conditions, these clusters mapped to anatomically regions; following angiotensin II infusion, the spatial relationship between similar R2* values was less well defined.

of acetylcholine suppressed the R2* signal throughout the kidney. This was probably not dependent on whole kidney perfusion, there being temporal separation between the reduction in blood flow and the reduction in R2*. The attenuation of R2* was dependent on NO generation, being inhibited by L-NAME, and had a delayed onset, being evident only in the second scan postinjection. A previous study also reported no immediate effect of NO on R2* intensity (31).

We recognize that NO reacts irreversibly with both oxy- and deoxyhaem moieties (8). These reactions are rapid, and hemoglobin and deoxyhemoglobin levels should be equivalently affected over each 3-min BOLD scan. We therefore ascribe the reduced R2* to an NO-dependent increase in Po_2 throughout the kidney, most probably reflecting inhibition of tubular sodium transport (11). The effect of acetylcholine was lost following chronic angiotensin II infusion. Prolonged exposure to angiotensin II causes oxidative stress in rats (18), and our data plausibly reflect accumulation of superoxide anion leading to NO deficiency and defects in renal oxygenation (35).

There are two important limitations to our study. First, it was not possible to measure renal blood flow and BOLD signal simultaneously. The invasive surgery required for Doppler measurements of renal arterial blood flow also mean that measurements were not made in the same animals: we chose instead to obtain repeated R2* measurements in a longitudinal study. Second, the BOLD MRI and renal blood flow data were obtained under differing anesthetic regimens. Maintenance of anesthesia within the MRI scanner required ECG monitoring under gas anesthesia (isoflurane) while stability of renal perfusion following the invasive abdominal surgery is best obtained with a long-lasting barbiturate (33). Renal hemodynamics may be differentially affected by the anesthetics, but it unlikely that this accounts for the temporally distinct dynamic response to acetylcholine of the R2* signal and blood flow.

In summary, we have developed an anatomically unbiased method for the assessment of renal function by BOLD MRI, employing signal analysis to remove errors inherent in manual ROI selection. These data indicate that protocols assessing the dynamic response of R2* to acetylcholine can provide information relating to renal NO bioavailability and offer temporal insight into renal oxygenation homeostasis.

ACKNOWLEDGMENTS

We thank Paul O'Connor and Chris Kenyon for critical reading of the manuscript.

This work has been published in abstract form at The Experimental Biology 2013 Meeting.

GRANTS

This work was funded through the University of Edinburgh Preclinical Imaging Initiative (to M. A. Bailey, J. W. Dear, J. J. Mullins, and D. J. Webb), an Engineering and Physical Sciences Research Council Shaping Capability Award (to G. Sanguinetti and M. A. Bailey), and a British Heart Foundation Centre of Research Excellence Award (to R. I. Menzies and A. Zammit-Mangion).

DISCLOSURES

No conflicts of interest, financial or otherwise, are declared by the author(s).

AUTHOR CONTRIBUTIONS

Author contributions: R.I.M., D.J.W., J.J.M., J.W.D., and M.A.B. conception and design of research; R.I.M., R.J.L., and M.A.J. performed experiments; R.I.M., A.Z.-M., L.M.H., G.S., and M.A.B. analyzed data; R.I.M., A.Z.-M., D.J.W., J.W.D., G.S., and M.A.B. interpreted results of experiments; R.I.M., A.Z.-M., and G.S. prepared figures; R.I.M., A.Z.-M., G.S., and M.A.B. drafted manuscript; R.I.M., A.Z.-M., D.J.W., J.W.D., G.S., and M.A.B. edited and revised manuscript; R.I.M., L.M.H., R.J.L., M.A.J., D.J.W., J.J.M., J.W.D., G.S., and M.A.B. approved final version of manuscript.

REFERENCES

1. **Ashek A, Menzies RI, Mullins LJ, Bellamy CO, Harmar AJ, Kenyon CJ, Flatman PW, Mullins JJ, Bailey MA.** Activation of thiazide-sensitive co-transport by angiotensin II in the cyp1a1-Ren2 hypertensive rat. *PLoS One* 7: e36311, 2012.
2. **Beierwaltes WH, Sigmon DH, Carretero OA.** Endothelium modulates renal blood flow but not autoregulation. *Am J Physiol Renal Fluid Electrolyte Physiol* 262: F943–F949, 1992.
3. **Bishop CM.** *Pattern Recognition and Machine Learning*. New York: Springer, 2006.
4. **Calhoun VD, Adali T, Pearlson GD, Pekar JJ.** Spatial and temporal independent component analysis of functional MRI data containing a pair of task-related waveforms. *Hum Brain Mapp* 13: 43–53, 2001.
5. **Chin SY, Wang CT, Majid DS, Navar LG.** Renoprotective effects of nitric oxide in angiotensin II-induced hypertension in the rat. *Am J Physiol Renal Physiol* 274: F876–F882, 1998.
6. **Dougherty ER, Barrera J, Brun M, Kim S, Cesar RM, Chen Y, Bittner M, Trent JM.** Inference from clustering with application to gene-expression microarrays. *J Comput Biol* 9: 105–126, 2002.
7. **Ebrahimi B, Gloviczki M, Woollard JR, Crane JA, Textor SC, Lerman LO.** Compartmental analysis of renal BOLD MRI data: introduction and validation. *Invest Radiol* 47: 175–182, 2012.
8. **Eich RF, Li T, Lemon DD, Doherty DH, Curry SR, Aitken JF, Mathews AJ, Johnson KA, Smith RD, Phillips GN, Jr, Olson JS.** Mechanism of NO-induced oxidation of myoglobin and hemoglobin. *Biochemistry* 35: 6976–6983, 1996.
9. **Evans RG, Gardiner BS, Smith DW, O'Connor PM.** Intrarenal oxygenation: unique challenges and the biophysical basis of homeostasis. *Am J Physiol Renal Physiol* 295: F1259–F1270, 2008.
10. **Evans RG, Gardiner BS, Smith DW, O'Connor PM.** Methods for studying the physiology of kidney oxygenation. *Clin Exp Pharmacol Physiol* 35: 1405–1412, 2008.
11. **Garvin JL, Herrera M, Ortiz PA.** Regulation of renal NaCl transport by nitric oxide, endothelin, and ATP: clinical implications. *Annu Rev Physiol* 73: 359–376, 2011.
12. **Gloviczki ML, Glockner J, Gomez SI, Romero JC, Lerman LO, McKusick M, Textor SC.** Comparison of 1.5 and 3 T BOLD MR to study oxygenation of kidney cortex and medulla in human renovascular disease. *Invest Radiol* 44: 566–571, 2009.
13. **Gloviczki ML, Glockner JF, Lerman LO, McKusick MA, Misra S, Grande JP, Textor SC.** Preserved oxygenation despite reduced blood flow in poststenotic kidneys in human atherosclerotic renal artery stenosis. *Hypertension* 55: 961–966, 2011.
14. **Gloviczki ML, Lerman LO, Textor SC.** Blood oxygen level-dependent (BOLD) MRI in renovascular hypertension. *Curr Hypertens Rep* 13: 370–377, 2011.
15. **Haque M, Franklin T, Prasad P.** Renal oxygenation changes during water loading as evaluated by BOLD MRI: effect of NOS inhibition. *J Magn Reson Imaging* 33: 898–901, 2011.
16. **Heyman SN, Goldfarb M, Darmon D, Brezis M.** Tissue oxygenation modifies nitric oxide bioavailability. *Microcirculation* 6: 199–203, 1999.
17. **Inoue T, Kozawa E, Okada H, Suzuki H.** Is there no future for renal BOLD-MRI? *Kidney Int* 82: 934, 2012.
18. **Laursen JB, Rajagopalan S, Galis Z, Tarpey M, Freeman BA, Harrison DG.** Role of superoxide in angiotensin II-induced but not catecholamine-induced hypertension. *Circulation* 95: 588–593, 1997.
19. **Manotham K, Ongvilawan B, Urusopone P, Chetsurakarn S, Tanamai J, Limkuansuwan P, Tungsanga K, Eiam-Ong S.** Angiotensin II receptor blocker partially ameliorated intrarenal hypoxia in chronic kidney disease patients: a pre-/post-study. *Intern Med J* 42: e33–37, 2012.
20. **Mason RP.** Non-invasive assessment of kidney oxygenation: a role for BOLD MRI. *Kidney Int* 70: 10–11, 2006.
21. **Mayer G.** Capillary rarefaction, hypoxia, VEGF and angiogenesis in chronic renal disease. *Nephrol Dial Transplant* 26: 1132–1137, 2011.
22. **Michaely HJ, Metzger L, Haneder S, Hansmann J, Schoenberg SO, Attenberger UI.** Renal BOLD-MRI does not reflect renal function in chronic kidney disease. *Kidney Int* 81: 684–689, 2012.

23. **Miyata T, Takizawa S, van Ypersele de Strihou C.** Hypoxia. 1. Intracellular sensors for oxygen and oxidative stress: novel therapeutic targets. *Am J Physiol Cell Physiol* 300: C226–C231, 2011.
24. **Nangaku M.** Chronic hypoxia and tubulointerstitial injury: a final common pathway to end-stage renal failure. *J Am Soc Nephrol* 17: 17–25, 2006.
25. **Neuhofer W, Beck FX.** Survival in hostile environments: strategies of renal medullary cells. *Physiology (Bethesda)* 21: 171–180, 2006.
26. **Norman JT, Stidwill R, Singer M, Fine LG.** Angiotensin II blockade augments renal cortical microvascular Po_2 indicating a novel, potentially renoprotective action. *Nephron Physiol* 94: 39–46, 2003.
27. **Palm F, Nordquist L.** Renal tubulointerstitial hypoxia: cause and consequence of kidney dysfunction. *Clin Exp Pharmacol Physiol* 38: 474–480, 2011.
28. **Pedersen M, Dissing TH, Morkenborg J, Stodkilde-Jorgensen H, Hansen LH, Pedersen LB, Grenier N, Frokiaer J.** Validation of quantitative BOLD MRI measurements in kidney: application to unilateral ureteral obstruction. *Kidney Int* 67: 2305–2312, 2005.
29. **Prasad PV, Priatna A, Spokes K, Epstein FH.** Changes in intrarenal oxygenation as evaluated by BOLD MRI in a rat kidney model for radiocontrast nephropathy. *J Magn Reson Imaging* 13: 744–747, 2001.
30. **Rosenberger C, Rosen S, Paliege A, Heyman SN.** Pimonidazole adduct immunohistochemistry in the rat kidney: detection of tissue hypoxia. *Methods Mol Biol* 466: 161–174, 2009.
31. **Schachinger H, Klarhofer M, Linder L, Drewe J, Scheffler K.** Angiotensin II decreases the renal MRI blood oxygenation level-dependent signal. *Hypertension* 47: 1062–1066, 2006.
32. **van der Mark J, Kline RL.** Altered pressure natriuresis in chronic angiotensin II hypertension in rats. *Am J Physiol Regul Integr Comp Physiol* 266: R739–R748, 1994.
33. **Walker LA, Buscemi-Bergin M, Gellai M.** Renal hemodynamics in conscious rats: effects of anesthesia, surgery, and recovery. *Am J Physiol Renal Fluid Electrolyte Physiol* 245: F67–F74, 1983.
34. **Welch WJ, Baumgartl H, Lubbers D, Wilcox CS.** Renal oxygenation defects in the spontaneously hypertensive rat: role of AT1 receptors. *Kidney Int* 63: 202–208, 2003.
35. **Welch WJ, Blau J, Xie H, Chabrashvili T, Wilcox CS.** Angiotensin-induced defects in renal oxygenation: role of oxidative stress. *Am J Physiol Heart Circ Physiol* 288: H22–H28, 2005.
36. **Welch WJ, Mendonca M, Aslam S, Wilcox CS.** Roles of oxidative stress and AT1 receptors in renal hemodynamics and oxygenation in the post-clipped 2K,1C kidney. *Hypertension* 41: 692–696, 2003.
37. **Xin-Long P, Jing-Xia X, Jian-Yu L, Song W, Xin-Kui T.** A preliminary study of blood-oxygen-level-dependent MRI in patients with chronic kidney disease. *Magn Reson Imaging* 30: 330–335, 2012.
38. **Zhao D, Seth DM, Navar LG.** Enhanced distal nephron sodium reabsorption in chronic angiotensin II-infused mice. *Hypertension* 54: 120–126, 2009.
39. **Zollner FG, Sance R, Rogelj P, Ledesma-Carbayo MJ, Rorvik J, Santos A, Lundervold A.** Assessment of 3D DCE-MRI of the kidneys using non-rigid image registration and segmentation of voxel time courses. *Comput Med Imaging Graph* 33: 171–181, 2009.